ELECTRONIC ENGINEERING

VOL. 39 No. 467

JANUARY 1967

Commentary

'PHYSICS, Electronics and Cybernetics' was the title of an Inaugural Lecture given at the University of Hull by Professor D. A. Bell, early last year. The object of the lecture was to explain the kind of work likely to be undertaken in a department of electronic engineering, and its relationship to other academic subjects. The lecture was a very able review of a complex subject and while space does not allow its reproduction in full, it is felt that certain sections of this lecture deserve a somewhat wider audience.

Professor Bell began by stating, "If physics is the study of the structure and behaviour of the physical universe, then any branch of engineering or technology must consist of applied physics; but electronics is a definable field which is particularly close to physics because it depends upon the detailed atomic structure of materials, the discovery of which was an important one out of the three stages which one can distinguish in the development of the science of physics. From the 17th to the 19th century physics was a study of the macroscopic behaviour of matter, exemplified by the 20th century description of physics as 'heat, light, sound, electricity and magnetism, properties of matter'. Examples of important macroscopic results are Newton's laws of motion, the rules of geometrical optics, Hooke's law for ideal elastic solids, the first and second laws of thermodynamics, the inverse-square law in electrostatics, Ampere's magnetic shell equivalent to a circuital electric current, and Maxwell's theory of electromagnetic radiation."

After giving examples from this phase and defining the position of chemistry, Professor Bell continued, "The second phase in physics could be called either atomic or electronic physics; it was concerned with relating the various properties of matter to the characteristics of the orbital electrons of the atom, the nucleus being regarded as a permanent unit of given charge and mass. This era commenced with the observation of cathode rays and the subsequent identification of the electron by J. J. Thompson, and its major feature was the Bohr-Rutherford model of the atom. The importance of this phase is that it was for the first time possible to observe the systematic behaviour of fundamental particles, in contrast to the achievements of statistical mechanics in explaining the kinetic theory of gases and the laws of thermodynamics in terms of the statistical behaviour of large numbers of particles. At the same time quantum theory was developing, first as a hypothesis to explain the bounded magnitude of black-body radiation and the fixed non-radiating orbits of electrons in the Bohr-Rutherfort atom, and later through the concepts of indeterminacy and wave-mechanics to something like an epistemology of physics. In a review of physics one should also note that Einstein's special theory of relativity was gaining universal acceptance in this same period.

It might have seemed logical to regard nuclear physics as the next phase after the physics of the Bohr-Rutherford atom, but it is now clear that the more general term is high-energy physics: high energy is needed both to explore the interior of the nucleus and to study the growing variety of fundamental particles which have no obvious place in the Bohr-Rutherford atom.

The function of electronic engineering is to put to practical use the various phenomena exhibiting the systematic behaviour of permanent charged particles, i.e. the phenomena discovered in the second phase of physics. It is in fact the attribute of charge which allows these particles to be manipulated systematically, in contrast to the statistical laws of thermal energy and of diffusion. A dramatic illustration of this is that chemical energy can be converted to electrical energy (and so subsequently to mechanical energy) at any temperature with high efficiency by an electro-chemical cell, whether one with consumable electrodes or a 'fuel cell', whereas the efficiency of conversion via thermal energy is limited to that defined by the Carnot cycle, and demands a large temperature difference between input and output. The motion of charged particles constitutes an electric current, and the science of electronics is concerned with the control of electric currents and electromagnetic fields, i.e. with controlling the flow and storage of electromagnetic energy, usually with the aid of electrical power smaller than that being controlled. Amplification is a frequently-used feature of electronic apparatus; and the ability to obtain readily a power gain of a million-fold or a thousand-million-fold has revolutionized techniques of measurement and control.

A system of components which can modify and temporarily store an electrical signal is known as an electric circuit, and there are two broad types, namely, passive and active circuits. The passive circuit can modify the signal by altering and delaying part or all of it, but the total energy leaving the circuit cannot be greater than the signal energy entering it. The active circuit, on the other hand, is able to control energy from a local source in accordance with the incoming signal, so that the controlled energy leaving the circuit is greater than the signal energy entering it. The active element in the circuit is usually either a thermionic valve or a transistor or some other quantum-electronic device such as a tunnel diode or a maser."

There is, of course, nothing new or revolutionary in the above extract from Professor Bell's lecture, but it does form a concise and aptly put summary of the evolution and function of electronic engineering.

Measurement of Speed Transients Using Optical Gratings

By D. K. Ewing*, B.Sc., D.I.C.

A frequency/voltage convertor is described, which is based on the phase-locked oscillator principle adapted to detect speed transients by using an optical grating as the speed transducer. Typical applications include the measurement of speed transients arising from transmission errors in the drive to the grating shaft and the provision of velocity feedback in machine-tool control systems where tachometric feedback would be too noisy.

(Voir page 62 pour le résumé en français: Zusammenfassung in deutscher Sprache auf Seite 69)

THE need in modern industrial processes for long term stability and high accuracy of measurement and control has brought about the development of digital methods. Because these have an incremental or numerical reference basis, they have an inherent precision which exceeds that of conventional analogue elements.

The use of optical gratings in machine tools as digital position transducers[1,2] has made automatic continuous measurement possible with an accuracy comparable with the best static measurements. The exceptional resolution of optical gratings can be used to measure the small dynamic transmission errors of precision gears. Their resolution and stability in dynamic measurement exceed those of the equivalent analogue components over the same wide range, and, in addition, they present the dimensional information directly in numerical form.

While the full potential of the radial grating, as a stable precision reference for angular movement, has been realized, its use in direct measurement of transient speed phenomena has not been widely appreciated. It has been shown[3,4] how a grating can, in effect, replace a tachometer, by counting the grating frequency over a given time interval and displaying a figure that indicates the average frequency over the counting period. Alternatively by converting the grating frequency to pulses of fixed duration and amplitude, a voltage is recovered by means of a low-pass filter, which is proportional to the average frequency over a number of cycles depending on the filter time-constant. Although these devices succeed in their main requirement of covering a wide range of frequencies (i.e. the tachometric application), inevitably because of the averaging process they may not be able to detect transients, and as a result the full resolution of the optical grating as a sensitive device for measuring speed may not be realized. To achieve this a frequency demodulator is required, which is capable of converting the change in pulse repetition frequency with minimum delay into a voltage proportional to the speed it represents. Indeed each grating pulse period is a sample, as it were, of the speed at that instant, and the problem is to recover from these changes in pulse period as much information about the speed variations as the grating is capable of resolving.

* *Ministry of Technology, National Engineering Laboratory.*

Thus, for the sensitive detection of speed transients the instrument must be capable of presenting in suitable analogue form each speed sample as it occurs; i.e. this implies that its bandwidth must be a sizeable fraction of the carrier frequency within the limits imposed by various sampling theorems.

This article describes such a frequency discriminator based on the phase-locked oscillator principle, but modified to include a sample-hold feature that in addition to its fast response also produces a direct voltage signal without the need for further filtering.

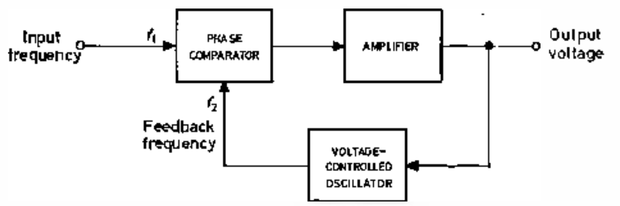

Fig. 1. Frequency demodulator using phase-locked oscillator

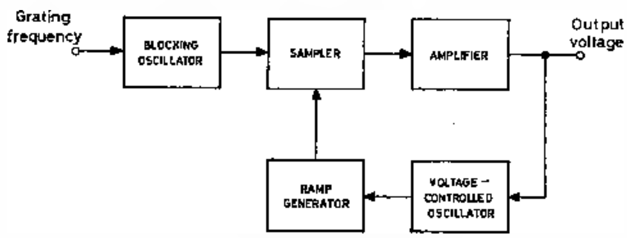

Fig. 2. Arrangement of circuit units

General Description

Fig. 1 shows the basic components of the phase-locked oscillator. The grating pulse frequency (f_1) is compared in phase with the frequency (f_2) from the internal voltage-controlled oscillator and the phase error voltage is amplified and used to control the internal oscillator, by means of negative feedback, to make the oscillator run in synchronism with the grating frequency.

In operation, f_2 and f_1 are phase-locked and since the output voltage is proportional to the feedback frequency it is also proportional to the input frequency. Thus sampling and feedback techniques combine to give the circuit an exceptional response to fast transients and provide a voltage output that needs no further filtering to obtain the analogue speed signal.

Circuit Description

Although there is a variety of circuit techniques capable of performing the functions shown in Fig. 2, nevertheless, during the circuit design process, certain novel features have been developed that not only minimize the number of adjustments when changing the frequency range but also take advantage of the exceptional flexibility of choice that is a characteristic feature of electronic design; namely, that careful selection of components can often result in great simplifications.

For instance the blocking oscillator (VT_1) in Fig. 3 not only standardizes the amplitude and duration of the input pulses, but also forms an integral part of the sampler by switching transistors VT_2 and VT_3 with pulses of the correct polarity to enable the capacitor C_1 to hold the voltage sample, V, by either charging or discharging through the bidirectional switch formed by these transistors. This voltage is converted to a current, I, by means of a direct-coupled amplifier, VT_4, VT_5 and VT_6, consisting of a long tailed pair with a high impedance input stage that does not discharge C_1 significantly. The current I, which is determined by V and R_1, charges the emitter capacitor, C_2, of the unijunction transistor VT_7 controlling the frequency of this type of relaxation oscillator[5]. Whenever the voltage on C_2 is charged up to the trigger level of VT_7, the unijunction transistor switches from its open-circuit to its short-circuit state and discharges C_2. Thus not only is the frequency proportional to the current I, but the sawtooth waveform on C_2 is also eminently suitable, after a certain amount of power amplification, for use as reference voltage in the sampler.

VT_8 and VT_9 form an appropriate yet simple impedance convertor, which is essentially an emitter-follower bootstrapped to produce the especially high input impedance needed if the waveform on C_2 is not to be distorted. It has, in addition, a certain amount of feedback to ensure that the output impedance is sufficiently low to supply a large charging current to C_1 during the brief sampling period. The capacitive coupling to this type of amplifier has provided the opportunity of attenuating the ramp waveform by means of C_3 and C_4, in addition to shifting the mean level of the sawtooth waveform to a suitable value for the d.c. amplifier, which greatly simplifies the biasing of this closed loop system.

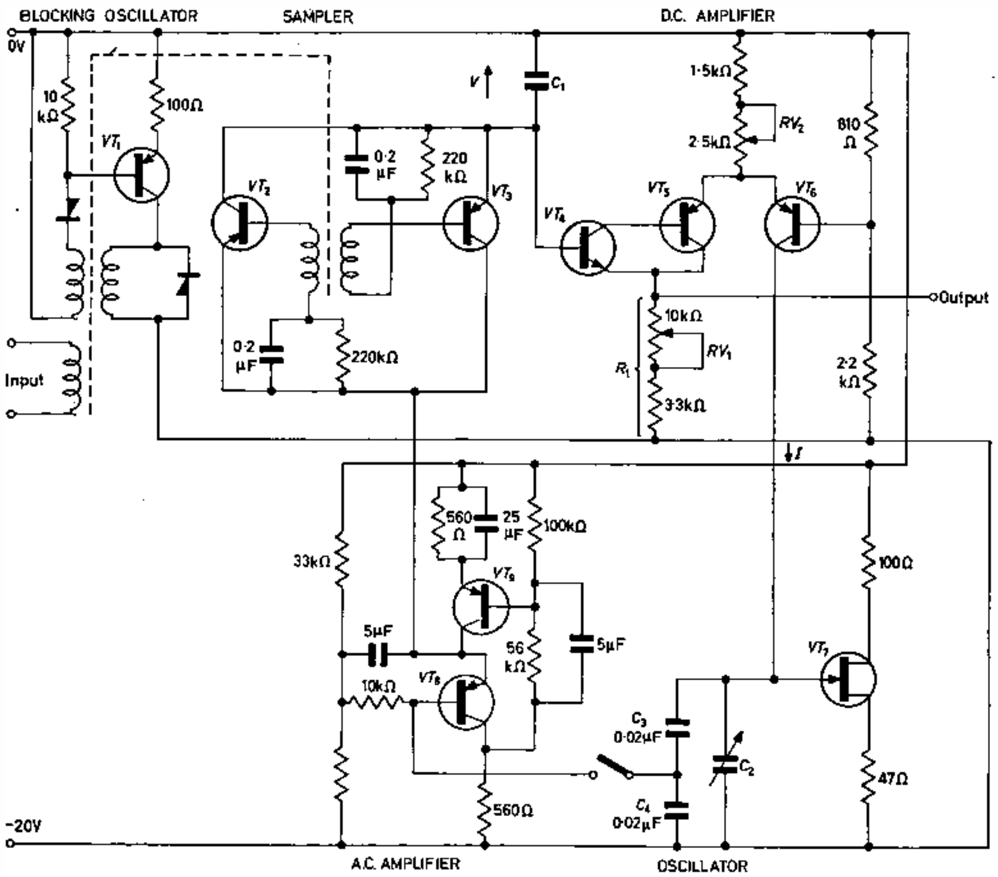

Fig. 3. Frequency to voltage convertor

Alignment

The frequency range of the instrument is restricted to the range of the internal oscillator and is therefore determined mainly by C_2 and its mean charging current; but, from the circuit design point of view, it is simpler to keep the charging current fixed and change only the capacitor C_2 to suit the particular input frequency. The main problem is to ensure that the centre frequency of the internal oscillator is within 5 per cent (say) of the mean frequency input so that the frequency modulation components can be detected symmetrically within the linear range of the oscillator. This alignment can be accomplished by breaking the feedback loop between the oscillator and its a.c. amplifier. The sampler then maintains the charging current at its mean value, which corresponds to the quiescent voltage of the a.c. amplifier output; thus by changing the charging capacitor C_2 in fine increments, it is easy to match the internal frequency to the input frequency. Too coarse a setting would cause the oscillator to operate off centre in closed loop, giving an unsymmetrical characteristic. For this reason, the range changing switch takes the form of a series-parallel connexion that allows the frequency to be changed in increments and not, as is more customary, in multiples. In fact by using the arrangement shown in Fig. 4, the correct combination of capacitors can be selected by the three decade switches to produce the internal frequency that is shown numerically on the switch positions.

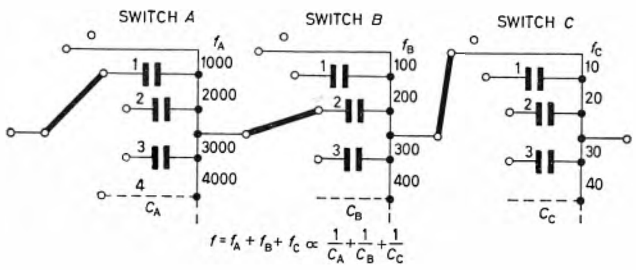

Fig. 4. Frequency selector decade switch, C_2

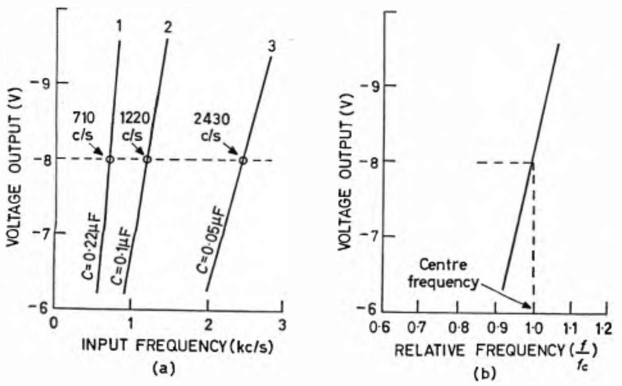

Fig. 5. Static frequency/voltage characteristics

Other pre-set adjustments (RV_1 and RV_2) allow the mean charging current to be set in addition to establishing the gain of the amplifying section of the system, and although the main problem is to make the static characteristic of frequency to voltage symmetrical and linear, some care must be also taken to ensure that the gain is suitable if feedback instability is to be avoided. Moreover to prevent the internal oscillator locking to some multiple of the input frequency, the amplifier gain must be further restricted so that its full range of voltage output (corresponding to the sawtooth amplitude of the phase error detector) results in less than a 2 : 1 change in oscillator frequency.

Performance

It is important that the main characteristic (Fig. 5(a)), showing the relationship between the input frequency and the output voltage, should be linear, although its slope changes with differing values of C_2 since the biasing of the circuit is always set to cover the same voltage range for a 2 : 1 change in frequency. However, if the frequency is normalized with respect to the centre frequency corresponding to each value of capacitance, then each of the characteristics becomes identical (Fig. 5(b)).

One of the essential features of the frequency/voltage convertor is that it should be able to detect fast speed-transients in the form of abrupt changes in the pulse period of the grating frequency. In fact the response of the circuit can be assessed in terms of bandwidth expressed as a percentage of the carrier frequency; i.e. the bandwidth of the system depends on the loop gain and the frequency limitations of its constituent parts. For this device, the open loop response (Fig. 6(a)) shows that the integrating effect of the oscillator predominates, although at the higher frequencies a 'fall-off' in response occurs, due mainly to the time-constant inherent in the limited charging current that can flow through the sampler to the holding capacitor. Apparently the fall-off points in Fig. 6(a) occur at a fixed fraction of the carrier frequency for not only does a smaller value of charging capacitor C_2 increase the gain (as can be inferred from the static characteristics) but also the higher sampling frequency produces a proportionate increase in the frequency at which the response falls off. Hence, within limits, the closed loop system having these characteristics has a bandwidth that can be expressed as a fixed percentage of the carrier frequency (Fig. 6(b)) in spite of changing the value of C_2. Normally some adjustment of the loop gain is required to give the system adequate bandwidth within the bounds of stability and the resulting dynamic characteristics for the complete frequency/voltage convertor are shown in Figs. 7(a) and 7(b).

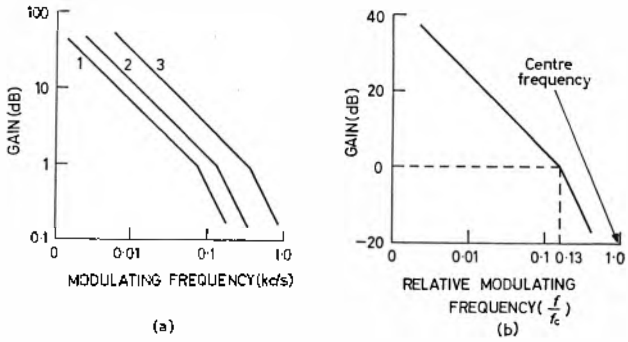

Fig. 6. Approximate open loop frequency response

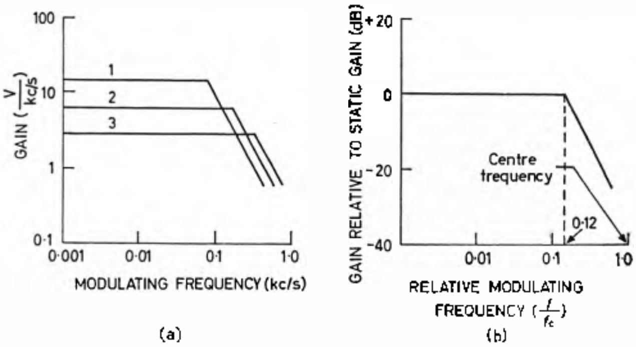

Fig. 7. Approximate closed loop frequency response

Inevitably there are limitations that restrict the overall frequency range. For example, the upper limit to the input frequency is determined by the fixed duration of the sampling pulse from the blocking oscillator, since the waveform from this oscillator must have a small mark-to-space ratio for the sampler to operate correctly. If, however, the pulse length was reduced, the holding capacitor would take longer to charge and the bandwidth would decrease. For low input frequencies, the main limitation is the input impedance to the d.c. amplifier which tends to discharge C_1, and hence at low frequencies the output voltage would show signs of ripple which might mask the signal as noise. In general, there is a limit to the accuracy and sensitivity of the frequency/voltage convertor, since drift in the oscillator and amplifiers, over long time intervals, will produce changes in the output voltage level. In addition, short term accuracy is limited by the noise level inherent in the hold and amplifier circuits, although this might be overcome by suitable filtering at the expense of bandwidth. Thus the requirement of high sensitivity with low noise is not compatible with wide bandwidth.

In general the performance of the circuit shows that although the main components of the system were selected mainly to generate a voltage proportional to the input frequency, yet, fortuitously, subsidiary characteristics have preserved the essential dynamic response of the system even when the charging capacitor C_2 is changed.

Applications

The principal application of the voltage/frequency convertor is the conversion of discrete grating-frequency signals into a direct analogue form which can be recorded or used as a continuous measure of such speed transients as might arise from torque pulsations or transmission errors in the drive to the grating shaft. Fig. 8 shows typical error signals obtained using a 21 600 line radial grating. The calibration marks from a known oscillator frequency enable the amplitude of the signal to be related to the speed of the grating shaft. Usually only direct speed measurement will show fast transients, movements that would otherwise be undetected because of the integrating effect of position transducers. Correspondingly slow transients can be more sensitively measured in terms of position rather than its derivative speed.

The circuit can also usefully function as a frequency demodulator within phase modulated machine-tool control systems in which stabilizing signals in the form of velocity feedback may be needed. Generally tachometric feedback is too noisy at slow traverse speeds on automatic machine-tool drives, whereas velocity signals derived from the phase modulated position measuring system would be an improvement.

Sometimes pulse frequencies derived by digital techniques contain short term changes in phase. The phase-locked oscillator circuit can be adapted to have a sluggish response, such that abrupt phase changes have little effect on the internal oscillator which nevertheless remains locked to the mean input frequency. Thus the internal frequency is a smoothed version of the input frequency and the whole circuit behaves rather like a 'flywheel' oscillator.

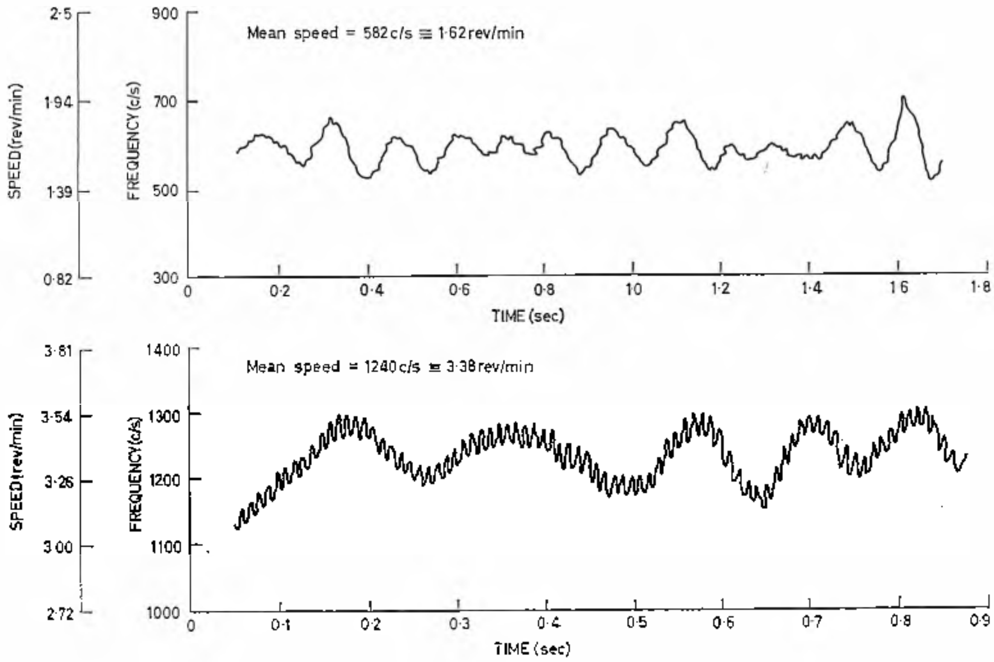

Fig. 8. Typical transient speed records using 21 600 line grating

Acknowledgments

The author wishes to acknowledge the assistance of Mr. D. A. McFarlane in the circuit development and construction of the frequency demodulator. This article is published by permission of the Director of the National Engineering Laboratory, Ministry of Technology. It is crown copyright and is reproduced by permission of the Controller of H.M. Stationery Office.

REFERENCES

1. LESLIE, W. H. P. Widening the Applications of Diffraction Gratings for Measurement and Control. *Int. J. Mach. of Tool Des. Res. 2*, 393 (1962).
2. TIMMS, C., SHARP, R., HUNTER, O. R., EWING, D. K. Performance of the NEL Single-flank Gear Tester. NEL Report No. 227. East Kilbride, Glasgow: National Engineering Laboratory (1966).
3. TOVE, P. A., CZEKAJEWSKI, J. Pulse Period Meter with Short Response Time, Applied to Cardiotachometry. *Electronic Engng. 36*, 290 (1964).
4. JAYAWANT, B. V., REA, D. P. A Tachometer Using Circular Diffraction Gratings. *Electronic Engng. 37*, 297 (1965).
5. Unijunction Transistor Circuits. General Electric Transistor Manual. (General Electric Company, New York, 1960).

The Design and Adjustment of M.F. Broadcasting Aerials

By P. Knight*, B.A., M.I.E.E.

The performance of a medium-frequency anti-fading aerial is critically dependent on the shape of its vertical radiation pattern. Although this pattern depends mainly on the height of the aerial and on its cross-section, it may be modified to some extent if the aerial has a capacitance top or a series-loading inductance. Formulae for calculating vertical radiation patterns of various types of aerials are contained in this article and procedures which may be used for the adjustment of aerials, to enable specified patterns to be obtained, are described.

(Voir page 62 pour le résumé en français: Zusammenfassung in deutscher Sprache auf Seite 69)

THE principles involved in the design of transmitting aerials for medium-frequency (m.f.) broadcasting are well-known and have been described elsewhere[1,2]. They may be summarized by saying that an m.f. aerial should launch a ground wave as efficiently as possible but should radiate a minimum of sky wave, since the latter causes fading and distortion during the hours of darkness. The quality of the service after dark therefore depends to a large extent on the shape of the vertical radiation pattern (v.r.p.) of the aerial. The factors which determine the optimum v.r.p. are discussed by Page and Monteath[1], the purpose of this article being to show how the desired v.r.p. may be achieved.

The principal types of m.f. broadcasting aerial are shown in Fig. 1. The T-aerial (Fig. 1(a)) consists of wires suspended between two masts in the form of a T. In the other two types (Figs. 1(b) and 1(c) the mast or tower itself is the actual aerial.

The almost horizontal wires of a T-aerial do not radiate to any great extent but they do enable the physical height to be less than would otherwise be necessary if a simple vertical wire were used. The height of a mast-radiator may likewise be reduced by adding radial spokes at its highest point; this is known as a capacitance top and is shown in Fig. 2(a). Alternatively the height may be reduced by dividing the mast into two sections separated by an insulator. If a small inductive reactance is connected across the mast break, as shown in Fig. 2(b), a discontinuity is introduced in the current distribution and the v.r.p. is similar to that of a taller unbroken mast. The simultaneous use of a capacitance top and series loading is frequently encountered.

Although mast-radiators are usually base-fed by driving them between their lowest point and earth, when they have an intermediate insulator they are sometimes 'centre-fed' at the break insulator via a transmission line passing through the lower section. This arrangement is shown in Fig. 2(c). The current distribution on the lower section of the mast is controlled by a reactance connecting it to earth, the transmission line being energized through a transformer.

In Fig. 3, current distributions and v.r.p.'s of centre-fed and base-fed masts about 0·5λ high are compared. It will be seen that the current distributions and v.r.p.'s both have deeper minima with centre-feeding and consequently the centre-fed aerial radiates less sky wave. In either case the current distribution may be regarded as the sum of a sinusoidally-distributed primary distribution, and a component in phase quadrature which fills the minimum of the primary distribution; the quadrature component is also responsible for filling the minimum in the v.r.p. In designing anti-fading aerials the most important parameter to control is the position and depth of the v.r.p. minimum. Its position is governed by the primary current distribution and its depth by the quadrature current, which depends on the cross-section of the mast or tower and on the method of feeding. The dimensions of the aerial must therefore be carefully chosen to achieve the correct primary current distribution.

Although the primary current is a sinusoidally-distributed standing wave, its velocity of propagation and therefore its wavelength is slightly less than that of light, by a factor k. The value of k depends on the cross-section of the aerial, approximate values being 0·95 for single wires, 0·90 for mast-radiators and 0·85 for self-supported towers. These figures are generally assumed for design calculations, more accurate values being measured during the setting up of the aerial, when allowance can often be made for any slight differences which arise; this will be discussed later.

In the next section, formulae are given for calculating v.r.p.'s of all types of m.f. aerials from their dimensions. These formulae also enable values to be calculated for break-loading reactances for base-fed masts, and base-

Fig. 1. Types of m.f. aerial
(a) T-aerial (b) Mast radiator (c) Self-supported tower radiator

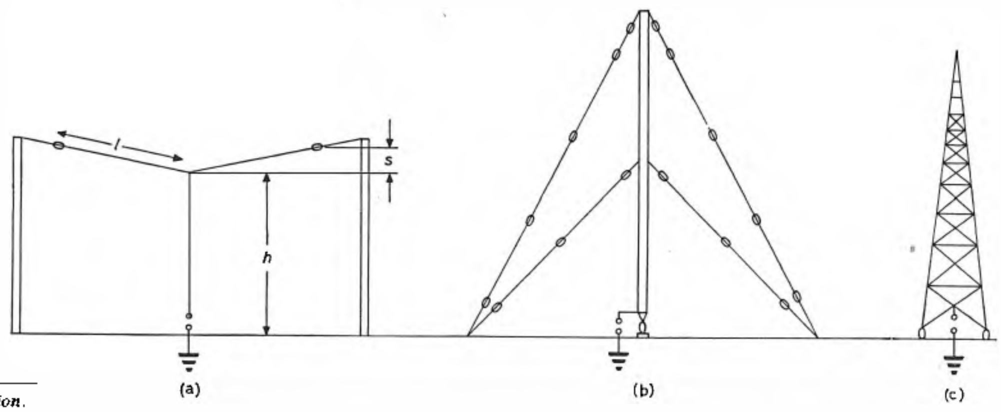

* *The British Broadcasting Corporation.*

terminating reactances for centre-fed masts, required to achieve prescribed v.r.p.'s. Methods are then discussed for adjusting the various types of aerials to obtain a specified v.r.p.

Vertical Radiation Pattern Formulae

Consider a vertical aerial of height h whose current distribution $I(z)$ is a function of z, the distance measured upwards from the ground. Since the main concern here is the position rather than the depth of the v.r.p. minimum, the ground in the vicinity of the aerial will be assumed to be perfectly-conducting; this assumption is justified because the principal effect of imperfect conductivity on high-angle radiation is to fill the v.r.p. minimum without changing its position. The radiation pattern of the aerial is then given by the expression:

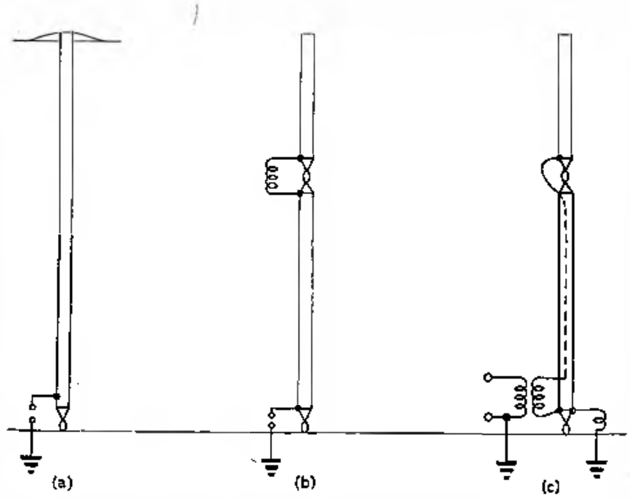

Fig. 2. Types of mast radiator
(a) Mast radiator with capacitance top
(b) Base-fed mast with series loading
(c) Centre-fed mast

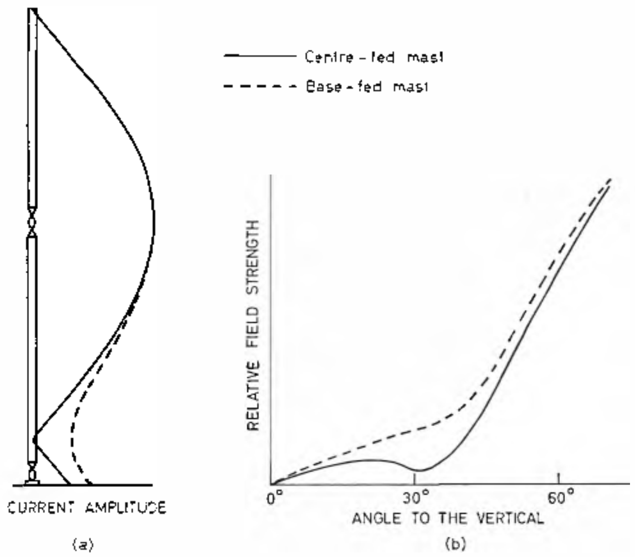

Fig. 3. Comparison of centre-fed and base-fed masts
(a) Current distribution *(b) Vertical radiation pattern*

$$E(\theta) \propto \sin\theta \int_0^h I(z)\cos(\beta z\cos\theta)\,dz \quad \ldots\ldots \quad (1)$$

where θ is the angle to the vertical, $\beta = 2\pi/\lambda$ and λ is the free-space wavelength.

In the sections which follow, solutions of this integral are given for various primary current distributions but, to simplify the expressions, all constants which are independent of θ have been omitted.

Simple Aerial

This is a vertical aerial without a capacitance top or series loading; its primary current distribution is shown in Fig. 4. The angular height of the top of the aerial is denoted by A and is equal to $360h/\lambda$ degrees, where h is the actual height of the aerial and λ the free-space wavelength. It is important to note that all the angular heights are expressed in terms of the free-space wavelength, not the wavelength of the current distribution.

Fig. 4 (right). Primary current distributions of simple aerials
(a) Aerial more than $\lambda/2$ high
(b) Aerial less than $\lambda/4$ high

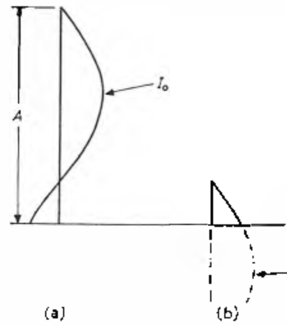

Fig. 5 (below). Radiation patterns of simple vertical aerials due to primary current only, assuming perfectly conducting ground
$v = 0{\cdot}9c$: h = physical height

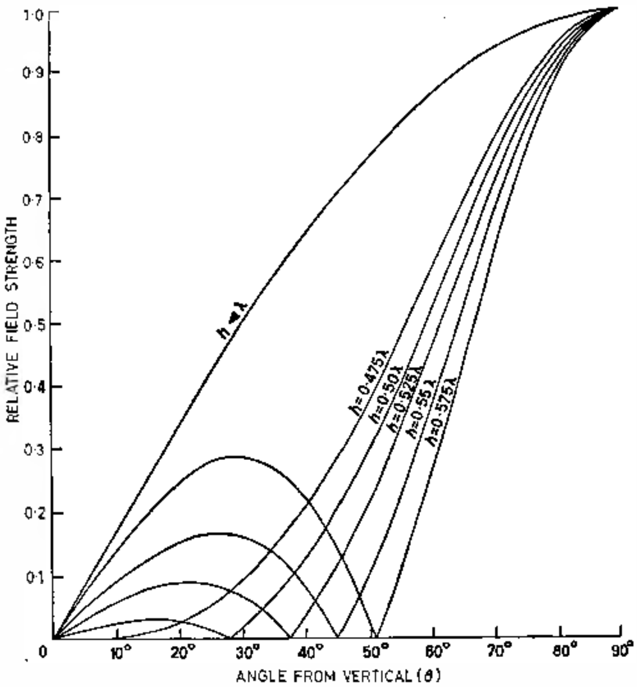

The primary current distribution is:

$$I(z) = I_0 \sin\left(\frac{A - \beta z}{k}\right) \quad \ldots\ldots\ldots\ldots \quad (2)$$

where I_0 is the maximum or 'loop' current, shown in Fig. 4; if the aerial is less than $\lambda/4$ high I_0 is the maximum current which would be attained if the distribution were extrapolated below ground level, as shown in Fig. 4(b).

The solution to equation (1) is:

$$E(\theta) \propto f(\theta)\,[\cos(A\cos\theta) - \cos(A/k)] \quad \ldots\ldots \quad (3)$$

where $f(\theta) = \sin\theta/(1 - k^2\cos^2\theta)$. Fig. 5 shows v.r.p.'s calculated from equation (3) for $k = 0{\cdot}9$. These are, of course, the contributions to the v.r.p. due to the primary current alone. The actual v.r.p.'s are similar but have maxima filled to an extent depending on the cross-sectional dimensions of the aerial, and on the ground conductivity.

A relationship between the height h and the angle of minimum radiation θ_o may be obtained by setting equation (3) to zero, giving:

$$\cos\theta_o = 1/(h/\lambda) - (1/k) \quad \ldots\ldots\ldots\ldots (4)$$

AERIAL WITH CAPACITANCE TOP

This section applies to T-aerials and mast-radiators with capacitance tops. The current distribution is shown in Fig. 6(a) and is given by:

$$I(z) = I_o \sin\left(\frac{B - \beta z}{k}\right) \quad \ldots\ldots\ldots\ldots (5)$$

$$0 < \beta z < D$$

where B is the angular height at which the current would fall to zero if extrapolated and D is the angular height of

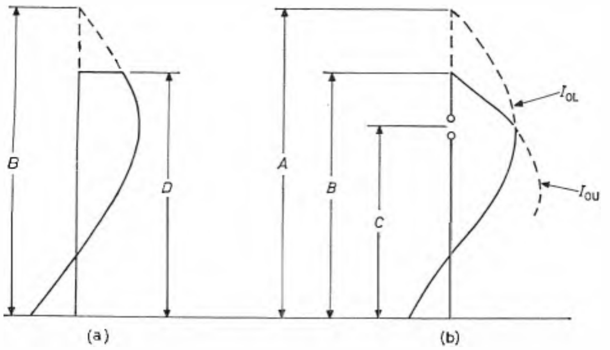

Fig. 6. Primary current distributions
(a) T-aerial or mast radiator with capacitance top
(b) Series loaded or centre-fed mast radiator

the aerial. The expression for the v.r.p. is:

$$E(\theta) \propto f(\theta)\left[\cos\left(\frac{B - D}{k}\right)\cos(D\cos\theta) - k\cos\theta\sin\left(\frac{B - D}{k}\right)\sin(D\cos\theta) - \cos(B/k)\right] \quad \ldots\ldots\ldots\ldots (6)$$

It is not convenient to obtain an expression for the zero radiation angle by setting equation (6) to zero since a transcendental equation results. Values of θ_o are more readily obtained by direct computation of the v.r.p.

Some discussion of the value of the extrapolated height B is called for. Experience with mast-radiators has shown that a capacitance top consisting of six arms joined with wires is equivalent to a section of mast of about three times the length of the arms. Thus $B - D$ may be assumed initially to be three times the radius of the capacitance top; a more precise value may be measured after the mast has been erected, as described later.

In estimating the electrical length of the capacitance top of a T-aerial it is assumed that the characteristic impedance of each horizontal arm is the same as that of the vertical section. The length is then found of a single conductor which has the same reactance as the two horizontal arms in parallel. Thus if l is the length of the individual arms [Fig. 1(a)], the length l' of the equivalent single conductor is given by $\cot\beta l' = \frac{1}{2}\cot\beta l$; this simplifies to $l' = 2l$ when l is small compared with the wavelength. B is taken, therefore, as the angular height corresponding to $h + l'$. In calculating D an allowance must be made for the sag s of the aerial, since currents in the sloping wires contribute to the vertically-polarized rediation. Provided l does not exceed $\lambda/4$, D may be assumed to be the angular height corresponding to $h + s/2$.

SERIES-LOADED AND CENTRE-FED AERIALS

The division of a mast-radiator into two sections enables a discontinuity to be introduced into its current distribution, as shown in Fig. 6(b). The extent of the discontinuity is determined by the loading reactance, but the same primary current distribution may be obtained with either base- or centre-feeding.

In Fig. 6(b), A is the angular height at which the current in the lower section would fall to zero if extrapolated, while B and C are the angular heights of the top of the mast and the break insulator respectively. The currents in the upper and lower sections (I_U and I_L respectively) are:

$$I_U = I_{OU}\sin\left(\frac{B - \beta z}{k}\right) \quad \ldots\ldots\ldots\ldots (7)$$

$$C < \beta z < B$$

$$I_L = I_{OL}\sin\left(\frac{A - \beta z}{k}\right) \quad \ldots\ldots\ldots\ldots (8)$$

$$0 < \beta z < C$$

where I_{OU} and I_{OL} are the maximum or 'loop' currents. At the mast break $I_U = I_L$ and thus:

$$I_{OU}\sin\left(\frac{B - C}{k}\right) = I_{OL}\sin\left(\frac{A - C}{k}\right) \quad \ldots\ldots (9)$$

Equation (9) enables the radiation pattern integral to be expressed in terms of either I_{OU} or I_{OL}; the solution (neglecting constants) is:

$$E(\theta) \propto f(\theta)\left[\sin\left(\frac{A - C}{k}\right)\cos(B\cos\theta) - \sin\left(\frac{A - B}{k}\right)\cos(C\cos\theta) - \cos(A/k)\sin\left(\frac{B - C}{k}\right)\right] \quad \ldots\ldots\ldots\ldots (10)$$

The value of A depends on the break or base loading reactance, which will be denoted by jK_SZ_O for series loading and jK_CZ_O for centre-feeding, where Z_O is the characteristic impedance* of the mast. The relationships between A and K_S and K_C are determined as follows. If the mast is base-fed the current in the lower section is the same as that which would be obtained if the length of the upper section were $A - C$ and the break were short-circuited; the reactance of this upper section would be $-jZ_O\cot((A - C)/k)$ and is equal to the actual reactance terminating the lower section. Since the reactance of the upper section of the mast is in fact $-jZ_O\cot((B - C)/k)$ it follows that the loading reactance must be equal to the difference of the two reactances, i.e.:

$$K_S = \cot\left(\frac{B - C}{k}\right) - \cot\left(\frac{A - C}{k}\right) \quad \ldots\ldots (11)$$

If the mast is centre-fed the base terminating reactance is equivalent to a short-circuited transmission line of the same characteristic impedance as the mast; the length of this line is equal to the distance to the first maximum below ground level of the extrapolated current distribution.

* *The characteristic impedance of an aerial is a slowly-moving function of its height and cross-sectional dimensions. For typical mast-radiators it is approximately 250Ω.*

Therefore:

$$K_C = \tan(270° - (A/k)) = \cot(A/k) \quad .... \quad (12)$$

With a certain amount of manipulation it is possible to eliminate A from equation (10) with the use of either equation (11) or equation (12) and this enables the radiation pattern to be expressed in terms of the loading reactances.

The resulting expressions are:

(a) *For series-loading (base-feeding)*

$$E(\theta) \propto f(\theta)\{\cos(B\cos\theta) - \cos(B/k) - K_S \sin((B-C)/k)[\cos(C\cos\theta) - \cos(C/k)]\} \quad .... \quad (13)$$

(b) *For centre-feeding*

$$E(\theta) \propto f(\theta)\{\cos(C/k)\cos(B\cos\theta) - \cos(B/k)\cos(C\cos\theta) - K_C[\sin(C/k)\cos(B\cos\theta) - \sin(B/k)\cos(C\cos\theta) + \sin((B-C)/k)]\} \quad .... \quad (14)$$

Useful relationships between K_S and K_C and the zero radiation angle θ_o may be derived from equations (13) and (14) by setting $E(\theta)$ to zero.

Series-loaded and Centre-fed Aerials with Capacitance Tops

The current distribution resembles that of Fig. 6(b) but with an additional parameter D specifying the overall height of the mast, as in Fig. 6(a). Equations (11) and (12) still apply and the radiation pattern formulae are as follows:

$$E(\theta) \propto f(\theta)\left\{ \sin\left(\frac{A-C}{k}\right)\left[\cos\left(\frac{B-D}{k}\right)\cos(D\cos\theta) - k\cos\theta\sin\left(\frac{B-D}{k}\right)\sin(D\cos\theta)\right] - \sin\left(\frac{A-B}{k}\right)\cos(C\cos\theta) - \cos(A/k)\sin\left(\frac{B-C}{k}\right)\right\} \quad .... \quad (15)$$

In terms of the loading reactances:

(a) *For series-loading (base-feeding)*

$$E(\theta) \propto f(\theta)\left\{\cos\left(\frac{B-D}{k}\right)\cos(D\cos\theta) - k\cos\theta\sin\left(\frac{B-D}{k}\right)\sin(D\cos\theta) - \cos(B/k) - K_S\sin\left(\frac{B-C}{k}\right)[\cos(C\cos\theta) - \cos(C/k)]\right\} \quad .... \quad (16)$$

(b) *For centre-feeding*

$$E(\theta) \propto f(\theta)\left\{\cos(C/k)\left[\cos\left(\frac{B-D}{k}\right)\cos(D\cos\theta) - k\cos\theta\sin\left(\frac{B-D}{k}\right)\sin(D\cos\theta)\right] - \cos(B/k)\cos(C\cos\theta) - K_C\left[\sin(C/k)\cos\left(\frac{B-D}{k}\right)\cos(D\cos\theta) - k\cos\theta\sin(C/k)\sin\left(\frac{B-D}{k}\right)\sin(D\cos\theta) - \sin(B/k)\cos(C\cos\theta) + \sin\left(\frac{B-C}{k}\right)\right]\right\} \quad .... \quad (17)$$

Relationships between K_S, K_C and θ_o may again be obtained by setting $E(\theta)$ to zero.

The Adjustment of Anti-fading Aerials for the Optimum V.R.P.

The design of an anti-fading aerial must be such that the desired v.r.p. can be achieved with confidence. The aerial dimensions must therefore be carefully chosen before erection, especially when there are no controls available for the fine adjustment of the v.r.p. The provision of adjustments is desirable because exact values of some of the design parameters, such as velocity factor, can only be determined after the aerial has been built, unless they are measured with models. Adjustments also allow an aerial to be re-aligned for optimum performance in the event of a small change of frequency allocation.

T-Aerials

The majority of T-aerials are less than $\lambda/4$ high and do not have anti-fading properties; at m.f. they are used mainly for low-power installations, where the service area is limited by ground-wave attenuation rather than fading. Their v.r.p.'s approximate closely to $\sin\theta$ and are almost independent of their dimensions, which are determined mainly by cost and radiation efficiency.

T-aerials more than $\lambda/4$ high are occasionally used as anti-fading aerials, although they are unlikely to be high enough for the optimum v.r.p. to be achieved. The v.r.p. is therefore not critically dependent on the velocity factor, which may be assumed to lie between 0·90 and 0·95, depending on whether the down lead consists of a cage of wires or simply a single wire. There is no convenient way of measuring the velocity factor.

There is no reason why a T-aerial of optimum height should not be built but the cost of the two tall masts supporting it would undoubtedly be greater than that of a single mast-radiator of equivalent height.

Mast-radiators of Uniform Cross-section

For the design calculations the velocity factor of a mast-radiator is usually assumed to be 0·90. A more precise value may be measured after the mast has been erected; this enables the v.r.p. to be calculated more accurately and to be correctly adjusted if controls have been provided.

The measured velocity factor is deduced from the impedance-frequency characteristic of the mast, measured at the lead-out insulator at the aerial tuning house over a frequency range of about two octaves. For this measurement the mast is arranged as a simple base-fed aerial; the capacitance top is therefore lowered and the break insulator (if any) shorted out with a non-inductive connexion.* If the mast is intended for centre feeding the base-loading reactance is temporarily disconnected.

The equivalent circuit of the mast, seen from the bridge terminals, is shown in Fig. 7; here Z represents the impedance of the aerial itself, C the stray capacitance of the base insulator, mast lighting transformers etc., and L the inductance of the lead between the bridge and the base of the mast. To determine k it is necessary to measure Z as accurately as possible.

The value of L is found by measuring the reactance obtained when the base of the mast is connected to the earth system with a non-inductive connexion. It is then a simple matter to calculate the impedance of the parallel combination of Z and C from the bridge measurements.

Fig. 8 shows a typical impedance-frequency characteristic corrected for lead reactance. It will be seen that

* *The inductance may be minimized by bridging the insulator with three or four wide strips of copper foil, spaced around its perimeter.*

the reactance curve crosses the axis at frequencies f_1, f_2 and f_3; if C were zero these three frequencies would be multiples of f_1 and would correspond to the $\lambda/4$, $\lambda/2$ and $3\lambda/4$ mast resonances respectively. Now at f_1 the reactance of C is large compared with Z and consequently f_1 does not differ greatly from the true $\lambda/4$ resonance frequency. It may, therefore, by assumed that the true $\lambda/2$ resonance frequency is approximately equal to $2f_1$; this is somewhat greater than f_2. Since Z is a pure resistance at the $\lambda/2$ resonance frequency, the reactance component at $2f_1$ is due only to C, which can therefore be calculated by converting the measured impedance to parallel form. Knowing C, it is then possible to calculate the value of Z and so find the true $\lambda/4$ and $3\lambda/4$ resonance frequencies; values of k may then be calculated from the relationships $k=4h/\lambda_1$ and $k=4h/3\lambda_3$ where λ_1 and λ_3 are the free-space wavelengths at the true $\lambda/4$ and $3\lambda/4$ resonance frequencies respectively. The two values of k should be approximately equal.

If the aerial has a capacitance top its effective height

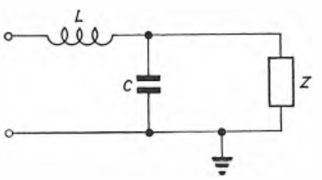

Fig. 7 (right). Equivalent circuit of a mast radiator

Fig. 8 (below). Impedance-frequency characteristic of a mast radiator

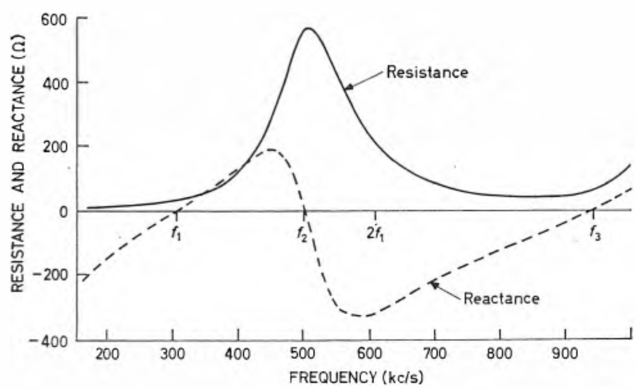

may be found by repeating the previous measurement with the capacitance arms extended. The increase in height Δh due to the capacitance top is equal to $0{\cdot}25k\Delta\lambda_1$ where $\Delta\lambda_1$ is the increase in the free-space wavelength corresponding to the reduction in the $\lambda/4$ resonance frequency. The value of Δh is used to calculate $B-D$ (Fig. 6).

If the aerial has no break insulator equation (6) is used to calculate the v.r.p. and θ_o, and to decide whether the capacitance top should be extended fully or only partially. If the mast has a break insulator, however, the loading reactance must now be adjusted to obtain the desired v.r.p.

The most reliable way of performing this adjustment is to measure the actual current distribution on the lower part of the mast, since the position of the current minimum provides a sensitive indication of the zero radiation angle*. Although the relationship between θ_o and the height of the current minimum is the same whether the mast is base- or centre-fed, it is easier to calculate if the mast is assumed to be base-fed. K_S is first calculated for the required value of θ_o from equation (13) or (16). The value of A is then calculated from equation (11) and the position of the current minimum, whose angular height in degrees is equal to A-$180k$, is finally determined.

A convenient way of measuring the current distribution is to energize the mast at the operating frequency with a power of about 10W, care being taken to provide a d.c. path to earth to prevent a build-up of static charge. A portable loop aerial is clamped at various heights to one of the corner members of the mast; the loop is held outside the mast in a vertical plane so that it couples with the magnetic field due to the current flowing in the corner member. A convenient size of loop is about 30cm square, screened and containing about 15 turns. It is tuned with a capacitor and connected to a detector, the d.c. output being fed through a short screened lead to a micro-ammeter.

Self-supported Towers and Mast-radiators of Non-uniform Cross-section

The v.r.p. of a self-supported tower, or of a mast-radiator of non-uniform cross-section, is more difficult to predict because its velocity factor varies along its length. For self-supported towers k may be assumed to be equal to 0·85, while for non-uniform mast-radiators the value of 0·90 may again be used; these figures, however, can only be regarded as guides in the initial design calculations. The most satisfactory way of determining the v.r.p. of this type of aerial with any degree of certainty is to model it together with its image in the ground, using the technique described by Page and Monteath[1]. This enables the position of the v.r.p. minimum to be found, and also the extent to which it would be filled if the ground were a perfect conductor. A further advantage is that the power gain or E_od_o of the aerial* may be found by integrating its power radiation pattern.

The v.r.p. of a self-supported tower may be adjusted with a capacitance top or by adding a light tubular extension, model measurements again providing the most satisfactory method of determining the resulting v.r.p. The use of series loading is generally considered to be impracticable.

Conclusions

Although the vertical radiation patterns of T-aerials and mast-radiators of uniform cross-section may be calculated with reasonable accuracy from their dimensions, this is not true of self-supported towers and non-uniform mast-radiators, whose v.r.p.'s are more accurately determined with models. The adjustment of self-supported towers should also be based on model measurements, but this method should not be used for inductively-loaded mast-radiators because loading inductances cannot be modelled accurately. The most reliable way of adjusting an anti-fading mast-radiator of uniform cross-section is to measure the current distribution on its lower part and to adjust it until it agrees with the theoretical distribution which gives the required v.r.p.

Acknowledgment

The author is indebted to the Director of Engineering of the British Broadcasting Corporation for permission to publish this article.

REFERENCES

1. Page, H., Monteath, G. D. The Vertical Radiation Patterns of Medium-wave Broadcasting Aerials. *Proc. Instn. Elect. Engrs. 102B*, 279 (1955).
2. Ballantine, S. High Quality Radio Broadcast Transmission and Reception. *Proc. Inst. Radio Engrs. 22*, 564 (1934).

* *On a typical mast-radiator operating at 647kHz, a 35m shift of the current minimum corresponded to a 20° change in θ_o.*

* *The E_od_o of an aerial is the product of the distance and the ground-wave field strength which would be measured if the earth were a perfect conductor, when 1kW is radiated. It is a measure of the overall efficiency of the aerial as a ground-wave radiator.*

A Simple High-Speed Analogue Multiplier

By J. P. Wilson*, B.Sc., Ph.D.

The analogue multiplier described is based on the non-linearity of valve characteristics. The accuracy of multiplication is 2 per cent with a long term drift of 1 per cent. The frequency range covered depends on the details of the circuit chosen and may extend from d.c. to a maximum of 2MHz. A number of input and output circuits are discussed which enable the multiplier to be used for computation, modulation, instantaneous power measurement, correlation and the accurate control of amplitude or envelope of auditory frequency signals.

(Voir page 62 pour le résumé en français: Zusammenfassung in deutscher Sprache auf Seite 69)

An analogue multiplier, in addition to performing a basic operation in analogue computation, has important applications as a phase sensitive detector, correlator, wide band power meter and modulator. Adequate performance in terms of accuracy, stability and wide bandwidth, is difficult to achieve and usually involves special units of complex construction and adjustment. The design proposed here can satisfy these requirements to an accuracy of 2 per cent and is suitable for use in the above applications.

The circuit to be described is essentially a development of a multiplier using two short suppressor base pentodes in which the x signals are fed in antiphase to the control grids and the y signals in antiphase to the suppressor grids; the product appearing in the anode output[1]. The replacement of each pentode by three triodes has two important advantages: for a given percentage error a very much greater proportion of the dynamic range can be used bringing the effects of drift down to a very low level and the circuit becomes self-balancing eliminating the need for push-pull inputs. These advantages have not been fully exploited in two circuits of a somewhat similar configuration for a modulator[2] and a phase sensitive detector[3] respectively.

Principle of Operation

The non-linearity of certain double triodes is such that the difference between the anode currents is proportional to both the voltage difference between their grids and the total current flowing through the strapped cathodes when the anode voltages are held constant.

Thus in Fig. 1:

$$i_1 - i_2 = a\,(i_1 + i_2)\,x = a\,i_0\,x \quad \ldots\ldots\ldots\ldots\ldots (1)$$

$$\therefore\ i_1 = i_0/2\,(1 + ax) \text{ and } i_2 = i_0/2\,(1 - ax) \quad \ldots\ldots (2)$$

By making these anode output currents the cathode supplies for two more double triodes and cross combining their outputs it is possible to obtain currents which depend only on the product of the grid input voltages, x and y.

Thus:

$$i_3 = i_1/2\,(1 + by) \text{ and } i_5 = i_2/2\,(1 - by) \quad \ldots\ldots\ldots (3)$$

substituting i_1 and i_2:

$$i_3 = i_0/4\,(1+ax)\,(1+by) = i_0/4\,(1+ax+by+abxy) \quad \ldots\ldots\ldots\ldots (4)$$

and:

$$i_5 = i_0/4\,(1-ax)\,(1-by) = i_0/4\,(1-ax-by+abxy) \quad \ldots\ldots\ldots\ldots (5)$$

$\therefore$ adding $i_3 + i_5 = i_0/2\,(1 + abxy) = i_7$

similarly:

$$i_2 + i_4 = i_0/2(1-abxy) = i_8$$

* *University of Keele.*

As i_0, a and b are constants both outputs depend only on the product of the two inputs. Taking the difference between the outputs eliminates a constant term but this normally has no practical advantage:

$$i_7 - i_8 = i_0\,abxy$$

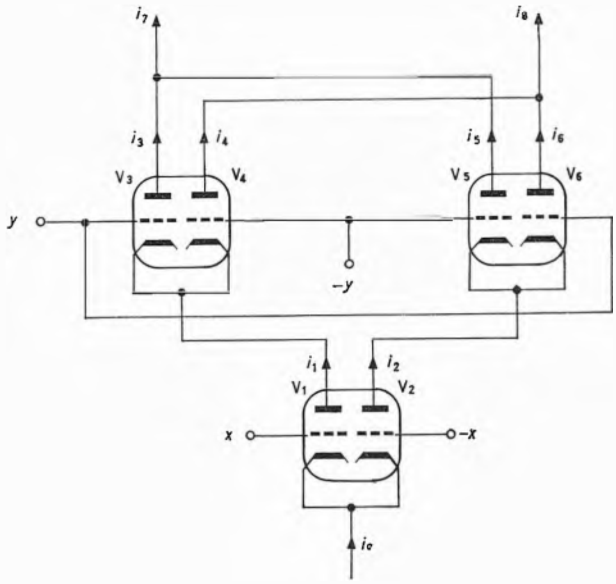

Fig. 1. Basic amplifier circuit

In practice this theory is not quite accurate as there are other much smaller terms present giving slightly curved forms to plots of i_3, i_4, i_5 and i_6 against x or y which fortunately cancel out when i_3 and i_5 and i_2 and i_4 are combined in the output. Although most triodes have an approximate square law characteristic, analysis of the circuit on this basis does not lead to an adequate solution.

The requirement for reasonably constant anode-cathode potentials has the fortunate advantage of eliminating Miller capacitance and is one of the reasons for the excellent high frequency response of the circuit. Normally triodes give linear amplification by virtue of the voltage feedback developed in the load and applied to the anode: in this circuit the linear amplification of the x and y inputs inherent in equations (2) and (3) is accomplished because even order terms which are in phase at the cathodes are degenerated by the large cathode load whereas the differential components of the input signals are not. As mentioned in the introduction it is unnecessary to provide anti-phase input signals because the cathode loads, whether resistance or anode impedance, are sufficiently high to provide adequate balance with the second grid grounded. (Some computer circuits, in fact, might take advantage of the second grid to perform a subtraction before multiplication). Normally small d.c. correcting voltages are applied to these grids in order to balance the circuit.

Practical Circuit Considerations

As already stated the output of the multiplier, i_7 and i_8 is in the form of a variation on a standing current. For display on a milliammeter or low impedance recorder it would be convenient to connect one side of the instrument to anodes 3 and 5, and the other side to anodes 2 and 4, with the appropriate current supplied by two equal resistors large compared with the instrument impedance. The low impedance of the meter would ensure that the anode voltages remained within a few volts of nominal during operation whatever the value of current supply resistors.

If a potential output of more than a few volts is required it is desirable to add a pair of grounded grid triodes in a cascode arrangement as shown in the circuit diagram (Fig. 2). The signal output voltage is then proportional to the load resistance and can be considerably greater than the operating input voltages so that a potential divider and cathode-follower could be added to bring the d.c. level to zero without losing stability.

If the product of more than two variables is required it is possible to obtain this without repeating the complete multiplier. Additional decks of the type $V_{3,4,5,6}$ may be inserted with i_7 and i_8 becoming the current sources for the stage above.

Either a.c. or d.c. coupling can be provided for the signal inputs. If d.c. operation of the x input is not needed however a.c. coupling as shown in Fig. 2 is preferable as it does not require accurately matched resistors, it operates at much higher frequencies without capacitive correction and has a higher sensitivity and input impedance. The d.c. input circuit shown in Fig. 3 is capable of operation up to 50kHz without correction and suffers no appreciable loss in stability when constructed with matched metal oxide resistors mounted close together. The need for a low d.c. source resistance can be relaxed somewhat by providing a bleeder resistance to V_4.

A number of different types of double triode have been tested in this circuit but the consumer types failed either because of drawing grid current at the necessarily low h.t. voltages used or because accurate multiplication could not be obtained. Two valve types were found to be satisfactory. Type E180CC is particularly linear and operates at a low current level and would be preferred for most applications. Type ECC88 has a very low impedance at high current and would be preferred for high frequency applications.

For the setting up of the circuit, testing of valve types, and the balancing procedure, extensive use was made of the 'bow-tie' input-output plot. In this each input in turn is fed to the X plates of an oscilloscope while the output is fed to the Y plates. The two inputs must be independent and have repetitive peak values symmetrical about zero (sine wave being the obvious choice).

Desirable features for the plot include identical positive and negative peak heights on the Y axis indicating equal gain in the four quadrants of operation: straight edges indicating linear output against the relevant input and a well defined central node indicating absence of phase shift and unwanted output components. Such a plot is of course limited in accuracy by the linearity of the oscilloscope. Examples of performance are shown in Fig. 4; (a) is typical of the circuit given while (b) shows how the linearity is degraded by the introducing of loading resistances into the anodes

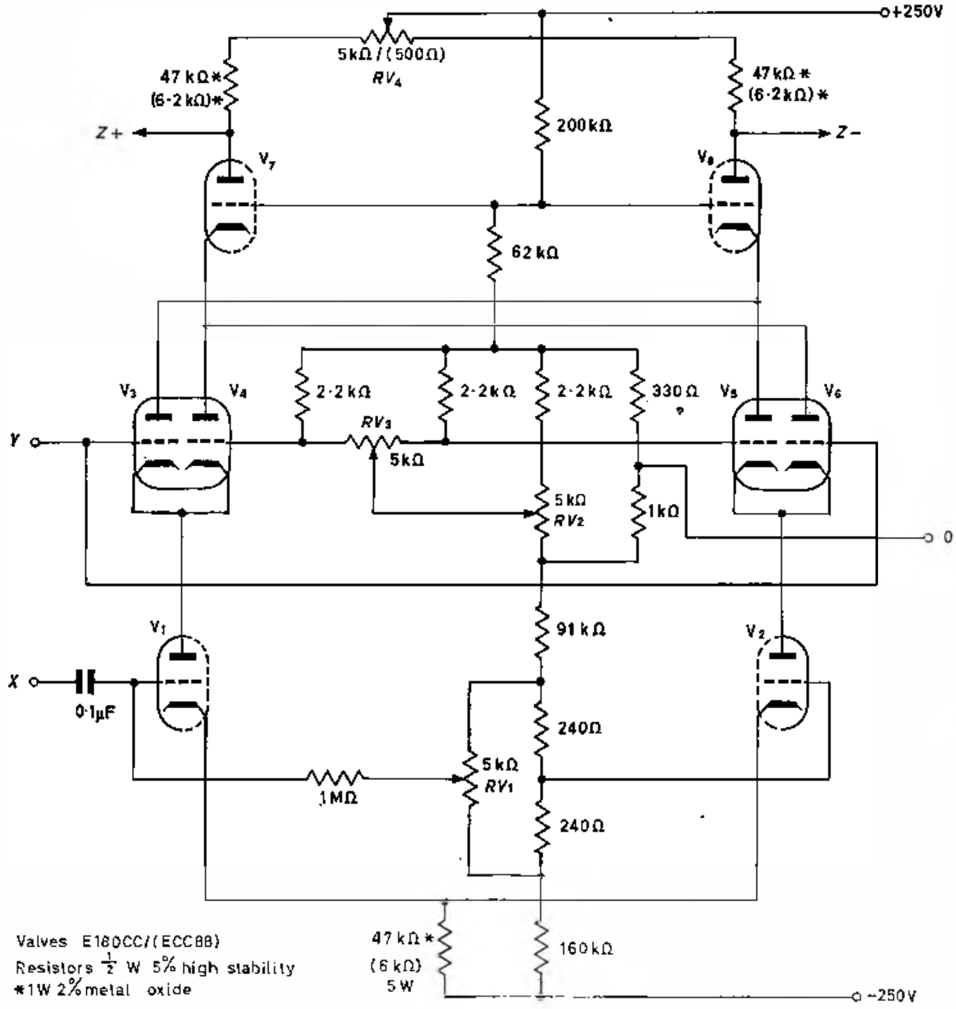

Fig. 2 (left). Complete multiplier circuit

Fig. 3 (below). D.C. x input circuit

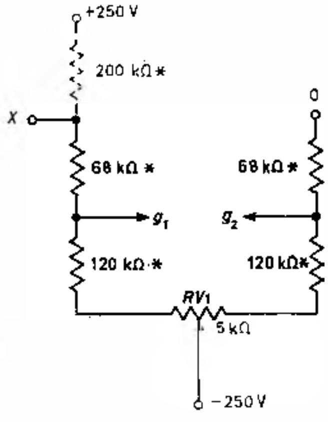

so that their voltages are no longer constant. A poor plot similar to this was obtained in a transistor version using type OC71; also for certain other valve types.

The complete circuit in Fig. 2 shows circuit values suitable for ±250V and type E180CC valves with values for the ECC88 type in brackets. 90V has been allowed across the valves taking the heavier current and 60V across the others: this is sufficient to avoid grid current or unbalance of the circuit when overloaded. Once the voltage levels have been set, the overall current is determined by the common cathode resistance, R. The optimum value in both cases was obtained by varying R and noting which value gave the best 'bow-tie' figure.

Fig. 4. Examples of performance
(a) Typical of circuit given
(b) Degradation due to loading resistors in anode circuits

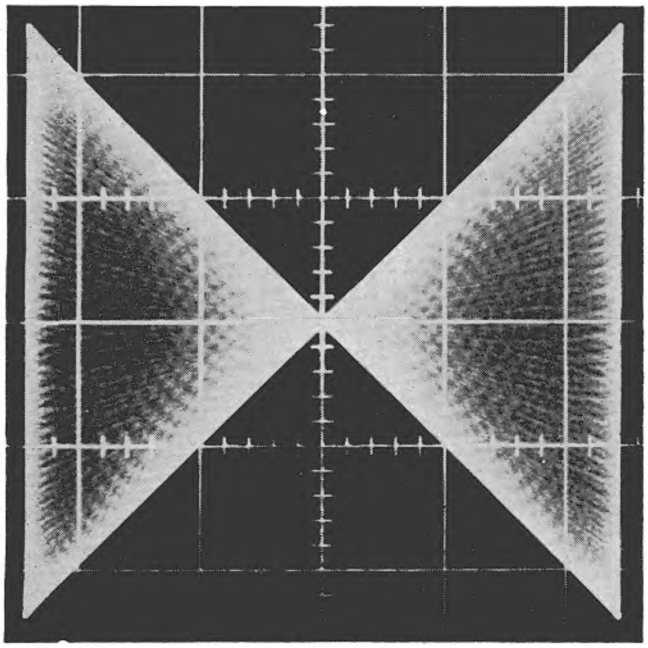

(a)

(b)

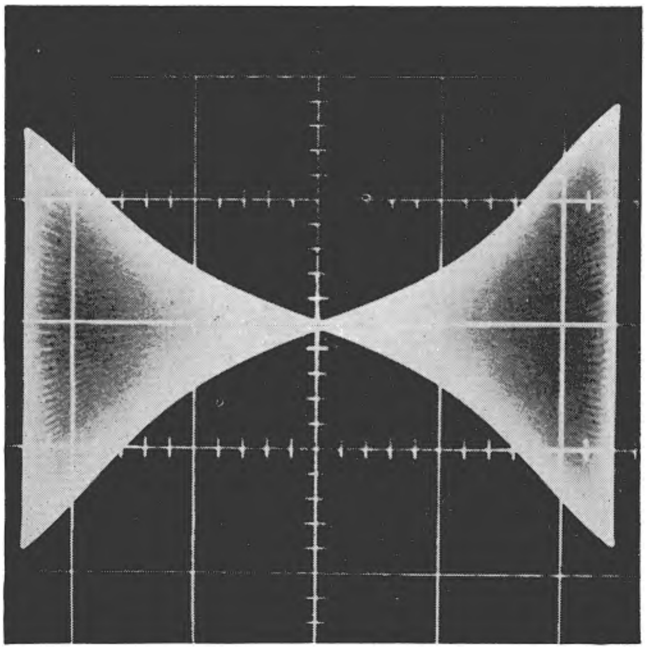

The balancing procedure is straightforward and rapid when performed in the following sequence. With the X input grounded and a sine wave of about 1V peak-to-peak on Y, adjust RV_1 for minimum signal output (a horizontal line on the input/output plot eliminating the fundamental of the y signal); then adjust RV_3 for a minimum of the second harmonic of the y signal in the output (minimum curvature of the input/output plot). Next with the sine wave applied to X, and Y grounded, adjust RV_2 for a minimum of x in the output (horizontal input/output plot). It may be necessary to repeat these steps after the initial adjustment as the controls RV_2 and RV_3 are slightly interdependent. RV_4 can be used either to eliminate any d.c. difference between the $Z+$ and $Z-$ outputs or to get exact balance of the differential signal outputs. For many applications it may be omitted. In general the balance point of RV_2 will not be quite the same for the two outputs so that final adjustment should be made using the appropriate output. In a properly balanced circuit the unwanted output with one of the inputs zero is generally $\frac{1}{4}$ to $\frac{1}{2}$ per cent of the maximum output.

Assessment of Performance

It is difficult to express the overall performance of a multiplier as there are a number of possible shortcomings and an improvement in one direction may lead to a deterioration in another. In the author's case a.c. output and one d.c. input only were required with a minimum of spurious frequency components rather than high arithmetical accuracy. Using two sine-wave inputs there are three types of component in the output: the required one consisting of the sum and difference frequencies; unwanted frequencies which can be cancelled out by the balancing procedure comprising the input frequencies and the second harmonic of the y input, and thirdly components which cannot be cancelled out, the remaining harmonics of the input frequencies and the harmonics of the sum and difference frequencies. The predominant unwanted components at the nominal operating levels are the third harmonics of the input signals.

The performance as a multiplier was determined using the 'bow-tie' plot as described above. Inputs and outputs were reversed and differences taken in order to cancel out non-linearities in the cathode-ray tube. The peak values in the four quadrants were within 2 per cent. D.C. drift of the anode voltages with constant input signals is less than 1 per cent of the peak output over several

TABLE 1
Performance

PERFORMANCE	INPUTS			OUTPUT	
	X		Y	Z (single ended)	
	A.C.	D.C.	D.C.	E180CC	ECC88
(a) 1% multiplication accuracy	±0·5V	±0·8V	±0·8V	±16V	±5V
(b) Spurious frequency components reach 1% of total output	±1·0V	±1·6V	±1·0V	±40V	±12V
(c) Overload voltages for maximum possible output	±2V	±3V	±2V	±80V	—

days of operation and is unimportant for a.c. output A.C. drift, or wandering of the balance points, is undesirable in all applications. With a maximal signal in one input and a zero signal in the other the unwanted output remains less than 1 per cent of the peak output over a period of a few days. Drift may also occur as a result of heater supply variations; but as this amounts to less than 2 per cent for a 10 per cent change in supply voltage it is normally negligible. H.T. variations of about 10 per cent also have little effect on the balance: the change in gain involved is +1 per cent for the E180CC and −7 per cent for the ECC88 and indicates that for the E180CC circuit at least, stabilization should not be necessary. Poor valveholder contacts for the heater pins can, however, lead to considerable instability and this should be checked during the balancing procedure by moving each valve in turn and any doubtful valveholder replaced. The possibility could be eliminated by series heater connexion.

The upper frequency limit at which additional errors due to valve and circuit capacitances reach 2 per cent, is about 2MHz for the a.c. coupled ECC88 circuit when the source impedances are low. It is not possible to correct the d.c. version to this frequency without providing balanced y inputs because of the capacitive coupling to the x input grid from the unbalanced y signal present at the first anode. The upper limit for the E180CC version is probably in the region of 250kHz.

Applications

The unit can be used in a number of applications where accuracy of the highest order is not required. In addition to analogue multiplication and double sideband modulation it can be used in phase sensitive detectors, correlation circuits, instantaneous power measurement from d.c. to h.f., or for an electronic signal controller in which the amplitude of a signal can be varied according to some function applied to the other input. Two of these units have now been in operation for several months in an audio frequency shifter employing the phasing method of single sideband modulation and are proving entirely satisfactory.

Acknowledgements

Grateful acknowledgement is made to Mr. R. R. Glover for assistance in devising this circuit and comments on the article and to the S.R.C. for financial support in this work.

REFERENCES

1. MACKAY, D. M., FISHER, M. E. Analogue Computing at Ultra High Speed, p. 57. (Chapman & Hall, London, 1962).
2. DE BOER, E. On the "Residue" in Hearing, pp. 95-7. (Ph.D. Thesis, University of Amsterdam, 1956).
3. FAULKNER, E. A., STANNETT, R. H. O. A General Purpose Phase-Sensitive Detector. *Electronic Engng.* *36*, 159 (1964).

A Wide Frequency Range Voltage Controlled Multivibrator *

By R. J. P. Jones, B.Sc.

A multivibrator is described which has a voltage controlled frequency range continuously variable over at least ten octaves (1 000:1). In its simplest form the frequency and mark-to-space ratio are sensitive to small changes in transistor characteristics and component values. A stabilizing circuit is used to overcome these deficiencies and also linearize the frequency versus control voltage relationship.

(Voir page 63 pour le résumé en français: Zusammenfassung in deutscher Sprache auf Seite 69)

THE basic circuit is shown in Fig. 1. The transistors VT_1 and VT_2 correspond to those used in a conventional multivibrator; VT_3 and VT_4 are emitter-followers (these have a function other than lowering the output impedance); VT_5 and VT_6 provide a constant charging current for the timing capacitors C_1 and C_2. At low frequencies operation is the same as in a conventional multivibrator except that the charging rate of the capacitors is constant instead of exponential (Fig. 2(a)). At high frequencies the voltages dropped across R_3 and R_4 due to the high charging currents, reduces the amplitude of the voltage changes across the capacitors. This combination of high charging current and low voltage change produces a high maximum frequency (Fig. 2(b)).

A simple analysis gives the following approximate relationship for a symmetrical circuit:

$$2CR_e \, . \, f = \frac{(I_c \, . \, R_e)/V_s}{1 - (I_c \, . \, R_e)/V_s}$$

where C is the timing capacitor (F)

R_e is the emitter resistor value (Ω)

f is the repetition frequency (Hz)

I_c is the charging current of the timing capacitors (A)

V_s is the supply voltage.

Stabilizing Circuit (Fig. 3)

The long-tailed-pair VT_7 and VT_8 is driven from the two anti-phase multivibrator outputs C and D after smoothing via R_7, R_8, C_3 and C_4. The outputs of the

Fig. 1. The basic circuit

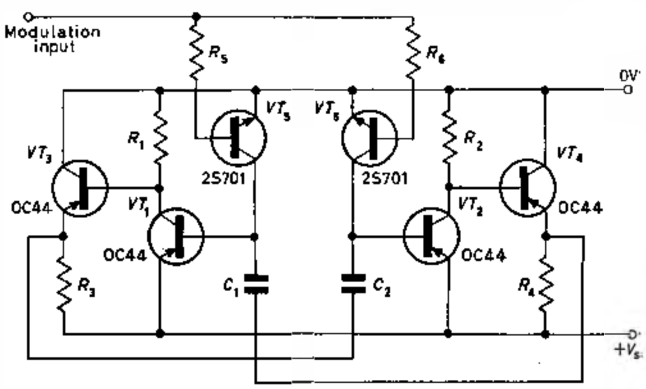

* *U.K. Patent Appl. 50768/65.*

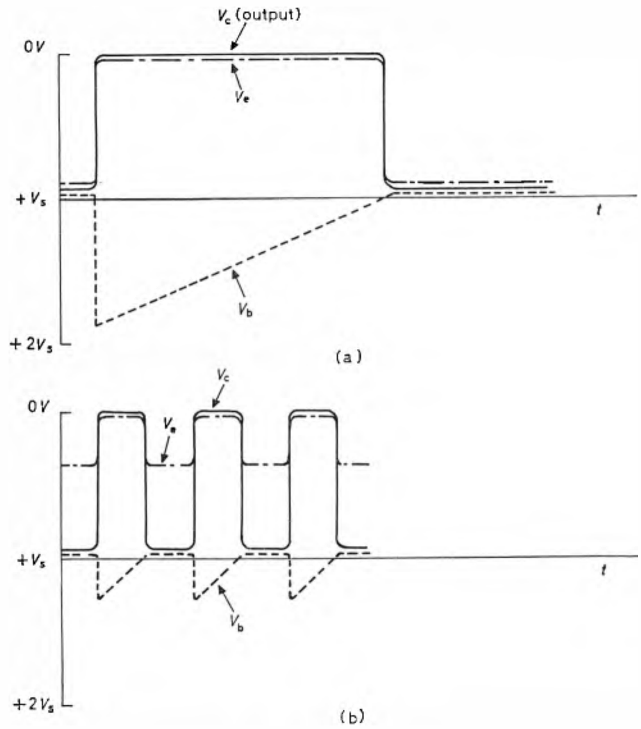

Fig. 2. Multivibrator voltage waveforms
(a) Low frequency *(b) High Frequency*

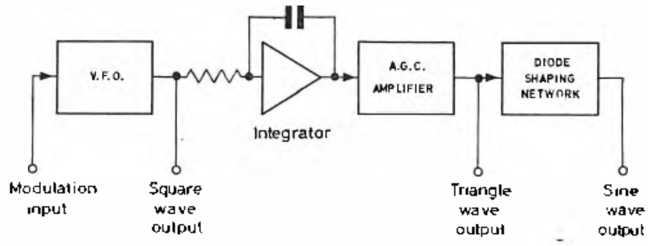

Fig. 4. Square/triangle/sine wave oscillator

is biased slightly more positive than E and provides a feedback current directly proportional to frequency. This current may be offset at E (which is a summing junction) by a positive controlling voltage at F. The linearity of the control voltage versus frequency characteristic depends on the quality of the summing junction E. Improvements in quality could be made by optimizing the existing circuit and employing further stages of amplification.

The frequency stability of the prototype multivibrator is 30 times better at 10kHz with the circuit in Fig. 3 than the unstabilized circuit in Fig. 1. The frequency range is 20Hz to 35kHz (1 750:1).

The response of frequency to a step control voltage input is necessarily worsened by stabilizing circuits of the type described, but improvements can be made to meet any specification by operating the multivibrator at a higher frequency and dividing down for the output.

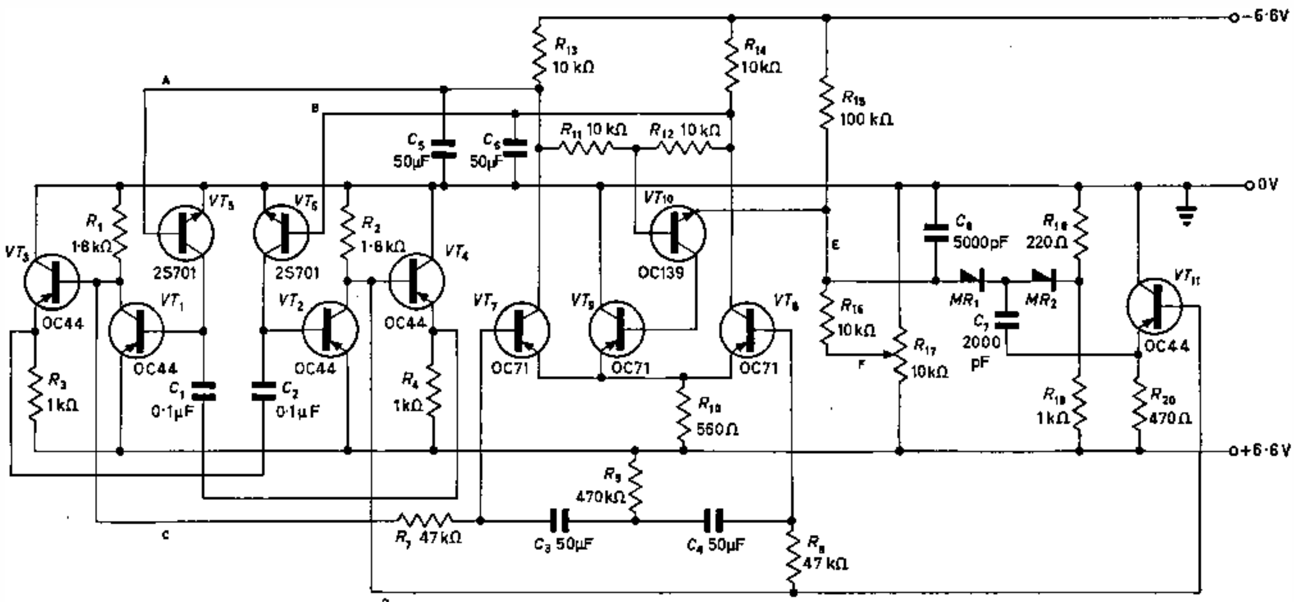

Fig. 3. Stabilizing circuit

long-tailed-pair are fed back to the multivibrator via the bases of VT_5 and VT_6 thereby forming a closed loop. An improvement in mark-to-space ratio stability of about 100 times is obtained by using this circuit.

The addition of VT_9, VT_{10}, R_{11} and R_{12} in the above circuit enables the long-tail-pair transistors to act in unison to feed in the frequency controlling signal. Study of the loop VT_{10}, VT_9, VT_7, VT_8 will show that the average of the voltages at A and B will follow the voltage at E, and that there is current gain from E through to AB. The emitter-follower driven ratemeter circuit MR_1, MR_2, C_7, C_8

Applications

Applications of the circuit include:

(1) Audio frequency oscillator with square/triangle/sine wave output (see Fig. 4).

(2) Automatic frequency response testing.

(3) Speech synthesis and electronic music.

(4) Synchronous motor or stepping motor speed controller for digital servo systems and tape recorders.

(5) Analogue to digital conversion.

A Dual Channel Stimulator

By J. W. Hinshelwood* and A. G. Seabridge*

A dual output rectangular pulse generator is described. The generator has been designed for physiological purposes; the two channels have a common frequency control but the amplitude and width of each is independently variable. The maximum output amplitude is 50V. It is suitable for stimulation by two routes, i.e., directly and transneurally.

(Voir page 63 pour le résumé en français: Zusammenfassung in deutscher Sprache auf Seite 70)

A TWO channel pulse generator with a frequency range of 0·05 to 10 pulses per second has been developed for physiological purposes. Both channels have a common frequency control, but each output is independently variable in respect of pulse width and amplitude. The pulse amplitude control is incorporated in the output stage in such a way as to present a constant output impedance at approximately 5Ω.

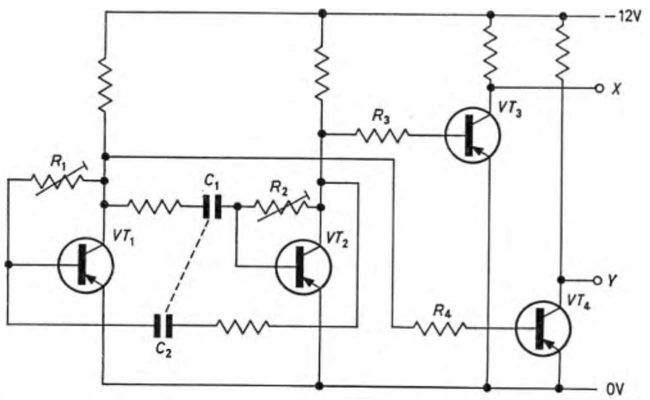

Fig. 1. Oscillator circuit

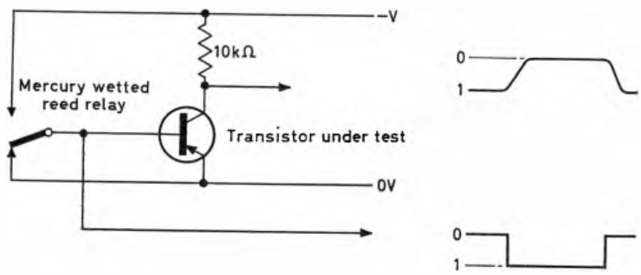

Fig. 2. Transistor matching test circuit

Pulse Repetitive Frequency

Pulses are initiated by a dual output multivibrator with outputs 180° out of phase. These outputs are capacitively coupled to generate a differentiated waveform and the positive going spikes are fed on to the collectors of the monostable transistors; the negative going spikes may be disregarded as they will serve only to further turn off the monostable. The circuit is shown in Fig. 1; for values of components see Fig. 8.

The mark-to-space ratio of the oscillator must be 1 : 1 at all frequencies so that at the final stage each pulse will begin exactly half way through the cycle of its opposite channel c.f. Fig. 4. Fine adjustments of this ratio may be made by means of resistors R_1 and R_2, and the rate may then be controlled in steps by switching capacitors C_1 and C_2 without altering the ratio since the timing resistors are fixed. The inconvenience of only being able to control rates in steps may be reduced by using plug-in timing capacitor cards or a remote programming unit so that ranges may be chosen to suit a specific purpose†.

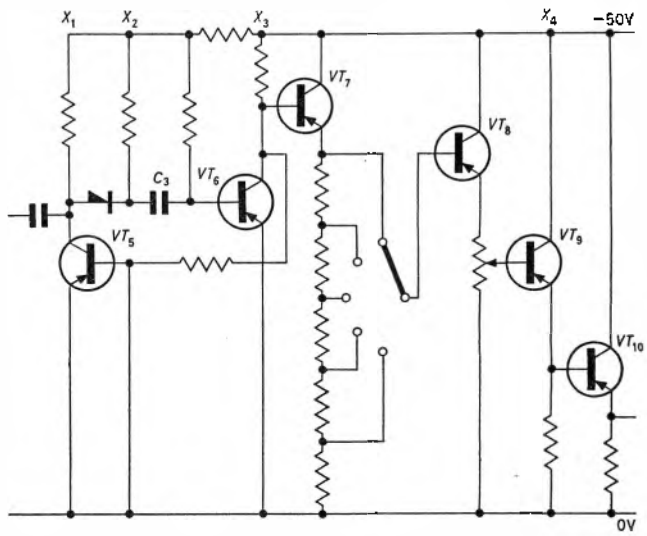

Fig. 3. Width and power stage circuit

To obtain square pulses with fast falling phase of about 10μsec that can be transmitted by the decoupling capacitors, the transistors VT_3 and VT_4 (Fig. 1), are incorporated in the circuit as shaping devices. By adjustment of R_3 and R_4 the rise and fall times can be reduced to a minimum value, which will be the average switching time of the transistors used. To ensure that the oscillator transistors have identical rise and fall phases they must be matched. This may easily be done by inserting them in the test circuit shown in Fig. 2. A negative potential is applied to the base of the transistor and the time taken for the circuit to change states is recorded.

Width

The width circuit is simply a monostable which is triggered by the output from C_3 and C_4.

The positive going spike from the oscillator is applied to the collector of VT_5. This turns the transistor 'on', so that it saturates and at the same time turns VT_6 'off', thus producing a voltage output. The length of time the circuit stays in this state is determined by the capacitor C_3.

The oscillator is decoupled from the monostable to limit the initiating pulses as much as possible. If this width was allowed to be longer than the pulse width required

* *University College, London.*

† *Frequency and width ranges may be extended by a remote programme unit which consists of a panel of switches arranged so that when connected to the stimulator and the rate and width switches turned to OFF the capacitors in the remote programme unit are connected in place of the function capacitors in the stimulator.*

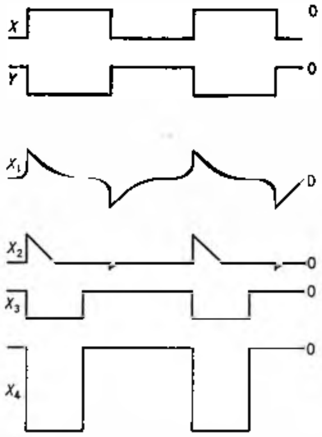

Fig. 4. Waveforms through circuit in Fig. 3

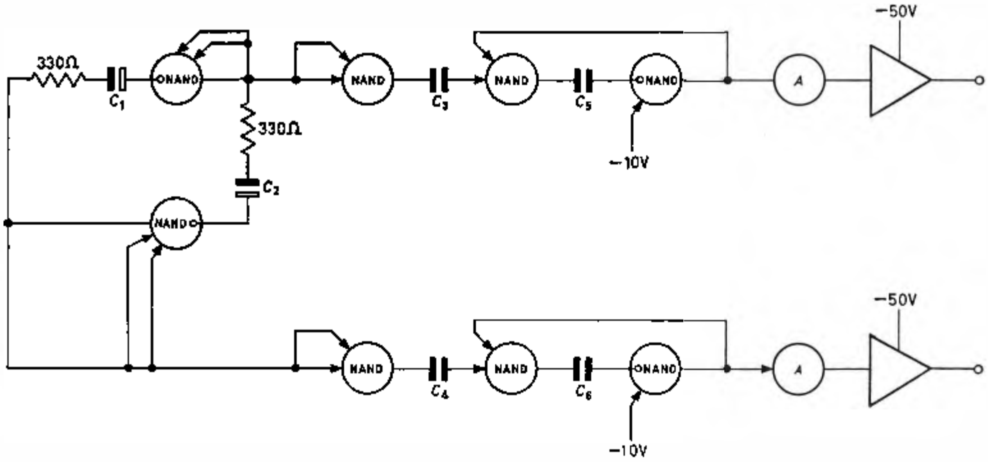

Fig. 5. Logical circuit configuration

the stability of the monostable would be greatly impaired. The periodic time of the fastest rate has a minimum value of twice the maximum width or conversely:

$$T_{W(max)} = 0{\cdot}5\, f_{max}$$

This relationship must be allowed in case the circuit is altered to accommodate for wide pulses and high frequencies.

VT_6 is run at a higher potential than VT_5 to provide sufficient base drive for the power output stage.

Power Stage

The shaped pulses are fed into an output stage with a

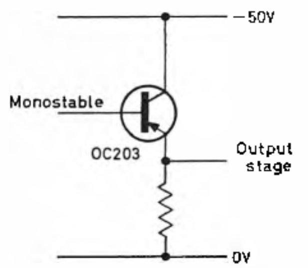

Fig. 6. Link to output stage, *A* in Fig. 5

maximum amplitude of 45V, controlled by a switch and potentiometer, in an emitter-follower driving chain. The final output is from the emitter of a power transistor, and this allows the instrument to work into low impedance preparations (Lewis[1]).

A width and power stage is required for each channel. Shown in Fig. 4 are the waveforms throughout the circuit, with reference to Fig. 3. This circuit although shown as a conventional electronic circuit may also be represented as logic functions, and constructed from commercial logic blocks of t.r.l. type. The logical configuration is shown in Fig. 5.

In the logical circuit the oscillator is applied to the base of the monostable transistors rather than to the collector. The link to the output stage is shown in Fig. 6 using an OC203 as an emitter-follower to drive an OC77 chain.

Controls

The frequency control is arranged with two six-way rotary switches with an 'off' position on each, thus giving ten frequency steps which are calibrated in absolute units. This incidentally gives a range of 25 uncalibrated steps if both switches are employed simultaneously.

The width control is a six-way rotary switch giving five width selections and an 'off' position.

In Fig. 7 are graphs of frequency and width against capacitance to give an approximate indication of values to be expected. The actual values encountered in practice will, of course, depart from these curves slightly due to electrolytic capacitor leakage and capacitance tolerance.

Amplitude is controlled by switch and potentiometer in a linear manner.

A master on-off switch is incorporated, together with a channel selector switch to give CHANNEL 1, 1 and 2 alternately, CHANNEL 2. These switches must be chosen with care, P.O. type 1000 key switches being preferable to mains type toggle switches.

The on-off control is effected by clamping the monostable input to zero in the off position, as shown in Fig.

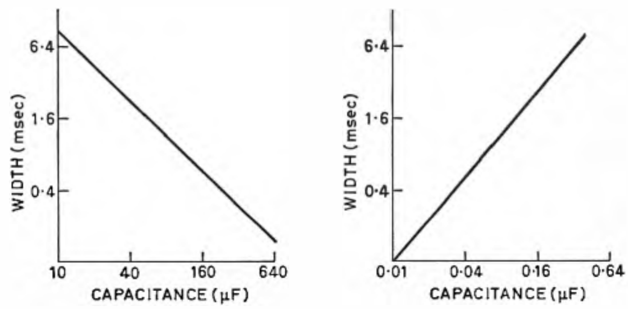

Fig. 7. (a) Frequency (b) Width against capacitance

Fig. 9. Mains voltage dependence graphs

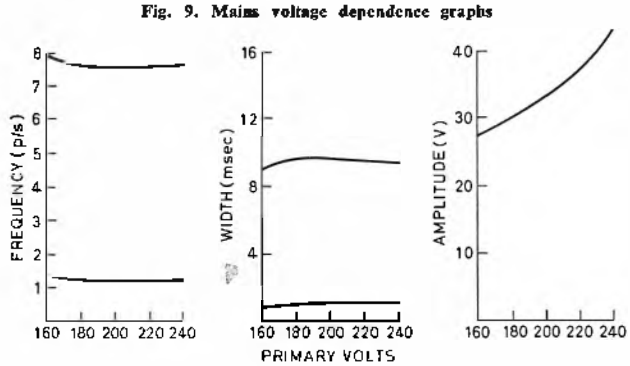

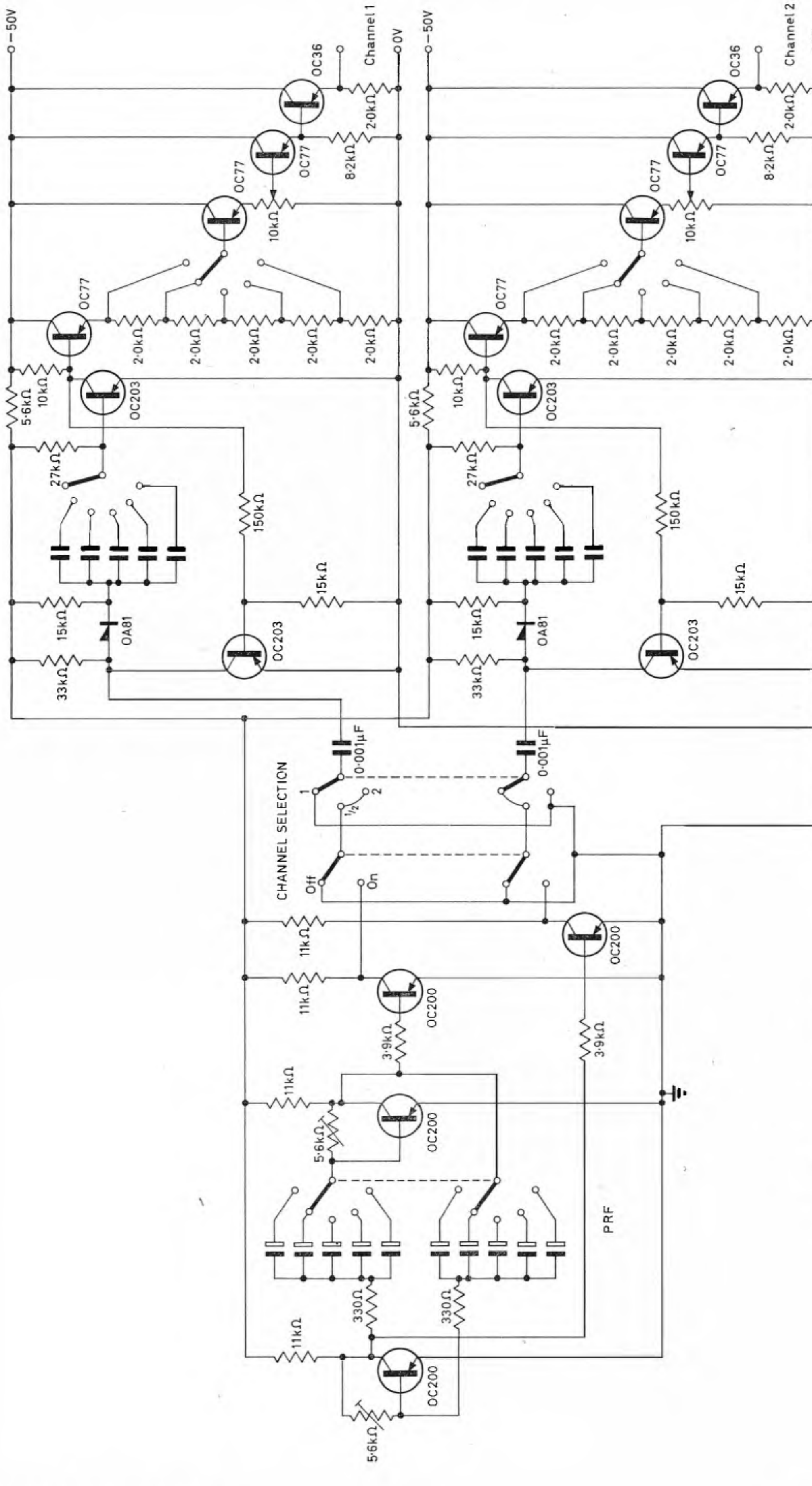

Fig. 8. The complete circuit

8. This was adopted in favour of merely switching the output which was found to produce spurious oscillations.

Stability

The stability of this device is obviously voltage dependent, and in this particular model a simple Zener diode stabilized power supply was employed, and tests were carried out to test the effect of mains voltage fluctuations upon performance, see Fig. 9.

Variation of load produced no appreciable shift in parameters. Obviously use of a more sophisticated regulated power supply would mean greater stability against mains variations as would the use of commercially available logic blocks against ambient temperature changes.

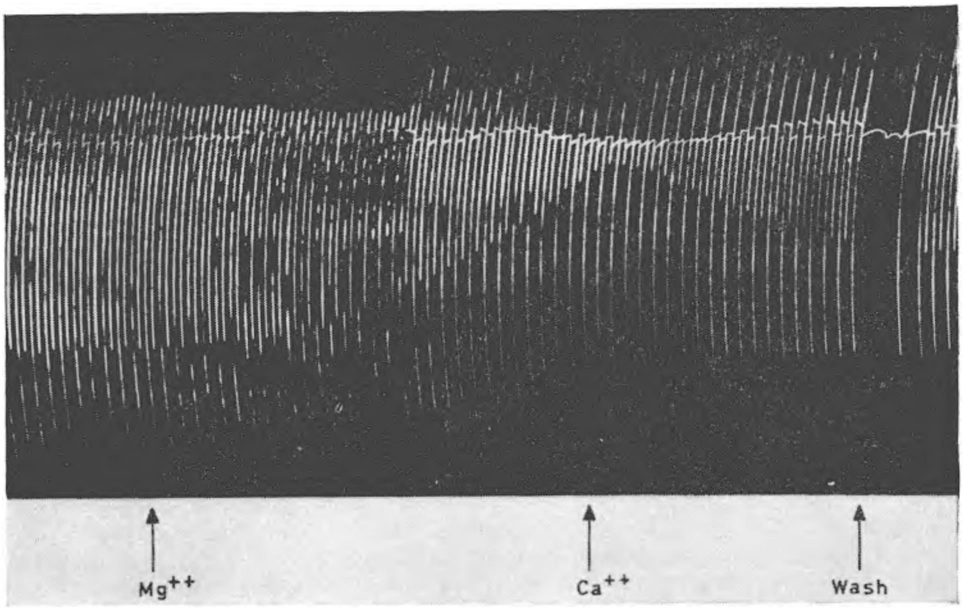

Fig. 10. Result of stimulation of rat phrenic nerve preparation

Performance

The stimulator behaved well on all ranges, and Fig. 10 shows its application to the stimulation of the rat phrenic nerve-diagram preparation in which shocks were applied alternately directly to the muscle and to the nerve suplying the muscle.

A presynaptic block was induced by increasing the magnesium concentration and relieved by restoring the calcium/magnesium balance. The result was that although neuro-muscular transmission was blocked the muscle was still active and responded maximally to direct stimulation. This illustrates the use of the instrument for comparing two routes of stimulation.

Acknowledgments

The authors wish to acknowledge Professor H. O. Schild for allowing this work to be carried out, Drs. D. H. Jenkinson and R. A. Webster for correcting the scripts and guidance for the biological aspects.

REFERENCES

1. LEWIS, A. F. *Proc. Phys. Soc.* (April 1964)
2. Elliott Bros., Minilog Applications.

Satellite Communications Terminal for the Royal Navy

Britain's first satellite communication terminal for shipborne use is being built for participation in the Interim Defence Communication Satellite Programme (I.D.C.S.P.). The project is part of the Royal Naval Scientific Service research programme at the Admiralty Surface Weapons Establishment. Initially the terminal has been set up on a land site, but early this year the equipment will be transferred into H.M.S. Wakeful to undergo sea trials.

The I.D.C.S.P. is an inter-Service project to test the efficacy of global communications in the military sphere. The 'space signment' is provided and financed by the U.S. Department of Defence and managed by the Defence Communications Agency in Washington. The satellites are active repeaters launched into near-stationary equatorial orbits by Titan 3C rockets.

A successful first launch of a group of eight satellites was made in June last year. Another launch is planned for early this year. Of the eight satellites in orbit seven are available for use in the military communications network. The interim programme will extend to the end of 1967.

The main advantage of the new system over present h.f. systems is its independence of relay stations. Higher quality of communication should be established and the signals will not suffer from variations in atmospheric conditions and hence reliability will be higher. Although this terminal is comparatively small, telegraphy, voice and facsimile traffic can be accommodated.

An agreement concluded between the U.S. Department of Defence and the British Ministry of Defence allows a limited number of earth stations to operate within the system. Three land-based stations with large aerials have been commissioned by the Ministry of Aviation. The first of these is located at Christchurch, Hampshire.

The provision of a shipborne system presents special problems and the Royal Navy's terminal facility has been built to explore these problems. In particular the terminal is being used to determine:

(a) The communication traffic capacity of a small terminal in a strategic network.

(b) The operational procedures necessary to provide an effective mobile communication centre.

(c) The technique for acquiring and maintaining communication in a ship environment of motion and radio interference.

The leader of the project is Dr. Glanville Harries at the Admiralty Surface Weapons Establishment and the aim has been to develop a system using mainly British equipment and components.

The terminal consists of a 6ft diameter aerial, with auto tracking facilities, fed by a high-powered transmitter operating in the military band of microwave frequencies. The signal from the satellite is retransmitted at a different frequency. Two separate receivers in the system enable the ship to monitor its own signals as well as those from another sending station.

The transmitter-receiver is being built in the Space Division of Plessey Radar Ltd, at Cowes, Isle of Wight, for the initial part of the trials programme. It incorporates a Mullard amplifier for small signal reception. The high power transmissions require water cooling of the transmitter valve and the waveguide systems. The transmitter, receiver, modulator equipment, aerial control and signal processing equipment are contained in two transportable cabins which are designed to be dropped into position on the ship's deck. An auxiliary power supply will be used to augment the ship's power supplies.

A specially designed stabilization system, using Ferranti gyros, is being installed in the ship by the Admiralty Surface Weapons Establishment.

Logarithmic Current-Measuring Transistor Circuits

By K. S. Højberg*

Two transistorized circuits for the logarithmic measurement of small currents with a view to nuclear reactor instrumentation are described. The logarithmic element is applied in the feedback path of an amplifier, and only one dual transistor is used as logarithmic diode and temperature-compensating transistor. A simple one-amplifier circuit is compared with a two-amplifier system. The circuits presented have been developed in connexion with an amplifier which incorporates a dual m.o.s. transistor input stage with diode-protected gates.

(Voir page 63 pour le résumé en français: Zusammenfassung in deutscher Sprache auf Seite 70)

An increasing number of types of instruments are being transistorized to achieve high reliability, small size and low power consumption. Development of m.o.s. transistors has enabled production of amplifiers with very low input currents and, by means of the planar, bipolar transistor used as a logarithmic element, simple and uncritical transistor circuits for the logarithmic measurement of currents down to relatively small values can be designed.

Logarithmic one- and two-amplifier current measuring circuits utilizing solid state components and temperature dependent resistors in the feedback networks have been described earlier[1]. The aim of the work presented here was to develop straightforward logarithmic networks for a transistorized electrometer amplifier[2], and two circuits were developed for the measurement of currents in the range approximately 10^{-10} to 10^{-3}A in view of nuclear reactor instrumentation. In each of the circuits described only one dual transistor, of silicon planar type, is applied as logarithmic diode and temperature compensating transistor.

The prototype amplifier[2] contains a dual m.o.s. transistor as a differential input stage, a circuit which is attractive as drift and supply voltage variations are in principle balanced out. One of the m.o.s. transistor gates was protected against punch-through due to excessive voltages by means of a neon bulb connected from the gate to the chassis and a series resistor was connected from the gate to the amplifier input. In the version of the amplifier used in the logarithmic circuits described here, the neon bulb was replaced by two parallel connected, but oppositely directed, low-leakage emitter base diodes from silicon planar transistors 2N930 and each gate was similarly protected. This type of protection circuit seems to be more effective against high frequency transients, but has a lower input resistance. Protection of the amplifier was intended both during handling and after insertion in the given circuit.

One-amplifier Circuit

A simple circuit for the logarithmic measurement of currents, e.g. from an ion chamber in a nuclear reactor, is shown in Fig. 1. Both the logarithmic and the temperature compensating elements are connected in one feedback loop. One half of a silicon planar transistor 2N2913 is diode connected and used as the logarithmic element VT_1. The other half VT_2 is an emitter-follower stage which gives a temperature-dependent offset. This stage is connected to a voltage divider which introduces a temperature-dependent gain.

The dual transistor $VT_1 - VT_2$ secures a good thermal contact between VT_1 and VT_2 and a good temperature compensation at one input current $I_1 = I_2$. However, if the input current I_1 is changed, the drift in transistor VT_1 is varied, i.e. the gain of the circuits is temperature dependent. This 'gain drift' is essentially stabilized by means of the n.t.c. resistor shown in the figure.

The principle of the one-amplifier logarithmic circuit is shown in Fig. 2. The original d.c. amplifier with the drift e_d referred to the input is here represented by a drift-free amplifier with zero input current, the gain $-A$, and a drift source e_d connected to the input. The internal resistance in the current source shown and the amplifier input resistance is considered to be high in comparison with the dynamic resistance in the feedback elements as seen from the amplifier input. The relation between the voltage e_{o1} and the ion chamber current I_1 can be specified as

$$e_{o1} = V_{be2} - V_{be1} + e_d - (e_{o2}/A) \quad \ldots\ldots\ldots \quad (1)$$

The emitter base voltages V_{be1} and V_{be2} of the transistors VT_1 and VT_2 respectively are approximated with the following expressions

$$V_{be1} = (kT/q) \ln ((I_1/I_s) + 1) \quad \ldots\ldots\ldots \quad (2)$$

$$V_{be2} = (kT/q) \ln ((I_2/I_s) + 1) \quad \ldots\ldots\ldots \quad (3)$$

I_s is the saturation current of the emitter base junction, T is the absolute temperature in degrees Kelvin, k is Boltzmann's constant and q is the charge of an electron ($kT/q = 26$mV at 27°C). For $I_1 \gg I_s$ and $I_2 \gg I_s$ the combination of equations (1), (2) and (3) gives

$$e_{o1} = e_d - (e_{o2}/A) - (kT/q) (\ln (I_1/I_s) - \ln (I_2/I_s)) \quad \ldots \quad (4)$$

or

$$e_{o1} = e_d - (e_{o2}/A) - (kT/q) \ln (I_1/I_2) \quad \ldots\ldots \quad (5)$$

The following relationship can be established in connexion with the voltage divider R_1, R_2

$$\frac{e_{o2} - e_{o1}}{R_2} = (e_{o1}/R_1) + (I_2/\beta_2) \quad \ldots\ldots\ldots \quad (6)$$

β_2 is the current gain of the transistor VT_2. R_2 includes the parallel connected resistor R_3 and the n.t.c. resistor R_4 in Fig. 1 as

$$R_2 = \frac{R_3 R_4}{R_3 + R_4} \quad \ldots\ldots\ldots\ldots\ldots\ldots \quad (7)$$

At 25°C, $R_4 = 4{\cdot}7\text{k}\Omega$, $R_3 = 0{\cdot}33\text{k}\Omega$ and thus $R_2 = 0{\cdot}31\text{k}\Omega$. If equation (5) is inserted in equation (6) and the latter is

* *Danish Atomic Energy Commission, Research Establishment Risö, Denmark.*

solved with respect to the output voltage e_{o2}, the following result is obtained

$$e_{o2} = \frac{\dfrac{R_1 + R_2}{R_1}\left[(I_2/\beta_2)\dfrac{R_1R_2}{R_1 + R_2} + e_d - (kT/q)\ln(I_1/I_2)\right]}{1 + (1/A)\dfrac{R_1 + R_2}{R_1}} \quad \ldots\ldots\ldots\ldots (8)$$

For simplicity, the complicated terms in equation (8) are replaced by single letters

$$e_{o2} = [k/(1 + a)]\,(e + e_d - v) \quad \ldots\ldots\ldots (9)$$

The following comments apply to the terms in equations (8) and (9). The voltage

$$v = (kT/q)\ln(I_1/I_2) \quad \ldots\ldots\ldots\ldots (10)$$

gives the basic contribution from one logarithmic element VT_1, referred to the amplifier input, and includes the practically constant current I_2 from the compensating transistor VT_2. The insertion of $I_1/I_2 = 0{\cdot}1$ and $kT/q = 26\text{mV}$ in equation (10) gives $v = -60\text{mV}$. Thus the contribution of v is 60mV per decade of input current change when one logarithmic diode is applied.

The mean value of the amplifier drift e_d measured on 10 amplifiers was 0·18mV/°C or 0·3 per cent of one decade per °C. This corresponds to 0·7 per cent of the scale reading at 1°C temperature change. The amplifier offset, which can be included in the diagram, Fig. 2, in the same way as the drift e_d, should be cancelled by proper amplifier balancing to avoid excessive currents through the gate-protecting diodes (not shown).

The term

$$e = (I_2/\beta_2)\,\frac{R_1R_2}{R_1 + R_2} \quad \ldots\ldots\ldots\ldots (11)$$

includes a constant offset which is referred to the amplifier input. The influence from this quantity on the final output voltage e_o, Fig. 1, can be removed by the zero adjustment potentiometer shown in Fig. 1. The term e is due to the finite current gain β_2 of the transistor VT_2, and therefore contains a contribution according to the current gain drift of VT_2. A rough approximation for this drift is $\Delta\beta/\beta = 1$ per cent/°C for bipolar transistors. For $R_1 = 0{\cdot}12\text{k}\Omega$, $R_2 = 0{\cdot}31\text{k}\Omega$, $I_2 = 7{\cdot}1\text{mA}$ and $\beta_2 = 280$, the insertion in equation (11) gives $e = 2{\cdot}2\text{mV}$ and the

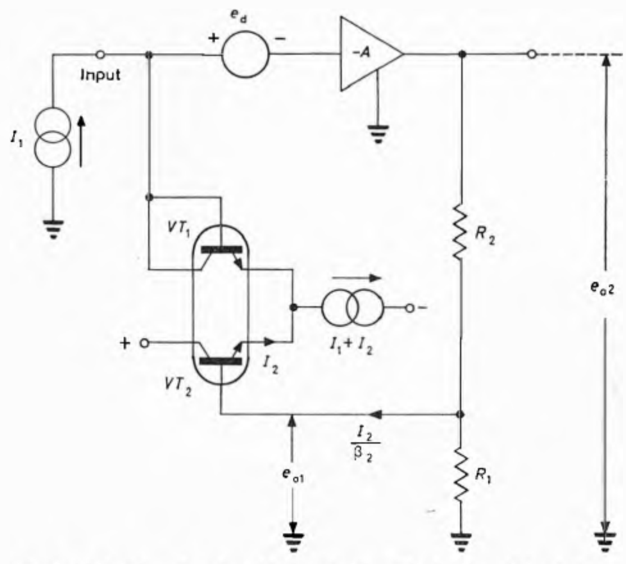

Fig. 2. Principle of a logarithmic circuit with d.c. amplifier drift e_d

drift for $\Delta\beta/\beta = 1$ per cent/°C is then 0·022mV/°C. As the logarithmic element contribution is 60mV per decade, this drift is 0·04 per cent of one decade per °C. The drift due to the leakage current in the transistor VT_2 is neglected as it is very small as compared with the above-mentioned drift of the relatively high base current. From equation (11) it is obvious that β_2 must be chosen high, I_2 low, and the resistance of the voltage divider as seen from the base of the transistor VT_2 must be kept low to obtain a low drift due to current gain changes. However, I_2 must exceed the input current I_1. For a given n.t.c. resistor and a given gain constant

$$k = \frac{R_1 + R_2}{R_1} \quad \ldots\ldots\ldots\ldots\ldots (12)$$

in equations (8) and (9), the smallest voltage divider resistance as seen from the transistor VT_2 base is obtained by shunting the n.t.c. resistor instead of using a series connexion. For this reason parallel connexion of the resistor R_3 and the n.t.c. resistor R_4 was chosen.

$$a = (1/A)\,\frac{R_1 + R_2}{R_1} \quad \ldots\ldots\ldots\ldots\ldots (13)$$

is the error due to finite gain A. For $A = 5\,000$ (d.c. gain measured on the prototype amplifier with maximum load), $R_1 = 0{\cdot}12\text{k}\Omega$ and $R_2 = 0{\cdot}31\text{k}\Omega$, the error a is ·00072 or only 0·07 per cent of the total output voltage e_{o2}.

In principle the influence of the above-mentioned error terms, e, e_d and a in equation (9) can be reduced by connecting more logarithmic diodes in series for the increase of the basic term v. If, however, e and e_d are considered small as compared with v and $a \ll 1$ in the case given, equation

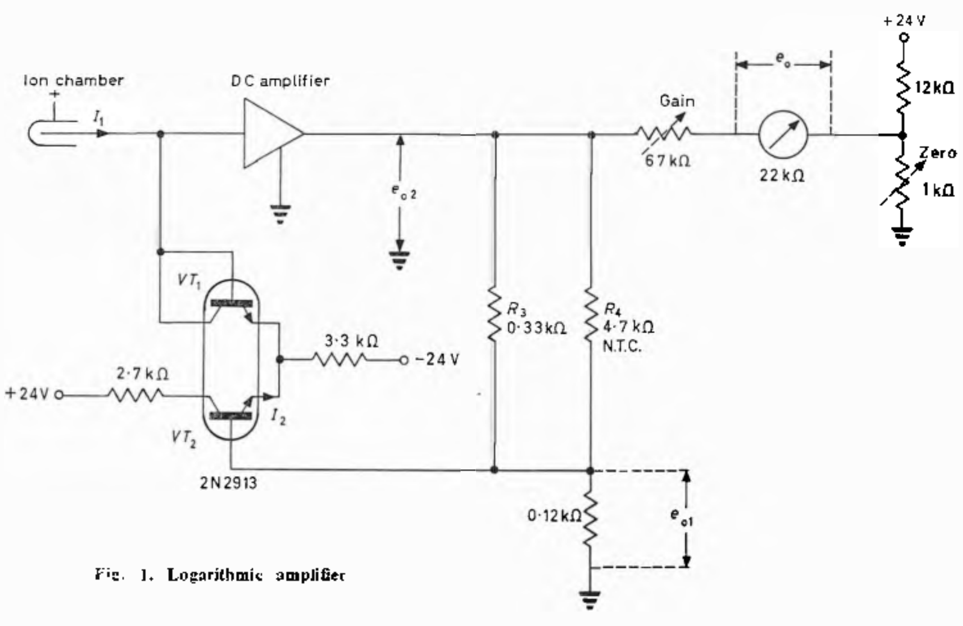

Fig. 1. Logarithmic amplifier

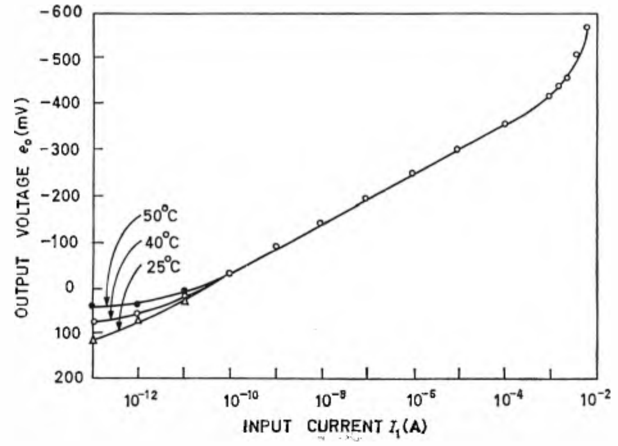

Fig. 3. Characteristics of the logarithmic current shown in Fig. 2

(9) is reduced to

$$e_{o2} = -kv \quad \ldots\ldots\ldots\ldots\ldots\ldots \quad (14)$$

or by the reinsertion of equations (10) and (12)

$$e_{o2} = -\frac{R_1 + R_2}{R_1}(kT/q)\ln(I_1/I_2) \quad \ldots\ldots\ldots\ldots \quad (15)$$

Insertion of $R_1 = 0{\cdot}12\text{k}\Omega$, $R_2\,0{\cdot}31\text{k}\Omega$ and $kT/q = 0{\cdot}0258\text{V}$ gives the following output voltage at 25°C

$$e_{o2} = -0{\cdot}2\log(I_1/I_2) \quad \ldots\ldots\ldots\ldots \quad (16)$$

The resistors R_1, R_3 and the n.t.c. resistor R_4 are chosen so that the insertion in equations (7) and (15) of the specified value of R_4 at 55°C together with kT/q at this temperature leads to the same gain factor 0·2 as obtained at 25°C.

The measured characteristics of the logarithmic circuit given in Fig. 1, including amplifier and power supply at 25, 40 and 55°C, are shown in Fig. 3. The deviation from the logarithmic characteristic at the low end of the current scale can essentially be explained by the fact that the proportion I_1/I_s is not small as compared with 1 in equation (2). In this connexion it should be noted that the collector resistor for the transistor VT_2 shown in Fig. 1 is important for the reduction of VT_3 power loss, and thus for the reduction of the temperature and the saturation current I_s of the transistor VT_1. The deviation at the other end of the current scale is partly due to the ohmic resistance in the logarithmic diode. When $I_1 \ll I_2$, I_2 is practically constant (Fig. 2). As I_1 approaches I_2, I_2 decreases and a deviation from the logarithmic characteristic can be expected according to equation (16).

Two-amplifier Circuit

A two-amplifier logarithmic circuit which is based on the same principles as that given in Fig. 1 is shown in Fig. 4. The compensation at one current $I_1 = I_2$ is introduced at amplifier 1 and the gain drift compensation is carried out by placing a n.t.c. resistor in the feedback network of amplifier 2. The diode-connected. compensating transistor is operated at very low power and there is no current limit due to the compensating current I_2 which is chosen at the middle of the current range ($2{\cdot}4 \times 10^{-7}$A). However, the ohmic resistance of the logarithmic element VT_1 has essential influence on the characteristic for currents $I_1 >$ 1mA as illustrated in Fig. 5. The compensation voltage from the transistor VT_2 is inserted at amplifier 1 differential input. The potential at this input is chosen as approximately zero to avoid excessive current through the gate-protecting diodes in the amplifier. The 10kΩ input resistor shown limits the current I_1 and protects the logarithmic element VT_1. A current is subtracted at amplifier 2 input to ensure that in principle a zero current is obtained through the n.t.c. resistor, giving a practically zero temperature drift in amplifier 2, when the temperature drift is zero in amplifier 1 output voltage. This situation occurs when the input current I_1 is equal to the compensating current I_2. If the subtraction mentioned is omitted, an unwanted temperature drift is introduced by means of the n.t.c. resistor.

The output voltage of amplifier 1 can be described as

$$e_{o1} = k_1 - (kT/q)\ln(I_1/I_2) \quad \ldots\ldots\ldots\ldots \quad (17)$$

where k_1 is the constant bias applied to the transistor VT_2 emitter. Infinite amplifier gain and zero amplifier offset is assumed. If $T = T_o + \Delta T$ the temperature drift included in equation (17) can be expressed as

$$e_g = \frac{k\,\Delta T}{q}\ln(I_1/I_2) \quad \ldots\ldots\ldots\ldots\ldots \quad (18)$$

where ΔT is the deviation in ambient temperature from the constant value T_o. If the compensating current I_2 and thus the zero drift point is placed at one end of the scale, the maximum drift (numerical value) obtained at the other

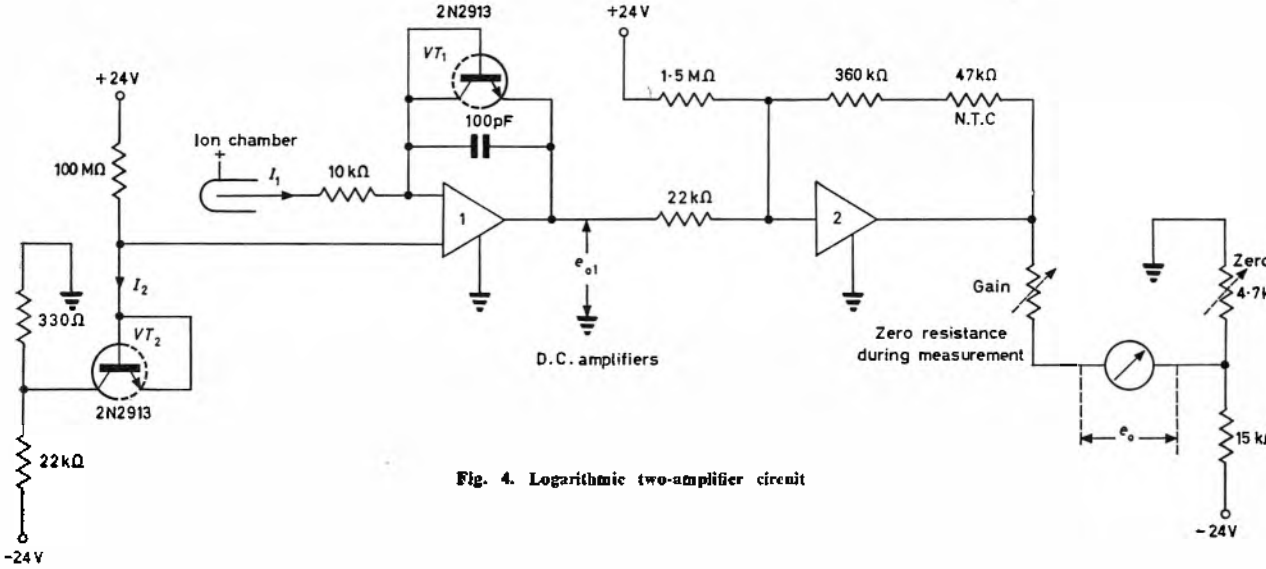

Fig. 4. Logarithmic two-amplifier circuit

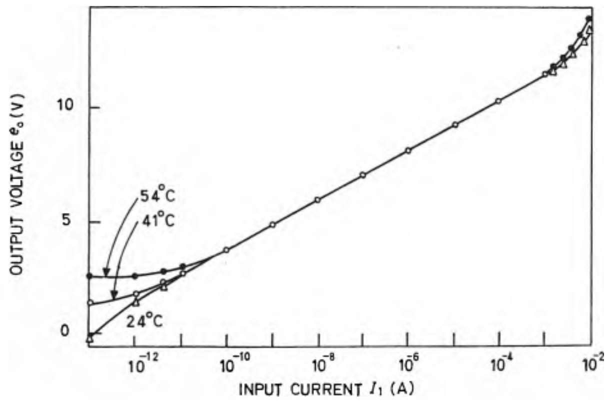

Fig. 5. Characteristics of the logarithmic circuit shown in Fig. 4

end of a scale with n decades is

$$e_{\max(1)} = \frac{k \Delta T}{q} \ln 10^{n} \quad \ldots\ldots\ldots\ldots\ldots\ldots (19)$$

When the compensating current I_2 is placed at the middle of the scale, zero drift is obtained here and the maximum drift (numerical value) at the ends of the scale is

$$e_{\max(2)} = \frac{k \Delta T}{q} \ln 10^{n/2} \quad \ldots\ldots\ldots\ldots\ldots (20)$$

or only half the value obtained in the previous case.

The logarithmic circuit output at 25 and 55°C is approximately

$$e_o = k_2 + k_3 \log (I_1/I_2) \quad \ldots\ldots\ldots\ldots (21)$$

With zero resistance setting of the gain control the constant k_3 is approximately 1. k_2 is a constant which can be altered by means of the zero potentiometer shown.

The advantages of the circuit given in Fig. 4 are, however, small as compared with the simple circuit in Fig. 1 with respect to the logarithmic range (Figs. 3 and 5).

Acknowledgment

Thanks are due to L. Buch, who tested several types of solid state components and suggested the use of the transistor 2N2913 and 2N930 as logarithmic elements.

REFERENCES

1. Furukawa, T., Wakayama, N. Solid State Neutron Flux Monitoring Instruments for the Nuclear Reactor. Paper No. CN22/48, IAEA Conf. Nuclear Electronics, Bombay. (Nov. 1965).
2. Hojberg, K. S. A Transistorized Electrometer Amplifier. (Letter). *Electronic Engng. 37*, 758 (1965).

Loading Effects in Two-Section RC Filters

By J. F. Young*, C.G.I.A., M.I.E.E., A.M.I.E.R.E.

By simple transformation of the circuit diagram, it is shown that loading effects in two-section RC ladder filters can be expressed in terms of an equivalent inverted Wien half-bridge circuit. This makes easy exact consideration of inter-section loading effects.

(Voir page 63 pour le résumé en français: Zusammenfassung in deutscher Sprache auf Seite 70)

SINGLE-SECTION *RC* filters are quite useful in electronics and their transfer characteristics are easy to deduce. When such circuits are cascaded with unity-gain buffer amplifiers separating each pair of circuits, the individual transfer characteristics are simply multiplied together to give the overall response. If the individual responses are expressed as curves of decibels against the logarithm of frequency, the overall response is easily obtained by addition of the individual curves. However, when a buffer-amplifier (having either high input and low output impedances or low input and high output impedances) is not used between filter sections, the overall characteristics are more complex. The reason for this is that later filter sections load earlier sections and so modify their characteristics.

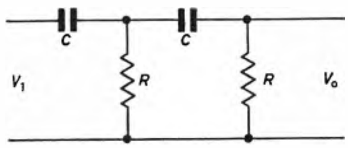

Fig. 1. Two section high-pass filter

Recently Gosling[1] has given an approximate method for dealing with this loading problem with the two-section *RC* filter. It might therefore be of interest to show as an alternative how an exact solution can easily be obtained by a simple transformation using elementary circuit theorems. The two-section filter considered by Gosling is shown in Fig. 1. This gives a transfer function:

$$V_o/V_1 = \frac{j^2\omega^2C^2R^2}{1 + 3j\omega CR + j^2\omega^2C^2R^2}\,.$$

The demominator of such an equation can be factorized, the roots taking a cosine-squared form[2]. However, it is possible to visualize the performance of the circuit more directly by operating directly on the circuit diagram,

Fig. 2. First equivalent circuit

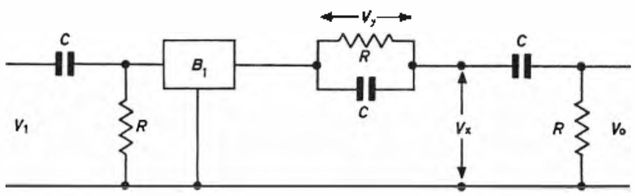

* *The University of Aston.*

making use of well-known circuit theorems. For example, application of Thevenin's theorem to Fig. 1 gives the equivalent circuit of Fig. 2. Here, B_1 is an imaginary buffer-amplifier, such as a cathode-follower, having unity voltage gain, infinite input impedance and zero output impedance. The part of this equivalent circuit to the right of the buffer amplifier will be recognized as an inverted version of the Wien half-bridge[3]. One can, in fact, redraw Fig. 2 incorporating yet another imaginary buffer-amplifier B_1 as shown in Fig. 3.

Here, the response of the centre section is obtained from the inversion of the Wien half-bridge:

$$V_x = V_z - V_y$$

$$= V_z - \frac{V_z j\omega CR}{1 + 3j\omega CR + j^2\omega^2C^2R^2}$$

hence

$$V_x/V_z = \frac{1 + 2j\omega CR + j^2\omega^2C^2R^2}{1 + 3j\omega CR + j^2\omega^2C^2R^2}$$

Also, the first and third sections of the equivalent circuit each have the response:

$$V_z/V_1 = V_o/V_x = \frac{R}{R + 1/j\omega C} = \frac{j\omega CR}{1 + j\omega CR}.$$

The overall response is therefore given by:

$$V_o/V_1 = V_o/V_x \,.\, V_z/V_1 \,.\, V_x/V_z$$

$$= \frac{j^2\omega^2C^2R^2}{(1 + j\omega CR)^2} \times \frac{1 + 2j\omega CR + j^2\omega^2C^2R^2}{1 + 3j\omega CR + j^2\omega^2C^2R^2}$$

$$= \frac{j^2\omega^2C^2R^2}{1 + 3j\omega CR + j^2\omega^2C^2R^2}$$

as stated previously. However, the expanded circuit diagram of Fig. 3 gives a clear insight into the meaning of this equation without the need for factorization. It shows that the overall response can be considered as due to a buffered cascade of two identical *CR* high-pass filters without loading effects, and the effect of loading can be considered as due to the inverted Wien half-bridge. The vector locus diagram for this inverted Wien half-bridge is as shown in Fig. 4. The output voltage V_x lags on the input voltage V_z at low frequencies and leads at high frequencies. Voltage V_x is in-phase with V_z at a frequency where $\omega CR = 1$. It has been shown elsewhere[3] that an alternative circuit which gives the vector-locus of Fig. 4 is the bridged-T circuit of Fig. 5.

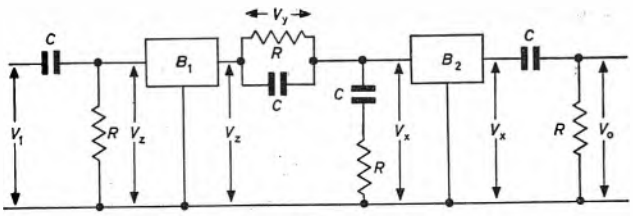

Fig. 3. Second equivalent circuit

Fig. 4. Vector locus diagram

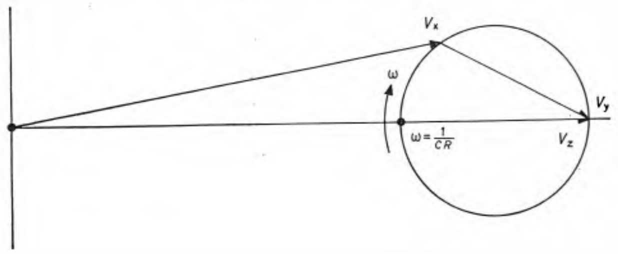

Fig. 5. Bridged-T filter

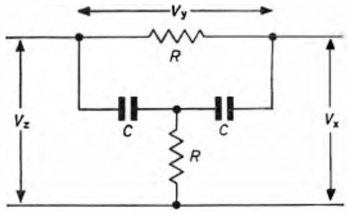

Fig. 6 (right). Two section low-pass filter

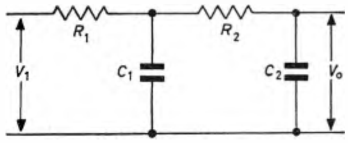

Fig. 7 (below). Equivalent circuit

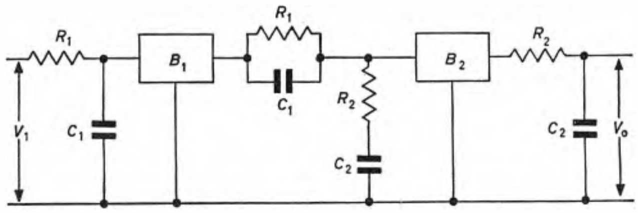

Thus it is quite simple to allow accurately for the effects of loading in this two-section *CRCR* high-pass filter. A similar approach can be made in the case of the two-section *RCRC* low-pass filter. The loading effect can again be expressed as the action of an imaginary inverted Wien half-bridge cascaded without loading effects with, in this case, two separate simple single section low-pass filters.

The same approach can be used when dissimilar component values are incorporated. For example, the action of the circuit of Fig. 6 is identical to that of the equivalent circuit of Fig. 7. Thus in this case the inverted Wien half-bridge of the equivalent circuit has dissimilar components. While the vector-locus diagram for such a Wien circuit is still a circle, the diameter of the circle is no longer necessarily 3. If $R_2 \gg R_1$ and $C_1 \gg C_3$, then the loading error represented by the Wien half-bridge is small. This would be expected from inspection of Fig. 6. The two-section high-pass *CRCR* filter can be considered in a similar way when dissimilar components are incorporated.

The approach described here gives the overall response of a circuit in the form of the response of a cascade of three simpler circuits. Consequently it is useful to consider the decibel-log (frequency) form of the response since it is simply formed from the sum of the three elementary decibel-log (frequency) curves. Thus the centre section in Fig. 7 has the effect of introducing a downward notch into the response. The sum of this notch and the conventional low-pass responses of the other two sections, produces the overall decibel-log (frequency) diagram.

A similar approach to that described here can be used with current input-current output filters, in this case Norton's theorem being used rather than Thevenin's theorem.

REFERENCES

1. GOSLING, W. A Simple Approximation for Calculating the Phase Shift of Two-Loop *CR* Networks. *Electronic Engng.* *38*, 186 (1966).
2. YOUNG, J. F. The Response of RC Ladder Filters. *Electronic Engng.* *35*, 525 (1963).
3. YOUNG, J. F. Alternatives to the Wien Bridge. *Wireless World*. *65*, 92 (1959).

An Asynchronous Binary-Coded-Decimal Circuit with Gated Feedback

By S. L. Hurst*

Binary-coded-decimal assemblies normally operate asynchronously, and employ some form of count detection logic to produce a non-binary transition at some stage of the count. A form of series gating is here described to obtain the necessary non-binary transition, which has the merit of eliminating transitory false counts which are present in most b.c.d. arrangements.

(Voir page 63 pour le résumé en français: Zusammenfassung in deutscher Sprache auf Seite 70)

BINARY-CODED-DECIMAL and all other types of sequential counter circuits may generally be divided into two main categories, namely synchronously operating or asynchronously operating. In the synchronous or 'gated' type of circuits, all the bistable circuits that constitute the assembly are driven by one common clock pulse driving signal, logic gating in each bistable 'set' and 'reset' pulse input line being necessary to allow through or block the clock pulses, as required, on each count. On the other hand, in the asynchronous type of counter each bistable circuit is driven by the change of state of some other circuit, usually the preceding one; hence the various changes of state that may be necessary between one count and the next are dependent upon the change-over times of the various bistable circuits themselves.

The synchronous or 'gated' type of counter thus is capable of faster operation than the asynchronous type. Also it does not generate any transitory false count which the asynchronous type normally does when generating any code other than pure binary. Against these advantages must be weighed the cost and complexity of the gating circuits required on each 'set' and 'reset' input line of every bistable circuit to correctly gate the common master clock signals.

In the case of a pure binary counter, with each circuit always operating at one half the rate of its predecessor, the simplicity of the normal a.c. coupled asynchronous type of circuit far outweighs its disadvantages. If a four-stage gated counter to produce pure binary counting is contemplated, the 'set' and 'reset' gates have to be operated as detailed in Fig. 1 to produce the normal divide-by-two action. The total logic required as a result of using a master clock pulse drive will be seen to be considerable.

The gated counter, however, begins to become more attractive, when coding other than pure binary is required, for example in the production of Gray cyclic coding sequences. To attempt to utilize an asynchronous type of counter to generate such a code is complex, as by definition a Gray code does not involve normal binary transitions between consecutive counts. The sequence of a typical four-stage Gray code is shown in Fig. 2(a) from which the lack of normal binary transitions between counts will be apparent. Thus there is little attraction in adopting an asynchronous type counter circuit for electronically generating such a code.

Hence the choice between using asynchronous or synchronous counter circuits for generating particular

Fig. 1. Gating required to produce pure binary coding from a 4-stage gated counter

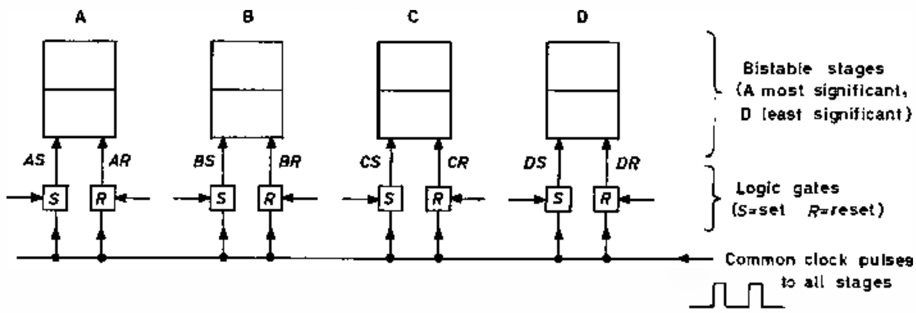

BINARY STATE				DECIMAL COUNT	GATES TO BE OPENED OR BLOCKED AS A RESULT OF PREVALENT COUNT IN ORDER TO PRODUCE THE FOLLOWING COUNT (O = Open, B = Blocked, DC = "Don't Care")							
A	B	C	D		*AS*	*AR*	*BS*	*BR*	*CS*	*CR*	*DS*	*DR*
0	0	0	0	0	B	DC	B	DC	B	DC	0	B
0	0	0	1	1	B	DC	B	DC	0	B	B	0
0	0	1	0	2	B	DC	B	DC	DC	B	0	B
0	0	1	1	3	B	DC	0	B	B	0	B	0
0	1	0	0	4	B	DC	DC	B	B	DC	0	B
0	1	0	1	5	B	DC	DC	B	0	B	B	0
0	1	1	0	6	B	DC	DC	B	DC	B	0	B
0	1	1	1	7	0	B	B	0	B	0	B	0
1	0	0	0	8	DC	B	B	DC	B	DC	0	B
1	0	0	1	9	DC	B	B	DC	0	B	B	0
1	0	1	0	10	DC	B	B	DC	DC	B	0	B
1	0	1	1	11	DC	B	0	B	B	0	B	0
1	1	0	0	12	DC	B	DC	B	B	DC	0	B
1	1	0	1	13	DC	B	DC	B	0	B	B	0
1	1	1	0	14	DC	B	DC	B	DC	B	0	B
1	1	1	1	15	B	0	B	0	B	0	B	0

* *Bath University of Technology.*

codes is normally dictated by ease of generation. The theoretically lower maximum counting speed of the asynchronous type and its transitory false counts when generating codes other than pure binary are accepted as preferable to the complexity of the synchronous counter in the majority of applications.

Binary-Coded-Decimal Counters

Possibly the most commonly encountered coding other than pure binary is the binary-coded-decimal assembly. The usual b.c.d. assembly, involving the use of four bistable circuits, has six 'forbidden' binary combinations in the states of its four circuits, in order that it performs the required cycle of ten rather than the pure binary cycle of sixteen.

Figs. 2(b) to (e) illustrate four typical four-stage b.c.d. coding patterns. It will be noticed that the incidence of non-binary transitions in the pattern of codes (d) and (e) is very high, while codes (b) and (c) each contain only one such non-binary transition, namely between counts 9 and 0 in (b) and between counts 1 and 2 in (c). It may also be noted that no positive weighting may be ascribed to a Gray cyclic code; indeed any conversion of a Gray code into decimal equivalents is difficult, and resort to other forms of cyclic coding may be necessary. Some of these alternatives may involve more than four bistable circuits per decade[1,2].

Gated counter circuits thus are more attractive for the electronic generation of codes such as (d) and (e), but asynchronous circuits are usually used for codes such as (b) and (c) due to the very high percentage of normal binary transitions in the latter patterns. Care must also be exercised in the design of the logic gating for any gated b.c.d. counter, as it is possible for such a counter to 'sub-cycle' continuously within the six forbidden counts of the four stages[3], should interference ever momentarily generate one of these forbidden counts. This interesting but undesirable feature can never occur with the asynchronous circuit, which always will automatically flow back into its normal cycle-of-ten should it ever be influenced into any of its forbidden counts.

However, it is possible to suggest a compromise between the simple asynchronous type counter and the gated synchronous type, which incorporates desirable features from each. For b.c.d. coding, the simplicity of the asynchronous driving pulses between stages may be retained with advantage to provide the normal divide-by-two action, but simple gating may be added to give a cycle of ten, and also to eliminate any transitory false count.

Now if all possible ways of utilizing four binary stages to produce a cycle of ten with only one non-binary transition are compiled, it will be found that of the ten possible codings one is weighted 8:4:2:1, seven are weighted 2:4:2:1, and two are unweighted. The 8:4:2:1 code is as shown in Fig. 2(b), while Fig. 2(c) illustrates the first of the seven possible 2:4:2:1 weighted codes. The remaining six such codes follow the normal binary pattern for an increasing number of counts before the non-binary 'jump' is made in the coding pattern. The two unweighted decimal codes are when the non-binary transition is made between decimal counts 0 and 1, or between decimal counts 8 and 9. These latter codes are of no attraction whatsoever for any application.

Of the seven 2:4:2:1 codes, it is found that the one with the non-binary transition between decimal 1 and 2

Fig. 2. Typical coding sequences other than pure binary

	A	B	C	D
0	0	0	0	0
1	0	0	0	1
2	0	0	1	1
3	0	0	1	0
4	0	1	1	0
5	0	1	1	1
6	0	1	0	1
7	0	1	0	0
8	1	1	0	0
9	1	1	0	1
10	1	1	1	1
11	1	1	1	0
12	1	0	1	0
13	1	0	1	1
14	1	0	0	1
15	1	0	0	0
0	0	0	0	0

(a) Gray cyclic

	A	B	C	D
0	0	0	0	0
1	0	0	0	1
2	0	0	1	0
3	0	0	1	1
4	0	1	0	0
5	0	1	0	1
6	0	1	1	0
7	0	1	1	1
8	1	0	0	0
9	1	0	0	1
0	0	0	0	0

(b) Binary-coded-decimal, weighted 8:4:2:1

	A	B	C	D
0	0	0	0	0
1	0	0	0	1
2	1	0	0	0
3	1	0	0	1
4	1	0	1	0
5	1	0	1	1
6	1	1	0	0
7	1	1	0	1
8	1	1	1	0
9	1	1	1	1
0	0	0	0	0

(c) Binary-coded-decimal, weighted 2:4:2:1

	A	B	C	D
0	0	0	0	0
1	0	0	0	1
2	0	0	1	1
3	0	1	0	1
4	0	1	1	1
5	1	0	0	0
6	1	0	0	1
7	1	0	1	1
8	1	1	0	1
9	1	1	1	1
0	0	0	0	0

(d) Binary-coded-decimal, weighted 5:2:1:1

	A	B	C	D
0	0	0	0	0
1	0	0	0	1
2	0	0	1	1
3	0	0	1	0
4	0	1	1	0
5	1	1	1	0
6	1	0	1	0
7	1	0	1	1
8	1	0	0	1
9	1	0	0	0
0	0	0	0	0

(e) Binary-coded-decimal, Gray cyclic unweighted

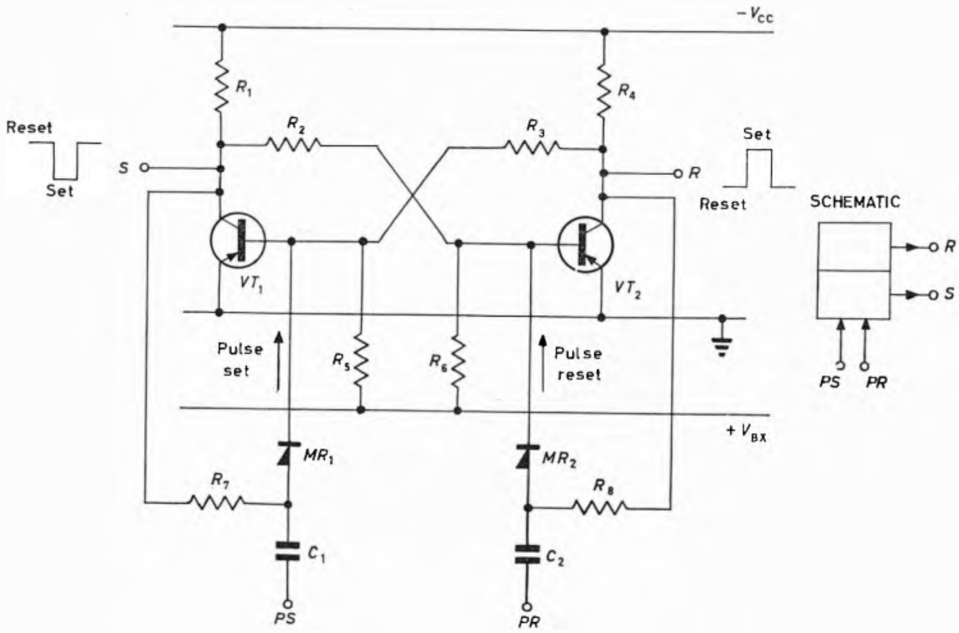

Fig. 3. Basic divide-by-two circuit of each stage of the b.c.d. assemblies

Fig. 4. Binary coded decimal assemblies with gated feedback
(a) *Weighted* $A = 8$, $B = 4$, $C = 2$, $D = 1$
(b) *Weighted* $A = 2$, $B = 4$, $C = 2$, $D = 1$

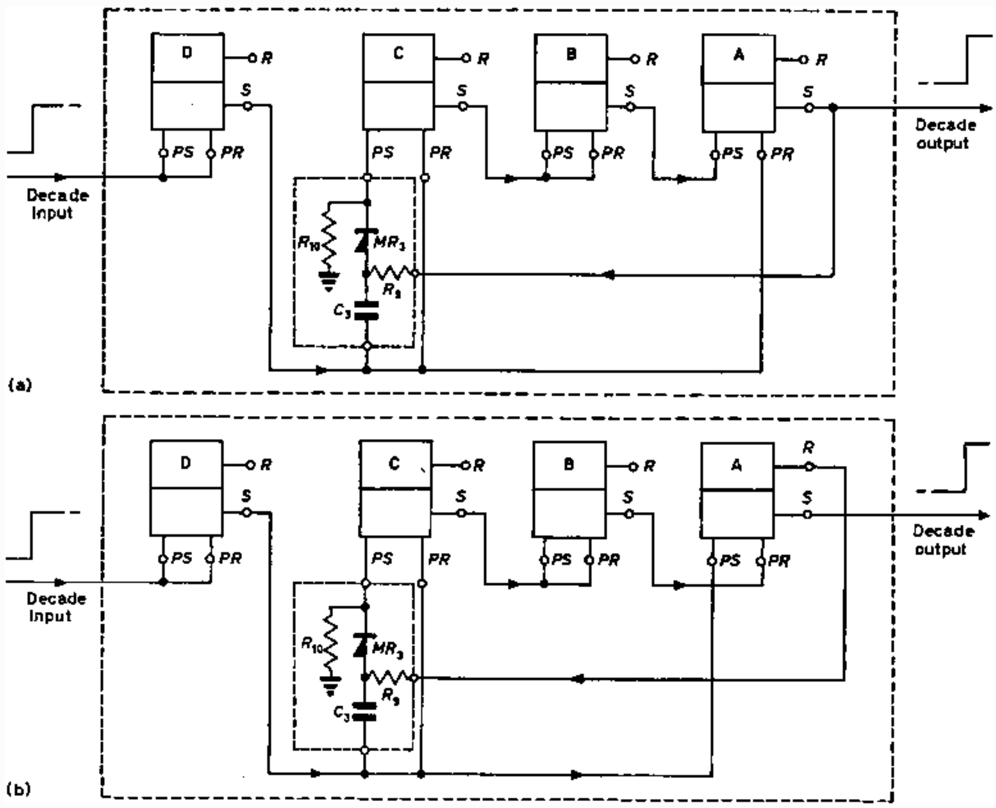

affords the easiest 'jump' to engineer by the gating circuits to be described. The complete 2:4:2:1 code is thus as given in Fig. 2(c).

The A.C. Coupled Asynchronous Gated B.C.D. Circuits

Fig. 3 illustrates the bistable circuit which constitutes each of the four stages of every b.c.d. assembly. This circuit is perfectly conventional, the pulse inputs being internally gated by the diode steering circuits to give the normal changeover action of the bistable when positive-going steps are applied to the capacitors C_1 and C_2.

The assembly of four such bistable circuits to produce b.c.d. coding weighted (a) 8:4:2:1, and (b) 2:4:2:1 is shown in Fig. 4(a) and (b) respectively. The main addition in both assemblies will be seen to be an additional biased diode-capacitor gate $R_9/C_3/MR_3$ placed in series with the normal internal $R_7/C_1/MR_1$ 'set' gate of the second stage. A negative voltage supply on either gate biasing resistor R_7 or R_9 affords a block to prevent a positive input step from influencing the state of the bistable circuit. Thus *both* these gates in series require zero voltage on their biasing resistors to allow an input signal to become effective.

In the action of the 8:4:2:1 assembly of Fig. 4(a), divide-by-two counting action proceeds normally until the eighth signal is registered. Following the completion of this count, a negative voltage from stage A is now present to block the additional series gate on stage C, thus making the next 1 to 0 change of stage D ineffective in influencing C. This next 1 to 0 change does, however, reset A, which thus reverts the whole decade to zero count on this the tenth input signal.

In a very similar manner, the 2:4:2:1 assembly of Fig. 4(b) completes a cycle of ten rather than sixteen. Here, however, the additional series gate of stage C is fed so as to be blocked at the commencement of the code, and unblocked following the operation of stage A at count 2. Thereafter the count proceeds in a perfectly normal binary fashion reaching zero count again on the tenth input signal.

It will thus be appreciated that with these circuit arrangements, there is no transitory false count during the non-binary transitions, as all the appropriate gates are prepared beforehand in readiness for this transition. The CR time-constant considerations of the additional series gate are precisely the same as those associated with the normal 'internal' gates of the basic bistable assemblies. Also as the additional gate is concerned with the second stage C, and not with the fastest operating stage D, the most critical time-constants will not be directly connected with this modified stage, but rather will be associated with stage D in the usual manner.

The final resistor R_{10} present between the diode MR_3 of the additional series gate and the normal 'set' gate capacitor C_1, is a high value resistor necessary merely as a leak to ground, thus preventing any build-up of voltage between MR_3 and C_1 which might continuously reverse bias MR_3.

The maximum operating speed of the whole decade in both arrangements is still dependent upon the cascade time of changeover of the four bistable circuits in series. The fully gated synchronous counter thus remains superior in this respect. However, the time taken for the non-binary transition in both these arrangements of Fig. 4, after application of the input signal, is no greater than the normal transition time associated with the changeover of stage C. In this respect, therefore, these asynchronous gated circuits show an improvement in speed compared with many b.c.d. arrangements, as these latter arrangements involve the cancellation of transitory false counts by the operation of appropriate logic feedback.

Conclusions

This technique of additional diode gating in series with the normal divide-by-two gating of bistable circuits is seen to offer attractions in the generation of simple modified binary coding, such as binary-coded-decimal arrangements.

The technique may be extended to produce further forms of non-binary coding if desired, though if used to generate codes which contain a very high proportion of non-binary transitions then the fully gated counter becomes a more satisfactory solution once more.

Acknowledgments

Acknowledgments with thanks are made to Professor A. J. Eales, Head of the School of Electrical Engineering, Bath University of Technology, for permission to publish this short article.

REFERENCES

1. RICHARDS, R. K. Arithmetic Operations in Digital Computers. (Van Nostrand, 1958).
2. YOUNG, J. F. Cyclic Binary-Decimal Complementing Codes. *Control*, *8*, 226 (1964).
3. BROWN, D. H. The Gated Counter. *J. Elect. Engng. Education*, *4*, 3 (1966).

Application of a pnpn Switch to Temperature Control*

By A. Lupic† and B. Kovac†

The possibility of converting temperature into frequency by temperature sensitivity of a relaxation oscillator circuit is discussed. The linear dependence of the temperature and frequency in the range of −10°C to +50°C has been measured. Results obtained during the continuous operation of the oscillator over 1 000 hours are presented.

(Voir page 63 pour le résumé en français: Zusammenfassung in deutscher Sprache auf Seite 70)

A TEMPERATURE sensing system based on frequency variation with temperature has advantages over systems with temperature expanding materials: it provides good repeatability and high sensitivity.

Relaxation Oscillator Using a pnpn Switch

Operation Principles

Fig. 1 is a schematic view of the circuit described below. The circuit works in the following way: the anode voltage of the pnpn switch increases exponentially and the gate voltage is proportional to it. At the moment the gate voltage reaches the trigger level, the switch is triggered and the capacitor C is discharged through the protecting resistor R_3. This causes the switch to cut-off, the cycle is repeated and the frequency is determined by the RC elements and the gate trigger level which is variable with temperature.

Oscillator Frequency Analysis

The anode voltage v of the pnpn switch (Fig. 1) increases according to the equation:

$$v = V[1 - \exp(-t/\tau)] \quad \ldots\ldots\ldots\ldots \quad (1)$$

* *Yugoslav Patent Application P-697/66.*

† *Boris Kidric Institute of Nuclear Sciences, Yugoslavia.*

where:

$$\tau = RC\,(R_1 + R_v)/(R + R_1 + R_v) \quad \ldots\ldots\ldots (2)$$

$V = V_o(R_1+R_v)/(R + R_1+ R_v)$; $R_v = (R_2R_g)/(R_2+R_g)$; $R_3 \ll R_g$; $R_g = e_g/i_g$.

R_g is obtained by characteristics of the gate voltage e_g and gate current i_g.

When the voltage v reaches v_1 (Fig. 2), thus the voltage e_g being equal to the gate trigger voltage e_{g1} (at temperature T_1) and the current i_g equal to the gate trigger current i_{g1}, the pnpn switch will be triggered and the capacitor C discharged through the protecting resistor R_3.

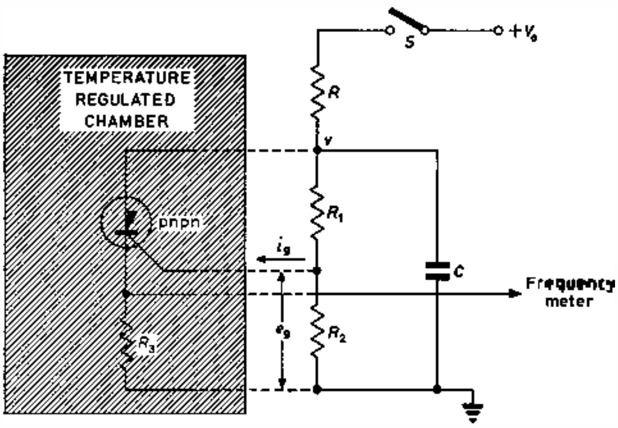

Fig. 1. The circuit described

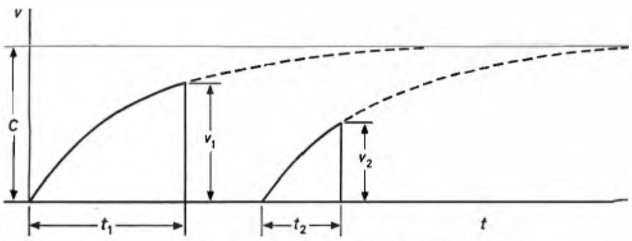

Fig. 2. Operational waveforms

Fig. 3. Calculated and measured response characteristics

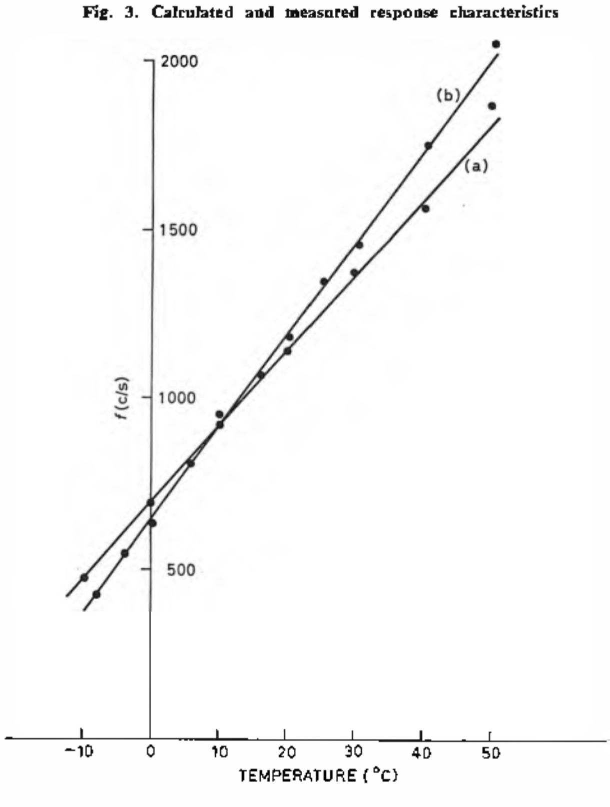

If the capacitor C is fully charged before e_g reaches the gate trigger level, the oscillator will not operate. Hence. the choice of the elements should be:

$$(VR_v)/(R_1 + R_v) > e_g$$

If the pnpn switch is to operate as a relaxation oscillator the following condition should be fulfilled:

$$R > V_o/I_H$$

where I_H is the switch holding current.

When the temperature increases from T_1 to T_2, the trigger voltage decreases from e_{g1} to e_{g2}. The gate trigger voltage-temperature variation is given by manufacture.

According to the dependence:

$$v \;=\; e_g\,(R_1 + R_v)R_v \quad \ldots\ldots\ldots\ldots\ldots (3)$$

it may be concluded that decreased trigger voltage causes an oscillation amplitude decrease from v_1 to v_2 (Fig. 2) and charge time-interval of the capacitor C from t_1 to t_2. Finally, it may be concluded that increase of temperature corresponds to increasing oscillator frequency.

Equation (1) gives the value of the charging time-interval of the capacitor t_k at the temperature T_K:

$$t_k \;=\; \tau \ln V/(V - v) \quad \ldots\ldots\ldots\ldots\ldots (4)$$

and the oscillator frequency:

$$f_k \;=\; 1/t_k$$

$$f_k \;=\; (1/\tau)\;[1/\ln V/(V - v)]$$

If τ is replaced from equation (2), and v from equation (3), it follows that:

$$f_k \;=\; \{1/[RC\;\;(R_1+R_v)/(R+R_1+R_v)\,]\}$$
$$\{1/\ln\;[V-e_g\;\;(R_1+R_v)/R_v]\} \quad \ldots\ldots\ldots\ldots (5)$$

Calculated response of the experimental oscillator equation (5)) is given in Fig. 3(a).

Experimental Results

The experimental oscillator consists of a 2N3032 type pnpn switch, produced by SSPI, and of the following elements:

R = 220kΩ, R_1 = 1MΩ, R_2 = 39kΩ, C = 15nF, R_3 = 5Ω. Power supply: V_o = 85V.

The stability with time of the temperature sensing oscillator was tested during a 1 000-hour run. The frequency temperature variation of the oscillator is shown in Fig. 3(b). It is seen that the curve is fairly linear in the range −10°C to +50°C, and it can be expressed by

$$f = 27{\cdot}6T + 640\ [\text{c/s}, {}^\circ\text{C}]$$

Conclusion

The results show that the described oscillator with a pnpn switch can be used for temerature measurement and regulation in the range determined by the operating characteristics of the switches. The simple construction and the small number of elements make possible its wide application and its further development in the form of integrated circuits.

The variation of errors of the experimental circuit that appeared during 1 000 hours were less than ±5 per cent. The circuit is considered reliable.

Acknowledgments

The authors wish to thank Dr. D. T. Jovanovic, Dr. M. M. Novakovic, and Dr. M. M. Vojinovic for helpful discussions and proof-reading of the manuscript.

Unified Transistor Calculations

By D. W. W. Rogers*, C.Eng., A.M.I.E.R.E.

A method of unifying junction transistor calculations is described based upon the impedance parameters and the equivalent T circuit. The method is particularly labour saving inasmuch that 'off the cuff' canonical calculations may be made in z, y, and h parameters, without matrix transformation.

(Voir page 63 pour le résumé en français: Zusammenfassung in deutscher Sprache auf Seite 70)

THE rapid evolution of semiconductors, transistors in particular, has increased considerably the demands from both student and experienced engineer. For example calculations such as small signal stage gain and input impedance, are now part of the daily routine, and are often required at a moments notice. Unfortunately the development of a facile calculating ability is hampered by a bewildering number of equivalent circuits and parameters, while textbooks invariably give page after page of proof culminating in tables of formulae for stage calculation. The method to be described here, besides going a long way towards a simple unified approach, may easily be memorized, so that with very little practice, the facility to make 'off the cuff' stage calculations in all configurations is soon acquired.

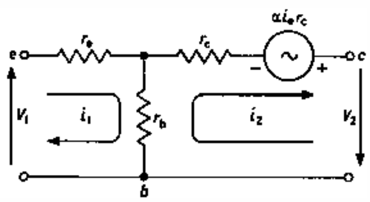

Fig. 1. Equivalent T circuit

As a rule transistor analysis is usually introduced by means of the equivalent T circuit, (see Fig. 1). This is because this circuit has almost a one to one correspondence with the physical idea of a transistor as a series combination of a forward and reverse biased diode. Further the transistor may be represented by simple impedance terms such as r_e, r_b, r_c and α, which besides being currently used by the manufacturers, are more readily accepted by the type of engineer who has been reared on impedance calculations rather than admittance. Also $r_e \simeq 26/i_e$(mA) is a fundamental relationship. There is a strong case therefore for using this circuit as a base for calculation. In order to emphasize the method rather than its proof, much of the initial mathematics is confined to the Appendix.

z Parameters and the Equivalent T Circuit

Consider first the z parameters of the grounded base (g.b.) equivalent T circuit shown in Fig. 1. The z parameters are defined by equations (1) and (2).

$$V_1 = i_1 z_{11} + i_2 z_{12} \qquad (1)$$

$$V_2 = i_1 z_{21} + i_2 z_{22} \qquad (2)$$

It should be noted in Fig. 1 that both the currents and the voltages have a clockwise sense. This convention is necessary in order to preserve the properties of the indefinite impedance matrix, although as stated previously matrix transformation is unnecessary in this method.

* *Sheffield College of Technology. The author holds the Diploma of Graduate Studies of the University of Birmingham.*

The z parameters are best obtained by means of the unit current technique[5,6]. Substituting $i_1 = 1$A and $i_2 = 0$, in equation (1) for example, then $Z_{11} = V_1$. More concisely Zadeh[5] has defined the impedance parameter as z_{mn}, where z_{mn} is the voltage induced in the m^{th} mesh by unit current in the n^{th} mesh. Thus Z_{11} is the voltage induced in the first mesh of Fig. 1 by a current of 1A in the first mesh, the second mesh being open-circuit. Hence $z_{11} = r_e \,.\, 1 + r_b \,.\, 1 = r_e + r_b \,.\, z_{12}$ is the voltage induced in the first mesh of Fig. 1 by a current of 1A in the second mesh, the second mesh being open-circuit. Hence $z_{12} = -r_b \,.\, 1 = -r_b$.

z_{21} is the voltage induced in the second mesh by a current of 1A in the first mesh, the first mesh being open-circuit. Hence $z_{21} = -r_b \,.\, 1 - \alpha \,.\, r_c = -r_b - \alpha \,.\, r_c$.

z_{22} is the voltage induced in the second mesh by a current of 1A in the second mesh, the first mesh being open-circuit. Hence $z_{22} = r_b + r_c \,.\, 1 = r_b + r_c$. It is possible therefore merely by inspection to write down the g.b. z parameters as follows:

$$\begin{vmatrix} z_{11} & z_{12} \\ z_{21} & z_{22} \end{vmatrix} \equiv \begin{array}{cc} C & B \\ \begin{vmatrix} r_e + r_b & -r_b \\ -r_b - \alpha \,.\, r_c & +r_b + r_c \end{vmatrix} & \begin{array}{c} C \\ B \end{array} \end{array}$$

Next, in order to deal with the g.c., g.b., and g.c. configurations, the indefinite impedance matrix is constructed. Shekel[1] has studied its dual, the indefinite admittance matrix, although this rarely appears in literature.

The Indefinite Impedance Matrix

Lest the reader is discouraged by such an impressive heading, he is reassured that this matrix is merely an array of terms such that all the columns and rows sum to zero. This rather remarkable property enables the z parameters of one configuration to be transformed simply to that of another by addition. The construction of the indefinite impedance matrix is illustrated in Fig. 2.

The set of z parameters representing any of the three configurations is now obtained by mentally crossing out the row and column corresponding to the grounded terminal, the four remaining parameters being those required.

Formulae for Stage Calculations

Conventional formulae are now employed to relate the parameters of the indefinite matrix to the stage calculations. These formulae are developed for reference in the

Fig. 2. Construction of the indefinite impedance matrix

$$\begin{array}{c} \begin{array}{cccc} & C & E & B \\ C & r_b + r_c & -r_b & - \\ E & -r_b - \alpha r_c & r_b + r_c & - \\ B & - & - & - \end{array} \\ \text{G.B. } z \text{ parameters} \end{array} \rightarrow \begin{array}{c} \begin{array}{cccc} C & E & B & \\ r_b + r_c & -r_b & -r_e & C \\ -r_b - \alpha r_c & r_e + r_b & -(r_e - \alpha r_c) & E \\ \alpha r_c - r_e & -r_e & -\alpha r_c + r_e + r_c & B \end{array} \\ \text{The indefinite impedance matrix} \end{array}$$

Appendix. Fortunately, it turns out that the voltage gain A_v, and the output impedance Z_o may be derived directly from the formulae for the current gain A_i, and the input impedance Z_i, so that only two formulae require to be memorized.

Current Gain A_i (see Appendix equation (1a))

$$A_i = -z_{21}/(z_{22} + z_L) \quad \ldots\ldots\ldots\ldots\ (3)$$

where z_L = the load impedance.

Input Impedance Z_i (see Appendix equation (2a))

$$Z_i = (\Delta z + z_{11}z_L)/(z_{22} + Z_L) \quad \ldots\ldots\ (4)$$

where $\Delta z = z_{11} \cdot z_{22} - z_{12} \cdot z_{21}$

Voltage Gain A_v (derived from equations (3) and (4))

$$A_v = V_2/V_1 = -i_2z_L/i_1Z_1 = -z_{21}/(z_{22}+z_L) \cdot z_L \Big/ \frac{(\Delta z + z_{11}z_L)}{(z_{22} + z_L)}$$

$$= -z_{21}z_L/(\Delta z + z_{11}z_L) \quad \ldots\ldots\ldots\ldots\ldots\ (5)$$

Output Impedance Z_o

The expression for Z_o is easily derived by changing z_L to z_g, z_{11} to z_{22}, and z_{22} to z_{11} in the formulae for Z_i, i.e.

$$Z_o = (\Delta z + z_{22}z_g)/(z_{11}+z_g) \quad \ldots\ldots\ldots\ldots\ (6)$$

where z_g = the source impedance

Application

Calculate the voltage gain of a g.b. stage given the impedance values, $r_e = 50\Omega$, $r_b = 500\Omega$, $r_c = 2{\cdot}0\text{M}\Omega$, $r_g = 20\Omega$, $r_L = 200\text{k}\Omega$, and $\alpha = 0{\cdot}98$.

The indefinite impedance matrix is first constructed as shown in Fig. 2, and the *B* rows and columns crossed out.

The g.b. parameters are therefore:

$$\begin{vmatrix} z_{11} & z_{12} \\ z_{21} & z_{22} \end{vmatrix} = \begin{vmatrix} r_b + r_e & -r_b \\ -(r_b + \alpha r_c) & r_b + r_c \end{vmatrix}$$

Next the formula for the voltage gain, equation (5), is derived from the memorized formulae of current gain and input impedance, equations (3) and (4).

then:

$$A_v = z_{21}z_L/(\Delta z + z_{11}z_L) = (r_b + r_c\alpha)z_L/(\Delta z + (r_b + r_e)r_L) \quad \ldots\ldots\ldots\ (7)$$

Another advantage of the z parameters is that the source impedance r_g may be taken into account quite simply by adding its value to the appropriate z element; in this case r_e. Including therefore r_g, and substituting $\Delta z = z_{11}z_{22} - z_{12}z_{21}$:

$$A_v = \frac{(r_b + \alpha r_c)\, r_L}{(r_b + r_c + r_L)\,(r_g + r_e + r_b) - r_b\,(r_b + \alpha r_c)}$$

$$\simeq \frac{\alpha r_c r_L}{(r_c + r_L)\,(r_g + r_e + r_b) - r_b \alpha r_c} \quad \text{as } r_b \ll r_c$$

$$= \frac{0{\cdot}98 \times 2{\cdot}0 \times 10^6 \times 200 \times 10^3}{2{\cdot}2 \times 10^6 \times 570 - 500 \times 0{\cdot}98 \times 2{\cdot}0 \times 10^6} = 1\,440$$

It is worthwhile summarizing what has been achieved with this technique. One can in fact work out from memory, stage calculations for any of the three configurations. This is quite a profit on the net cost of memorizing two formulae, the g.b. equivalent T circuit, and the letter order *C.E.B.*

Frequency Modifications

In order to account for the effects of frequency in the g.e. equivalent circuit, it is necessary to study the frequency dependence of the z parameters. Consider the circuit shown in Fig. 3(a), in which Ce and Cc, the emitter transit capacitance and collector junction capacitance respectively, have been added to the circuit of Fig. 1. Van de Ziel[3] has shown that such a circuit is a very close approximation to a junction transistor at relatively high frequencies.

An application of Norton's theorem to the collector arm of Fig. 3(a), results in the circuit shown in Fig. 3(b), which may likewise be transformed to the circuit of Fig. 3(c). The emitter current which controls the current generator is the current which flows in r_e, or:

$$i_e' = \frac{i_e}{1 + j\omega C_e r_e} = \frac{i_e}{1 + sC_e r_e}$$

where $s = j\omega$.

The final modified circuit is shown in Fig. 3(d). Except for very complex circuits, the T circuit is the most accurate, although other forms and arrangements of the equivalent circuit are more convenient for particular purposes such as measurements of parameters. It is apparent that by substituting $z_e' = 1/((1/r_e) + sC_e)$ and $z_c' = 1/((1/r_c) + sCc)$, for r_e and r_c respectively, and $\alpha_f = \alpha/(1 + sr_eC_e)$ for the current gain, in the low-frequency T circuit of Fig. 1, the indefinite impedance matrix of Fig. 2 may now be used for high frequency calculations. For convenience write:

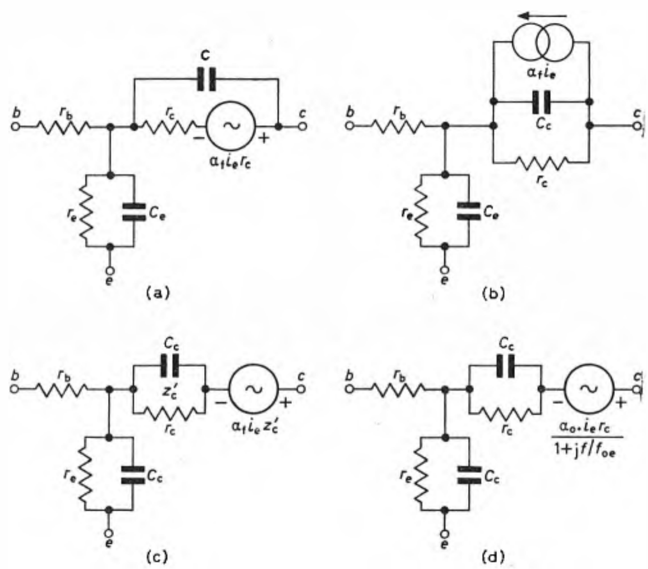

Fig. 3. Grounded emitter high frequency equivalent T circuit

$$z_e' = \frac{r_e}{1 + sr_eC_e} = \frac{r_e}{1 + jf/f_{oe}}$$

and:

$$z_c' = \frac{r_c}{1 + sr_cC_c} = \frac{r_c}{1 + jf/f_{oc}}$$

where f_{oe} is the 3dB point cut-off frequency of the emitter to collector current gain, and $f_{oc} = 1/2\pi C_c r_c$.

y Parameters

The indefinite admittance matrix may be derived from the indefinite impedance matrix by changing the position of its elements, dividing each element by Δz, and reversing the order of the letters *C.E.B.* Such a transformation is based on the inverse matrix. For clarity the transformation is shown diagrammatically using equivalent T parameters.

$$
\begin{array}{c|ccc|}
 & C & E & B \\
\hline
C & r_b+r_e & -r_b & -r_e \\
E & -(r_b+\alpha r_c) & r_b+r_c & -(r_c-\alpha r_c) \\
B & -r_e+\alpha r_c & -r_c & r_c+r_e-\alpha r_c
\end{array}
\quad z \quad \text{to} \quad
\begin{array}{|ccc|c}
B & E & C & \\
\dfrac{r_e + r_c - \alpha r_c}{\Delta z} & \dfrac{-(r_c - \alpha r_c)}{\Delta z} & \dfrac{-r_e}{\Delta z} & B \\
\dfrac{-r_c}{\Delta z} & \dfrac{r_c + r_b}{\Delta z} & \dfrac{-r_b}{\Delta z} & E \\
\dfrac{\alpha r_c - r_e}{\Delta z} & \dfrac{-r_b - \alpha r_c}{\Delta z} & \dfrac{r_e + r_b}{\Delta z} & C
\end{array}
\quad y
$$

Similarly, employing the principle of duality, the formulae for stage calculations in terms of the y parameters may be derived from the corresponding formulae in the z form by substituting y for z, i for v, and v for i (see Table 1).

In the example to follow, the y matrix for a series impedance, shown in Fig. 4 will be used. Whereas the z parameters are characterized by their open-circuit properties, the y parameters are characterized by their short-circuit properties. One can therefore write down from inspection of the series circuit below, that $y_{11} = y_{22} = 1/z$; similarly $y_{12} = y_{21} = -1/z$.

The y equations are:

$$i_1 = V_1 y_{11} + V_2 y_{12} \quad \ldots\ldots\ldots\ldots\ldots \quad (8)$$

$$i_2 = V_1 y_{21} + V_2 y_{22} \quad \ldots\ldots\ldots\ldots\ldots \quad (9)$$

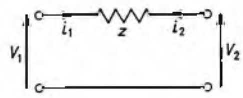

$$\begin{vmatrix} 1/z & -1/z \\ -1/z & +1/z \end{vmatrix} = \begin{vmatrix} y_{11} + y_{12} \\ y_{21} + y_{22} \end{vmatrix}$$

Fig. 4. y parameters for a series impedance

Application

The following example of unilateralization in the equivalent T circuit is intended to emphasize certain useful aspects of the indefinite admittance matrix for circuit analysis. Unilateralization is a particular neutralization process which eliminates the inherent undesirable feedback property of a bilateral four terminal network, and converts it into a unilateral four terminal network. The aim then is to synthesize a simple network which when connected between the collector and base of a g.e. stage effectively neutralizes feedback from the collector to base. Consider first the unilateralized stage shown in Fig. 5,

where Y_n, Y_t and Y_L represent the neutralized matrix, the transistor high frequency indefinite admittance matrix, and the load matrix respectively. The admittance circuits may be connected in shunt, simply by adding together the corresponding matrices in an appropriate manner. For example, the neutralizing matrix is embedded on the C and B column and rows, whereas the load matrix is similarly embedded on the C and E column and rows. (Y_n and Y_L are designated by an asterisk).

The required g.e. matrix

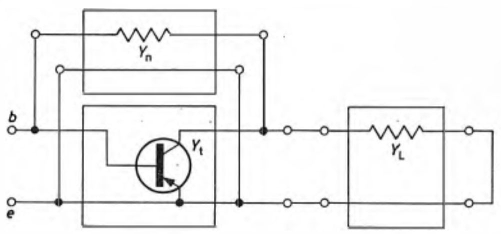

$$\equiv \begin{vmatrix} y_{11} & -y_{12} \\ -y_{21} & +y_{22} \end{vmatrix}$$

$$
\begin{array}{c|ccc|}
 & B & E & C \\
B & \dfrac{z_e' + z_c'(1-\alpha_f)}{\Delta z'} + 1^*/z_n & \dfrac{-z_c'(1-\alpha_f)}{\Delta z'} & \dfrac{-z_e'}{\Delta z'} - 1^*/z_n \\
E & \dfrac{-z_c'}{\Delta z'} & \dfrac{z_c' + r_b}{\Delta z'} + 1^*/R_L & \dfrac{-r_b}{\Delta z'} - 1^*/R_L \\
C & \dfrac{\alpha_f z_c' - z_e'}{\Delta z'} - 1^*/z_n & \dfrac{-r_b - \alpha_f z_c'}{\Delta z'} - 1^*/R_L & \dfrac{z_e' + z_b}{\Delta z'} + 1^*/R_L + 1^*/z_n
\end{array}
$$

Fig. 5. G.E. unilateralized stage

is obtained as usual by crossing out the row and column E. For neutralization, the reverse transfer admittance y_{12} is equated to zero:

$$-z_e'/\Delta z' - (1/z_n) = 0, \text{ and } z_n = -(\Delta z'/z_e') \quad \ldots\ldots \quad (10)$$

The minus sign indicates that a phase reversing transformer will be required. It is shown in the Appendix that

$$\Delta z' = z_e'(z_c' + r_b(1-\alpha_f)) + z_c' r_b$$

and that substituting for $\Delta z'$ in equation (10), and neglecting the sign:

$$1/z_n = \frac{r_e + s\,.\,C_e r_c r_e}{r_c(r_e + r_b(1-\alpha)) + r_b r_e + s\,.\,r_e r_b r_c(C_e + C_c)} = \frac{(1+s\,.\,T_1)}{R'(1+s\,.\,T_2)} \quad \ldots\ldots\ldots\ldots \quad (11)$$

Further it is shown in the Appendix that the impedance z_n may be synthesized into the following form of network, which is merely one of the many forms it can take. However it should be noted that the particular form shown in Fig. 6 closely resembles the transistor network, which of course is only to be expected of a neutralizing circuit.

TABLE 1. Stage Formulae

	z	y
Current Gain A_i	$-z_{21}/(z_{22} + z_L)$	$-y_{21}y_L/(y_L y_{11} + \Delta y)$
Input Impedance Z_i	$\Delta z + z_{11}z_L/(z_{22} + z_L)$	$Y_i = \Delta y + y_{11}y_L/(y_{22} + y_L)$
Voltage Gain A_v	$-z_{21}z_L/(\Delta z + z_{11}z_L)$	$-y_{21}/(y_{22} + y_L)$
Output Impedance Z_o	$\Delta z + z_{22}z_g/(z_{11} + z_g)$	$Y_o = \dfrac{\Delta y + y_{22}y_g}{(y_{11} + y_g)}$

Conclusions

An attempt has been made to outline a simple unified approach to small-signal calculations. The equivalent T circuit, when related to the indefinite impedance matrix

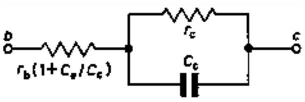

Fig. 6. Neutralizing network

is shown to provide a canonical basis, whereby the z parameters in algebraic form of one configuration may be transformed directly to another. Transformation from impedance to admittance form is similarly direct. For the student, it is emphasized that although the object here has been to avoid nodal analysis[3], and successive matrix operation, the former merits first place as an introduction. The indefinite impedance matrix for h parameters is included in the Appendix; and the reader is recommended to round off this technique by relating the h parameters and the hybrid π equivalent circuit to the indefinite admittance matrix.

Acknowledgment

The author is indebted to Mr. R. Walker, Senior Lecturer, Sheffield College of Technology for stimulating discussions and criticisms in connexion with this article.

Appendix

Formulae for Stage Calculations

Current Gain A_i

Substituting $V_2 = -i_2R_L$ into equation (2) then $-i_2R_L = -i_1z_{21}+i_2z_{22}$; therefore:

$$A_i = (-i_2/i_1) = \frac{-z_{21}}{z_{22}+R_L} \quad \ldots\ldots\ (1a)$$

Input Impedance

Substituting for A_i into equation (1), then:

$$Z_i = V_1/i_1 = z_{11} - \frac{z_{21}z_{12}}{z_{22}+R_L}$$

therefore:

$$Z_i = \frac{\Delta z + z_{11}R_L}{z_{22}+R_L}$$

where:

$$\Delta z = z_{11}z_{22} - z_{12}z_{21}. \quad \ldots\ldots\ldots\ldots\ldots\ldots\ (2a)$$

It should be noted carefully, that Δz is invariant for a given transistor, for any configuration provided external elements are not added. In the formulae for stage calculations above, Δz is made up of the final matrix elements.

Neutralizing Network

$\Delta z'$ is evaluated using the elements of the g.c. stage matrix of Fig. 5. i.e.:

$$\Delta z' = (r_b+z_e')(r_b+z_c') - r_b(r_b+\alpha_t z_c')$$
$$= z_c'(z_c'+r_b(1-\alpha_t)) + z_e'r_b \quad \ldots\ldots\ldots\ldots\ (3a)$$

As $z_c' \gg r_b$, $z_e'r_b$ is often neglected.

From equations (3a) and (10),

$$-z_n = \Delta z'/z_c' = \frac{1+s\,.\,C_er_c}{r_c}\left[\frac{r_c}{1+s\,.\,C_cr_c}\,.\,\left[\frac{r_e}{1+s\,.\,C_er_e} + r_b\left(1-\frac{\alpha}{1+s\,.\,C_cr_c}\right)\right] + \frac{+\,r_br_e}{1+s\,.\,C_er_e}\right]$$

Rearranging:

$$-z_n = \frac{r_cr_e + r_cr_b(1-\alpha) + r_br_e + s\,.\,(C_e+C_c)\,r_br_er_c}{r_e + s\,.\,r_eC_cr_c}$$

To identify z_n as a network, the following continued-fraction is made[4], which may be arranged in ascending, or descending orders of s. Choosing the latter, then by long division:

$$s\,.\,C_cr_cr_e + r_e / \frac{r_b(1+(C_e/C_c))}{s\,.\,r_cr_br_e(C_e+C_c) + r_c[r_e+r_b(1-\alpha)] + r_br_e}$$
$$\frac{s\,.\,r_cr_br_e(C_e+C_c) + r_er_b(1+(C_e/C_c))}{\ldots\ldots\ldots\ldots\ r_c[r_e+r_b(1-\alpha)]} - r_er_b\,.\,(C_e/C_c)$$

and:

$$-z_n = r_b(1+(C_e/C_c)) + \frac{r_c[1+r_b(1-\alpha)/r_e - r_bC_e/r_cC_c]}{1+s\,.\,C_c\,.\,r_c}$$
$$\simeq r_b(1+(C_e/C_c)) + \frac{1}{(1+s\,.\,C_c\,.\,r_c)/r_c}$$

as $r_b(1-\alpha)/r_e - r_bC_e/r_cC_c \ll 1$;

$$= r_b(1+(C_e/C_c)) + \frac{1}{(1/r_c)+s\,.\,C_c} = R_1 + \frac{1}{G_2+Y_2}$$

The corresponding network is shown in Fig. 6.

h Parameters (Indefinite Impedance Matrix)

$$\begin{array}{c|ccc|} & C & E & B \\ C & \Delta h_b/h_{ob} & -h_{rb}/h_{ob} & (h_{rb}-\Delta h_b/h_{ob} \\ E & h_{fb}/h_{ob} & 1/h_{ob} & -(1+h_{fb})/h_{ob} \\ B & -(h_{fb}+\Delta h_b)/h_{ob} & (h_{rb}-1)/h_{ob} & \dfrac{-h_{rb}+\Delta h_b+(1+h_{fb})}{h_{ob}} \end{array}$$

Note here that $\Delta h_b = h_i\,.\,h_o + h_f\,.\,h_r$, where these parameters are measured in the g.b. configuration as is the normal practice of the manufacturers. The invariant ΔH of the above matrix is however h_{ib}/h_{ob}; h_{fb} is negative.

References

1. Shekel, J. Voltage-Reference Node. *Wireless Engr. 31*, 6 (1954).
2. Van der Ziel. Solid State Physical Electronics, p. 344. (Macmillan).
3. Jones, F. R. B. Nodal Analysis. *Wireless World. 66*, 556 and 599 (1960).
4. Hazony, D. Elements of Network Synthesis. (Chapman & Hall. 1963).
5. Zadeh, L. P. A. A Note on the Analysis of Vacuum Tubes and Transistor Circuits. *Proc. Inst. Radio Engrs. 41*, 989 (1953).
6. Rogers, D. W. W. Direct Reduction of a Multi-Mesh Circuit to a Four Terminal Network. *Electronic Engng. 37*, 678 (1965).
7. Shekel, J. Matrix Representation of Transistor Circuits. *Proc. Inst. Radio Engrs. 45*, 1493 (1957).

A Diamond Thermistor

General Electric (USA) has developed a diamond thermistor which can be used as a temperature sensor over the range −325° to +1200°F.

In addition to its extremely wide temperature range, the new thermistor has demonstrated excellent long-term stability and repeatability. It also offers fast response to temperature changes—since the diamond sensing element is small and has a high thermal conductivity. In addition, it is small, rugged, hermetically sealed, and corrosion resistant. Because of its small and uniform size, the G-E thermistor is ideally suited for either probes or permanent installation, and it can be used in almost any fluid medium.

Semiconducting diamond is extremely rare in nature, and accounts for less than 1 per cent of natural diamond. But it can be grown at will using a high temperature, ultra high-pressure process discovered at the G.E. Research and Development Center.

The starting material for man-made diamond is graphite. The transformation of this into diamond may be accomplished by the action of a molten metal catalyst and the simultaneous application of pressures of about one million pounds per square inch and temperatures above 2 000°F. (Without the metal catalyst, the process requires pressures as high as three million pounds per square inch and temperatures above 9 000°F.)

The invention of made-made diamond was announced by the General Electric Company in 1955. Several years later, it was discovered that semiconducting diamond may be grown by adding impurities (such as boron, beryllium, or aluminium) to the starting mixture of graphite and catalyst. The semiconducting diamond crystal produced for G.E.'s new thermistor weighs about ·0004 carats and approaches a cube in shape, with about 0·015in per side.

Semiconducting diamond also has been prepared by diffusing boron and aluminium into man-made or natural diamond at high pressures and temperatures. All semiconducting diamonds made so far by these two processes has been p-type (positive current carriers).

A Thermocouple Wattmeter for Magnetic Loss Measurement

By J. K. Choudhury*, M.Sc., M.Sc.(Tech.), D.Phil., M.I.E.E., R. K. Mondal*, M.Sc.(Tech), M.E.E, and S. N. Bhattacharyya*, M.Sc., M.E.E., Ph.D.

The article describes a thermal wattmeter circuit employing a matched pair of vacuo-junction thermocouples for core-loss measurements. The circuit employed by the authors differs from the conventional thermal wattmeter circuit. High sensitivity has been achieved by using a suspended moving-coil galvanometer as the indicating instrument.

Selected experimental results are included to illustrate the suitability and simplicity of the method for core-loss measurements under normal and incremental conditions of excitation in the test core. Measurements have been carried out over a frequency range of 50Hz to 50kHz. The overall accuracy obtained was of the order of 1 per cent of the full-scale deflexion.

A combined set-up incorporating the present thermal wattmeter and an electrostatic wattmeter was devised for the measurement and comparison of core-loss under identical test conditions. Excellent agreement was obtained between the results of the two methods.

(Voir page 63 pour le résumé en français: Zusammenfassung in deutscher Sprache auf Seite 70)

A.C. bridges[1,2] constitute the most widely used method for core-loss measurements at audio and higher frequencies. The method however suffers from certain limitations; the presence of harmonics in the exciting current wave, particularly during incremental measurements, causes difficulty in obtaining a sharp balance. Furthermore, multiple-screened components and special forms of earthing such as Wagner earthing are often necessary for the reduction of the effects of earth capacitances. The electrostatic wattmeter[3] has been used for core-loss measurements at audio and higher frequencies. Unless the sensitivity is increased by the use of amplifiers for the current and voltage circuits, the electrostatic wattmeter cannot measure very small power dissipation occurring in small cores or at low flux densities.

Thermal methods employing calorimeter[4] and vacuum thermocouples[5] offer certain advantages for core-loss measurements. The upper frequency limits of these methods may be quite high. Also, methods employing thermocouples are essentially simpler than a.c. bridges. The calorimetric method is rather slow and tedious, and requires the dissipation of several watts for accurate measurements. In the thermocouple wattmeter advantage is taken of the sensitivity and accuracy of the permanent magnet moving-coil instrument, and low power can be measured conveniently with the help of it.

The thermocouple wattmeter[6,7,8,9] employs two matched thermal elements (insulated vacuum thermojunctions) in such a manner as to obtain a d.c. voltage proportional to the average power in the load. It thus offers potentiality for use as a method of core-loss measurement at power, audio, and higher frequencies although no such attempt appears to have been made. The present authors employ a circuit involving two matched thermocouples which in conjunction with a high sensitivity d.c. galvanometer gives a direct indication of core-loss in a magnetic sample. The circuit differs from the conventional thermal wattmeter circuits.

Theory of the Present Method

The circuit arrangement of the present method for core-loss measurements is shown in Fig. 1. The switch S_w is normally to be used in position 1. The sample has a magnetizing winding of n_1 turns and a centre-tapped secondary winding of n_2 turns. A non-reactive shunt S is connected in series with the primary winding n_1 of the sample, the ohmic value of S being very small compared to the impedance of the exciting winding. Evidently the voltage-drop across S will be proportional to and in phase with the exciting current i. The heaters of two matched thermocouples T_1 and T_2 in series with high resistances R_1 and R_2 are connected across the secondary as shown. The total resistances R_t of each thermocouple heater circuit are made equal. The voltage-drop across S is connected between the points O and P of the secondary circuit of the sample, O being the centre-tap of the secondary winding n_2 and P the junction of the heater circuits. Ideally, the points O and P are equipotential. The outputs of the thermocouples in series opposition are connected across a sensitive d.c. galvanometer G.

The total current flowing through the heater of each thermocouple consists of (a) a circulating component i_e proportional to the induced voltage e in the exciting winding, and (b) a component i_s proportional to the excit-

* *Jadavpur University, Calcutta, India.*

ing current i. These two components are:

$$i_o = \frac{n_2 e}{n_1 2R_t} \quad \ldots\ldots\ldots\ldots\ldots\ldots\ldots\ldots\ldots\ldots (1)$$

$$i_s = \frac{Si}{R_t + 2S} \quad \ldots\ldots\ldots\ldots\ldots\ldots\ldots\ldots\ldots (2)$$

While the currents i_o and i_s [as given by equations (1) and (2) respectively] add together in the heater of the thermocouple T_1, they oppose each other in the other heater circuit. So the heater current i_1 of the thermocouple T_1 will be:

$$i_1 = \frac{n_2 e}{2n_1 R_t} + \frac{S}{R_t + 2S}\, i \quad \ldots\ldots\ldots\ldots\ldots\ldots (3)$$

and that for the thermocouple T_2 will be:

$$i_2 = \frac{n_2 e}{2n_1 R_t} - \frac{S}{R_t + 2S}\, i \quad \ldots\ldots\ldots\ldots\ldots\ldots (4)$$

Now, if the thermocouples are matched, the output voltage e_c may be assumed to be ideally related to the heater current i_c by the same law:

$$e_c = K i_c^2 \quad \ldots\ldots\ldots\ldots\ldots\ldots\ldots\ldots\ldots\ldots\ldots (5)$$

So the total output E of the thermocouple circuit, acting

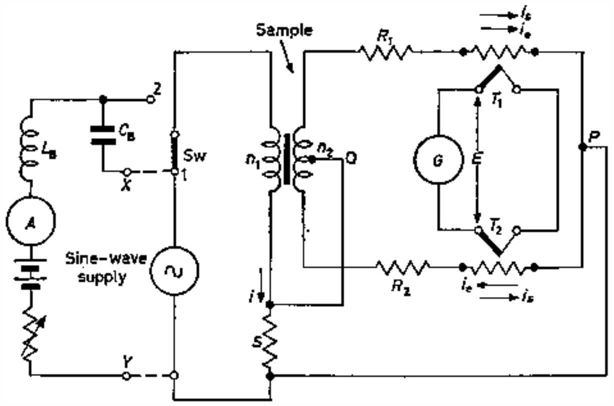

Fig. 1. The present thermocouple wattmeter

across the galvanometer G, will be given by:

$$E = f \int_0^{1/f} K\,[i_1^2 - i_2^2]\, dt$$

$$= f \int_0^{1/f} K \left[\left(\frac{n_2 e}{2n_1 R_t} + \frac{Si}{R_t + 2S} \right)^2 - \left(\frac{n_2 e}{2n_1 R_t} - \frac{Si}{R_t + 2S} \right)^2 \right] dt \quad \ldots\ldots (6)$$

f being the supply frequency. Thus:

$$E = f \int_0^{1/f} \left[2K\,(n_2/n_1)\, \frac{S}{R_t\,(R_t + 2S)} \right] . \, ei\, dt$$

$$= C\, [f \int_0^{1/f} ei\, dt] \quad \ldots\ldots\ldots\ldots\ldots\ldots\ldots\ldots\ldots\ldots (7)$$

where

$$C = 2K\,(n_2/n_1)\, \frac{S}{R_t\,(R_t + 2S)}$$

Therefore, the indication of the galvanometer is proportional to the core-loss in the sample. The value of C is easily calculated from known constants of a given set-up, the magnitude of K being obtained by an experimental determination of the thermocouple characteristic in accordance with equation (5).

It may be noted that the exciting winding copper loss along with power loss in the resistance S is eliminated from the output indication. However, the ohmic loss in the heater circuit due to the circulating current i_o through the two resistances R_t is included in the reading. This loss is usually very small as R_t is quite large; in any case, it can easily be corrected for if required.

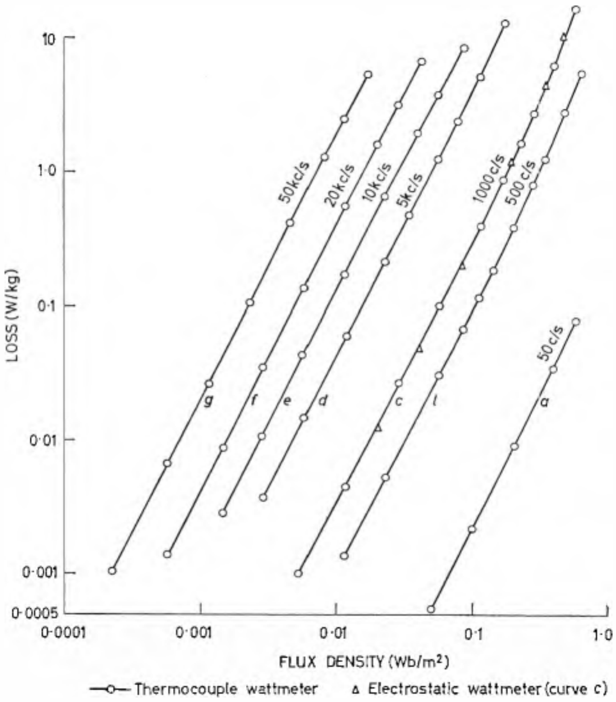

Fig. 2. Variation of core-loss with flux density for coiled Mumetal strip

Strip section: 0·0125m × 0·000375m

Effects of Harmonics in the Current Wave

It is well known that due to the non-linear B/H relation of a magnetic core, the exciting current will contain harmonics for a sinusoidal flux variation in the core. So the exciting current i can be written, in the general form, as:

$$i = \sum_{n=1,2,3\ldots} I_{n(pk)} \sin\,(n\omega t + \phi_n) \quad \ldots\ldots\ldots\ldots (8)$$

(normally, except for the incremental case, the even harmonics are absent). Hence the output E as given by equation (7) should be modified to read as:

$$E = Cf \int_0^{1/f} [\, e \sum_{n=1,2,3\ldots} I_{n(pk)} \sin\,(n\omega t + \phi_n)]\, dt \ldots . (9)$$

So long as flux density in the core is sinusoidal, e will also be sinusoidal (containing only the fundamental). Since the output is the average voltage as represented by the right-hand side of equation (9), the current wave harmonics will have no effect on the indication. In this respect the present circuit behaves as a true wattmeter method, requiring no correction for the harmonics in the current wave. This gives it a distinct advantage over bridge methods in which a correction[4] must be applied for the harmonic ohmic dissipation in the external resistance (S) of the exciting circuit.

Modification for Incremental Measurement

The circuit of Fig. 1 may easily be adapted for incremental core-loss measurements[10]. For this purpose, the switch S_w of Fig. 1 is changed over to position 2 from position 1 and the circuit between the terminals X and Y is connected across the alternating supply source along the dotted lines. The same winding on the sample is used for both a.c. and d.c. excitations. A high inductance choke coil L_B limits the a.c. in the battery circuit whereas a large value capacitor C_B blocks d.c. from flowing through the a.c. supply source but presents low impedance to the a.c. A part of the direct current flowing through the shunt S finds its path through the heaters of T_1 and T_2. However this direct current divides itself equally in the two halves of the secondary winding n_2 of the sample and also through the two heater circuits. This additional direct current has no adverse effect on the performance and accuracy of the equipment as long as the total current through the heaters does not exceed the rated value.

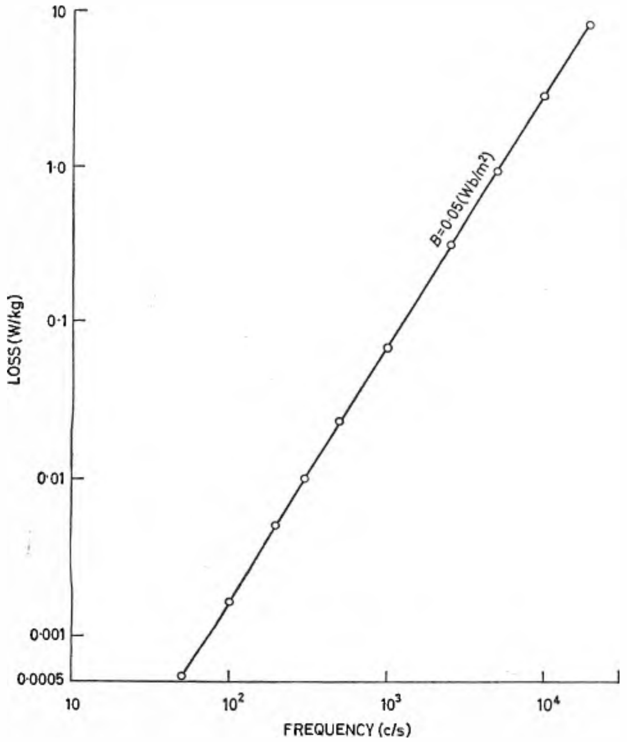

Fig. 3. Variation of core-loss with frequency for coiled Mumetal strip
Strip section: 0·0125m × 0·000375m

Matching of the Thermocouples

A batch of six precision grade thermocouples of insulated vacuo-junction type (Cambridge Instrument Co.) of identical current ratings was taken and the individual heater current/thermo-e.m.f. characteristics were determined separately, the open-circuit thermo-e.m.f. being measured by a d.c. potentiometer. Of the six thermocouples tested, two were chosen to form a nearly matched pair. The constants of the thermocouples forming the matched pair are shown in the table given below:

Thermocouple	T_1	T_2
Rated current	1·25mA	1·25mA
Heater-resistance	1370Ω	1410Ω
Couple-resistance	8·7Ω	8·0Ω
Thermo-e.m.f. at rated current	7·30mV	7·23mV

The exact matching of the thermocouple characteristics could be done in two ways:

(1) The heaters of T_1 and T_2 were connected in series and the thermocouple e.m.f.s were connected in series opposition. A variable resistance (of relatively high value) was connected across the output terminals of T_1 and matching of T_1 and T_2 was accomplished by gradually varying the said resistance till zero output voltage was obtained across the series combination of the thermocouples, with the same current flowing through the two heaters.

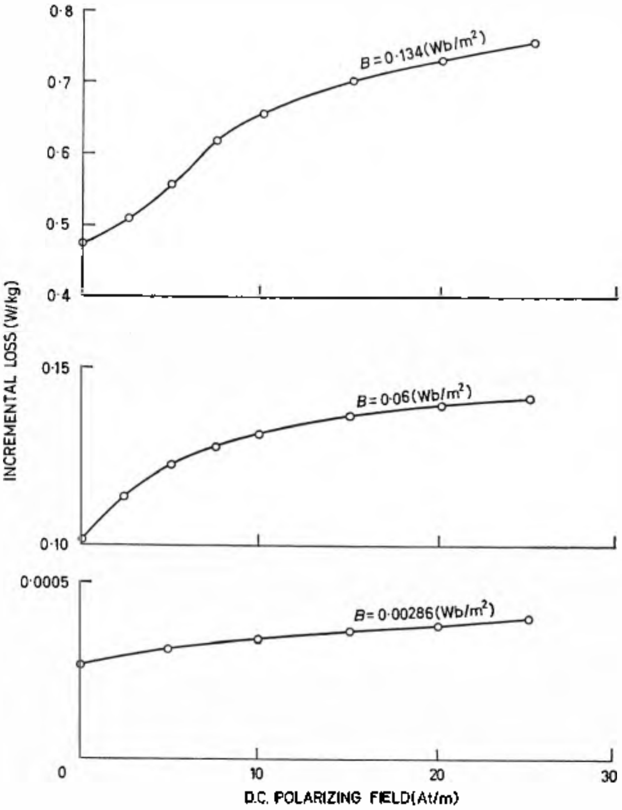

Fig. 4. Variation of incremental core-loss with polarizing field for coiled Mumetal strip
Strip section: 0·0125m × 0·000375m
Frequency: 1kHz

(2) A variable resistance (of relatively high value) could be connected across the heater of T_1 and the same adjusted till the thermocouple output voltages exactly balanced, with the same total current in the heater circuit.

It was found that very close matching of the thermocouple pair could be obtained by either of the above two methods over the entire heater current range.

Examples of Measurements

For the purpose of core-loss measurements, a reflecting galvanometer was used as indicator for the output voltage

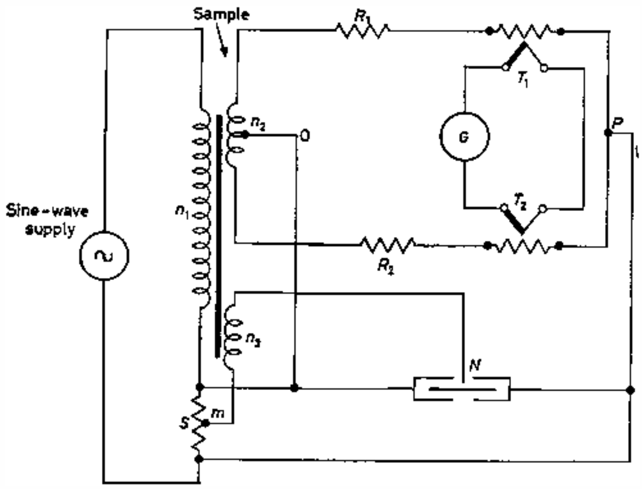

Fig. 5. Combined set-up for the thermocouple wattmeter and the electrostatic wattmeter

E of the oppositely-connected and matched thermocouple pair T_1 and T_2 of Fig. 1. The sensitivity of the galvanometer was of the order of 1 000mm/μA at a distance of 1m from the moving coil. For different flux densities in the test core, the total resistance R_t of the individual heater circuits of T_1 and T_2 was changed so as to operate the heaters at currents between 0·5mA and 1·0mA approximately.

The test sample consisted of a ring core of spirally coiled, 0·0125m wide and 0·000375m thick Mumetal tape, weighing approximately 0·25kg.

The examples of core-loss measurements given below and illustrated in Figs. 2, 3 and 4 have been selected to show

(a) The wide range of frequencies and power levels for which the method is suitable.

(b) The versatility of the method.

(c) The consistency of the results obtained.

Fig. 2 illustrates the variation of core-loss with flux density in Mumetal at seven different frequencies covering a power range of $3 \times 10^4 : 1$, and frequency range of 50Hz to 50kHz.

Fig. 3 shows the variation of core-loss with frequency at a constant flux density of 0·05Wb/m^2, covering a frequency range of 50Hz to 20 kHz.

The results of the incremental core-loss measurements are shown in Fig. 4 wherein the variation of core-loss with d.c. polarizing field at constant frequency and alternating flux density, is illustrated.

Comparison with the Electrostatic Wattmeter

The present circuit of the thermocouple wattmeter has marked similarities with the circuit of the electrostatic wattmeter in theory of operation. Matched thermal elements are used in the former in place of matched capacitances of the latter.

Fig. 5 illustrates a combined set-up incorporating an electrostatic wattmeter for the purpose of comparing some of the test results. A commercial portable electrostatic wattmeter[11] was used. In this figure, the resistance S serves as the quadrant shunt of the wattmeter. The induced voltage in a tertiary winding n_3 (preferably having the same number of turns as n_2) was applied between the mid-point m of the shunt S and the needle N of the electrostatic wattmeter. The combined test was carried out at a frequency of 1000Hz for the measurement of core-loss with varying flux density. Curve C of Fig. 2 shows the close agreement between the results obtained by the two methods under identical conditions.

Discussion

The principal merits of thermocouple instruments in general and the present thermocouple wattmeter in particular, are: comparative simplicity in construction, relative inexpensiveness, high sensitivity, and coverage of a very wide range of frequencies. The present equipment is particularly suitable for measurements at higher audio and radio frequencies at which other conventional methods are either complicated or inconvenient. Screening and earthing which pose considerable difficulty in a.c. bridge measurements, are remarkably simpler in the thermal wattmeter.

One of the serious limitations of thermocouple instruments is their rather high sensitivity to variation in the ambient temperature. The change in the heater resistance and change of thermo-e.m.f.'s due to change of base temperature tend to affect the performance[8] by 0·1 to 0·3 per cent/°C. In order to avoid this particular limitation of thermocouple equipment, the present series of tests was carried out in a temperature-controlled room.

An obvious source of error in the thermocouple type wattmeter is the non-conformity to a strictly square-law relationship between the heater current and the output thermo-e.m.f. of the thermo elements. Vacuum thermojunctions have been made in which the output is proportional to a power of the heater current higher than 2 and also to a power lower than 2, so that it should be possible to produce them with an output which is closely proportional to the square of the heater current[9]. In the present investigation, the error from this cause was estimated to be less than 0·3 per cent of the full-scale deflexion.

The overall accuracy of the present thermocouple wattmeter method was of the order of one per cent of full scale indication, which is considered to be reasonably good for most magnetic loss measurement purposes.

Acknowledgments

The authors thank the authorities of the Jadavpur University, Calcutta, for providing laboratory facilities for the investigation. Thanks are due to Mr. N. C. Dey, laboratory assistant of the electrical measurement section for useful services.

REFERENCES

1. Hague, B. Alternating Current Bridge Methods. (Pitman, 1957).
2. Lynch, A. C. Bridge Methods for Measurement of Magnetic Materials at Communication Frequencies. *Proc. Symposium on Precision Electrical Measurements*, pp. 1 and 11. (H.M. Stationery Office, 1955).
3. Choudhury, J. K., Glynne, A. The Use of an Electrostatic Wattmeter for Magnetic Loss Measurement. *Proc. Instn. Elect. Engrs. 98*, Pt. 2. 539 (1951).
4. Greig, J., Kayser, H. Iron-loss Measurements by A.C. Bridge and Calorimeter. *J. Instn. Elect. Engrs. 95*, Pt. 2, 205 (1948).
5. Brailsford, F., Bradshaw, C. G. Iron Losses at High Magnetic Flux Densities in Electrical Sheet Steels. *Proc. Instn. Elect. Engrs. 102A*, 463 (1955).
6. Brown, G. H., Epstein, J., Peterson, D. W. Direct-reading Wattmeters for Use at Radio Frequencies. *Proc. Inst. Radio Engrs. 31*, 403 (1943).
7. Kinnard, I. F. Applied Electrical Measurements. (John Wiley, 1962).
8. Harris, F. K. Electrical Measurements. (John Wiley, 1957).
9. National Physical Laboratory. Audio Frequency Power Measurements. (Notes on Applied Science, No. 8).
10. B.S. 933:1941, Specification for Magnetic Materials for Use Under Combined D.C. and A.C. Magnetisation.
11. Axworthy, F. R., Choudhury, J. K. The Design and Application of a Portable Electrostatic Wattmeter. *Trans. Soc. Instrum. Tech.*, *4*, No. 2, 2 (1952).

An Analysis of the Action of a Schmitt Trigger Circuit

By D. W. H. Hampshire*, B.Sc., M.I.E.E. and D. Petersen*, B.Sc., M.I.E.E., A.M.I.E.R.E.

This article considers in detail one of the several possible modes of operation of a transistor Schmitt trigger circuit. Conditions for regenerative switching are analysed and stable state conditions are calculated and compared with practice.

(Voir page 63 pour le résumé en français: Zusammenfassung in deutscher Sprache auf Seite 70)

THE Schmitt trigger circuit has been used extensively for many years, originally with valves and then with transistors, and its advantages are well known. A particularly useful feature of the circuit is that it will work satisfactorily over a wide range of circuit designs. Indeed, it is difficult to build a Schmitt circuit which will not work! It is perhaps for this reason that the theory behind the operation of the circuit is rather inadequately covered in the literature and in this article an attempt will be made to develop the theory and to show how it applies in practice to a particular design.

In the basic Schmitt circuit in Fig. 1 the mode of operation will be considered in which, in the initial state of the circuit, VT_1 is saturated and VT_2 is off and, on the application of a sufficiently positive voltage, VT_1 cuts off and VT_2 saturates.

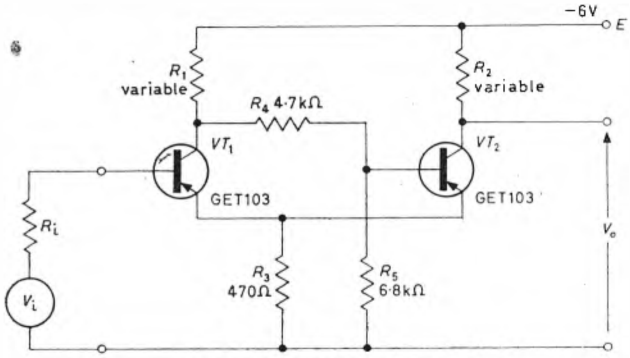

Fig. 1. The basic Schmitt circuit

Initial Conditions

A transistor is saturated when both junctions are forward biased. Thus, using the notation V for voltage with respect to earth, together with the appropriate subscript to denote the terminal and transistor, the condition for VT_1 to be saturated is:

$$V < V_{C1} < V_E \qquad (1)$$

These voltages will differ by only a few tenths of a volt and the critical condition for saturation to just occur will be

$$V_{B1} = V_{C1} \qquad (2)$$

If VT_1 is initially saturated VT_2 will be cut off by the voltage divider R_4R_5 holding the base potential of VT_2 positive with respect to V_E

i.e.

$$V_{B2} = V_{C1}\frac{R_5}{R_4 + R_5} \qquad (3)$$

and since $V_{B2} > V_E$, then, neglecting leakage current,

$$V_{B2} = E \qquad (4)$$

Switching Action

If VT_1 is initially saturated its terminal voltages will depend on the input source voltage and its internal impedance. Consider the two extreme cases: where this impedance is zero and then infinite. In the former case all the terminal voltages of VT_1 will follow the input voltage until

$$V_1 = V_E = E\frac{R_3}{R_1 + R_3} \qquad (5)$$

when the transistor just comes out of saturation and switching occurs. When the source impedance is infinite the base potential of VT_1 is clamped to the emitter potential given by equation (5) and the base current will fall until VT_1 comes out of saturation. Under some conditions between these two extremes the emitter and collector potentials of VT_1 will rise as the input voltage rises until VT_1 comes into its active region, after which its collector potential will fall while its emitter potential continues to rise. Thus the base voltage of VT_2 will fall while its emitter voltage rises and therefore a point will be reached where VT_2 begins to conduct.

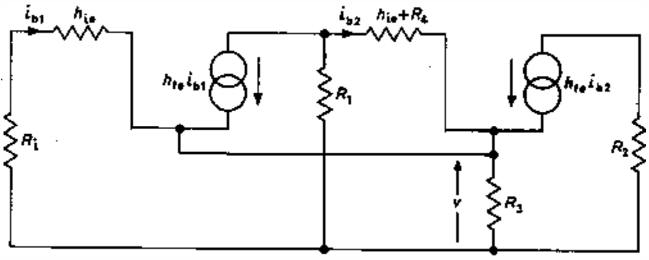

Fig. 2. An equivalent circuit for the switching state

When both transistors are in their active regions, the collector of VT_1 is driving the base of VT_2 whose emitter will vary in phase with it by emitter-follower action. The emitter-follower's output is the input to VT_1 which behaves therefore as a common base amplifier. If the loop gain of this system is greater than unity the changeover action will be regenerative and rapid switching will occur. When the circuit has switched VT_1 is cut off and VT_2 is conducting. In most applications VT_2 is required to saturate in order to minimize its collector power dissipation.

Conditions for Switching to be Regenerative

In order to determine the conditions for the regenerative switching action outlined in the previous section, an

* *Portsmouth College of Technology.*

incremental equivalent of the circuit of Fig. 1 is required. Fig. 2 shows such an equivalent circuit drawn on the assumptions that R_5 has negligible shunting effect on the input of VT_2 and both transistors are in their active regions during switch-over.

In Fig. 2 the resistor R_i is the input generator internal resistance. The transistors are represented by their simplified common emitter hybrid equivalent circuits and, therefore, since the switching action is extremely rapid, and the transistor parameters depend on the operating point, this will not give an accurate analysis. In practice it was found to be difficult to demonstrate the precise conditions at which the switching action became regenerative, so that the complicated work involved in a more exact analysis would be unable to be verified.

Referring to Fig. 2, for a loop gain of unity:

$$v \simeq h_{fe}(i_{b1} + i_{b2})R_3 \simeq -i_{b1}(h_{ie} + R_i)$$

$$\therefore h_{fe}R_3 i_{b2} \simeq -i_{b1}(h_{ie} + R_i + h_{fe}R_3)$$

Also $(h_{ie} + R_4)\,i_2 + v \simeq -(h_{fe}i_1 + i_2)\,R_1$

$$\therefore \quad (h_{ie} + R_4 + R_1)\,i_2 \simeq -i_1\,(h_{fe}R_1 - h_{ie} - R_1)$$

Dividing the equations to eliminate the base currents:

$$(h_{ie} + R_4 + R_1)/h_{fe}R_3 \simeq (h_{fe}R_1 - h_{ie} - R_i)/(h_{ie} + R_1 + h_{fe}R_3)$$

Since $h_{fe}R_3 \gg h_{ie} + R_1$ then:

$$R_1 \simeq (2h_{ie} + R_4 + R_i)/h_{fe}$$

Since the input resistance between the base of VT_2 and the common line is approximately $2h_{ie} + R_i$, the shunting effect of R_5 may be accounted for by putting:

$$R_1 \simeq \frac{2h_{ie} + R_4 + R_i}{h_{fe}} \div \frac{R_5}{2h_{ie} + R_i + R_5} \quad \ldots\ldots\ldots\ldots\ldots (6)$$

If the loop gain is less than unity, the circuit will behave as a two stage amplifier, the first stage of which has two antiphase outputs one from the collector and the other from the emitter of VT_1. These are applied simultaneously to the base and emitter of VT_2 so that the input and output of the Schmitt circuit are in phase (Fig. 3). In contrast to the regenerative switching conditions, the emitter voltage always follows the input voltage because the decrease in current through R_3 due to VT_1 switching off is greater than the increase in current through R_3 due to VT_1 switching on.

Starting Conditions

To find the voltage at the base of VT_1 to just start VT_2 conducting, it is assumed that

$$V_{B1} = V_E$$

Now

$$V_{B2} \simeq V_{C1}\frac{R_5}{R_4 + R_5}$$

and

$$V_{C1} = E - R_1 I_{R1}$$

where

$$I_{R1} = (V_E/R_3) + \frac{V_{C1}}{R_4 + R_5}$$

therefore

$$V_{B2} = \frac{R_5}{R_1 + R_4 + R_5}\,(E - (R_1/R_3)V_E)$$

and since

$$V_{B2} \simeq V_E$$

$$V_{B1} \simeq \frac{R_3R_5 \,.\, E}{R_1R_3 + R_3R_4 + R_3R_5 + R_1R_5} \quad \ldots\ldots (7)$$

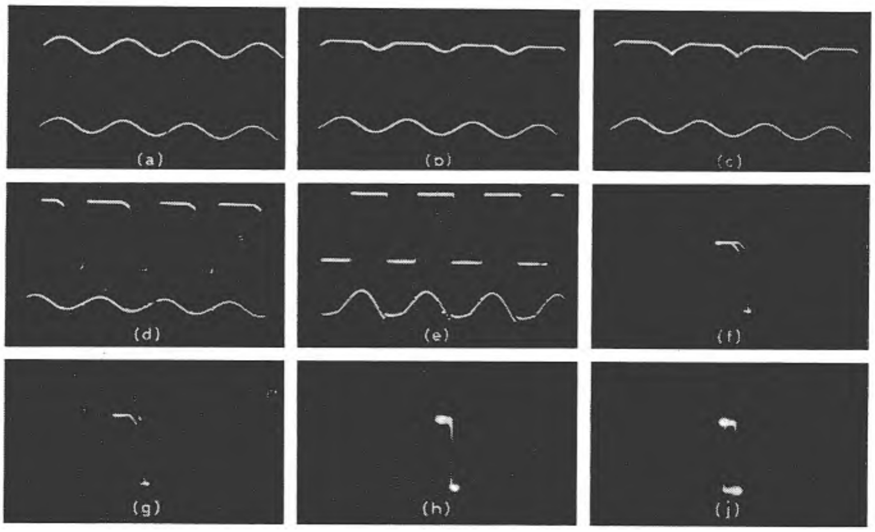

Fig. 3. Circuit waveforms

(a) Input and output voltages when the circuit is non-regenerative. (b) Input and output voltages when the circuit is just becoming regenerative. (c) The onset of regenerative switching. (d) Switching with negligible backlash. (e) Switching with backlash. (f) to (j) The hysteresis loop when R_1 = (f) 20Ω, (g) 50Ω, (h) 200Ω, (j) 640Ω

This gives the critical value of V_{B1} required to initiate switching.

Conditions When VT_2 is Saturated

These are found on principles similar to those used for finding the conditions for VT_1 to be saturated.

If R_2 is small, VT_2 will not be saturated.

Therefore, applying Thevenin's theorem,

$$V_{B2} = \frac{ER_5}{R_1 + R_4 + R_5} - \frac{R_1(R_4 + R_5)}{R_1 + R_4 + R_5}\,I_{B2}$$

If R_2 is large VT_2 will be saturated.

For VT_2 to be just saturated, $V_{B2} = V_{C2}$

Now

$$I_{C2} \simeq \frac{E - V_{CE(sat)}}{R_2 + R_3}$$

therefore

$$V_{C2} \simeq \frac{ER_3}{R_2 + R_3} + \frac{V_{CE(sat)}R_2}{R_2 + R_3} \quad \ldots\ldots\ldots (8)$$

When VT_2 is saturated VT_1 is off and its collector potential will be given by:

$$V_{C1} \simeq E \frac{R_4 + R_5}{R_1 + R_4 + R_5} \quad \ldots\ldots\ldots\ldots \quad (9)$$

Backlash in the Schmitt Circuit

When VT_2 saturates the emitter voltage is given by:

$$V_E \simeq \frac{R_3}{R_2 + R_3} E \quad \ldots\ldots\ldots\ldots \quad (10)$$

This will be the approximate voltage required at the base of VT_1 to switch on this transistor. The base voltage required to switch off VT_1 is given by equation (6) and the difference between these voltages is the backlash.

Experimental Results

INITIAL CONDITIONS

R_1 was adjusted until VT_1 just saturated.

The value of R_1 required was 640Ω. The terminal voltages of the transistors were measured under these conditions and found to be:

V_E	V_{B1}	V_{C1}	V_{B2}	V_{C2}
−2·4	−2·6	−2·6	−1·5	−6

These results confirm the equations (2), (3) and (4).

STARTING CONDITIONS

When R_1 was set to 1kΩ (i.e. VT_1 saturated initially) it was found that the base voltage of VT_1 at which the circuit switched was −2·7V. The theoretical value given by equation (7) is −2·5V.

CONDITIONS FOR VT_2 TO BE SATURATED

When R_2 was set to 500Ω it was found that VT_2 just saturated, with $V_{C1} = -5{\cdot}5$V and $V_{C2} = -3$V. Assuming a value of −0·2V for $V_{CE(sat)}$, equations (8) and (9) give $V_{C1} = -5{\cdot}5$V and $V_{C2} = -2{\cdot}9$V.

CONDITIONS FOR REGENERATIVE SWITCHING

In practice it was difficult to assess the precise value of R_1 at which switching became regenerative. Fig. 3(a) shows the input (lower trace) and output waveforms when $R_1 = 20\Omega$. When the base of VT_1 was connected to a variable supply regeneration was observed when $R_1 \geqslant 100\Omega$.

If a value of h_{ie} equal to 1kΩ is assumed then from equation (5) it is found that the circuit just becomes regenerative at $R_1 \simeq 100\Omega$ if the source impedance is negligible compared with h_{ie}. Fig. 3(b) shows the effect of increasing R_1 from 20Ω to 50Ω just before regeneration begins.

When $R_1 = 200\Omega$ the circuit switches regeneratively with little backlash as shown in Fig. 3(d). When $R_1 = 640\Omega$ the circuit gives a good switching waveform and has backlash as shown in Fig. 3(e). The hysteresis loops corresponding respectively to the values of R_1 given above are shown in Figs. 3(f) to 3(j). All the oscillographs were taken with $R_2 = 500\Omega$ (i.e. VT_2 just saturated) using a sine wave input at 1kHz, whose amplitude was just sufficient to trigger the circuit.

Conclusion

The stable conditions for one mode of operation of a Schmitt circuit have been found theoretically and experimentally. Allowing for the simplifying assumptions made in the analysis and the tolerance on components, good agreement was obtained between theory and practice.

The unstable state of the circuit, during which switching occurs, is easy to describe qualitatively but very difficult to analyse accurately. The approximate theoretical analysis used does, however, give a result which is consistent with the behaviour of the circuit in practice.

Acknowledgment

The work described in this article was performed in the Electrical Engineering Department, Portsmouth College of Technology and the authors wish to thank the Board of Governors of the college for the facilities provided and for permission to publish.

REFERENCES

Mullard Tech. Commun. 6, No. 51 (1961).
Mullard Tech. Commun. 7, No. 65 (1963).
STRAUSS, W. Wave Generation and Shaping. (McGraw-Hill, 1960).
MILLMAN, J., TAUB, H. Pulse, Digital and Switching Waveforms. (McGraw-Hill, 1965).

An Automatic Kidney Machine

Successful trials of a new automatic kidney machine, which could free hospital nurses for other duties, have just been completed at the Cardiff Royal Infirmary. The machine, the first on the European market to use the peritoneal dialysis technique, was built by the Industrial Automation Division of Hawker Siddeley Dynamics in association with the doctors at the Infirmary.

Peritoneal dialysis is an approved method of treatment for patients suffering from acute renal failure, and provides for the extraction of waste products from the blood normally dealt with by the kidneys. In cases where there is bleeding due to renal failure, peritoneal dialysis has an advantage of not requiring the use of anticoagulant as is necessary when cleansing the blood externally by haemodialysis.

In peritoneal dialysis, a sterilized dialysis fluid is pumped into the peritoneal (abdominal) cavity. Impurities in the blood, normally extracted by the kidneys, pass from the numerous blood vessels in the peritoneal lining into the liquid by a process called dialysis. This technique is simpler than the best known method for removing the waste products, in which the patient's blood is washed as it passes through a machine.

Previously the repeated peritoneal dialysis liquid changes have been made every hour by a nurse who has had to be in constant attendance for 12 to 24 hours.

The machine provides means of transferring under electronic control pre-determined quantities of solution at controlled pressure, temperature, and rate of flow, to and from the peritoneal cavity.

The system incorporates a number of safety devices for making a local visual and remotely situated audible alarm. These operate when temperature and pressure go out of limits, when there is a mains electricity power failure or when the supply of aqueous solution has reached a dangerously low level. Under any of these conditions the pump is automatically stopped and the system has to be manually checked and restarted.

The new automatic kidney machine, built by the Industrial Automation Division of Hawker Siddeley Dynamics in association with doctors at the Cardiff Royal Infirmary hospital

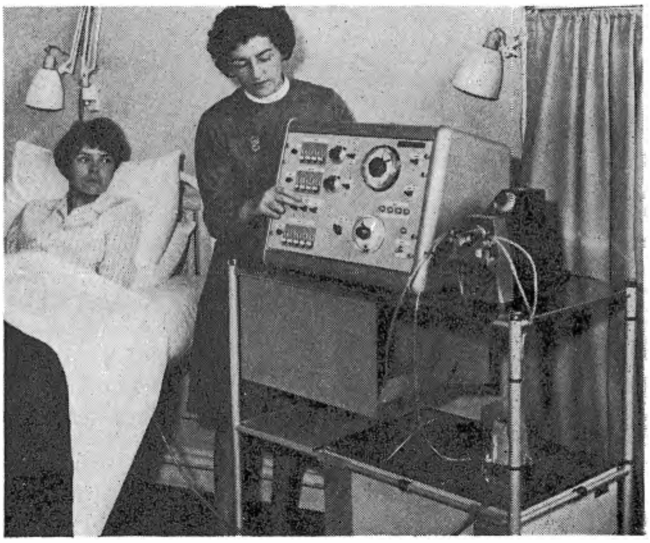

Firing an Adjustable-Frequency Three-Phase Invertor

By R. L. V. de Lima Mendes*

Three circuits are given for firing a three-phase invertor using silicon controlled rectifiers. The advantages and disadvantages of the three circuits are discussed and detailed circuit diagrams are given.

(Voir page 63 pour le résumé en français: Zusammenfassung in deutscher Sprache auf Seite 70)

THREE circuits for firing a three-phase invertor using s.c.r.'s are described.

The circuits were designed to fire a single d.c. side commutated invertor[2] (Fig. 1), however, with small changes they will apply to any three-phase bridge invertor.

Analysis of operation of such an invertor under reactive load conditions imposes the following conditions on the firing circuits:

(a) The circuit must supply two kinds of signals: Six 60° phased firing signals to invertor s.c.r.'s at the same frequency as the wave generated by the invertor and, two 180° phased firing signals to commutation s.c.r.'s at three times the invertor frequency.

(b) To allow for operation under inductive loads, the firing signals to invertor s.c.r.'s must be somewhat lengthened.

(c) The firing signals to invertor s.c.r.'s must be able to reset each s.c.r. 60° after its turn-on because commutation action does not apply to a single s.c.r., but to a whole side of the invertor each time. It seems advisable to provide resetting pulses after all commutations, for during the commutation period a transient may turn off a conducting s.c.r., even when the commutation pulse acts on the opposite side of the invertor. Such a need for resetting was also found when operating another kind of invertor (complementary impulse-commutated three-phase bridge invertor[3]) where no intrinsic unwanted commutations existed.

(d) Firing signals to invertor s.c.r.'s and to commutation s.c.r.'s must be phased in such a way as to allow for an s.c.r. to be turned off before firing of the opposite one, to avoid short-circuiting of the d.c. supply which would make commutation action difficult or even impossible.

Besides, the gate of a s.c.r. being turned off must have no positive drive during the commutation period. A similar feature concerning the other s.c.r.'s is recommended to minimize reverse leakage during commutation.

Three firing circuits for a single d.c. side commutated invertor which satisfy the above requirements were designed and tested. They all derive from the same basic sequential unit.

Basic Sequential Unit (Fig. 2)

A unijunction transistor relaxation oscillator supplies pulses at six times the invertor frequency to a flip-flop and a ring-counter.

The frequency of the oscillator may be manually controlled, by means of a potentiometer, or may follow an automatic programme.

The flip-flop divides by two providing two 180° phased signals at three times the invertor frequency suitable for firing the commutation s.c.r.'s.

The ring counter has three flip-flops interlocked by their steering networks.

This interlocking allows for two working modes: in the first the counter divides by six, providing 60° phased signals and in the other it makes no division and oscillates in synchronism with the input signal. This useless mode,

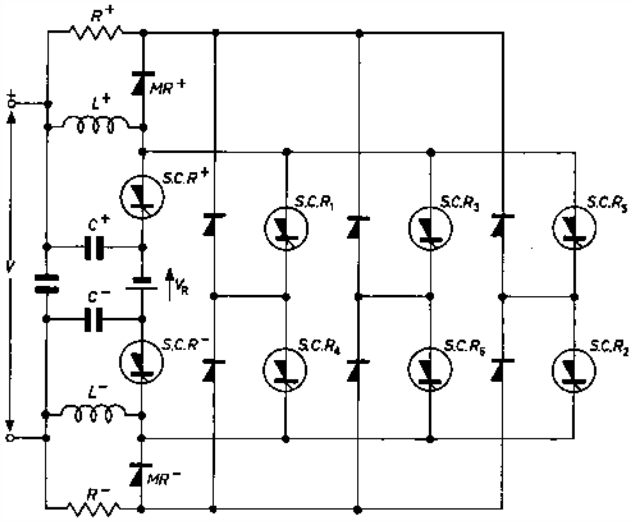

Fig. 1. Single d.c. side commutated three-phase invertor

Fig. 2. Basic sequential unit

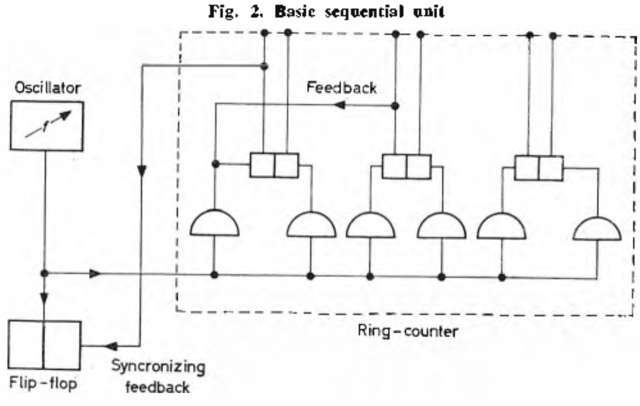

* *Laboratório de Fisica e Engenharia Nucleares, Sacavem, Portugal.*

with occurrence probability of 1/4, has been inhibited by feedback taken from the second to the first flip-flop.

Firing signals to invertor and to commutation s.c.r.'s are synchronized by means of another feedback network connected from ring-counter to commutation flip-flop.

Firing Circuits

Circuit of Fig. 3

Oscillator pulses are supplied to a 40μsec delay time single-shot multivibrator.

Switching of the multivibrator supplies a pulse to the commutation flip-flop and to the ring-counter, giving this the correct configuration for the next working 60°. Signals to the invertor s.c.r.'s are taken between the six outputs of the ring counter and the collector of the unstable side of the multivibrator (common point *G*).

In this way, during the multivibrator off time there are no firing signals to the invertor s.c.r.'s, which are only supplied when the multivibrator returns to its stable state. Thus one obtains delay, and the condition of no gate drive required for proper commutation.

Firing signals are supplied directly to the negative side

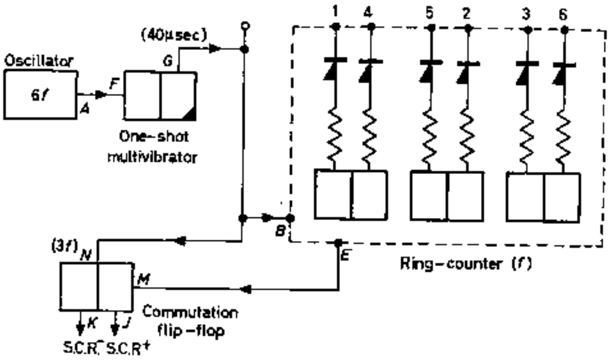

Fig. 3. Continuous wave firing circuit

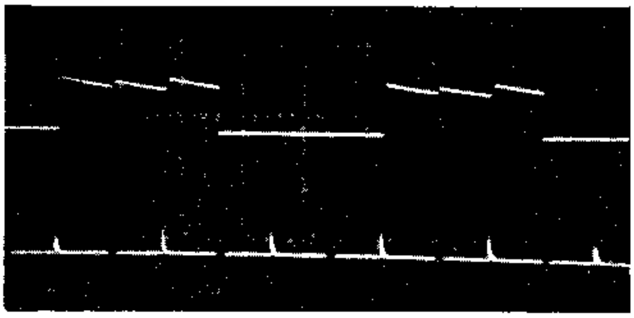

Fig. 4. Firing waveforms to a plus side invertor s.c.r. (top) and to SCR− commutation s.c.r. (bottom) 0.5msec/cm

Fig. 5. Same waveforms as in Fig. 4. 40μsec/cm

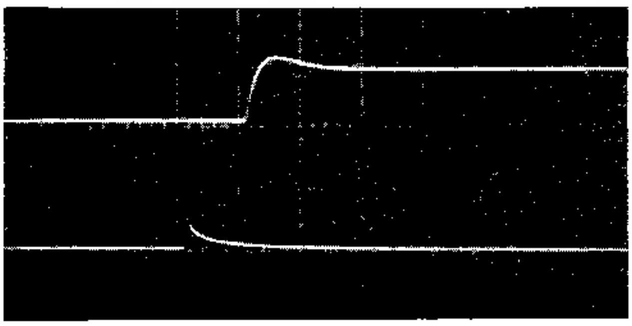

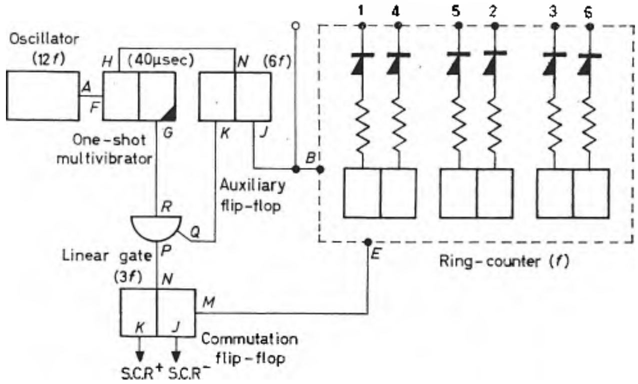

Fig. 6. Pulsed wave firing circuit

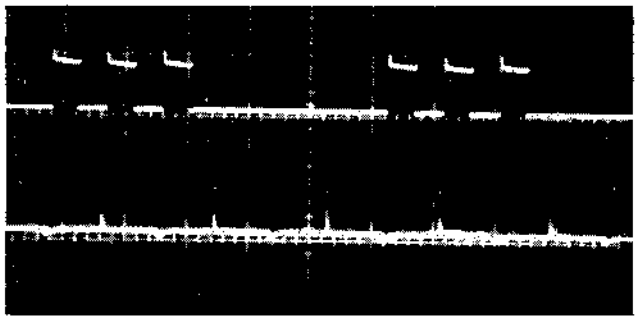

Fig. 7. Firing waveforms to a plus side invertor s.c.r. (top) and to SCR+ commutation s.c.r. (bottom) 0.2msec/cm

invertor s.c.r.'s and through an isolating transformer (non-differentiating) to positive side s.c.r.'s.

Firing signals to commutation s.c.r.'s are supplied through small differentiating transformers.

The upper trace of Fig. 4 shows the firing waveform to a positive side invertor s.c.r. and the lower trace the firing waveform to SCR^- commutation s.c.r. The scale is 5msec/cm.

In Fig. 5 the same waveforms in a faster scale (40μsec/cm) show the delay between a commutation pulse and the firing pulse to the s.c.r. opposite to the one turned off.

Circuit of Fig. 6

The unijunction oscillator is working now at 12 times the invertor frequency and supplies pulses to a 40μsec time delay one-shot multivibrator. Switching of the multivibrator supplies a pulse to the commutation flip-flop through a linear gate controlled by an auxiliary flip-flop.

Controlled by a flip-flop switching at half the frequency of the unijunction oscillator, the linear gate is open to each second pulse. Joint action of the linear gate and flip-flop provide the division by four, required to impose on the commutation flip-flop a working frequency equal to three times the invertor frequency.

When the multivibrator returns to its stable state it supplies a pulse to the auxiliary flip-flop feeding the ring counter. The firing signals to the invertor s.c.r.'s are taken between the six outputs of the ring counter and one collector of the auxiliary flip-flop (*J*). In this way, firing signals are obtained only when the *J* side of the flip-flop is not conducting. By auxiliary flip-flop and single-shot multivibrator actions the requirements of no gate drive during commutation and firing delay for safe turn-off are satisfied simultaneously. Fig. 7 shows the firing waveforms to a positive side invertor s.c.r. (top) and to SCR^+ commutation s.c.r. (bottom). Scale is 2msec/cm. The delay

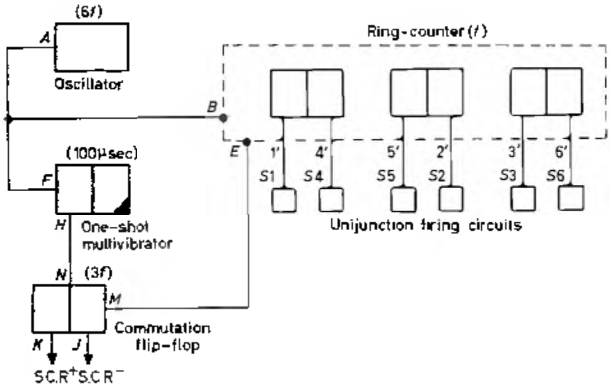

Fig. 8. Unijunction firing circuit

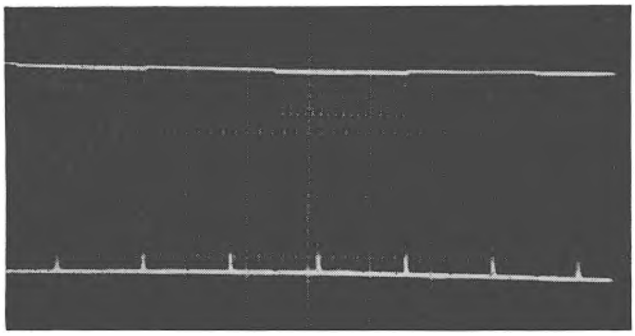

Fig. 9. Firing waveforms to a plus side invertor s.c.r. (top) and to SCR+ commutation s.c.r. (bottom) 0.5msec/cm

between commutation and firing signals is similar to that shown in Fig. 5.

CIRCUIT OF FIG. 8

Oscillator pulses are supplied directly to the ring counter and through a single-shot multivibrator to the commutation flip-flop. To each ring counter output are connected s.c.r. firing circuits. These are 1kc/s unijunction transistor oscillators.

Collector points of ring counter flip-flops supply capacitor-side voltage to unijunction oscillator firing circuits. When one of these flip-flops switches, the voltage supply to the firing circuit connected to the turned off side stops, causing cut-off of its firing pulses.

On account of the capacitor initial charge, the firing circuit connected to the opposite side does not supply pulses for one millisecond, thus providing the required delay for proper commutation.

The unijunction oscillator firing pulses last for some tens of microseconds, so commutation action can be disturbed if the last pulse supplied to a s.c.r. which is going to be turned off, is too close to the commutation time. To avoid such disturbances the signal to the commutation flip-flop is delayed by 100μsec.

Fig. 9 shows the firing waveforms to a positive side invertor s.c.r. (top) and to SCR$^+$ commutation s.c.r. (bottom). Scale is 5msec/cm. These pulses were supplied to the s.c.r.'s through small transformers; however negative side invertor s.c.r. firing signals can be supplied directly as before.

Remarks and Conclusions

The choice between the circuits described must be based on considerations such as component economy, gate dissipation, commutation losses.

The first circuit provides the greater components economy, nevertheless if it is intended to operate the invertor at very low frequencies there will be some trouble with firing transformer dimensions for non-saturating conditions. The second circuit supplies higher frequency waveforms to the firing transformers thus being less critical at low frequency operation. Also, after each commutation, this circuit always supplies a similar pulse to reset the s.c.r.'s, thus decreasing firing deficiencies by voltage drop and saturation. However, as its pulses last only for 30 electrical degrees, some problems may be found under very inductive load operating conditions.

As far as firing reliability is concerned, the third is the more valuable circuit, providing always similar pulses, using small transformers and having low gate dissipation. It is, however, the most expensive in semiconductor components and presents the highest commutation losses. The reason is as follows: in the other circuits the s.c.r.'s to be reset are fired 40μsec after commutation begins, and in this circuit that delay can be as high as 1msec, which allows for a large decrease of current through the commutation winding, thus increasing commutation losses.

It must be remembered that firing signals to commutating s.c.r.'s supplied through a small differentiating transformer which supplies one short pulse each 120° have been considered. This is the procedure to follow when the invertor d.c. supply has little ripple, or when it is intended to use commutation transients, to obtain high charging voltages of commutation capacitors, with a low voltage auxiliary supply V_R.

However, when dealing with a large ripple d.c. supply, one may, in this way, charge commutation capacitors when voltage is low, and not obtain enough reverse voltage for the next commutation if this takes place when the supply voltage is high.

Now, between two commutations the capacitor must be able to follow the increasing d.c. supply voltage, so commutation s.c.r.'s must have a continuous firing waveform. This will be satisfactorily obtained using two unijunction oscillator firing circuits, connected to each side of the commutation flip-flop.

In the circuits described the following changes should be made:

Single-shot multivibrators of the first and second circuits must have a larger delay time than the period of the commutation s.c.r. firing circuits.

Fig. 10. Unijunction oscillator

For arrangement of:

Fig. 3	*Fig. 6*	*Fig. 8*
$V = 10V$	$V = 10V$	$V = 20V$
$R = 3k\Omega$	$R = 3k\Omega$	$R = 6{\cdot}2k\Omega$
$C = 0{\cdot}68\mu F$	$C = 0{\cdot}33\mu F$	$C = 0{\cdot}33\mu F$

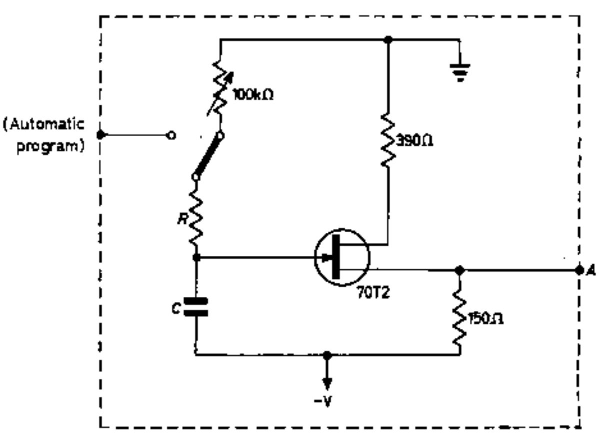

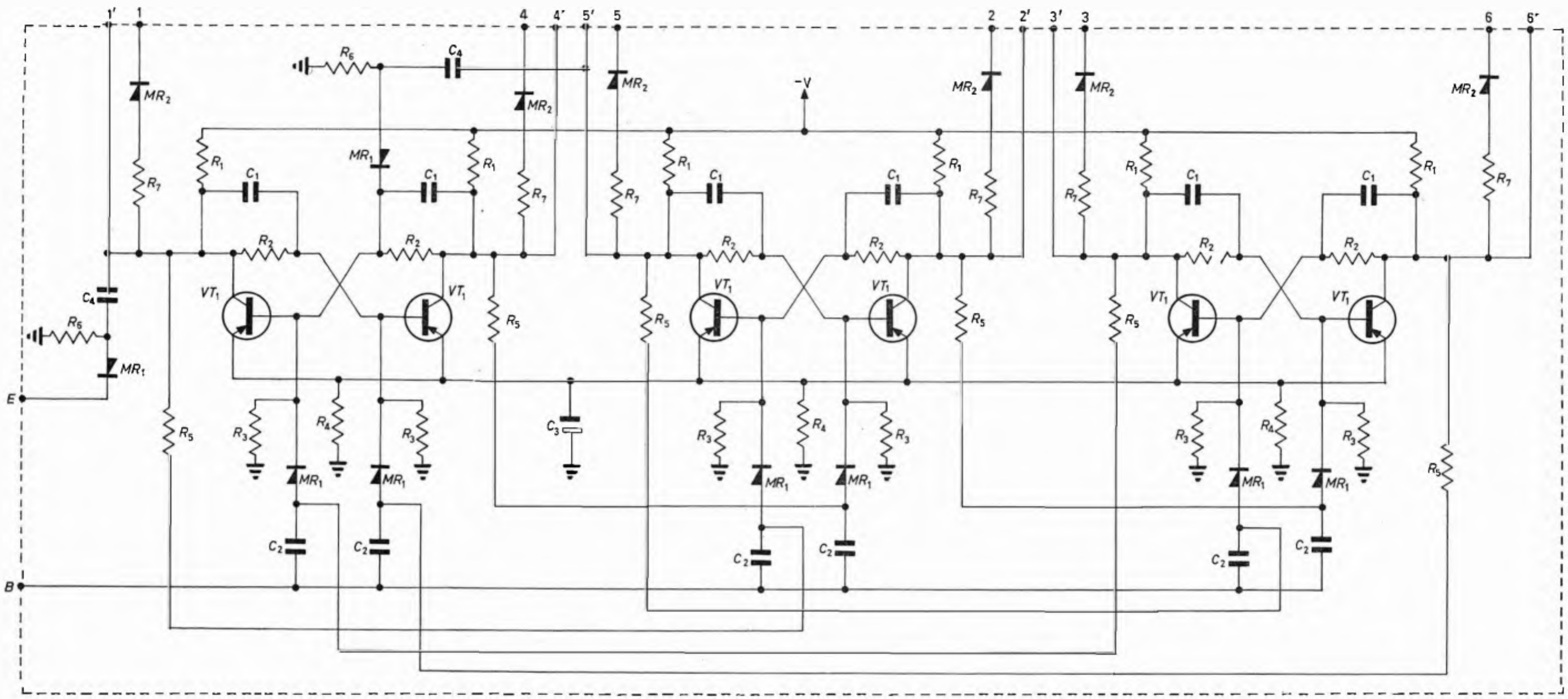

Fig. 11. Ring counter

For arrangement of:

	Figs. 3 and 6	*Fig. 8*
V	$10V$	$20V$
R_1	100Ω	510Ω
R_2	$2{\cdot}4k\Omega$	$10k\Omega$
R_3	$1{\cdot}2k\Omega$	$2{\cdot}4k\Omega$
R_4	10Ω	10Ω
R_5	$30k\Omega$	$51k\Omega$
R_6	$30k\Omega$	$51k\Omega$
R_7	180Ω	
C_1	$1000pF$	$500pF$
C_2	$0{\cdot}01\mu F$	$4700pF$
C_3	$10\mu F$	$10\mu F$
C_4	$0{\cdot}015\mu F$	$4700pF$

$MR_2 = 1N277$ $\quad VT_1 = 2N526$ $\quad MR_1 = 1N198$

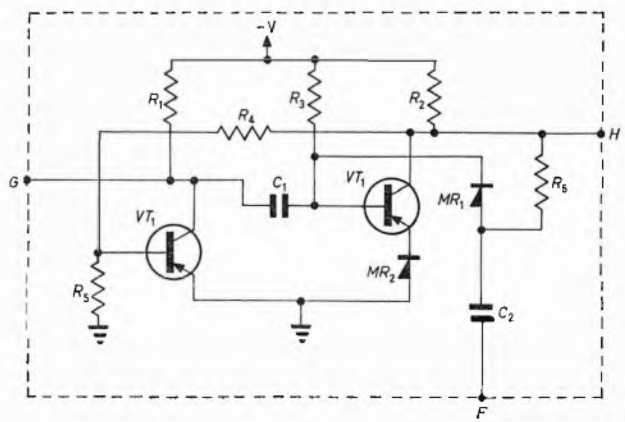

Fig. 12. One shot multivibrator

$VT_1 = 2N526$ $\quad MR_1 = 1N198$

	Fig. 3	*Fig. 6*	*Fig. 8*
V	$10V$	$10V$	$20V$
R_1	33Ω	510Ω	$1k\Omega$
R_2	100Ω	510Ω	$1k\Omega$
R_3	$3k\Omega$	$15k\Omega$	$30k\Omega$
R_4	510Ω	$15k\Omega$	$30k\Omega$
R_5	100Ω	$3{\cdot}3k\Omega$	$6{\cdot}2k\Omega$
R_6	$30k\Omega$	$30k\Omega$	$51k\Omega$
C_1	$0{\cdot}022\mu F$	$4700pF$	$5000pF$
C_2	$0{\cdot}01\mu F$	$0{\cdot}01\mu F$	$4700pF$
MR_2	not used	not used	$1N277$

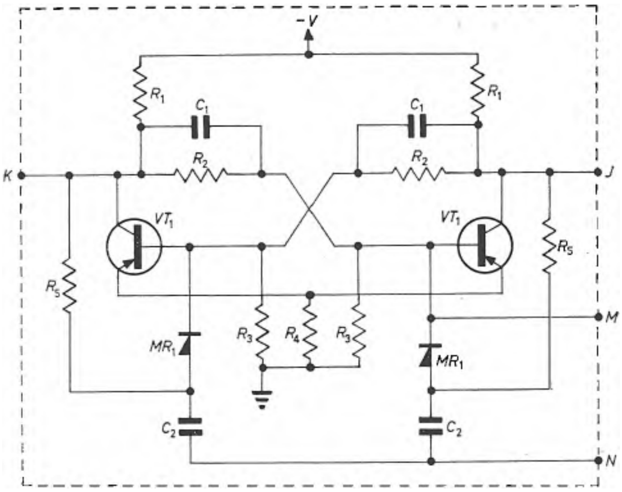

Fig. 13. Flip-flops

Commutation flip-flop		Auxiliary flip-flop
Figs. 3 and 6	*Fig. 8*	*Fig. 6*
$V = 10V$	$V = 20V$	$V = 10V$
$R_1 = 100\Omega$	$R_1 = 510\Omega$	$R_1 = 100\Omega$
$R_2 = 2{\cdot}4k\Omega$	$R_2 = 10k\Omega$	$R_2 = 2k\Omega$
$R_3 = 1{\cdot}2k\Omega$	$R_3 = 2{\cdot}4k\Omega$	$R_3 = 1k\Omega$
$R_4 = 10\Omega$	$R_4 = 10\Omega$	$R_4 = 0$
$R_5 = 30k\Omega$		$R_5 = 30k\Omega$
$C_1 = 1000pF$	$C_1 = 500pF$	
$C_2 = 0{\cdot}01\mu F$	$C_2 = 4700pF$	$C_1 = 1000pF$
$MR_1 = 1N198$	$MR_1 = 1N198$	$C_2 = 0{\cdot}01\mu F$
$VT_1 = 2N526$	$VT_1 = 2N526$	$MR_1 = 1N198$
		$VT_1 = 2N526$

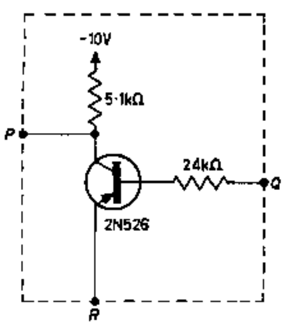

Fig. 14. Linear gate

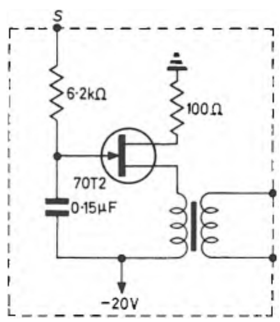

Fig. 15. S.C.R. unijunction firing circuit

The single-shot multivibrator of the third circuit is not necessary provided the commutation s.c.r. firing circuits are designed with a smaller period than the invertor s.c.r.'s firing circuits.

Circuit Diagrams

Circuits designed for firing an 8 h.p. invertor are shown in Figs. 10 to 15.

Acknowledgments

The author wishes to express his thanks to M. J. Campos Costa, E.E., for his comments and helpful suggestions and to the Director of "Laboratório de Física e Engenharia Nucleares" for permission to publish this article.

REFERENCES

1. Hey-Simple Circuits for Triggering SCR's into Fast-rising Load Currents. GE Application Note 200.41-3/65.
2. Bradley, Clarke, Davis, Jones. Adjustable-frequency Invertors and their Application to Variable-speed Drives. *Proc. Instn. Elect. Engrs. 111*, Pt. 2, 1839 (1964).
3. Bedford, Hoft. Principles of Invertor Circuits, p. 207 (J. Wiley & Sons, 1964).
4. Texas Instruments Inc. Transistor Circuit Design, p. 396 (McGraw-Hill, 1963).

UK-3 Satellite in America

The principal prototype model of UK-3, the first all-British satellite, commissioned by the Science Research Council, and which is due to carry five British scientific experiments into space early this year is now undergoing compatibility tests in America. It will undergo mechanical and other tests with the actual launch vehicle at Dallas, Texas.

UK-3 is a 198 lb satellite which will be launched into a circular orbit some 325 miles above the earth. As well as its scientific instruments the satellite will carry a data handling and storage system, a command receiver and telemetry system for relaying information back to ground stations (which will include the Radio and Space Research Station at Slough) and an array of thousands of solar cells for converting the sun's energy into electricity. The overall height of the satellite is about 5ft and its span with booms extended (which are erected simultaneously and symmetrically) 10ft.

Co-ordination of this most significant British project in space has been undertaken by the Space Research Management Unit of the Science Research Council, together with Ministry of Aviation, acting as the design authority.

The British Aircraft Corporation has constructed the spacecraft and GEC Electronics has been the principal firm responsible for the complex electronic system.

The design aim is that the satellite should transmit experimental data for a year.

The five experiments the satellite will be carrying will:

Measure the characteristics of radio frequency emissions from natural terrestrial sources such as thunderstorms (the Radio and Space Research Station);

Study the vertical distribution of molecular oxygen in the Earth's atmosphere at about 150km (the Meteorological Office);

Study the spatial and temporal characteristics of v.l.f. radiation (1 to 20kHz) above the Earth's ionosphere (Sheffield University);

Effect a world wide survey of the ionosphere by measuring the electron density and temperature at frequent points along the path of the satellite (Birmingham University);

Measure the emission of radio noise from sources in the galaxy at frequencies too low to be observed on the ground. (Jodrell Bank).

UK-3 showing the compartment containing apparatus for the Radio and Space Research Station's experiment to measure high frequency atmospheric noise received in the satellite

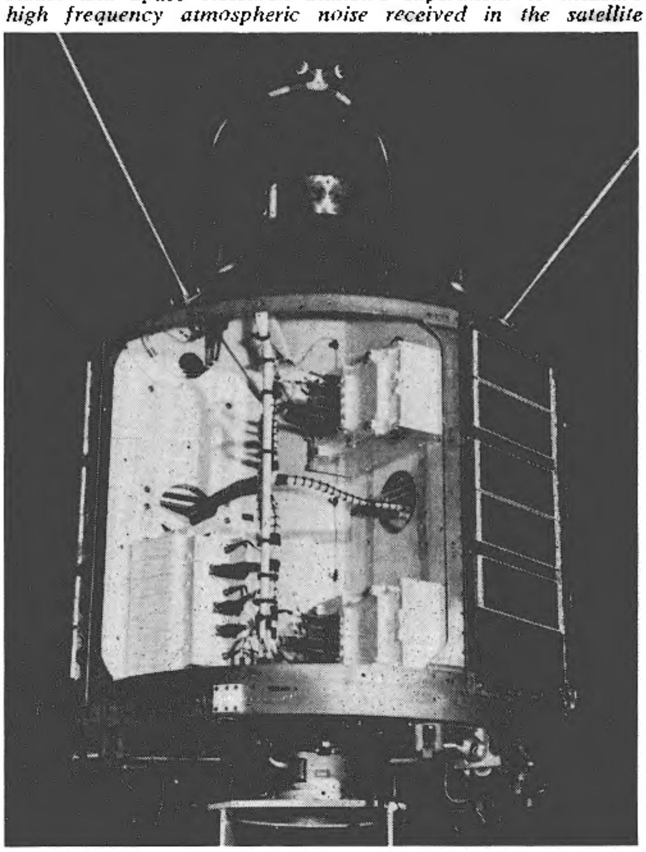

SHORT NEWS ITEMS

The International Electronics Conference, sponsored by the Canadian Region of the Institute of Electrical and Electronic Engineers, is to be held in Toronto, Canada, on 25 to 27 September 1967, for which papers are invited on electronics and related subjects.

Further information is obtainable from Dr. Rudi de Buda, Technical Programme Chairman, International Electronics Conference, 1819 Yonge Street, Toronto 7, Canada.

The Council of the Royal Society has awarded one of its Royal Medals for the year 1966 to Mr. J. A. Ratcliffe, C.B., C.B.E., F.R.S., formerly director of the Science Research Council's Radio and Space Research Station, for his distinguished studies in the ionosphere on the propagation of radio waves.

The twenty-second Exhibition and Conference relating to Electronics, Instruments, Controls and Components, sponsored by the Northern Division of the Institution of Electronics, is to be held in the Exhibition Halls, Belle Vue, Manchester, on 26 to 30 September this year.

Further details are obtainable from M. W. Birtwistle, General Secretary of the Institution of Electronics, Balderstone, Rochdale, North Manchester.

The BBC is to introduce a new television series of ten programmes on solid state physics starting on 8 January on BBC-1.

These programmes, intended for electrical engineers, teachers in schools and colleges, undergraduates and sixth forms, will explain how the devices are made, how they work and some of their uses.

The British Standards Institution has just published supplement No. 1 to B.S. 448: Dimensions of electronic tubes and valves. This supplement contains the following new and revised sections for insertion in Part 2 of the Standard which contains the data sheets B4G, B5D, B5E, B7G/F, B8D, B9A, B10B, B12A, B13B, B15B and B19A.

This is the first of the supplements which will be printed when necessary for the revision of the 1964 reprint of B.S. 448 : 1953, Part 2.

Copies may be obtained from B.S.I., Sales Department, Newton House, 101-113 Pentonville Road, London, N.1, price £1 each (postage 1s. extra will be charged to non-subscribers).

The Marconi Company has developed a new 10kW medium wave broadcasting transmitter (type B6029) which is tropicalized and suitable for operation in extremes of temperature and humidity. The whole of the equipment occupies a floor area of 20 sq. ft. and requires neither rear access nor the use of underfloor cable trenches, access for servicing the transmitter being provided through the interlocked front doors.

The power output of the transmitter is generated in a single tetrode valve, the only thermionic device in the whole of the equipment. It is driven by a completely solid-state drive unit which is 'low level' modulated. Under excessive audio input powers the equipment automatically limits the modulation to just over 100 per cent, preventing the equipment from transmitting radio interference across a wide bandwidth.

Power supplies for the equipment employ solid state rectifiers with generous ratings. The equipment automatically isolates the high tension power supplies in the event of faults occurring in the equipment. However, in order to prevent closedown in the event of momentary faults, the equipment only 'locks out' permanently after three attempts have failed to restore the supply.

Control of the transmitter is simple, and can be connected for remote operation by a switch after which the switching-on procedure is timed and executed automatically. For manual operation the same switch is all that is required to start up the transmitter.

The transmitter is suitable for paralleling with another identical unit to double the output power or to increase the reliability and introduce a standby facility if a breakdown of either unit occurs.

The General Post Office has now introduced a new data transmission service that provides, for the first time, simultaneous two-way transmission of digital data over an ordinary telephone circuit.

The new service, known as Datel 200, is capable of operating at speeds up to 200 bits per second and is therefore suitable for connecting remote keyboard type terminals to multi-access computers.

Datel 200 is the latest addition to the expanding range of Datel services which includes Datel 100, capable of speeds up to 100 bits per second on telegraph circuits, and Datel 600, with an operating speed range of up to 600 or 1 200 bits per second in one direction at a time over telephone circuits. Facilities are also available for higher speeds.

The Datel 600 service, started in 1964, now operates nationally, and between this country and France, Denmark, Austria, West Germany and the U.S.A.

The British Radio Valve Manufacturers' Association (BVA) and the Electronic Valve and Semiconductor Manufacturers' Association (VASCA) have issued details concerning the export of electronic valves, tubes and semiconductor devices for the first nine months of 1966 as follows: Electronic valves and tubes, £7 706 831; semiconductor devices, £2 956 418.

The level of exports has remained fairly static in the third quarter but is slightly up over the corresponding period of 1965, valves showing an increase of 2 per cent and semiconductors an increase of 3 per cent. These were largely due to increased exports of industrial valves over 50W, electron optical devices including camera tubes, thyristors, and silicon transistors.

The Post Office V.L.F. transmitter at Rugby Radio Station (GBR) which has for 40 years provided a vital link with British ships all over the world, has recently been re-opened, following extensive modernization and reconstruction.

Originally designed and built in the early 1920s by engineers of the 'Wireless Section' of the Post Office Engineers Department, the station made history as the world's most powerful transmitter using thermionic valves.

As well as the GBR call-sign, it also broadcast the Greenwich Time Signal at specific times of the day.

More recently it was decided to increase the radiated power and modernize the operating capability of the transmitter, and this has involved complete re-design of the valve amplifiers and the modulating equipment, as well as extensive modification of the main aerial tuning circuit. The old transmitter ceased operations at the end of 1965, and has been rebuilt by the Post Office Engineers Department in the space of a few months. The most striking changes are in the main amplifier stages, where three amplifier panels each of 18 water-cooled valves have been replaced by three vapour-cooled amplifier valves which can be used singly or in combination, and in the modulator which can generate precision frequency-shift signals as well as the original c.w. signals, at speeds up to 72 bauds. A new control centre has been installed which will also serve the other two low-frequency transmitters in the building.

The new transmitter now goes into regular use for Navy Department traffic and Time Signal emissions. The output power of the transmitter will be 450-500kW and the power radiated from the aerial will exceed 60kW at 16kHz. Both power and signalling speed have been approximately doubled. The transmitter is rated, together with Anthorn, the most powerful and effective unit in Western Europe.

It was the first in the world to have its carrier frequency stabilized to the accuracy of a primary frequency standard and this has been progressively improved over the last 15 years, the present limit of variation being less than 5 parts in 10^{10}. It is expected that this can be improved still further, to 1 part in 10^{10} or better, with the aid of an atomic frequency standard, a rubidium gas cell, in place of the existing quartz resonator. This development will enhance the value of the 16kHz emission, already extensively used by scientific investigators throughout the world, as an international standard of frequency and time.

At the Fourth General Assembly of the European Organization for Civil Aviation Electronics (EUROCAE), Dr. B. J. O'Kane, General Manager, Electronics, The Marconi Company, was elected President for 1966/67. Dr. O'Kane was one of the architects of this organization, which was formed in 1963 to provide a co-ordinating body for European aviation electronics, both manufacturers and users, and has been Chairman of the steering committee of EUROCAE since its inception. EUROCAE is analogous to the American Radio Technical Commission for Aeronautics.

Standard Telephones and Cables Ltd has received an order valued at over £4½M from the General Post Office for a 1 000-mile transistorized under-sea telephone cable system to be laid between Cornwall and Lisbon, and to become operative in the early part of 1969.

This cable, the first deep sea long haul transistorized cable of its kind in the world, will leave Sesimbra, 20 miles south of Lisbon, and in the 1 000-mile run to Kennick Sands, near the Lizard in Cornwall, 133 of S.T.C.'s new deep-sea transistorized repeaters will be laid at 7½ nautical mile intervals.

The cable will be able to carry 480 simultaneous high quality (4kHz) telephone conversations. About 700 nautical miles of the cable will be Post Office Mark II lightweight 0·99in cable, with 300 miles of heavily armoured type for use at the shore-ends. Ten equalizers will be spliced into the cable at intervals to achieve the best possible transmission quality.

The satellite communications ground station designed and built by The Marconi Company for Cable and Wireless Ltd has now been handed over by the Marconi installation team on Ascension Island, and will shortly be brought into full operational use for the first of the American APOLLO launchings. This satellite tracking system was designed, manufactured, tested, delivered, erected on site and commissioned, all within a year.

The Cyprus Broadcasting Corporation has awarded a contract valued at £60 000 to E.M.I. Electronics Ltd for television studio solid-state equipment which includes both versions of the new 4½in image orthicon camera channels type 206 and 207, twenty-five picture monitors (types 1402 and 1902), vision mixing and special effects equipment, stabilizing amplifiers, soundmixing and communications equipment. The bulk of the equipment is to be used to equip a new studio from which a commercial television service is scheduled to begin operations early this year.

G.E.C. Electronics Communications Division, Spon Street, Coventry, has received orders totalling £62 000 for v.h.f. radio equipment for police use. Five hundred 'AM Courier' personal radiotelephones have been ordered by the Home Office on behalf of several police forces, and 120 f.m. duplex transceivers are to be supplied to Lancashire Constabulary for use in police cars.

Elliott-Automation is consolidating the activities of two of its subsidiaries in the nucleonic field by amalgamating the industrial nucleonic work of the Baldwin Instrument Company at Dartford, Kent, with the medical and laboratory instrumentation of Isotope Developments Limited at its factory at Beenham, near Reading.

Deutsche Lufthansa AG has ordered the latest crystal controlled automatic direction finding equipment from The Marconi Company for a new fleet of 21 Boeing 737-130 aircraft, which is due for delivery starting this year. Two direction finders will be fitted on each aircraft.

The Marconi direction finder, type AD370, is designed to provide the maximum simplicity in operation, to enable radio bearings to be taken more rapidly by the pilot. The outstanding technical feature of this equipment is that it is the only a.d.f. available in the world using truly solid state crystal controlled electronic tuning with no moving parts. Tuning is performed automatically and instantaneously. Frequencies can be selected, in ½kHz steps on a simple control unit, using decade switches and counters which display the chosen frequency. The elimination of moving parts in the tuning system conforms fully with the latest international specification, ARINC 550, and is fully approved by The British Air Registration Board and Federal Aviation Agency.

Decca Radar Ltd has recently installed an Electron Spin Resonance Spectrometer at the University of Warwick. The instrument, the most advanced model in the Decca range of Electron Spin Resonance (e.s.r.) Spectrometers, uses the Newport Instruments type M2 magnet system and was supplied complete with a Decca Variable Temperature Cavity Insert and a Decca Liquid Nitrogen Accessory.

Special features include simple and superheterodyne detection with high and low-frequency field modulation and dual fixed operating frequency is accurately determined by phase-locking the signal source to a quartz crystal oscillator; this and the direct magnetic field readout allow precise measurement of 'g' values, line widths and separations directly from the chart recorder.

The Decca spectrometer is to be used for structural research on synthetic and natural diamonds. Comparisons between e.s.r. spectra from dispersed substitutional nitrogen donors in natural and synthetic single stones have been possible with particular reference to their previous heat-treatment.

The spectrometer is being used direct on line to a computer of Average Times to enhance the signal-to-noise ratio of weak signals. The information obtained from many successive sweeps through the required spectrum is stored in the computer before being averaged, thus cancelling part of the random noise surrounding the signal. This relatively new technique can extend the application of electron spin resonance spectroscopy with very weak signals, particularly where the spectral information obtainable is normally masked by the system noise level.

NEW BOOKS

'Electronic Digital Systems'

By R. K. Richards. 637 pp. Med. 8vo. J. Wiley. 1966. Price 115s.

SEVERAL years ago Dr. Richards wrote two books, one on arithmetic operation the other on digital components and circuits; both appeared at a time when, although there was a demand for that kind of work among machine designers, few books had yet been published.

Dr. Richards' sense of timing is demonstrated again in the volume under review, for he deals not only with digital computers but places them in the systems concept, a topic of great current interest again not covered by many authors.

The book contains approximately 600 pages with only a dozen or so illustrations and could be described as a collection of essays. The contents are easy to read and it is not necessary to read chapters consecutively; subject matter is only loosely related to previous material.

The first chapter is a detailed history of, and introduction to, digital computers. Dr. Richards' purpose is to arrive at the description of a 'system', his concept of which comprises not only the central processor with conventional peripherals such as tape readers, punches, backing stores and so on, but includes the data transmission components which connect a computer to a real-time system and the transducers at the remote ends of the lines; in short, the total environment.

Chapter 2, in which Dr. Richards covers the theory of digital systems, discusses the philosophical aspects at some length. Topics range from the derivation of a theoretical model and assignment of system states to basic storage elements, system synthesis, nets, asynchronous systems and Turing machines.

Chapter 3 is concerned with the stored program concept. Detailed comment would make the review too long and this reviewer can do no more than list the more important topics. These are comparison of single- and multiple-address formats, modifiers, multiple accumulators, variable instruction length, index registers, sort, merge, micro and macro programming techniques, the interrupt concept, supervisor programs and multiprogramming. These last three are, of course, of great current interest in the context of real-time systems and it is further testimony to Dr. Richards' foresight that his book should include them.

Chapter 4, Automatic Programming, is a series of essays on, typically, mnemonic notation, assembly programs, generators, symbol strings, Polish notation, compilers, translators, error checking, documentation and operating procedures.

Chapter 5 deals with digital data transmission. After a general discussion Dr. Richards discusses information-carrying ability and bandwidth, noise, channel capacity equation, error rates, modulation methods, synchronization and feedback systems.

It seems more logical to take Chapter 7 as a natural sequence to data transmission for here Dr. Richards writes on telephone and message switching systems. First he discusses the stored programme computer as a message switching centre then the interconnexion of two or more centres, an introduction to time-sharing and ultimately the relative merits of time and frequency division multiplexing.

To return to Chapter 6, this deals with combined analogue and digital techniques. After comparisons, the author discusses combination techniques, how each can be used to perform corresponding functions and the programming of a digital computer to simulate an analogue computer.

Chapter 8 is mainly philosophical being called 'The Relationship between Digital Systems and Thinking.' Fortunately the author immediately dispels any suggestion that a digital computer 'thinks' thus placing this chapter outside the realms of science fiction. His main subjects are game playing, neural nets, neuron hardware and character recognition.

Chapter 9 deals with miscellaneous digital systems such as those for control by means of tape, cord and plugboards and voice and television systems.

In Chapter 10, Digital System Reliability, Dr. Richards ensures that this vital aspect of any digital system is emphasized in his system concept. He deals both with component reliability and redundancy techniques.

Chapter 11 'The Automatic Design of Digital Systems' contains such topics as circuit parameters, minimization of numbers of components, determination of physical lay-out and so on. It is the least interesting chapter, could well have been reduced in length and added as a section to an earlier chapter.

To quote the author from p. 345, 'A translator for preparing translators contains the same triple language characteristics but with the added complication that the programme to be translated is itself a translator involving three different languages. Because this programme is actually a translator, the programme for preparing translators could be called a translator translator,' unquote; such germane observations together with all the foregoing topics contained in a book which although only 6in by 9in weighs 2 lb 12 oz gives rise to the question: at 115s what more could one ask?

T. R. H. SIZER

Théorie et Pratique des Circuits à Transistors (Theory and Practice of Transistor Circuits)

By A. Petitclerc. 440 pp. Med. 8vo. Dunod (Paris). 1966. Price 86F.

IN the field of textbooks for universities and technical colleges, as regards semiconductor technology, French speaking engineers and would-be engineers often have to rely on publications in other languages. In this book, the author has striven to provide a comprehensive basis for teachers and students, with particular reference to radio, television and frequency modulation applications.

The first two chapters define the static and dynamic properties of transistors in terms of their physical characteristics. The various equivalent circuits are introduced in Chapter 3 with special emphasis on the y parameters. As matrix methods are used to a great extent, an appendix on their application is given at the end of Chapter 3.

After dealing with the operating point and its stabilization in Chapter 4, nearly half of the book is devoted to developing the expressions for the various types of amplifiers. Practical examples are given in each case. Low frequency, power and wide-band amplifiers are considered in Chapters 5, 6 and 7. Then the losses and band-pass of interstage circuits are analysed in detail in Chapter 8 as preparation for the following chapters.

H.F. amplifiers, with and without band-pass filters, are dealt with in Chapters 9 and 10. Large signal amplification, with the attendant problems of distortion and cross-modulation, is discussed in Chapter 11. The main types of transistor oscillators are covered at length in Chapter 12 and this is followed by a short treatment of transistor mixers.

In the last chapter, the various kinds of transistor noise and their effects are given careful attention.

The author has treated each subject methodically with a step-by-step mathematical presentation. The main criticism which can be made is that only general references are given at the end of each chapter and, as these mainly refer to publications in English or German, the French-speaking readers would be at a decided disadvantage in doing further research unless they had sufficient fluency in these languages. The topics in this book are covered adequately by existing publications in English, thus obviating the need for an English translation.

D. K. HILLS

Longitudinal Space-Charge Waves

By R. E. Trotman. 219 pp. Crown 8vo. Chapman and Hall. 1966. Price 35s.

PROBABLY the most accurate description of the operation of many (including all those employing long transit times) is in terms of space-charge waves.

The book under review is concerned exclusively with longitudinal waves along straight electron beams; that is, with the space-charge wave theory of a class of devices, of which the klystron and the travelling wave tube are currently the most important members. The author had final year undergraduate and post-graduate students of electrical engineering and physics in mind, and a feature of the work is a critical survey of the various attacks on a given problem by different workers, or teams of workers. Such a style should induce in the reader a good understanding of the subject as well as a healthy disrespect for the printed word, including those under review, possibly.

After a brief historical survey and some introductory theory, the propagation of space-charge waves on monovelocity (i.e. zero thermal fluctuation) electron beams is treated beginning with the ideal one-dimensional case, and then passing on to Brillouin beams and beams in arbitrary magnetic fields. This constitutes Chapter 2 which finishes on a practical note with applications of the theory and experimental work.

The third chapter gives an excellent review of the various methods in which the space-charge waves might be amplified as they propagate along a beam or beams. The author has selected those proposals which have shown some degree of experimental success as reported in the literature up to about 1961, and in most cases he has developed the theory behind the proposal.

All theoretical discussion so far has been restricted to monovelocity beams. In Chapter 4 a discussion of the theory when this restriction is removed is presented. Detailed theory is not given but a review (with full references) acquaints the reader with the principal published work up to 1965. In particular he mentions experimental evidence of noise suppression by means of damping due to multi-velocity effects. It is therefore rather surprising that he appears to have overlooked the work of Currie and his associates.

Chapter 5 gives a development of Chu's Kinetic Power Theorem, and discusses some applications made by various authors. In particular, he highlights the significant difference in the power flow between 'fast' space-charge waves and 'slow' space-charge waves.

The book ends with a final chapter on general conclusions and a series of appendices in which some pieces of analysis are given which might have deflected the reader's attention had they been included in the main text.

To sum up: the reviewer likes the book and is happy to recommend it to anyone interested in the subject.

R. H. C. NEWTON

Silicon and Germanium Power Rectifier Technology

By R. Wells. 210 pp. Demy 8vo. Sir Isaac Pitman and Sons Ltd. 1966. Price 47s. 6d.

THE first chapter deals with the characteristics and testing of both germanium and silicon rectifiers. The testing is described in a practical way from the point of view of a manufacturer. The second chapter is based on a table of ten different rectifier/transformer connexions and each connexion is considered in detail from the point of view of currents, ripple, kVA transformer rating, power factor, etc. but proofs are not given. Protection, series and parallel operation and cooling are then considered. Many interesting problems are dealt with in connexion with series and parallel operation. Finally chapters are included on special performance considerations and equipment testing.

The book is well produced with clear diagrams and can be readily understood. The book is written from the practical point of view of a practising engineer and many interesting problems are well illustrated by practical examples. The author uses a number of abbreviations and although these are adequately explained when they first occur it would have been helpful if a list of these abreviations had been included. It is a most useful book for all concerned with the manufacture and design of semiconductor rectifiers, and also for the users of such devices. A useful bibliography is included.

G. N. PATCHETT

Physical Laboratory Handbook

By W. Sommer. 609 pp. Demy 8vo. Sir Isaac Pitman & Sons Ltd. 1966. Price 85s.

This book is an English translation of the original German book entitled 'Technische Kunstgriffe bei Physikalischen Untersuchungen', which is now in its twelfth edition, and is intended as a reference source for physical laboratory workers.

Measuring Methods and Devices in Electronics

By A. C. J. Beerens. 182 pp. Demy 8vo. Cleaver-Hume Press Ltd. 1966. Price 35s.

Part I of this book describes the various measuring instruments ranging from the simple meter to signal generators and impedance bridges.

Part II deals with the actual measurements of the fundamentals followed by measurements of active and passive networks, valves and transistors.

Phasor Diagrams

By M. G. Scroggie. 181 pp. Demy 8vo. Iliffe Books Ltd. 1966. Price 42s.

In this book the author has introduced a new approach to such concepts as Kirchhoff's laws, duality and Maxwell's cyclic current and applications to dealing with a.c. circuits valid in all branches of electrical engineering.

Design and Construction of Electronic Equipment

By G. Shiers. 362 pp. Med. 8vo. Prentice/Hall International. 1966. Price 84s.

The two objectives of this book are to acquaint beginners with the problems and processes related to the equipment design and manufacture, and to provide practical assistance to technicians, draughtsmen and designers in the electronic industry.

The book includes information on wiring, sub-assemblies, miniature constructions and microelectronic techniques.

Other features include chassis design and layout, component boards, printed circuits and connexion methods.

Short Wave Listening

By J. Vastenhoud. 107 pp. Demy 8vo. Iliffe Books Ltd. 1966. Price 12s. 6d.

Regulations for the Electrical Equipment of Buildings

241 pp. Demy 8vo. The Institution of Electrical Engineers. 1966. Price 17s. 6d.

Computer Programming for Science and Engineering

By B. A. M. Moon. 238 pp. Foolscap 8vo. Butterworth & Co. (Publishers) Ltd. 1966. Price 28s.

The general principles on which a computer operates are described in this book, together with a brief description of the computer elements.

The book is intended for undergraduates and others learning how to use digital computers.

Progress in Nuclear Energy Series IX Analytical Chemistry Volume 7

Edited by H. A. Elion and D. C. Stewart. 288 pp. Med. 8vo. Pergamon. 1966. Price 90s.

Volume 7 of this series contains further advances in nuclear energy including Electron Diffraction Techniques and their application to the study of Surface Structure. Other subjects are Liquid Scintillator Solutions in Nuclear Physics and Nuclear Chemistry, and On-line Analytical Instrumentation of Nuclear Fuel Reprocessing Plants.

Physical Principles of Magnetism

By F. Brailsford. 274 pp. Med. 8vo. D. Van Nostrand Co. Ltd. 1966. Price 60s. clothbound, 30s. paperback

The main subject of this book intended for engineers, physicists and metallurgists is ferromagnetism, including diamagnetism and paramagnetism. Also included are anti-ferromagnetism and ferrimagnetism.

The rationalized metre-kilogram-second system is used throughout and references to the literature and problems for solution together with answers are given with each chapter.

NEW EQUIPMENT

A description, compiled from information supplied by the manufacturers, of new components, accessories and test instruments.

(Voir page 57 pour la traduction en français; Deutsche Übersetzung Seite 64)

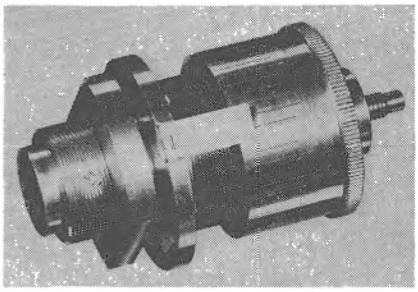

PROXIMITY VIBRATION TRANSDUCER

Southern Instruments Ltd, Camberley, Surrey

(Illustrated above)

The T.510 proximity vibration transducer is designed to measure the relative amplitude of vibration, without contact, between the transducer and a moving surface. The surface should be of high conductivity material or if non-conducting or ferrous, have a thin shim of beryllium copper brass attached to it.

To facilitate simple setting of the initial gap between transducer and surface, and to give ease of calibration the inductive measuring element can be moved relative to the transducer body. This movement is controlled by a micrometer type adjustment calibrated in 0·0005in divisions up to 0·4in.

The T.510 is designed solely for use with the Southern Instruments f.m. preamplifier system type TE.7, and it contains a miniature oscillator circuit, the output of which is a frequency (nominally 2MHz) proportional to applied displacement. The f.m. preamplifier will convert this frequency into a corresponding voltage or current signal.

Mounting of the transducer is by means of a 13/16in reamed hole or 13/16in × 40 t.p.i. threaded hole.

EE 02 751 *for further details*

SOLID STATE OSCILLOSCOPE

Hewlett-Packard Ltd, 224 Bath Road, Slough, Buckinghamshire

(Illustrated above right)

A new 50MHz plug-in all solid-state oscilloscope from Hewlett-Packard has a screen 30 per cent larger (8 × 10cm) than earlier large 50MHz oscilloscopes. It weighs 30lb, measures 8in × 11in × 22½in deep. The rack-mounting version, also available, measures 5¼in high. Designed to exceed earlier laboratory oscilloscopes in precision, the new HP model 180A is of small size, light weight, and wide adaptability to environment, for laboratory, field and production use. It is specified to operate normally from −28°C to +65°C, at 95 per cent relative humidity to 40°C, and at altitudes up to 15 000ft.

There are two plug-in positions. One is for the vertical amplifier. The first of these to become available is a two-channel unit which achieves a deflexion factor (sensitivity) of 5mV/cm at 50MHz. The trace will not jump when the calibrated sensitivity control is switched. There is virtually no trace drift when the instrument is turned on. These characteristics result from the use of new low-noise all solid-state circuits, with matched pairs of field-effect transistors kept constantly in the same thermal environment, permitting all attenuation to precede the amplifiers.

Two new time-base plug-ins are offered for the HP model 180A. The first of

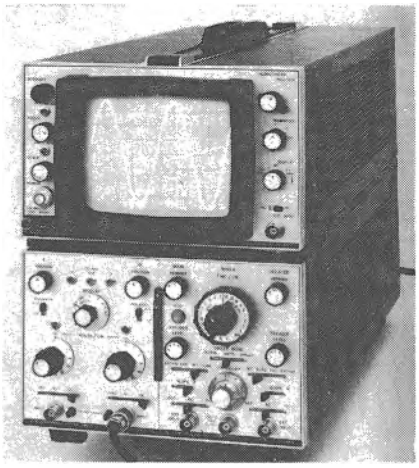

these, model 1820A, achieves a sweep speed of 5nsec/cm, when its ×10 magnifier is turned on at the fastest (0·05µsec/cm) calibrated setting. With reliable triggering to 90MHz, the result is greater resolution in the observation of high-speed traces than has previously been attained in an oscilloscope of this class. Variable hold-off permits the user to synchronize smoothly on asymmetrical pulse trains.

Optional with the model 180A is the new model 1821A time-base and delay generator plug-in. The delayed time-base begins to sweep after a time-delay from the main sweep, which is controllable. A bright dot on the screen identifies the point on the trace where the delayed sweep begins: this locates and identifies that part of any trace which the observer may wish to expand for detailed examination. By its use, also, the leading edge of the trace, after the delay-time, may be used to actuate the delay trigger, resulting in jitter-free full-screen presentation for measurement.

Despite the small size of the 180A, delay lines are built-in, so the leading edge of any pulse may always be brought into view. These delay lines are of entirely new construction, being etched-circuit strip lines. While of entirely adequate delay for the purpose, their bandwidth exceeds 140MHz, and a differential pair is built into the instrument.

A full array of accessories is offered for the 180A. The new HP model 197A electronic-shutter camera fits directly, and adaptors are offered for most other cameras. Flexible viewing hood, panel cover, carrying cover, and high-impedance divider probe are all designed to match.

EE 02 752 *for further details*

MINIATURE MOULDED TRACK POTENTIOMETERS

Davall Electronics Ltd, Rothersthorpe Avenue, Northampton

(Illustrated below)

The new Davall type 80 miniature moulded track preset potentiometer uses a one-piece high grade mineral filled phenolic moulding which allows the insulating base, resistive track and terminals to be moulded into a single solid integrated unit. This type of construction gives high stability under all conditions of humidity, temperature and vibration. Variation in performance is less than 5 per cent over the temperature range −40°C to +70°C. Specification DEF 5214 has been used as a minimum standard in the development of this unit.

The linear type 80 potentiometer has a power rating of 0·25W at 70°C and a maximum working voltage of 500V d.c.

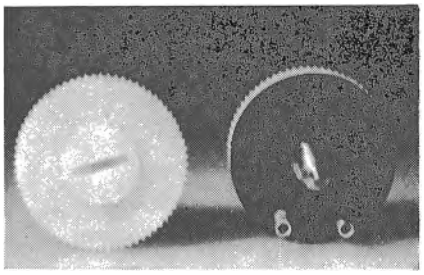

The resistance range available is 20Ω to 1MΩ.

Two versions are available, one with tags for direct soldering into printed circuits, the other for mounting on insulated boards using a 6 B.A. centre stud. The standard type 80 is very compact and can be contained in a cylinder 0·60in in diameter and 0·26in deep (excluding mounting and tags).

The type 80 can be adjusted manually or by screwdriver and a variant, type 80/1, is available with a larger knob for user adjustment.

EE 02 753 *for further details*

POLYCARBONATE CAPACITORS

Standard Telephones & Cables Ltd, Components Group, Footscray, Sidcup, Kent

(Illustrated below)

The Capacitor Division of Standard Telephones and Cables Ltd has introduced a comprehensive series of resin-protected polycarbonate capacitors intended specifically for the numerous applications where severe environmental conditions are not encountered.

Polycarbonate capacitors are high-reliability components wound from ultra-thin plastic-film of metallized polycarbonate. Their electrical and physical characteristics are superior to other plastic-film capacitors and remain stable over a wide temperature range.

Based on the Division's tubular units (which meet H6 environmental protection requirements of DEF specification 5011), the new units have the same high electrical performance but are housed in robust rectangular-moulded cases of thermo-setting resin providing environmental protection to H3 of DEF 5011—more than adequate for the operating conditions encountered by the vast majority of commercial electronic equipments. Terminal wires are radial and spaced to suit printed-circuit mounting.

STC resin-protected polycarbonate capacitors are available in values from 0·01 to 4·7μF 100V d.c. working, and are suitable for operation over the temperature range −40°C to +85°C. Their superior all-round performance makes them attractive alternatives or replacements for metallized polyester (polyethylene terephthalate) capacitors—particularly since the new capacitors are available at general polyester price levels.

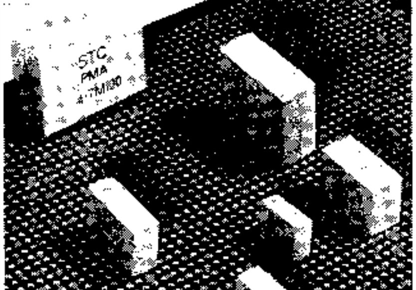

EE 02 754 *for further details*

MAGNETIC BEARING INDICATOR

Aviation Division, Smiths Industries Ltd, Kelvin House, Wembley Park Drive, Wembley, Middlesex

(Illustrated below)

Incorporating a number of improvements over previous models, a new radio magnetic indicator for displaying v.o.r. or a.d.f. bearings is now being produced by the Aviation Division of Smiths Industries. Contained in a standard 3 ATI case, the unit conforms to ARINC recommendations, and is provided with integral lighting.

Magnetic heading of the aircraft is indicated by a rotating compass card which is read against a fixed lubber mark at the top of the instrument. The card is driven by a servo, which has its amplifier contained within the case, from a signal supplied by the master compass system in the aircraft. Failure of the compass is indicated by a flag.

Magnetic bearings of two navigational beacons are indicated on the compass card by the two pointers, while relative bearing information is provided by the relationship of the pointers to the fixed lubber mark. Particular attention has been given to the accuracy of the relative bearing pointers which are driven from torque receiver synchros. V.O.R. or a.d.f. inputs to these synchros are selected by external switching.

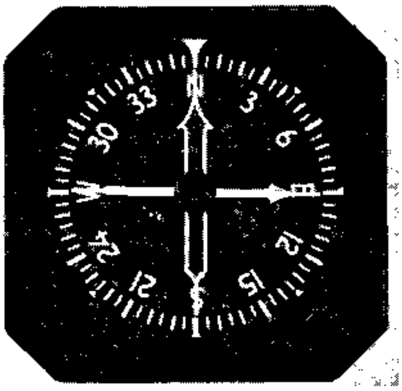

The unit also incorporates a bootstrap synchro transmitter which supplies an aircraft heading signal output. This is available for other flight equipment which requires such a signal.

EE 02 755 *for further details*

DIGITAL D.C. VOLTMETER

Hewlett-Packard Ltd, 224 Bath Road, Slough, Buckinghamshire

(Illustrated above right)

This new digital voltmeter (type 3430A) has an accuracy of 0·1 per cent plus 1 digit and a stability such that the specified calibration period is 90 days. It has a floating input: with its 'low' input terminal unstrapped from ground, the voltmeter can make measurements up to ±500V d.c. removed from ground. The input impedance is 10MΩ on all ranges.

The instrument has five manually-selected ranges, from 100mV d.c. full-scale to 1kV d.c. full scale, and a three-digit read out. A fourth digit (one or

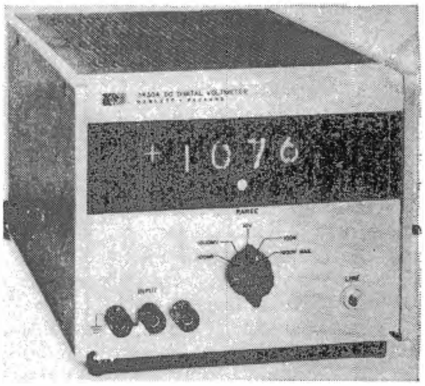

blank) permits over-range measurements up to 60 per cent above full-scale (except on the 1kV range) at full accuracy. Overload above 60 per cent is indicated by flashing of the illuminated display. The instrument automatically responds to the polarity of the input and indicates whether the input is a positive or negative voltage.

Among other features, the new digital voltmeter has an amplifier output that provides a d.c. voltage proportional to the input with a gain accuracy of ±0·1 per cent. The non-inverting voltage gain of the amplifier is 100 on the 100mV range, decreasing by a factor of 10 on each higher range. The amplifier output, handy for driving a recorder, is capable of driving any load that has an impedance greater than 10kΩ without degrading the accuracy of the reading.

An optional version of the instrument permits ratio measurements, a useful feature for normalizing the readings of d.c. transducer outputs. The display shows the input voltage divided by the reference voltage. Any fixed voltage between 0·8 and 1·2V (either polarity) may be used as the reference input and ratios from ·0001:1 to 1000:1 can be measured.

The new digital voltmeter is of the staircase comparator type which compares the input voltage to an internally-generated voltage derived from a Zener reference diode and precision resistors. The internally-generated voltage starts from zero and is stepped automatically to successively higher values until it matches the input voltages. Each step advances a counter one digit; when coincidence is reached, the number of accumulated counts, which represents the input voltage, is displayed on the front panel display. The instrument retains the displayed number until the next measurement cycle is completed, thus assuring a continuous display without blinking. The instrument completes two readings per second.

EE 02 756 *for further details*

STATIC SWITCHING UNITS

Vosper Ltd, Hamilton Road, Paulsgrove, Portsmouth, Hampshire

(Illustrated on page 52)

A range of static switching devices for a variety of duties is now in full production at the Portsmouth works of

Vosper Electric, a member of the Vosper-Thornycroft Group. Four main classes of unit are made: delay timers giving a simple switching function; delay timers driving double-pole double-throw (changeover) relays; multi-pole d.c. static switches; and multi-pole a.c. static switches, the latter two units being equivalent to electromechanical relays or contactors. As there are no moving parts the problems inherent in electromechanical devices, contact sticking and burning, wide range of pick-up and drop-out, wear, and so on, are eliminated. The multi-pole switches are offered with or without timers in the same module. All the timers are adjustable, a number of different ranges being available, giving delays up to a maximum of 300sec.

Emphasis has been placed on repeatability and reliability in the design of all these units. All components are encapsulated in an inert synthetic resin, and the whole assembly enclosed in an anodized aluminium cover. As a result the units are highly resistant to damp

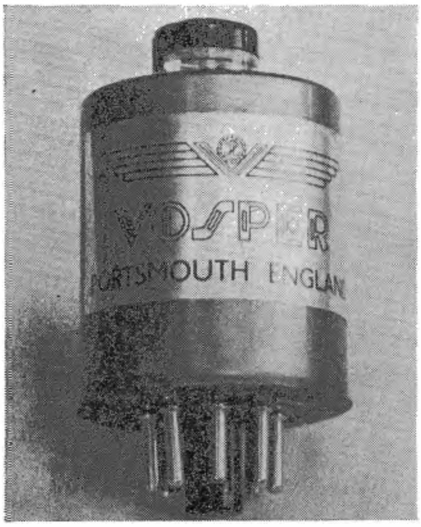

and corrosive environments, acceleration forces and vibration. An acceleration limit of 150*g* is specified for most of the units, and 50*g* for the delay timer containing the relay. All units can withstand vibratory forces equivalent to 25*g* at 2 or 3kc/s, and temperature from −65 or −55 to +60°C.

Output load currents range from 1·0 to 5·0A according to type, and input powers (equivalent to the operating coil current of a relay) are low enough for direct operation by transistor circuits −22mA d.c. or 5W a.c. A range of input and output voltage is available, from 12 to 150V d.c. and 12 to 250V a.c.

EE 02 757 *for further details*

R.F. SHIELDING BOXES

Hatfield Instruments Ltd, Burrington Way, Plymouth, Devon

(Illustrated above right)

This range of die-cast aluminium housings is designed to offer an effective answer to the problem of providing r.f. shielding for small groups of components

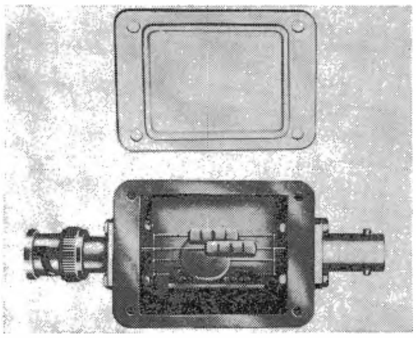

in such applications as attenuators, filters, networks, voltage dividers, etc. The boxes are strongly made and supplied complete with die-cast lids secured by four screws and can be fitted with B.N.C. plugs and sockets, so that they may be inserted in series with cables and existing equipment.

The boxes can be supplied fitted with 50Ω B.N.C. connectors as standard, socket one end and plug the other. They can be used with 75Ω systems up to approximately 100MHz without significant reflection taking place. This is because the B.N.C. connectors are only a small fraction of a wavelength at the lower radio frequencies.

The three sizes at present available are:

3·5 ×3·18 × 4·76cm; 7·3 × 4·76 × 7·3cm; 4·12 × 4·7 ×14·29cm.

EE 02 758 *for further details*

SUB-MINIATURE POTENTIOMETER

Pandect Precision Components Ltd, Wellington Road, High Wycombe, Buckinghamshire

(Illustrated below)

A sub-miniature wirewound trimmer potentiometer, one of the smallest of its type currently being produced in the United Kingdom, has been added to the range of resistive components manufactured by Pandect. Its physical outline corresponds to that of a standard TO-5 transistor, and the component is intended primarily for use in aeronautical, military and other high-grade electronic equipment meeting rigorous specifications.

The new potentiometer will be available in resistance values of 5Ω to 15kΩ. It offers the exceptionally high power rating for such a small device of 1W at +75°C. Resistance-welding together of the base and lid ensure 100 per cent environmental proofing over an ambient temperature range of −70 to +150°C.

Adjustment of the potentiometer setting is made by applying a screwdriver

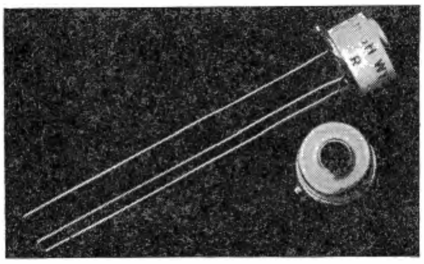

to a slotted spindle. The mechanism incorporates a simple slipping-clutch to guard against accidental damage due to excessive force being applied at the extremes of wiper movement. A silicone-rubber 'O' ring is fitted to maintain the sealing between the case and spindle.

Micro-welded connexions are used internally, to ensure maximum strength under severe vibration. The lead-out wires, which are gold-plated, are brought out through a glass-to-metal seal.

EE 02 759 *for further details*

MOLECULAR SIEVE SORPTION PUMPS

Mullard Ltd, Mullard House, Torrington Place, London, W.C.1

(Illustrated below)

Mullard Ltd has added two new molecular sieve sorption pumps to its range of ultra-high vacuum devices. Both are designed to give a fast pump-down from atmospheric pressure down to the starting pressure of Penning pumps (approximately 10^{-2} tor). The sorption

material is 13X alimino silicate which gives a higher efficiency than other grades of this material, and the sieve is constructed so that the maximum possible surface area of the sorption material is exposed to the coolant.

The pumps, type VAP-12 and VAP-40, have volume pumping capabilities of approximately 1 atmospheric litre and 10 atmospheric litres respectively. Larger volumes are best evacuated by using a sequential pumping arrangement in which one pump is pumping while the other is recovering.

Connexions to the pumps are made via stainless steel flanges, the seal being formed with the simple Mullard gold-wire system. A safety valve is fitted on both pumps to give complete protection from excesses of pressure. Specially designed dewar flasks are available for both types. Adequate room has been left in the flask assembly to accommodate the sensing head of the recently introduced Mullard liquid nitrogen replenishing system which can be incorporated to automatically maintain the coolant level while the pumping system is unattended. On the larger model (VAP-40), a bake-out heater is incorporated into the sieve to facilitate regeneration.

EE 02 760 *for further details*

MICROWAVE SIGNAL GENERATOR

Marconi Instruments Ltd, Sanders Division, Gunnel's Wood Road, Stevenage, Hertfordshire

(Illustrated below)

This instrument, type 6459, is claimed to have the widest frequency coverage of any signal generator available today. It has the following characteristics: Frequency range, 3·5 to 12·0GHz; direct reading frequency dial; direct reading attenuator, calibrated in voltage and dBm; high stability and accuracy; internal f.m., c.w. pulses or square wave modulation; optional conversion to rack mounting; f.m., c.w., square wave and pulse waveforms are generated internally and the instrument has facilities for the application of external modulations. The pulse repetition rate is variable from 40 to 4000p/s and pulse width from 0·5 to 10μsec. Synchronizing signals are simultaneous with the r.f. pulse, or between 3 and 300μsec in advance of the r.f. pulse. The internal pulse generators can also be synchronized by means of external signals.

The signal generator incorporates a plug-in klystron oscillator in an external coaxial line cavity. Frequency is determined by the position of a movable non-contacting piston which is coupled to the frequency scale and an automatic tracking network, and the output level is read in dBm and microvolts from the directly calibrated, internal, high precision attenuator. Temperature compensation, applied to the power meter bridge, ensures virtual freedom from the effects of ambient temperature changes.

Power output is as follows:

(a) Direct—an insertion probe couples out power to 80mW max.

(b) 0·223V to 0·1μV (0 to -127dBm) between 4·5 to 11·0GHz and -6dBm to -127dBm between 3·5 and 4·5GHz. Above 11·0GHz the output power is generally better than -6dBm into a 50Ω load.

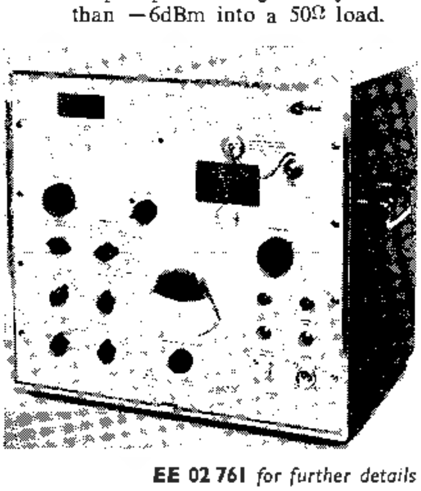

EE 02 761 *for further details*

TRACE READER

Normalair Ltd, Yeovil, Somerset

(Illustrated below)

Normalair Ltd announce a new addition to the 'Westland' range of data logging equipment—the Westland trace reader. Operation of this machine is very simple and does not involve the use of cursors, servos, electromechanical components or any special skill by the operator.

The reading table incorporates a flat metallic area across which is passed a linear electric potential (this is an isolated a.c. signal well below 1V in amplitude). The chart, film or photograph etc. to be sampled, is positioned over the sensitive area and readings are made by placing the stylus tip of a hand-held probe on the point to be read.

The sampling probe is held like an ordinary pen or pencil and has a spring-loaded stylus tip. The stylus tip is placed on the record at the point chosen for digitizing and the operator presses down on the body of the probe. This action causes the stylus to pierce the record

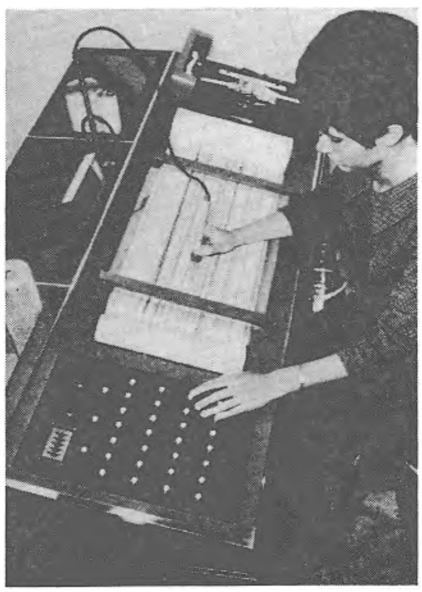

and make contact with the sensitive plate beneath. The machine then automatically completes the conversion process and punches the sampled value on the output tape.

The machine can accept a maximum working speed of up to two readings per second.

All functional controls are grouped together on a keyboard which also incorporates press button facilities for inserting additional data, such as trace identification and special symbols to suit customer's computer programming etc., on to the punched tape.

EE 02 762 *for further details*

MULTI-POLE JACK PLUG AND SOCKET

Render Instruments Ltd, Victoria Road, Burgess Hill, Sussex

(Illustrated above right)

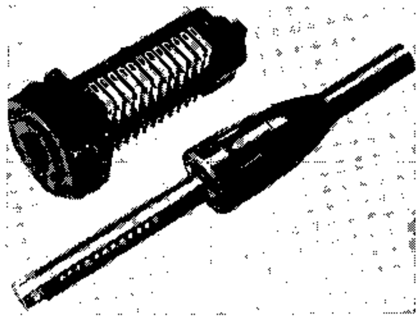

Render announce the introduction of a multipole jack plug and jack socket in addition to their established range of 2 pole, 3 pole and miniature jack plugs and jack sockets.

This innovation provides an easy, quick and secure method of connexion for use with miniature cables having up to 12 cores. In addition to its form as a connector it can be supplied with a large number of combinations of make and/or break contacts on the socket.

Electrical contact is made by a slight clockwise turn of the plug, after insertion, the plug automatically remaining locked in this position. A slight turn in the opposite direction releases the plug, which may then be withdrawn from the socket.

These components provide an alternative method of connexion to multi-pin types of plug and socket already available and have the added advantage of switching facilities.

EE 02 763 *for further details*

'PENCIL-FOLLOWER' ANCILLARY EQUIPMENT

d-mac Ltd, Queen Elizabeth Avenue, Hillington, Glasgow, S.W.2

(Illustrated on page 54)

A new range of ancillary equipment increases the scope, speeds up and further simplifies the operation of the 'Pencil Follower' manufactured by d-mac Ltd.

The unit, which converts graphic material into digital form for computer processing, can now be fitted with a projection system to facilitate the analysis of data from films.

Sprocketted or unsprocketted film of 16, 35, 50 or 70mm is projected on to its reading table. Film movement, both forward and reverse, is controlled by a variable-speed motor which can be de-clutched so that specific frames can be inched to precise positions manually.

Once the image has been selected, the operator traces the required data with a 'pencil' to which the 'follower', located under the reading surface, is tied magnetically. The position of the 'follower' is transmitted to the electronics console where it is converted into digital form and fed to an output device such as a tape punch.

The Pencil Follower can also be fitted with a paper reel unit consisting of two spools mounted at opposite sides of the reading table and a tensioning device to position the paper accurately on the reading surface. Charts

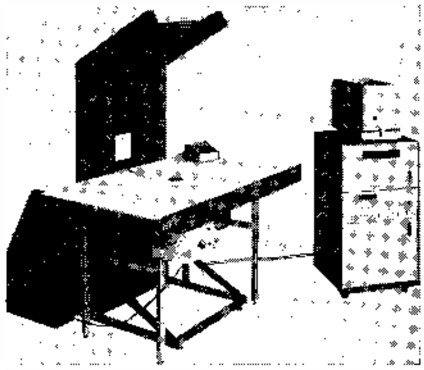

up to 18in wide are wound manually from one to the other, easing the handling of lengthy recordings.

A new type of 'pencil', laid along a line, supplies the co-ordinates of two points from which an angle may be calculated. This is already being applied to the analysis of spark chamber and kinetheodolite records.

An incremental readout facility is also available. By means of this, readings are taken at pre-selected intervals between a millimetre and a centimetre along the X-axis of a trace.

The Pencil Follower can now be supplied with a reading table measuring 100 × 100cm instead of the standard 100 × 45cm.

EE 02 764 *for further details*

LASER EQUIPMENT

System Computers Ltd, Fossway, Newcastle upon Tyne, 6

(Illustrated below)

A range of laser equipment which includes five helium-neon and three ruby lasers is being manufactured by System Computers Ltd. In addition, the company supplies ancillary equipment such as output meters, passive and rotating Q switches, glassware and special quality crystals for particular applications.

The R1 ruby laser is designed specifically for general demonstration and research purposes in industry and educational establishments. The output from the 2in long ruby element is sufficiently powerful for applications such as cutting or welding very fine wires.

The larger ruby lasers, the R5 and R10, have outputs of about 25 and 80 joules respectively and can be used as research or production process tools. Special features include an air cooled hyperpure aluminium cavity and a 6¼in long ruby or neodymium-in-glass rod operating at 6943Å or 10600Å depending on which material is used. Both models have an external prism and mirror and optional extras include rotating prisms or dye cell Q switching, optical focusing,

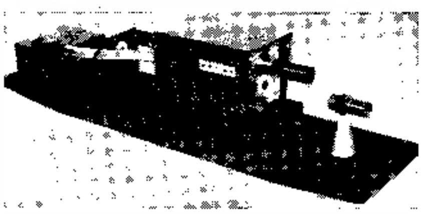

water cooling of the crystal and special quality crystals.

The illustration shows the R5 high energy solid state ruby laser.

EE 02 765 *for further details*

TORQUE TRANSDUCER

Ether Engineering Ltd, Park Avenue, Busbey Hertfordshire

(Illustrated below)

This torque transducer embodies high output solid state strain-sensing elements mounted on a short quill shaft with circular coupling flanges. The assembly is slim and flat and is particularly suitable for such applications as steering-wheel torque measurement during the performance testing of automotive vehicles; the transducer mounts below the steering-wheel with negligible addition to overall height and with no effect on the handling characteristics of the vehicle. A safety link is incorporated which maintains steering control in the unlikely event of the failure of the quill shaft. The unit may also be in a shaft coupling for torque and horse-power measurement.

The high signal output from the solid-state strain elements is adequate to drive

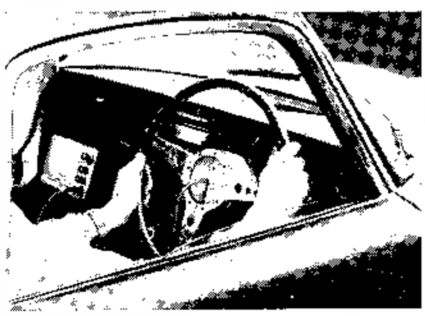

direct a robust moving-coil indicator or recorder. When used in conjunction with a slip-ring assembly in a shaft coupling, the effect of brush noise on the output will be negligible.

In addition to possessing infinite resolution and rapid response, the unit is remarkably insensitive to bending forces.

Standard Instrument range is 50 lb-ft but other ranges may be supplied to special order.

A battery powered portable indicator unit (type RML 8-225) is available to operate this transducer.

EE 02 766 *for further details*

DELAY LINE

Sealectro Ltd, Farlington, Portsmouth, Hampshire

(Illustrated above right)

A new, low cost 500µsec delay line that can be mass-produced for use in desk-size electronic calculators has been introduced by the "Deltime" division of Sealectro.

This new delay line, designated model 300, features any fixed delay up to 500µsec. It operates in the return-to-zero mode at 1MHz with a worst case signal-to-noise ratio of 3:1 between +15°C and +55°C.

Specifications include an input volt-

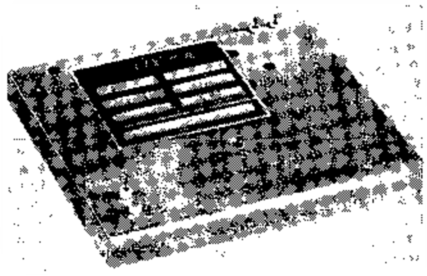

age of 20V and peak current of 50mA maximum. Output voltage is specified as 15mV minimum across a load of 2700Ω.

EE 02 767 *for further details*

MICROMINIATURE RESISTORS

Distributed by: Nutec Electronics Ltd, Mercantor House, 5 East Street, Shoreham-by-Sea, Sussex

Type RKL2 high stability carbon film resistors, manufactured by L. Siegart in Western Germany, are among the smallest in the world. They have a length of 0·102in and a diameter of 0·035in.

The new resistor is of similar design to the RKL10. A carbon deposit, applied by pyrolysis to the ceramic substrate, is extended to coat cavities at the ends of the rod. The leads are soldered to nickel plating overlaying the carbon film in these cavities. This eliminates the usual compression type end cap, assures a more stable electrical contact and provides a resistance tract extending the full length of the ceramic rod.

The leads are gold plated to facilitate rapid soldering. They are of copper nickel alloy which combines high strength with low thermal conductivity and reduces the danger of heat damage during soldering. However, it is recommended that solder with a melting point not greater than 180°C should be used.

These resistors, which are available in values between 47Ω and 100kΩ have a power rating of 30mW at 65°C.

EE 02 768 *for further details*

MINIATURE SYNCHRONOUS MOTOR

Magnetic Devices Ltd, Exning Road, Newmarket, Suffolk

(Illustrated below)

This small synchronous motor, 36mm in diameter and 20mm long, weighs 90g and requires an input power of 0·6W. The motor is reversible and on 50Hz has a synchronous speed of 300rev/min. Quick starting and reversing is achieved by a low moment of rotor inertia of 25g.cm². There is a direct connexion for voltages up to 100V but the motor may be used at up to 380V,

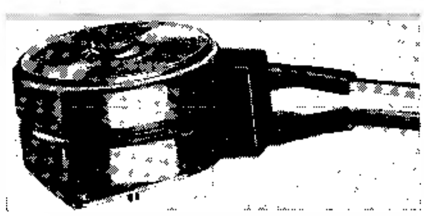

single or three-phase, via a series connected resistor or capacitor. As a stepping motor the RSM36 can operate at a maximum of 300 step/sec. Gearboxes are available for operation down to 1 revolution in 30 hours.

EE 02 769 *for further details*

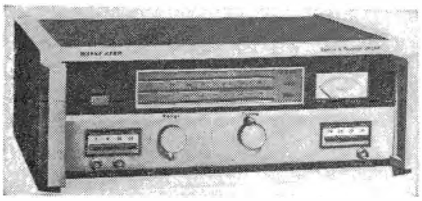

R.F. SOURCE/DETECTOR

The Wayne Kerr Co. Ltd, Sycamore Grove, New Malden, Surrey

(Illustrated above)

Wayne Kerr has introduced a solid-state source/detector with single-knob tuning from 100kHz to 100MHz. Although designed principally for its r.f. and v.h.f. bridges B201, B601 and B801, the new SR268 has a wide range of source output level and receiver gain, making it suitable for most measurement applications.

Output level is 2V r.m.s. across 75Ω with push-button attenuation available in 3dB steps to −39dB. Short-term frequency stability is 0·01 per cent.

Detector sensitivity is from 1μV or better, an input attenuator giving steps of 20dB each. At each setting the operating range of the a.g.c. circuit is automatically adjusted to provide ideal conditions for rapid location of balance with a precise final null. A null meter is fitted.

Operation is from 110 or 230V supplies, using an internal rectifier unit, but the SR268 can also be powered from batteries.

EE 02 770 *for further details*

MOTOR PROTECTION UNITS

Standard Telephones & Cables Ltd, Components Group, Footscray, Sidcup, Kent

(Illustrated above right)

This small solid-state plug-in module eliminates the possibility of electric motors overheating. Without contacts or moving parts of any kind, it automatically cuts off the motor contactor supply immediately the temperature of the motor windings exceeds a safe value.

Experience has shown that even minor overheating of motor windings adversely affects motor performance and, if prolonged, considerably shortens motor life.

The new module controls the motor a.c. supply via a built-in thyristor. Instant protection against excessive temperature operation is achieved by employing an external positive-temperature-coefficient (p.t.c.) thermistor embedded in the motor windings, to control the thyristor switching action. A rise in motor temperature causes the thermistor resistance to increase; when the resistance exceeds a critical value, the thyristor changes state and cuts off the contactor supply. Self-latching operation is possible with the addition of an external resistor.

Any type of p.t.c. thermistor can be employed. Three-phase motors can be protected by three thermistors—one per phase—connected in series so that all three windings can be monitored simultaneously by one module.

Since operation depends solely on the direct monitoring of actual winding temperature, effective protection is provided against overheating due to all forms of malfunction or abuse.

In practice, it has been found that the use of these modules rapidly brings to light any mechanical, electrical and environmental shortcomings, both in the installation design and the load, which normally would have passed unnoticed for some time—possibly not before failure occurred.

The module consists of a transistorized

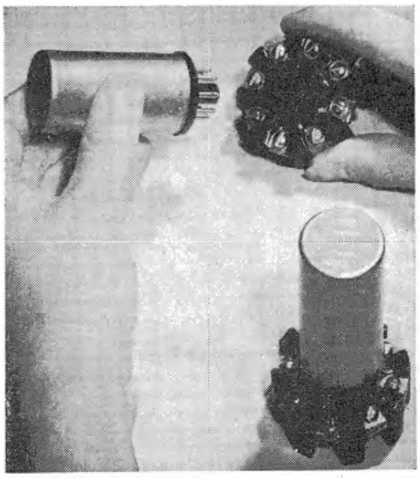

assembly containing the thyristor and its associated control circuit, engineered in STC's Ministac modular construction system for mechanical strength and small size. For increased ruggedness, the assembly is encapsulated and hermetically sealed in an anodized aluminium can. The small size of the module facilitates installation in restricted places such as motor starter boxes. Connexions are via an International octal plug to facilitate easy replacement in the unlikely event of failure.

The reliability of the new module is such that the designers claim a mean-time-between-failure rate of 45 years.

EE 02 771 *for further details*

PAPER/POLYESTER CAPACITORS

Telegraph Condenser Co. Ltd, Whales Farm Road, Acton, London, W.3

A new range of rectangular can capacitors using a mixed paper/polyester dielectric has been introduced by the Telegraph Condenser Co. Ltd, a member of the Plessey Components Group. Intended for use in high grade professional electronic equipment, they are designed to meet DEF-5131, styles CP 10 and CP 11 category 55/100 H6, and will shortly be submitted for approval to these standards.

Higher voltage stresses made possible by the new dielectric enable the capacitors to be considerably smaller than the established paper dielectric range for similar ratings. For example, the dimensions of a 2μF 5000V paper capacitor are reduced from 9in by $5\frac{1}{8}$in to only $4\frac{5}{8}$in by $5\frac{1}{8}$in by $3\frac{7}{8}$in with the mixed dielectric. Operating temperature is from −55°C to +70°C; suitably de-rated, operation is permissible up to 100°C.

Capacitance values are between 0·05μF and 12μF with d.c. rated voltages from 200V to 10kV at 70°C. Used as reservoir and smoothing capacitors in rectifier circuits, and for decoupling in amplifiers, both the established and the mixed dielectric types are especially suitable for use in high voltage d.c. circuits.

EE 02 772 *for further details*

FILM RESISTANCE MONITOR

Edwards High Vacuum Ltd, Manor Royal, Crawley, Sussex

(Illustrated below)

The Edwards film resistance monitor is a control device used with a vacuum coating plant to measure the changing electrical resistance of a film during deposition and to terminate the deposition when a preset value of resistance is reached. The resistance range covered is 10Ω to 10kΩ, in three steps. The film resistance monitor is used when depositing resistors or in conjunction with the film thickness monitor when depositing thin film circuits.

Either the resistance of the thin film itself is measured or that of a convenient monitor strip. This resistance forms one arm of a Wheatstone bridge and another, reference arm, of the bridge is adjustable from the front panel of the monitor.

The front panel reference arm, a helical potentiometer with a calibrated

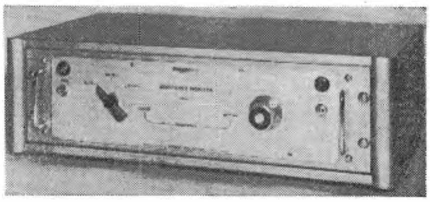

control, is set to correspond to the required thin film resistance. When the correct value is reached the bridge balances, triggering a high gain transistorized amplifier which energizes a relay which in turn closes the source shutter thus terminating the film deposition. The shutter remains closed until the reset button is depressed.

External use terminals on the relay, one pair normally closed and one pair normally open, are provided for control of ancillary apparatus.

The bridge is designed so that the power dissipation in the monitored film remains below 50mW on all ranges. Overheating or partial braking of the deposited film is thereby avoided.

EE 02 773 *for further details*

Meetings THIS Month

THE INSTITUTION OF ELECTRICAL ENGINEERS

Date: 4 January.
Discussion: Modular Construction in Electronic Instrumentation.
(Further details to be announced in I.E.E. News.)
Date: 5 January.
Discussion: Electrically Signalled Aircraft Flying Controls.
(Joint meeting with the Automatic Control Group of the I.Mech.E. at 1 Birdcage Walk, London, S.W.1, at 6 p.m.)
Date. 6 January.
Colloquium: Methods of Interpreting Biological Signals.
(Joint meeting with the Automatic Control Group of the I.Mech.E.)
Date: 9 January.
Discussion: The Application of Data Processing in a Large Manufacturing Plant.
(Joint meeting with the Automatic Control Group of the I.Mech.E. at 1 Birdcage Walk, London, S.W.1. at 6 p.m.)
Date: 9 January.
Discussion: Recent Developments in Fuel Cells.
Opened by: Dr. D. P. Gregory.
Date: 10 January.
Lecture: Glow and Corona Discharge Tubes.
By: Dr. F. A. Benson and others.
Date: 10 January.
Discussion: Are the Safety Arrangements on British Aircraft Electrical Systems Entirely Logical?
Opened by: D. O. Burns.
Time: 6 p.m.
Date: 11 January.
Discussion: High-Speed Fuses for the Protection of Diodes and Thyristors.
Opened by: E. Jacks.
Date: 12 January.
Discussion: M.H.D. Generation.
Opened by: Dr. P. R. Howard.
Date: 13 January.
Colloquium: Standardization, Servicing, Maintenance and Organization of Medical and Biological Instrumentation.
Joint meeting with the I.E.R.E. Medical and Biolological Group at 10.30 a.m.)
Date: 16 January.
Discussion: Laboratory Work Policy.
Opened by: Dr. K. R. Sturley and A. D. Collop.
Date: 18 January.
Lecture: Multi-Access Computer Systems.
By: Prof. M. V Wilkes.
Date: 19 January.
Discussion: Practical Applications of Computer Programmes in Electronic Engineering.
(Joint meeting with the I.E.R.E. Computer Group at the I.E.R.E., 8-9 Bedford Square, London, W.C.1, at 6 p.m.)
Date: 23-26 January.
Conference: Acoustic Noise and its Control.
Date: 24 January.
Lecture: Coding in the Auditory Nervous System.
By: Dr. I. C. Whitfield.
Date: 26 January.
Lecture: Ion Propulsion.
By: D. Gignoux and J. Lazar.
Date: 27 January.
Colloquium: Pseudo-Random Sequences Applied to Control Systems.
(Joint meeting with the Automatic Control Group of the I.Mech.E.)
Date: 27 January.
Discussion: Use of Electric Optic Effect for Light Modulation.
Opened by: J. M. Ley.
Date: 30 January.
Discussion: Ion Implantation.
Opened by: Dr. J. Dearneley and L. Large.
Date: 31 January.
Colloquium: Adaptive Control for Aircraft.
(Joint meeting with the Automatic Control Group of the I.Mech.E. and the IEE/RAeS London Joint Group, at 2.30 p.m.)

London District Meetings
Chelmsford

Date: 16 January.
Time: 6.30 p.m.
Lecture: Post Office Towers and Trunks.
By: J. H. H. Merriman.
Held at: The Lion and Lamb Hotel, Chelmsford, Essex.
(Joint meeting with the I.E.R.E.)

THE INSTITUTION OF POST OFFICE ELECTRICAL ENGINEERS

Formal Meetings

Formal meetings will be held at the Institution of Electrical Engineers, Savoy Place, W.C.2, commencing at 5 p.m.
Date: 17 January.
Lecture Production and Evaluation of Highly Reliable Transistors.
By: R. C. Corke.

Informal Meetings

Informal meetings will be held in the Conference Room, Fleet Buildings, 70 Farringdon Street, E.C.4, commencing at 5 p.m.
Date: 3 January.
Lecture: Postal Mechanization with Minimum Machinery.
By: S. W. Godfrey.
Date: 31 January.
Lecture: Application of Transistors to TV Line Equipment.
By: W. G. Simpson.

THE INSTITUTION OF ELECTRONIC AND RADIO ENGINEERS

Radar and Navigational Aids Group
Held at: Middlesex Hospital Medical School, Cleveland Street, London, W.1.
Date: 11 January.
Time: 10.30 a.m.
Symposium: Navigational Aids for Ground Vehicles.

Joint I.E.E/I.E.R.E.

Medical and Biological Electronics Group
Held at: Institution of Electrical Engineers, Savoy Place, London, W.C.2.
Date: 13 January.
Time: 10.30 a.m.
Symposium: Standardization, Servicing and Maintenance of Medical and Biological Electrical Instrumentation.

Electro-Acoustics Group

Held at: London School of Hygiene and Tropical Medicine, Keppel Street, Gower Street, London, W.C.1.
Date: 17 January.
Time: 6 p.m.
Symposium: Radio Microphones.
Speakers: M. L. Gayford, G. R. Pontzen and R. W. Swain.

Joint I.E.R.E./I.E.E.

Computer Groups
Held at: Institution of Electronic and Radio Engineers, 8-9 Bedford Square, London, W.C.1.
Date: 19 January.
Time: 6 p.m
Discussion: Practical Applications of Computer Programmes in Electronic Engineering.
The following contributions will be given:
Applications in an Integrated E.D.P. System—F. Barker.
Digital Circuit Simulation— Dr. M. W. Bradshaw.
Practical Experience with Computer Design Automation—H. G. Adshead.

South-Western Section

Held at: University of Bristol, Main Lecture Theatre, University Walk, Clifton, Bristol 8.
Date: 19 January.
Time: 7 p.m.
Lecture: Automation in North Atlantic Air Traffic Control.
By: H. Cherry.
(Joint I.E.R.E./R.Ae.S./I.E.E.)

South Wales Section

Held at: Welsh College of Advanced Technology, Cardiff.
Date: 11 January.
Time: 6.30 p.m.
Lecture: Silicon Controlled Rectifiers.
By: R. G. Dancy.

East Anglian Section

Held at: Lion and Lamb Hotel, Chelmsford, Essex.
Date: 16 January.
Time: 6.30 p.m.
Lecture: Post Office Towers and Trunks.
By: J. H. H. Merriman.
(Joint meeting with I E.E.)
Held at: College of Further Education, Ardleigh Green Road, Hornchurch, Essex.
Date: 25 January.
Time: 6.30 p.m.
Lecture: Some Applications of Electronics to Oceanographic Sensors.
By: A. M. East.

South Midland Section

Held at: North Gloucestershire Technical College.
Date: 20 January.
Time: 7 p.m.
Lecture: Quality and Reliability.
By: J. G. Adler and D. Newton.

East Midland Section

Held at: University of Nottingham, Department of Physics.
Date: 11 January.
Time: 6.30 p.m.
Lecture: The Engineering of Computer Control in the Engineering Industry.
By: K. A. MacKenzie and B. Revell.

West Midland Section

Held at: Stafford College of Further Education, Tenterbanks.
Date: 17 January.
Time: 7.15 p.m.
Lecture: Electronic Exchanges.
By: E. S. Grundy.

Merseyside Section

Held at: Liverpool College of Technology, Byrom Street.
Date: 18 January.
Time: 7 p.m.
Lecture: Modern Trends in Nuclear Electronics and Why.
By: H. Bisby.

North Eastern Section

Held at: Institute of Mining and Mechanical Engineers, Neville Hall, Westgate Road, Newcastle.
Date: 11 January.
Time: 6.30 p.m.
Lecture: Micro Miniaturized S.S.R. Transponder.
By: D. H. Mehrtens.

Southern Section

Held at: Highbury Technical College, Cosham, Portsmouth.
Date: 25 January.
Time: 6.30 p.m.
Lecture: Circuit and Systems Design by Digital Computer.
By: J. S. Reynolds.
Held at: Lanchester Theatre, University of Southampton.
Date: 17 January.
Time: 6 30 p.m.
Lecture: Colour Television.
By: S. M. Edwardson.
(Joint meeting with I.E.E.)
Held at: Farnborough Technical College, Boundary Road, Farnborough, Hants.
Date: 12 January.
Time: 7 p.m.
Lecture: Proximity Sensing by Magnetic Induction.
By: D. Barnard.

Scottish Section

Held at: Institution of Engineers and Shipbuilders, 39 Elmbank Crescent, Glasgow.
Date: 12 January.
Time: 7 p.m.
Lecture: The Use of Graphic Input/Output Equipment with Computers.
By: E. J. C. Fowell.

Thames Valley Section

Held at: J. J. Thomson Physical Laboratory, University of Reading.
Date: 18 January.
Time: 7.30 p.m.
Lecture: Self-Adaptive Control Systems.
By: P. Atkinson.

NOUVELLES Réalisations

Traduction des pages 50 à 55

Une description basée sur des renseignements fournis par les fabricants de nouveaux composants, accessoires et instruments d'essai

TRANSDUCTEUR DE VIBRATIONS DE PROXIMITÉ

Southern Instruments Ltd, Camberley, Surrey

(Illustration à la page 50)

Le transducteur de vibrations de proximité T.510 a été étudié pour mesurer l'amplitude relative des vibrations, sans contact entre le transducteur et une surface mobile. La surface doit être en un matériau à haute conductivité ou, si ce matériau n'est pas conductif ou ferreux, elle doit avoir une mince cale de laiton au cuivre de béryllium.

Pour faciliter la simplicité du réglage de l'entrefer initial entre le transducteur et la surface et pour faciliter également l'étalonnage, l'élément de mesure inductif peut être déplacé par rapport au corps du transducteur. Ce mouvement est contrôlé par un réglage de type micrométrique étalonné en divisions de 0,0005 pouce jusqu'à 0,4 pouce.

Le T.510 a été conçu exclusivement pour l'emploi avec le système préamplificateur à modulation de fréquence type TE.7 Southern Instruments, et il contient un circuit oscillateur miniature dont la sortie est une fréquence (nominalement de 2 MHz) proportionnelle au déplacement appliqué. Le préamplificateur à modulations de fréquence transforme cette fréquence en un signal correspondant de tension ou de courant.

Le montage du transducteur s'effectue au moyen d'un trou alésé de 20,6 mm ou d'un trou fileté de 20,6 mm à 40 spires par pouce.

EE 02 751 *pour plus amples renseignements*

OSCILLOSCOPE CONSTITUÉ DE CORPS SOLIDES

Hewlett-Packard Ltd, 224 Bath Road, Slough, Buckinghamshire

(Illustration à la page 50)

Le nouvel oscilloscope à fiches entièrement constitué de corps solides de 50 MHz de la société Hewlett-Packard a un écran de 30% plus grand (8 × 10 cm) que le modèle précédent de 50 MHz. Il pèse environ 13 kg, mesure 20,32 cm × 27,94 cm × 57,15 cm de profondeur. Le modèle pour montage sur bâti mesure 19,33 cm de hauteur. Conçu pour dépasser en précision les oscilloscopes de laboratoire précédents, le nouveau modèle Hewlett-Packard 180 A est d'un encombrement réduit, de poids léger et très adaptable aux diverses utilisations en laboratoire et de production. Il est étudié pour fonctionner normalement de −28°C à +65°C, à une humidité relative de 95% jusqu'à 40°C et à des altitudes allant jusqu'à 4572 m.

Il comporte deux prises pour fiches. L'une est pour l'amplificateur vertical. Le premier de ces amplificateurs à être disponible est un appareil à deux canaux et qui produit un facteur de déviation (sensibilité) de 5 mV/cm à 50 MHz. La trace ne se déplace pas lorsque la commande de sensibilité étalonnée est mise en action. Il n'y a pratiquement aucune dérive de trace lorsque l'instrument est mis en marche. Ces caractéristiques résultent de l'emploi de nouveaux circuits entièrement constitués de corps solides et à faible bruit, avec des paires adaptées de transistors à effet de champ maintenu constamment dans le même environnement thermique, permettant ainsi à toutes les atténuations de précéder les amplificateurs.

Deux nouveaux éléments interchangeables de base de temps sont offerts pour le modèle Hewlett-Packard 180 A. Le premier de ces modèles, type 1820A, réalise une vitesse de balayage de 5 nsec/cm, lorsque son appareil de grossissement est tourné au réglage d'étalonnage le plus rapide (0,05 µsec/cm). Grâce au déclenchement sûr à 90 MHz, le résultat en est une plus grande résolution dans l'observation de traces à grande vitesse que celle qui a pu être obtenue précédemment avec les oscilloscopes de cette catégorie. Une commande variable permet à l'utilisateur de synchroniser harmonieusement les trains d'impulsions asymétriques.

Le modèle 180 A peut être complété sur demande de la nouvelle base de temps, type 1821A et d'un dispositif à fiche de générateur à retard. La base de temps retardée commence à effectuer le balayage après un retard de temps par rapport au balayage principal, ce dernier étant contrôlable. Un point brillament éclairé sur l'écran identifie le point de la trâce où le balayage différé commence: ce dernier détecte et identifie la partie de la trace que l'observateur désire agrandir pour un examen détaillé. On peut également utiliser le bord principal de la trace, après le temps de retard, pour actionner le déclencheur de retard, et on obtient ainsi une présentation sur l'ensemble de l'écran exempte de tout tremblement.

Malgré les faibles dimensions du 180 A, les lignes à retard sont incorporées, de sorte que le bord principal de n'importe quelle impulsion peut toujours être observé. Ces lignes à retard sont d'une construction entièrement nouvelle tout en étant parfaitement appropriées au but auquel elles sont destinées; la largeur de bande de ces lignes à retard dépasse 140 MHz et une paire différentielle est incorporée à l'instrument.

Un assortiment complet d'accessoires est offert avec le modèle 180 A. La nouvelle caméra à obturateur électronique, HP modèle 197A, peut être montée directement sur l'appareil et des adapteurs sont fournis pour la plupart des autres caméras. Un capot de vision souple, un couvercle de panneau, un couvercle de support et une sonde de division à haute impédance sont tous conçus pour s'adapter à l'appareil.

EE 02 752 *pour plus amples renseignements*

POTENTIOMÈTRES MINIATURE À PISTE MOULÉE

Davall Electronics Ltd, Rothersthorpe Avenue, Northampton

(Illustration à la page 50)

Le nouveau potentiomètre préréglé miniature à piste moulée, Davall type 80, utilise un moulage phénolique d'une seule pièce rempli de minéraux de haute qualité qui permet à la base d'isolemment, à la piste résistive et aux bornes d'être moulés en un seul élément intégré solide. Ce type de construction assure une grande stabilité dans toutes les conditions d'humidité, de température et de vibration. Les variations de performance sont inférieures à 5 % dans la gamme de température de −40° C à +70° C. La spécification DEF 5214 a été utilisée comme norme minima dans la mise au point de ce composant.

Le potentiomètre linéaire type 80 a une puissance nominale de 0,25 W à 70° C et une tension de régime maxima de 500 V c.c. La gamme de résistance s'étend de 20 Ω à 1MΩ.

Il existe deux versions à savoir une version avec cosses pour le soudage direct au circuit imprimé, l'autre pour le montage sur plaquette isolée. Le type standard 80 est très compact et peut être enfermé dans un cylindre de 0,60 pouce de diamètre et de 0,26 pouce de profondeur (sans le montage et les cosses).

Le type 80 peut être à la main ou par tourne-vis et une variante, le type 80/1, peut être fournie avec un plus gros bouton pour le réglage par l'utilisateur.

EE 02 753 *pour plus amples renseignements*

CONDENSATEURS AU POLYCARBONATE

Standard Telephones & Cables Ltd, Components Group, Footscray, Sidcup, Kent

(Illustration à la page 51)

La division des condensateurs de la société Standard Telephones and Cables Ltd a introduit une série complète de condensateurs au polycarbonate protégés à la résine et spécifiquement prévus pour les nombreuses utilisations ne rencontrant pas des conditions d'environnement sévères.

Les condensateurs au polycarbonate sont des composants d'une haute fiabilité, bobinés à partir d'un film plastique ultra-mince de polycarbonate métallisé. Leurs caractéristiques électriques et physiques sont supérieures à celles d'autres condensateurs à film plastique et ils demeurent stables dans une gamme étendue de températures.

Basés sur les éléments tubulaires de la division (qui répondent aux conditions de protection d'environnement H6 de la spécification DEF 5011), les nouveaux éléments ont la même performance électrique élevée mais sont logés dans des coffrets moulés rectangulaires et robustes en résine à prise thermique fournissant une protection d'environnement au H3 de la spécification DEF 5011, c'est à dire une protection plus que suffisante pour les conditions d'utilisation de la plus grande partie des matériels électroniques commerciaux. Les fils terminaux sont radiaux et espacés pour le montage sur circuit imprimé.

Les condensateurs au polycarbonate protégés à la résine STC sont fournis à des valeurs de 0,01 à 4,7 μF, 100 Vc.c., et peuvent être utilisés dans la gamme de températures de −40°C à +85°C. Leur performance générale supérieure en fait des variantes intéressantes aux condensateurs au polyester métallisés (terephthalate au polyéthylene), particulièrement en raison du fait que les nouveaux condensateurs sont fournis aux prix généraux des condensateurs au polyester.

EE 02 754 *pour plus amples renseignements*

INDICATEUR MAGNÉTIQUE DE RELÈVEMENT

Aviation Division, Smiths Industries Ltd, Kelvin House, Wembley Park Drive, Wembley, Middlesex

(Illustration à la page 51)

Le nouvel indicateur combiné de position pour l'affichage des relèvements du radiogoniomètre d'approche ou du radiogoniomètre automatique, comportant un certain nombre de perfectionnements par rapport au modèle précédent, est actuellement en cours de production par la Division d'Aviation de la Société Smith Industries. Enfermé dans un coffret standard de 3 ATI, l'appareil est conforme aux recommandations de l'ARINC et il est muni de l'éclairage intégral.

Le cap magnétique de l'avion est indiqué par une carte de compas rotative qui se lit par rapport à un repère fixe sur le haut de l'instrument. La carte est entraînée par un mécanisme asservi dont l'amplificateur se trouve à l'intérieur du coffret, à partir d'un signal fourni par le compas principal de l'avion. Toute panne du compas est indiquée par un drapeau.

Les positions magnétiques de deux radars de navigation sont indiqués sur la carte du compas par les deux aiguilles, tandis que les renseignements sur le relèvement relatif sont fournis par la position des aiguilles par rapport au repère fixe. Un soin particulier a été donné à la précision des aiguilles de relèvement relatif qui sont actionnées par des synchros récepteurs de couple. Les entrées du radiogoniomètre d'approche ou du radiogoniomètre automatique vers ces synchros sont obtenus par commutation externe.

L'appareil comprend également un émetteur à contre-réaction qui fournit une sortie de signal du cap de l'avion. Cet élément peut être utilisé pour d'autres appareils de vol qui ont besoin de ce signal.

EE 02 755 *pour plus amples renseignements*

VOLTMÈTRE NUMÉRIQUE À TENSION CONTINUE

Hewlett-Packard Ltd, 224 Bath Road, Slough, Buckinghamshire

(Illustration à la page 51)

Le nouveau voltmètre numérique type 3430A a une précision de 0,1 % plus 1 chiffre et une stabilité telle que la période d'étalonnage prévue est de 90 jours. Il a une entrée flottante: lorsque sa borne d'entrée "basse" est détachée du sol, le voltmètre peut mesurer jusqu'à ±500 V c.c. loin du sol. L'impédance d'entrée est de 10 MΩ sur toutes les gammes.

L'instrument comporte cinq gammes sélectionnées manuellement allant de 100 mV c.c. sur la totalité de l'échelle à 1 kV c.c. sur la totalité de l'échelle et une lecture à trois chiffres. Un quatrième chiffre (un ou blanc) permet d'effectuer des mesures au-delà de la gamme allant jusqu'à 60% au-dessus de la totalité de l'échelle (excepté dans la gamme de 1 kV) à une précision absolue. Une surcharge dépassant 60% est indiquée par des éclairs sur l'affichage éclairé. L'instrument répond automatiquement à la polarité de l'entrée et indique si l'entrée est une tension négative ou positive.

Entre autres caractéristiques, le nouveau voltmètre numérique a une sortie d'amplificateur qui fournit une tension continue proportionelle à l'entrée avec une précision de gain de ±0,1%. Le gain de tension non-inverseur de l'amplificateurs est de 100 dans la gamme de 100 mV, décroissant d'un facteur de 10 sur chacune des gammes supérieures. La sortie de l'amplificateur, commode pour entraîner un enregistreur, peut entraîner n'importe quelle charge ayant une impédance supérieure à 10 kΩ sans dégradre la précision de la lecture.

Une version différente de l'instrument permet les mesures de rapport, un avantage certain pour normaliser les lectures de sortie de transducteurs à courant continu. L'affichage montre la tension d'entrée divisée par la tension de référence. N'importe quelle tension fixe entre 0,8 et 1,2 V (l'une ou l'autre des deux polarités) peut être utilisée comme entrée de référence et des rapports de 0,0001 : 1 à 1000 : 1 peuvent être mesurés.

Le nouveau voltmètre numérique est un instrument dit "en escalier" du type comparateur, pouvant en effet comparer la tension d'entrée par rapport à une tension produite intérieurement à partir d'une diode de référence zéner et de résistance de précision. La tension produite intérieurement commence à zéro et elle est automatiquement élevée à des valeurs successivement supérieures jusqu'à ce qu'elle s'accorde avec les tensions d'entrée. Chacun des plots fait avancer le compteur d'un chiffre; lorsque la coïncidence est atteinte, le nombre de comptages accumulé, qui représente la tension d'entrée, est affiché sur le tableau du panneau frontal. L'instrument retient le nombre affiché jusqu'à ce que le cycle de mesure suivant soit achevé, assurant ainsi un affichage continu. L'instrument complète deux lectures par seconde.

EE 02 756 *pour plus amples renseignements*

COMMUTATEURS STATIQUES

Vosper Ltd, Hamilton Road, Paulsgrove, Portsmouth, Hampshire

(Illustration à la page 52)

Une gamme de dispositifs statiques de commutation pour une variété d'utilisations est actuellement en pleine production à l'usine de Portsmouth de la société Vosper Electric, qui est une filiale du groupe Vosper Thornycroft. Quatre catégories principales d'éléments sont construits: des minuteries à retard assurant une fonction de commutation simple; des minuteries à retard entraînant des relais de permutation bipolaires et à deux directions; des commutateurs statiques de courant continu multipolaire, des commutateurs statiques de courant alternatif multipolaire. Ces deux derniers composants correspondent aux relais ou contacteurs électromécaniques. Etant donné qu'il n'y a pas de parties mobiles, les problèmes inhérents aux dispositifs électromécaniques sont éliminés. Les commutateurs multipolaires sont offerts avec ou sans minuterie dans le même module. Toutes les minuteries sont réglables, un nombre de gammes différentes étant prévu, donnant des retards jusqu'à un maximum de 300 sec.

Une attention particulière a été accordée à la répétabilité et à la fiabilité dans le dessin de tous ces éléments. Tous les composants sont encapsulés dans de la résine synthétique inerte et l'ensemble de l'assemblage est enfermé dans un couvercle en aluminium anodisé. Il en résulte des éléments hautement résistants à l'humidité et à la corrosion, aux forces d'accélération et de vibration. Une limite d'accélération de 150 g est prévue pour la plupart de ces commutateurs, et 50 g pour la minuterie à retard contenant le relais. Tous les commutateurs peuvent résister à des forces vibratoires équivalent à 25 g à 2 ou 3 kHz et à des températures de −65 ou moins 55 à +60 C.

Les courants de charge de sortie allant de 1,0 à 5,0 A, suivant le type, et des puissances d'entrée (correspondant au courant de bobine de régime d'un relais) sont suffisamment bas pour le fonctionnement direct par circuit à transistor de 22 mA c.c. ou 5 Wc.a. Une gamme de tension d'entrée et de sortie est prévue de douze à 150 V c.c. et de 12 à 250 V c.a.

EE 02 757 *pour plus amples renseignements*

BOÎTES DE PROTECTION R.F.

Hatfield Instruments Ltd, Burrington Way, Plymouth, Devon

(Illustration à la page 52)

Cette gamme de carters moulés en aluminium a été conçue pour répondre de manière efficace aux problèmes de la protection H.F. de petits groupes de composants faisant partie d'atténuateurs de filtres, de réseaux, de diviseurs de tension, etc. Ces boîtes sont de construction solide et elles sont fournies complètes avec couvercle moulé fixé par quatre vis. Elles peuvent être munies de douilles et prises B.N.C. de manière à pouvoir les introduire en série avec des cables et du matériel existant.

Ces boîtes peuvent être fournies en outre avec des connecteurs standard de 50 Ω B.N.C., avec une prise à une extrémité et une fiche à l'autre. Elles peuvent être utilisées avec des systèmes de 75 Ω jusqu'à environ 100 MHz sans qu'une réflexion sensible se produise. Ce cas est dû au fait que les connecteurs B.N.C. ne sont qu'une faible fraction d'une longueur d'onde aux hautes fréquences inférieures.

Les trois dimensions prévues actuellement sont:

3,5 × 3,18 × 4,76 cm; 7,3 × 4,76 × 7,3 cm; 4,12 × 4,7 × 14,29 cm.

EE 02 758 *pour plus amples renseignements*

POTENTIOMÈTRE SUBMINIATURE

Pandect Precision Components Ltd, Wellington Road, High Wycombe, Buckinghamshire

(Illustration à la page 52)

Un potentiomètre d'appont bobiné sub-miniature, l'un des plus petits de son genre actuellement produit au Royaume-Uni, a été ajouté à la gamme de composants résistifs fabriqués par la société Pandect. Sa forme physique correspond à celle d'un transistor standard TO-5, et il a été prévu principalement pour l'emploi dans le matériel aéronautique, militaire et électronique de haute qualité répondant à des spécifications rigoureuses.

Le nouveau potentiomètre est fourni dans des valeurs de résistance de 5Ω à 15 kΩ. Il offre une puissance nominale exceptionnellement élevée pour un aussi petit dispositif de 1 w à +75°C. Le soudage par résistance de la base et du couvercle assure une protection d'environnement de 100% dans une gamme de température ambiante de −70 à +150°C.

Le réglage du potentiomètre s'effectue en applicant un tourne-vis à un pivot à fentes. Le mécanisme comprend un simple embrayage qui patine pour le protéger contre l'endommagement accidentel par suite de l'application d'une force excessive aux extrémités du mouvement d'essuyage. Un anneau "O" en caoutchouc de silicone maintient le scellement entre le boîtier et le pivot.

Des connexions microsoudées sont utilisées intérieurement pour assurer une résistance maxima aux fortes vibrations. Les fils de sortie dorés passent à travers un scellement de verre/métal.

EE 02 759 *pour plus amples renseignements*

POMPES D'ADSORPTION DE CRIBLAGE MOLÉCULAIRE

Mullard Ltd, Mullard House, Torrington Place, London, W.C.1

(Illustration à la page 52)

La société Mullard Ltd a ajouté deux nouvelles pompes d'adsorption de criblage moléculaire à sa gamme de dispositifs à vide ultra poussé. Les deux nouveaux modèles ont été conçus pour assurer un pompage rapide de la pression atmosphérique jusqu'à la pression de départ des pompes Penning (environ 10^{-2} torr). Le matériau d'adsorption est du silicate d'alumine 13X qui donne une plus grande efficacité que d'autres qualités de ce matériau et le crible a été conçu de manière à ce que la plus grande surface possible du matériau d'adsorption soit exposé au fluide réfrigérant.

Les pompes, type VAP-12 et VAP-40, ont des capacités de pompage de volume d'environ 1 litre atmosphérique et 10 litres atmosphériques respectivement. Des volumes supérieurs peuvent être évacués par l'emploi d'un dispositif de pompage séquentiel dans lequel une des pompes travaille tandis que l'autre se rétablit.

La connexion aux pompes s'effectue au moyen de flasques en acier inoxydable, le scellement étant formé par le simple système Mullard à fil d'or. Une soupape de sûreté est fixée sur les deux pompes pour assurer une protection complète contre les excès de pression. Des bouteilles d'une conception spéciale sont prévues pour les deux types. Un espace suffisant a été laissé dans l'assemblage à bouteilles pour recevoir la tête sensible du système de remplissage à azote liquide Mullard, de création récente, qui peut être incorporé pour maintenir automatiquement le niveau du fluide réfrigérant pendant que le système de pompage est laissé sans observateur. Sur le plus grand modèle (VAP-40), un dispositif de chauffage est incorporé au crible pour faciliter la régénération.

EE 02 760 *pour plus amples renseignements*

GÉNÉRATEUR DE SIGNAUX MICROONDES

Marconi Instruments Ltd, Sanders Division, Gunnel's Wood Road, Stevenage, Hertfordshire

(Illustration à la page 53)

Cet instrument type 6459 offre la plage de fréquence la plus étendue de tous les générateurs de signaux pouvant être obtenus actuellement. Il a les caractéristiques suivantes:

Gamme de fréquence: 3,5 à 12,0 GHz.
Cadran de fréquence à lecture directe.
Atténuateur à lecture directe, étalonné en volt et en dBm.
Stabilité et précision élevées.
Modulation de fréquence interne, impulsion d'onde progressive ou modulation d'onde carrée.
Transformation facultative pour montage sur bâti.

Les formes d'ondes d'impulsion et d'ondes carrées sont produites intérieurement et l'instrument offre la possibilité d'utiliser les modulations externes. La fréquence de répétition des impulsions varie de 40 à 4 000 impulsions par seconde et la largeur d'impulsion est de 0,5 à 10 µsec. Les signaux de synchronisation sont simultanés avec l'impulsion HF, ou entre 3 et 300 µsec en avance sur l'impulsion HF. Les générateurs d'impulsion interne peuvent également être synchronisés au moyen des signaux externes.

Le générateur de signaux comporte un oscillateur à klystron à fiches dans une cavité à ligne coaxiale externe. La fréquence est déterminée par la position d'un piston mobile sans contact accouplé à l'échelle de fréquence et à un réseau de repérage automatique, et le niveau de sortie peut se lire en dBm et les microvolts à partir d'un atténuateur de haute précision interne, étalonné directement. La compensation de température appliquée au pont de mesure de la puissance, assure l'absence des effets de changement de température ambiante.

La sortie de puissance est comme suit:

(a) Direct: Une sonde d'introduction accouple la puissance à un maximum de 80 mW.

(b) 0,223 V à 0,1 μV (0 à −127 dBm) entre 4,5 et 11,0 GHz et −6 dBm à −127 dBm entre 3,5 et 4,5 GHz. Au-dessus de 11,0 GHz, la puissance de sortie est généralement supérieure à −6 dBm dans une charge de 50 Ω.

EE 02 761 *pour plus amples renseignements*

LECTEUR DE TRACE

Normalair Ltd, Yeovil, Somerset

(Illustration à la page 53)

La société Normalair Ltd vient d'ajouter un nouvel appareil à la gamme des instruments de concentration de données "Westland": le lecteur de trace Westland. Le fonctionnement de cet appareil est très simple et n'implique pas l'amploi de curseur, de mécanisme à asservissement de composants électromécanique et n'exige aucune habileté spéciale de la part de l'opérateur.

La table de lecture comporte une surface métallique plate à travers laquelle on fait passer un potentiel électrique linéaire, à savoir un signal de courant alternatif isolé bien au-dessous de 1 V en amplitude. Le diagramme, le film ou la photographie devant être examinés, sont placé sur la surface sensible et le lectures s'effectuent en plaçant l'extrémité à style d'une sonde tenue à la main sur la pointe devant être lue.

La sonde d'échantillonnage se tient comme une plume ou un crayon ordinaire et comporte un style à ressort. Ce dernier est placé sur l'enregistrement au point voulu pour chiffrer et l'operateur presse vers le bas le corps de la sonde. Cette action force le style à percer l'enregistrement et à établir le contact avec la plaque sensible se trouvant au-dessous. La machine complète ensuite automatiquement le processus de conversion et perfore la valeur échantillonnée sur la bande de sortie.

La machine peut être utilisée à une vitesse de régime maxima de une à deux lectures par seconde.

Toutes les commandes fonctionnelles sont groupées ensemble sur un clavier qui comprend également des boutons poussoirs pour ajouter des données supplémentaires, telles que l'identification de trace et de symboles spéciaux pour les programmes de calcul du client, etc. sur la bande perforée.

EE 02 762 *pour plus amples renseignements*

FICHE ET DOUILLE DE JACK À PLUSIEURS PÔLES

Render Instruments Ltd, Victoria Road, Burgess Hill, Sussex

(Illustration à la page 53)

La société Render vient d'annoncer l'introduction d'une fiche et douille de jack multipolaire qui vient s'ajouter à sa gamme de fiches et douilles de jack bipolaires, tripolaires et miniature.

Cette innovation constitue une méthode facile rapide et sûre de connexion pour l'emploi avec des câbles miniature ayant jusqu'à 12 âmes. En plus de sa forme de connecteur, ce composant peut être fourni avec un grand nombre de combinaisons de contact rupteurs sur la douille.

Le contact électrique s'effectue en tournant la fiche légèrement à droite, après insertion, la fiche restant automatiquement fixée dans cette position. En tournant légèrement la fiche dans le sens opposé, cette dernière est alors libérée et peut être retirée de la douille.

Ces composants constituent une méthode différente de connexion pour les types de fiche et douille à plusieurs broches déjà disponibles et ils ont l'avantage supplémentaire de permettre la commutation.

EE 02 763 *pour plus amples renseignements*

ÉQUIPEMENT AUXILIAIRE À "CRAYON-SUIVEUR"

d-mac Ltd, Queen Elizabeth Avenue, Hillington, Glasgow, S.W.2

(Illustration à la page 54)

Une nouvelle gamme d'équipement auxiliaire augmente les possibilités, la rapidité et la simplicité du fonctionnement du "suiveur de crayon" fabriqué par la société d-mac Ltd.

Cet élément qui convertit le matériau graphique en une forme numérique pour le traitement de données de calculatrices peut être muni maintenant d'un système de projection qui facilite l'analyse de données provenant de films.

Des films à cames ou sans cames de 16, 35, 50 ou 70 mm sont projetés sur sa table de lecture. Le mouvement de film tant en avant qu'en arrière est commandé par un moteur à vitesse variable pouvant être débrayé de sorte que des images spécifiques peuvent être fixées à la main à des positions précises.

Une fois l'image choisie, l'opérateur trace les données requises au moyen d'un "crayon" auquel le "suiveur" logé sous la surface de lecture est relié magnétiquement. La position du "suiveur" est transmise à la console d'éléctronique où elle est convertie en une forme numérique et injectée à un dispositif de sortie tel qu'un perforateur de bande.

Le crayon suiveur peut être également muni d'un rouleau de papier consistant de deux bobines montées au côté opposé de la table de lecture et un dispositif de tension pour placer le papier avec précision sur la surface de lecture. Des diagrammes d'une largeur de 45 cm sont enroulés à la main de l'un à l'autre, facilitant ainsi la manipulation de longs enregistrements.

Un neuveau type de "crayon" vient d'être mis au point pour assurer à l'appareil la possibilité de lecture angulaire. Ce crayon, placé le long d'une ligne, fournit les coordonnées de deux points à partir desquels un angle peut être calculé. Cette réalisation est déjà appliquée à l'analyse des enregistrements de chambre à étincelles et de kinéthéodolites.

Une possibilité de lecture différentielle est également prévue. Au moyen de cette dernière, des lectures sont obtenues à intervalles présélectionnés entre un millimètre et un centimètre le long de l'axe X d'une trace.

Le crayon suiveur peut être fourni avec une table de lecture mesurant 100 × 100 cm au lieu de la dimension standard de 100 × 45 cm.

EE 02 764 *pour plus amples renseignements*

EQUIPEMENT DE LASER

System Computers Ltd, Fossway, Newcastle upon Tyne, 6

(Illustration à la page 54)

La société System Computers Ltd fabrique une gamme de laser qui comprend cinq lasers au hélium-néon et trois lasers de rubis. Cette société fournit en outre le matériel auxiliaire dont les instruments de mesure de la sortie, les commutateurs Q à prisme passif et rotatif, les pièces de verre et des cristaux de qualité spéciale pour les applications particulières.

Le laser à rubis R1 a été spécialement conçu pour les démonstrations générales et pour les travaux de recherche dans l'industrie et les établissement d'enseignement. La sortie de l'élément à rubis de 5 cm de long est suffisament puissante pour des applications telles que le coupage ou le soudage de fils métalliques très minces.

Les grands lasers au rubis, modèles R5 et R10, ont des sorties d'environ 25 et 80 joules respectivement et peuvent être utilisées en tant qu'outils de processus de production. Les caractéristiques spéciales de ces lasers comprennent une cavité en aluminium hyperpure à refroidissement par air et une tige de 16,25 cm de long de rubis ou de néodymium-dans-le-verre fonctionnant à 6943Å ou 10600Å suivant le matériau utilisé. Les deux modèles ont un prisme extérieur et un miroir et les accessoires facultatifs comprennent un prisme rotatif ou une cellule de coloration, la commutation Q, la focalisation optique, le refroidissement par eau du cristal et des cristaux de qualité spéciale.

Notre gravure montre le laser R5 à rubis constitué de corps solides et à haute énergie.

EE 02 765 *pour plus amples renseignements*

TRANSDUCTEUR DE COUPLE

Ether Engineering Ltd, Park Avenue, Bushey Hertfordshire

(Illustration à la page 54)

Ce transducteur de couple comprend des éléments sensibles à la tension constitués de corps solides à sortie élevée montes sur une petite tige avec des flasques de couplage circulaire. L'assemblage est mince et plat et il convient particulièrement pour les applications telles que la mesure du couple d'un volant pendant le contrôle des véhicules automoteurs; le tranducteur se monte au-dessous du volant et ajoute très peu au poids total et demeure sans effet aucun sur les caractéristiques de manipulation du véhicule. Un joint de dans le cas improbable d'une panne de la tige. L'appareil peut également se trouver dans un couplage d'arbre pour la mesure du couple et de la puissance en chevaux.

La sortie à signaux élevé de l'élément de tension constitué de corps solides est suffisante qour entrainer directement un indicateur ou un enregistreur à cadre mobile robuste. Lorsqu'il est utilisé en liaison avec un assemblage à bague collectrice dans un couplage d'arbre, l'effet du bruit de balai sur la sortie est négligeable.

L'appareil possède non seulement une résolution infinie et une réponse rapide mais il est remarquablement insensible aux forces de flexion.

La gamme standard est prévue pour 50 livres par pied mais d'autres modèles peuvent être fournis sur commande spéciale.

Un indicateur portatif fonctionnant sur batterie (type RML 8-225) peut être fourni pour actionner le transducteur.

EE 02 766 *pour plus amples renseignements*

LIGNE À RETARD

Sealectro Ltd, Farlington, Portsmouth, Hampshire

(Illustration à la page 54)

Une nouvelle ligne à retard et à bas prix de 500 µsec pouvant être produite en série pour l'utilisation dans des calculatrices électroniques de format de bureau a été mise au point par la division "Deltime" de la société Sealectro.

Cette nouvelle ligne à retard, modèle 300, prévoit n'importe quel délai fixe jusqu'à 500 µsec. Elle fonctionne suivant le mode du retour à zéro à 1 MHz avec un rapport signal-bruit dans le cas le plus défavorable de 3:1 entre +15°C et +55°C.

La spécification comprend une tension d'entrée de 20 V et un courant de pointe de 50 mA au maximum. La tension de sortie est prévue à 15 mV minimum à travers une charge de 2700 Ω.

EE 02 767 *pour plus amples renseignements*

RÉSISTANCES MICROMINIATURES

Distributeurs: Nutec Electronics Ltd, Mercantor House, 5 East Street, Shoreham-by-Sea, Sussex

La résistance type RKL2 à film de carbone et à haute stabilité, fabriqué par la société L. Siegart d'Allemagne Occidentale, est une des plus petites au monde. Sa longueur est de 0,102 pouce et son diamètre de 0,035 pouce.

La nouvelle résistance est d'une conception analogue au type RKL 10. Un dépôt de carbone, appliqué par pyrolyse à la couche sous-jacente de céramique, est étendu pour revêtir les cavités aux extrémités de la tige. Les câbles sont soudés au revêtement de nickel du film de carbone dans ces cavités. On élimine ainsi la capsule d'extrémité ordinaire du type à compression et on assure un contact électrique plus stable et un passage de résistance s'étendant sur toute la longueur de la tige de céramique.

Les câbles sont dorés pour faciliter le soudage rapide. Ils sont en alliage de cuivre/nickel qui allie une grande solidité à une faible conductibilité thermique et réduit le danger d'endommagement par la chaleur durant le soudage. On recommande cependant d'utiliser une soudure dont le point de fusion n'est pas supérieur à 180°C.

Ces résistances qui sont fournies dans des valeurs entre 47 Ω et 100 kΩ ont une puissance nominale de 30 mW à 65°C.

EE 02 768 *pour plus amples renseignements*

MOTEUR SYNCHRONE MINIATURE

Magnetic Devices Ltd, Exning Road, Newmarket, Suffolk

(Illustration à la page 54)

Ce petit moteur synchrone de 36 mm de diamètre et 20 mm de long ne pèse que 90 g et exige une puissance d'entrée de 0,6 W. Il est réversible et il a une vitesse synchrone de 300 tours/min à 50 Hz. La mise en marche et l'inversion rapide sont réalisés par un faible moment d'inertie de rotor de 25 g/cm^2. Il existe une connexion directe pour les tensions allant jusqu'à 100 V mais le moteur peut être utilisé jusqu'à 380 V, monophasé ou triphasé, au moyen d'une résistance ou d'un condensateur relié en série.. En tant que moteur élévateur, le RSM36 peut fonctionner à une vitesse maxima de 300 plots/sec. Des boîtes de vitesse sont prévues pour le fonctionnement jusqu'à 1 tour par 30 heures.

EE 02 769 *pour plus amples renseignements*

SOURCE HF/DÉTECTEUR

The Wayne Kerr Co. Ltd, Sycamore Grove, New Malden, Surrey

(Illustration à la page 55)

La société Wayne Kerr a réalisé un détecteur/source constitué de corps solides avec un seul bouton à accord de 100 kHz à 100 MHz. Bien que principalement conçu pour ses ponts HF et VHF B201, B601 et B801, le nouvel appareil a une gamme étendue de niveaux de sortie de source et de gain de récepteur, ce qui le rend convenable pour la plupart des applications.

Le niveau de sortie est de 2 V efficaces à travers 75 Ω avec atténuation par bouton-poussoir en plots de 3 dB jusqu'à −39 dB. La stabilité de la fréquence à court terme est de 0,01 pour cent.

La sensibilité de détection est de 1 µV ou supérieure, un atténuateur d'entrée donnant 4 plots de 20 dB chacun. A chaque réglage la gamme de fonctionnement du circuit est automatiquement réglée pour fournir des conditions idéales pour la détection rapide de l'équilibre avec un zéro final précis. Un instrument de mesure du zéro est également fourni.

Le fonctionnement s'effectue sur alimentation de 110 ou 230 V, à l'aide d'un redresseur interne mais l'appareil SR268 peut être également actionné par batterie.

EE 02 770 *pour plus amples renseignements*

ÉLÉMENT DE PROTECTION DU MOTEUR

Standard Telephones & Cables Ltd, Components Group, Footscray, Sidcup, Kent

(Illustration à la page 55)

Ce petit module à fiches constitué de corps solides élimine le risque de surchauffement des moteurs électriques. N'ayant ni contact ni partie mobile, il coupe automatiquement l'alimentation du contacteur du moteur dès que la température des bobinages du moteur dépasse le niveau de sécurité.

L'expérience a montré que même le plus faible surchauffement des bobinages du moteur a un effet défavorable sur le comportement du moteur et que si ce surchauffement se prolonge il réduit considerablement la durée de vie du moteur.

Le nouveau module commande l'alimentation en alternatif du moteur au moyen d'un thyristor incorporé. La protection instantanée contre le fonctionnement de température excessif s'effectue par l'emploi d'un thermistor externe à coefficient de température positif logé dans les bobinages du moteur pour contrôleur l'action de commutation du thyristor. Toute hausse de température du moteur augmente la résistance du thermistor; lorsque la résistance dépasse une valeur critique, le thyristor change d'état et coupe l'alimentation du contacteur. On peut effectuer le fonctionnement à auto-verrouillage en ajoutant une résistance externe.

On peut employer n'importe quel type de thermistor à coefficient de température positive. Les moteurs triphasés peuvent être protégés par trois thermistors—un par phase—reliés en série de manière à ce que tous les trois bobinages puissant être contrôlés simultanément par un module.

Etant donné que le fonctionnement dépend entièrement du contrôle direct de la température effective du bobinage, une protection efficace est assurés contre le surchauffement causé par toutes les formes de mauvais fonctionnement ou d'utilisation incorrecte.

En pratique, on a constaté que l'emploi de ces modules révèle rapidement tout défaut mécanique électrique et d'environnement, tant dans l'installation que dans la charge, défaut qui aurait normalement passé inaperçu pendant quelques temps, probablement avant qu'une panne ne se produise.

Le module se compose d'un assemblage transistorisé contenant le thyristor et le circuit de commande connexe, fabriqués suivant le système de construction modulaire STC "Ministac" assurant la résistance mécanique et des dimensions réduites. Afin d'en accroître la robustesse, l'assemblage est encapsulé et scellé hermétiquement dans un boîtier en aluminium anodisé. Le faible encombrement du module facilite son installation dans les plus petits coins tels que dans les boîte de starter du moteur. Les connexions se font à travers une fiche octale International pour faciliter le remplacement au cas improbable d'une panne.

La fiabilité du nouveau module est telle que les ingénieurs lui accordent une durée de 45 années en moyenne avant qu'une panne ne se produise.

EE 02 771 *pour plus amples renseignements*

CONDENSATEURS AU PAPIER/POLYESTER

Telegraph Condenser Co. Ltd, Whales Farm Road, Acton, London, W.3

Une nouvelle gamme de condensateurs rectangulaires utilisant une diélectrique mixte au papier/polyester a été créée par la Telegraph Condenser Co. Ltd, une filiale du groupe des composants Plessey. Conçus pour l'emploi dans le matériel électronique de haute qualité, ces contacts répondent à la norme DEF-5131, styles CP 10 et CP 11, catégorie 55/100H6 et seront prochainement soumis pour approbation suivant ces normes.

Les contraintes de tension élevée rendues possibles par la nouvelle diélectrique permettent aux condensateurs d'être considérablement plus petits que la gamme classique diélectrique en papier pour des puissances nominales analogues. Par exemple, les dimensions d'un condensateur au papier de 2 μF 5000 V sont réduites de 22,86 cm × 13,01 cm à 11,74 cm × 13,01 cm × 15,23 cm avec le condensateur à diélectrique mixte. La température de fonctionnement s'étend de −55° C à +70° C; le fonctionnement est cependant permissible jusqu'à 100° C.

Les valeurs de capacitance sont entre 0,05 μF et 12 μF avec les tensions nominales continues de 200 V à 10 kV à 70° C. Utilisés comme condensateurs réservoirs et d'approximation dans les circuits redresseurs, ainsi que pour le découplage dans les amplificateurs, tant le type conventionnel que le type à diélectrique mixte conviennent spécialement pour l'emploi dans les circuits c.c. à haute tension.

EE 02 772 *pour plus amples renseignements*

CONTRÔLEUR DE RÉSISTANCE DE FILM

Edwards High Vacuum Ltd, Manor Royal, Crawley, Sussex

(*Illustration à la page 55*)

Le contrôleur de résistance de film Edwards est un dispositif de contrôle utilisé avec une installation de revêtement au vide pour mesurer le changement de résistance électrique d'un film pendant le dépôt et pour mettre fin au dépôt lorsqu'une valeur préréglée de résistance est obtenue. La gamme de résistance couverte va de 10 Ω à 10 Ω en trois plots. Le contrôleur de résistance de film est utilisé lorsqu'on dépose des résistances ou en liaison avec le contrôleur d'épaisseur de film lorsqu'on dépose des circuits à film mince.

On mesure soit la résistance du film mince lui-même, soit celle d'une bande de contrôle appropriée. Cette résistance form l'un de bras d'un pont de Wheatstone et un autre bras de référence du pont est réglable à partir du panneau frontal du contrôleur.

Le bras de référence du panneau frontal, c'est à dire un potentiomètre hélicoïdal avec commande étalonnée, est réglé de manière à correspondre à la résistance requise de film mince. Lorsque la valeur voulue est atteinte, le pont s'équilibre, déclenchant un amplificateur transistorisé à gain élevé qui amorce un relai, ce dernier à son tour fermant l'obturateur de source et mettant fin ainsi au dépôt de film. L'obturateur reste fermé jusqu'à ce que le bouton de réenclenchement soit pressé.

Des bornes d'usage externe sur le relai, une paire normalement fermée et une paire normalement ouverte, sont prévus pour le contrôle d'appareils auxiliaries.

Le pont a été conçu de manière à ce que la dissipation de puissance dans le film contrôlé reste au-dessous de 50 mW sur toutes les gammes. Le surchauffement ou la cuisson partielle du film déposé peut être évitée.

EE 02 773 *pour plus amples renseignements*

Résumés des Principaux Articles

Mesure des phénomènes transitoires rapides à l'aide d'une grille optique par D. K. Ewing

Résumé de l'article aux pages 2 à 5

L'auteur décrit un convertisseur de fréquence/tension, basé sur le principe de l'oscillateur à verrouillage de phase, adapté pour détecter les phénomènes transitoires rapides par l'emploi d'une grille optique comme transducteur de vitesse. Les utilisations typiques comprennent la mesure des phénomènes transitoires rapides produits par les erreurs de transmission dans l'entraînement vers l'arbre de grille et la réaction de vitesse dans les systèmes de commandes de machines-outils pour lesquels la réaction tachymétrique serait trop bruyante.

La conception et le réglage des antennes d'émission de fréquence moyenne par P. Knight

Résumé de l'article aux pages 6 à 10

Le comportement d'une antenne d'antifading de fréquence moyenne dépend de manière critique de la forme de son réseau à radiations verticales. Bien que ce réseau dépende principalement de la hauteur de l'antenne et de sa section, il peut être modifié dans une certaine mesure si l'antenne a un sommet de capacité ou une inductance à charge série. Des formules pour calculer les réseaux de radiations verticales de divers types d'antennes sont donnés dans cet article ainsi que les processus pouvanté être utilisés pour le réglage des antennes afin de pouvoir obtenir des réseaux spécifiés.

Un multiplicateur analogique simple à action rapide par J. P. Wilson

Résumé de l'article aux pages 11 à 14

Le multiplicateur analogique décrit dans cet article est basé sur la non-linéarité des caractéristiques de tube. La précision de la multiplication est de 2% pour une dérive à long terme de 1%. La gamme de fréquence couverte dépend des détails du circuit choisi et peut s'étendre du courant continu à un maximum de 2MHz. Un certain nombre de circuits d'entrée et de sortie sont étudiés, ces circuits permettant au multiplicateur d'être utilisé pour le calcul, la modulation, la mesure de puissance instantanée, la corrélation et la commande précise d'amplitude ou d'enveloppe de signaux à fréquence acoustique.

Un multivibrateur à gamme de fréquence étendue et à tension contrôlée par R. J. P. Jones

Résumé de l'article aux pages 14 à 15

L'auteur décrit un multivibrateur dont la gamme de fréquence à tension contrôlée est à variation continue pendant au moins dix octaves (1000:1). Dans leur forme la plus élémentaire, la fréquence et le rapport de marque-espace sont sensibles aux petits changements des caractéristiques de transistors et de valeurs de composants. Un circuit stabilisateur a été utilisé pour surmonter cette carence ainsi que pour linéariser les rapports entre la fréquence et la tension de commande.

Stimulateur à deux voies par J. W. Hinshelwood et A. G. Seabridge

Résumé de l'article aux pages 16 à 19

Les auteurs décrivent un générateur d'impulsions rectangulaire à double sortie. Le générateur a été étudié pour des utilisations physiologiques; les deux voies comportent une commande de fréquence commune mais l'amplitude et la largeur de chacune d'elles est à variation indépendante. L'amplitude de sortie maxima est de 50V. Elle peut être utilisée pour la stimulation par deux moyens, c'est à dire, directement et par le système nerveux.

Circuit à transistors de mesure logarithmique du courant par K. S. Højberg

Résumé de l'article aux pages 20 à 23

Cet article décrit deux circuits transistorisés pour la mesure logarithmique des petits courants pour l'instrumentation des réacteurs nucléaires. L'élément logarithmique est appliqué sur le parcours de réaction d'un amplificateur et en seul transistor double est utilisé en tant que diode logarithmique et transistor à compensation de température. Un circuit simple à un seul transistor est comparé à un système à deux amplificateurs. Les circuits presentés ont été mis au point en liaison avec un amplificateur qui comprend un étage d'entrée à transistor double MOS avec portes protégées par diode.

Effets de charge dans les filtres RC à deux sections par J. F. Young

Résumé de l'article aux pages 23 à 24

Par une simple transformation du diagramme de circuit, il est montré que les effets de charge dans les filtres RC à deux sections peuvent être exprimés en fonction d'un circuit de Wien équivalent inversé à demi-pont. Cela permet d'étudier de façon très précise les effets de charge d'inter-sections.

Un circuit décimal codé binaire asynchrone avec réaction à porte par S. L. Hurst

Résumé de l'article aux pages 25 à 28

Les assemblages décimaux codés binaires fonctionnent normalement de manière asynchrone et emploient une forme de logique de détection de comptage pour produire une transition non-binaire à un stade quelconque de comptage. Une forme nouvelle de déclenchement périodique en série est décrite dans cet article pour obtenir la transition non-binaire nécessaire dont le mérite et d'eliminer les faux comptages transitoires qui se produisent dans la plupart des montages décimaux codés binaires.

L'application d'un commutateur PNPN au contrôle de la température par A. Lupic et B. Kovac

Résumé de l'article aux pages 28 à 29

La possibilité de convertir la température en fréquence par la sensibilité de température du circuit oscillateur de relaxation est examinée dans cet article. La dépendance linéaire de la température et de la fréquence dans la gamme de —10°C à +50°C a été mesurée. Les résultats obtenus pendant l'oscillation continue de l'oscillateur pendant 1000 heures sont présentés.

Calculs de transistors unifiés par D. W. W. Rogers

Résumé de l'article aux pages 30 à 33

L'auteur décrit une méthode pour unifier les calculs de transistors à jonction, basés sur les paramètres d'impédance et le circuit T équivalent. Cette méthode est d'autant plus simple qu'elle permet d'effectuer les calculs canoniques sans difficulté dans les paramètres z,y_1 et h, sans transformation de matrice.

Un wattmètre à couple thermoélectrique pour la mesure des pertes magnétiques
par J. K. Choudhury, R. K. Mondel et S. N. Bhattacharyya

Résumé de l'article aux pages 34 à 37

Cet article décrit un circuit de wattmètre thermique utilisant une paire équilibrée de couples thermoélectriques à jonction au vide pour la mesure des pertes de noyau. Le circuit utilisé par les auteurs diffère du circuit de wattmètre thermique classique. Une haute sensibilité a pu être obtenue par l'emploi d'un galvanomètre à cadre mobile suspendu comme instrument indicateur.

Les résultats expérimentaux choisis montrent la simplicité et les qualités de cette méthode pour la mesure de perte de noyau dans des conditions normales et différentielles d'excitation dans le noyau d'essai. Les mesures on été effectuées dans une gamme de fréquence de 50Hz à 50kHz. La précision d'ensemble obtenue fut de l'ordre de 1% de la déviation sur la totalité de l'échelle.

Un montage combiné comprenant le wattmètre thermique et un wattmètre électrostatique fut mis au point pour mesurer et comparer la perte de noyau dans des conditions d'essai identiques. Un accord excellent fut obtenu entre les résultats de ces deux méthodes.

Analyse de l'action d'un circuit de déclenchement Schmitt par D. W. H. Hampshire et D. Petersen

Résumé de l'article aux pages 38 à 40

Cet article étudie en détail l'un des nombreux modes de fonctionnement du circuit de déclenchement Schmitt à transistors. Les conditions pour la commutation régénérative sont analysées et les conditions d'état de stabilité sont calculées et comparées à la pratique.

Amorçage d'un inverseur triphasé à fréquence réglable par R. L. V. de Lima Mendes

Résumé de l'article aux pages 41 à 45

Trois circuits sont indiqués pour l'amorçage d'un inverseur triphasé utilisant des redresseurs pilotés au silicium. Les avantages et désavantages des trois circuits sont examinés et des diagrammes de circuit détaillés sont donnés.

NEUE AUSRÜSTUNGEN

Übersetzung der Seiten 50 bis 55

Beschreibung neuer Bauelemente, Zubehörteile und Prüfgeräte auf Grund der von Herstellern gemachten Angaben.

Vibrations-Nahmesswandler

Southern Instruments Ltd, Camberley, Surrey

(Abbildung Seite 50)

Der Vibrations - Nahwirkungsmesswandler T.510 ist für das Messen der relativen Vibrationsamplitude ohne Kontakt zwischen Messwandler und einer sich bewegenden Oberfläche ausgelegt. Die Oberfläche muss entweder aus hochleitendem Werkstoff bestehen oder eine dünne Berylliumbronze tragen, wenn sie nichtleitend ist oder aus Eisen besteht.

Zur vereinfachten Einstellung des Anfangsspaltes zwischen Wandler und Oberfläche sowie zur Erleichterung des Eichens kann das induktive Fühlerelement mittels einer Mikrometereinrichtung relativ zum Wandlerkörper verstellt werden. Die Unterteilung ist in 0,0005" (0,0127 mm) bis zu 10,16 mm.

Der T.510 wurde ausschliesslich für Einsatz mit dem FM-Vorverstärkersystem TE.7 der Southern Instruments entwickelt und enthält eine Miniatur-Oszillatorschaltung, deren Ausgangsfrequenz (Nennwert 2 MHz) proportional zur auftretenden Verschiebung ist. Der FM-Vorverstärker setzt diese Frequenz in ein entsprechendes Spannungs- oder Stromsignal um.

Montage des Messwandlers erfolgt entweder mittels eines Passloches von 20,6 mm Durchmesser oder eines Gewindeloches 13/16" × 40 Gänge/Zoll.

EE 02 751 *für weitere Einzelheiten*

Festkörper-Oszillograf

Hewlett-Packard Ltd, 224 Bath Road, Slough, Buckinghamshire

(Abbildung Seite 50)

Ein neuer 50-MHz-Festkörper-Oszillograf in Einschubtechnik von Hewlett-Packard hat einen 30 % grösseren Schirm (8 × 10 cm) als ältere grosse 50-MHz-Oszillografen. Bei Abmessungen von 203 × 279 × 572 mm tief wiegt das Gerät 13,6 kg. Beim Entwurf des neuen HP-Modells 180A wurde auf höhere Präzision als bei älteren Labor-Oszillografen Wert gelegt. Es ist klein, leicht und mit breiter Anpassungsfähigkeit an die Umgebung für Anwendung im Labor, Aussendienst und der Fertigung geeignet. Grenzwerte für normalen Betrieb sind −28° C ... +65° C, 95 % relative Feuchtigkeit bei 40° C und etwa 4570 m Höhe.

Von den zwei Einschubpositionen ist eine für den Vertikalverstärker bestimmt. Der erste dieser Einschübe ist jetzt als Zweikanaleinschub lieferbar und erreicht einen Ablenkfaktor von 5 mV/cm bei 50 MHz. Die Spur springt nicht, wenn der unterteilte Empfindlichkeitsregler geschaltet wird. Bei Einschalten des Gerätes tritt praktisch keine Drift der Spur auf. Die Eigenschaften sind auf die Anwendung der neuen rauscharmen Voll - Festkörperschaltungen zurückzuführen, in denen gepaarte Feldeffekttransistoren dauernd in derselben thermischen Umgebung gehalten werden, so dass die gesamte Abschwächung von den Verstärkern erfolgen kann.

Mit dem HP-Modell 180A werden zwei neue Zeitablenkeinschübe angeboten. Der erste—Modell 1820A—erreicht bei Einschaltung zehnfacher Dehnung und der schnellsten geeichten Ablenkung (0,05 μs/cm) eine Schreibgeschwindigkeit von 5 ns/cm. Mit zuverlässiger Triggerung bis zu 90 MHz können bei Beobachtung schnellgeschriebener Spuren höhere Auflösungen erreicht werden, als bisher mit einem Oszillografen dieser Klasse möglich war. Asymmetrische Impulsreihen können mittels regelbarer Verzögerung glatt synchronisiert werden.

Gegen Zuschlag ist auf Wunsch der Zeitablenk- und Verzögerungsgeneratoreinschub 1821A erhältlich. Die verzögerte Zeitbasis beginnt die Ablenkung nach einer regelbaren Zeitverzögerung gegenüber der Hauptablenkung. Ein heller Punkt auf dem Schirm kennzeichnet den Punkt auf der Spur, in dem die verzögerte Ablenkung beginnt; dadurch wird der Teil der Kurve, den der Beobachter für eingehende Untersuchung dehnen möchte, positioniert und gekennzeichnet. Sein Einsatz gestattet weiterhin Anwendung der Spurvorderflanke nach Verzögerung für die Betätigung des Verzögerungstriggers, wodurch eine zitterfreie Darstellung auf dem gesamten Schirm für Messzwecke erreicht wird.

Trotz der kleinen Abmessungen hat der 180A eingebaute Laufzeitketten, so dass die Vorderkante jedes Impulses in das Blickfeld gebracht werden kann. Diese Laufzeitketten sind völlig neue Streifenleitungen in geätzter Schaltungstechnik. Die Verzögerung ist für diesen Zweck völlig ausreichend, und ihre Bandbreite überschreitet 140 MHz. Jedes Instrument enthält ein Differenzpaar.

Ein breites Zubehörsortiment wird mit dem 180A angeboten. Die neue HP-Kamera 197A mit elektronischem Verschluss passt direkt, und für die meisten anderen Kameras gibt es Zwischenstücke. Passende flexible Einblickmasken, Bedienfelddeckel, Transportkasten und hochohmige Teilersonden sind auch lieferbar.

EE 02 752 *für weitere Einzelheiten*

Miniaturpotentiometer mit Pressbahn

Davall Electronics Ltd, Rothersthorpe Avenue, Northampton

(Abbildung Seite 50)

Das neue Davall-Miniatur-Einstellpotentiometer Typ 80 mit gepresster Bahn hat ein Formstück aus Phenolharz mit mineralischem Füllstoff, in dem Isolierkörper, Widerstandbahn und Anschlüsse in einem massiven Pressling integriert sind. Diese Konstruktion gibt unter allen Feuchtigkeits-, Temperatur- und Schwingungsbedingungen hohe Konstanz. Die Leistungsstreuung ist im Temperaturbereich −40°C ... +70°C unter 5 Prozent. In der Entwicklung dieses Bauelements wurde die britische Norm DEF 5214 als Mindestanforderung betrachtet.

Das lineare Potentiometer Typ 80 ist bis zu 0,25 W bei 70°C belastbar; die maximale Betriebsspannung ist 500 V−. Widerstandswerte von 20 Ω bis zu 1 MΩ sind lieferbar.

Der Typ kommt in zwei Ausführungen, und zwar mit Lötfahnen für direktes Einlöten in gedruckte Schaltungen und für Einlochmontage auf isolierte Platten.

Die Abmessungen des kompakten Typs 80 (ohne Montagebolzen und Lötfahnen) sind 15,2 mm Durchmesser und 6,6 mm tief.

Typ 80 kann von Hand oder mittels Schraubenzieher eingestellt werden. Typ 80/1 ist eine Abwandlung mit grossem Einstellknopf.

EE 02 753 *für weitere Einzelheiten*

Polycarbonat-Kondensatoren

Standard Telephones & Cables Ltd, Components Group, Footscray, Sidcup, Kent

(Abbildung Seite 51)

Der Geschäftsbereich Kondensatoren der Standard Telephones and Cables Ltd hat eine umfassende Baureihe kunststoffgeschützter Polycarbonat-Kondensatoren eingeführt, die besonders für die zahlreichen Anwendungsmöglichkeiten in rauhen Umgebungsbedingungen bestimmt sind.

Polycarbonat-Kondensatoren sind hochzuverlässige Bauelement, die mit ultradünner Kunststoffolie aus metallisiertem Polycarbonat gewickelt werden. Ihre elektrischen und mechanischen Eigenschaften sind denen anderer Kunststofffolien-Kondensatoren überlegen und bleiben über einen breiten Temperaturbereich konstant.

Die neuen Elemente beruhen auf den Rohrkondensatoren der Firma, die den Ansprüchen der Norm DEF 5011 Klasse H6 für Umgebungsschutz genügen, und haben dieselben hohen elektrischen Eigenschaften. Sie sind jedoch in einem robusten, rechteckigen Duroplastgehäuse untergebracht, das Umgebungsschutz nach DEF 5011 Klasse H3 gibt. Dieser Schutz ist für die Arbeitsbedingungen, denen der weitaus grösste Teil kommerzieller elektronischer Ausrüstungen ausgesetzt ist, mehr als ausreichend. Die radialen Anschlussdrähte sind für Montage auf gedruckte Schaltungen ausgelegt.

Die kunststoffgeschützten STC-Polycarbonat-Kondensatoren sind in Werten von 0,01 bis zu 4,7 μF für 1 000 V— Betriebsspannung und Temperatur von $-40°$ ... $+85°$C lieferbar. Mit ihren allseitig überlegenen Eigenschaften sind diese Kondensatoren eine ansprechende Alternative und Ersatz für Polyester-(Polyäthylenterephthalat-) Kondensatoren, da das allgemeine Preisniveau der neuen Kondensatoren dem der Polyestertypen entspricht.

EE 02 754 *für weitere Einzelheiten*

Missweisender Peilungsanzeiger

Aviation Division, Smiths Industries Ltd, Kelvin House, Wembley Park Drive, Wembley, Middlesex

(Abbildung Seite 51)

Die Fertigung eines neuen missweisenden Funkanzeigers für VOR- oder ADF-Peilergebnisse, der Verbesserungen gegenüber älteren Modellen aufweist, ist jetzt beim Geschäftsbereich Luftfahrt der Smiths Industries angelaufen. Die Ausrüstung ist in drei ATI-Standardgehäusen untergebracht, entspricht den ARINC-Empfehlungen und hat integrale Beleuchtung.

Der missweisende Flugzeugkurs wird durch eine rotierende Kompassrose angezeigt und gegen eine Feststeuerlinie oben am Gerät abgelesen. Ein vom Hauptkompass der Maschine abgegebenes Signal treibt die Rose über eine Servoeinrichtung, deren Verstärker im selben Gehäuse eingebaut ist. Ausfall des Kompasses wird durch ein Schauzeichen angezeigt.

Missweisende Peilungen von zwei Funkbaken werden auf der Kompassrose durch zwei Zeiger angezeigt, während die relative Peilinformation durch das Verhältnis der Zeiger zur Feststeuerlinie gegeben wird. Besondere Aufmerksamkeit wurde der genauen Einstellung der Zeiger für die relative Peilung gewidmet, die durch Moment-Drehfeldempfänger erfolgt. VOR- oder ADF-Eingänge zu den Synchros werden durch externes Schalten gewählt.

Die Ausrüstung enthält ausserdem einen mitlaufenden Drehmelder, der das Flugzeugkurssignal abgibt, das für andere, dieses Signal benötigende Fluggeräte zur Verfügung steht.

EE 02 755 *für weitere Einzelheiten*

Digital-Gleichspannungsmesser

Hewlett-Packard Ltd, 224 Bath Road, Slough, Buckinghamshire

(Abbildung Seite 51)

Die Messunsicherheit des neuen Digitalvoltmeters 3430A ist 0,1 Prozent plus 1 Ziffer und seine Konstanz so hoch, dass die vorgeschriebene Eichungsperiode 90 Tage ist. Der Eingang ist erdfrei: mit der Verbindung der "niedrigen" Eingangsklemme zu Masse unterbrochen, können Messungen von ± 500 V— gegen Masse durchgeführt werden. Die Eingangsimpedanz ist für alle Bereiche 10 MΩ.

Das Gerät hat fünf manuell wählbare Bereiche mit Endwerten von 100 mV— bis zu 1 kV— und eine dreistellige Anzeige. Eine vierte Stelle (eins oder leer) gestattet mit Ausnahme des 1-kV-Bereiches Überbereichmessungen von bis zu 60 Prozent über Endwert bei voller Genauigkeit. Bei Überlastungen von über 60 Prozent wird durch Blinken der beleuchteten Anzeige gewarnt. Das Gerät spricht automatisch auf die Eingangspolarität an und zeigt, ob es sich um eine positive oder negative Eingangsspannung handelt.

Eins der Merkmale des neuen Digitalvoltmeters ist Abgabe einer dem Eingang proportionalen Gleichspannung mit einer Verstärkertoleranz von $\pm 0,1$ Prozent. Die nichtinvertierende Spannungsverstärkung für den 100-mV-Bereich ist 100 und nimmt für jeden höheren Bereich um einen Faktor von 10 ab. Der für das Treiben eines Schreibers geeignete Verstärkerausgang kann jeden Verbraucher treiben, dessen Impedanz grösser als 10 kΩ ist, ohne dass die Anzeigegenauigkeit verringert wird.

Eine wahlweise lieferbare Ausführung gestattet, Quotientenmessungen durchzuführen, was für Normierung der Gleichstromausgänge von Messwandlern nützlich ist. Die Anzeige stellt die durch die Bezugsspannung dividierte Eingangsspannung dar. Jede beliebige Festspannung zwischen 0,8 und 1,2 V beliebiger Polarität kann als Bezugseingang Verwendung finden, und man kann Quotienten von 0,0001:1 bis zu 1000:1 messen.

Das neue Digitalvoltmeter arbeitet nach dem Treppenvergleichsverfahren und vergleicht die Eingangsspannung mit einer intern mittels einer Zener-Bezugsdiode und Präzisionswiderständen erzeugten Spannung. Die intern erzeugte Spannung fängt bei Null an und wird automatisch auf den nächsthöheren Stufenwert gebracht, bis sie der Eingangsspannung gleich ist. Jede Stufe stellt den Zähler eine Ziffer vorwärts. Sowie Koinzidenz erreicht ist, wird die Anzahl der die Eingangsspannung darstellenden gesammelten Zählstösse auf der Frontplatte angezeigt. Die dargestellten Anzeigewerte werden festgehalten, bis die nächste Zählung beendet ist, was eine laufende Anzeige ohne Blinken gewährleistet. Zwei Zählungen je Sekunde werden vorgenommen.

EE 02 756 *für weitere Einzelheiten*

Statische Schaltgeräte

Vosper Ltd, Hamilton Road, Paulsgrove, Portsmouth, Hampshire

(Abbildung Seite 52)

Statische Schaltgeräte für die verschiedensten Aufgaben sind im Werk Portsmouth der Vosper Electronic, einer zum Firmenverband Vosper-Thornycroft gehörenden Firma, in voller Produktion. Die Erzeugnisse fallen in vier Hauptgruppen: Verzögerungszeitgeber mit einfacher Schaltfunktion; durch zweipolige Umschaltrelais getriebene Verzögerungszeitgeber; mehrpolige statische Gleichstromschalter; und mehrpolige statische Wechselstromschalter. Die letzteren zwei Klassen entsprechen elektromechanischen Relais oder Kontaktgebern. Da sie keine beweglichen Teile haben, spielen die elektromechanischen Bausteinen innewohnenden Probleme wie Kontaktkleben und -abbrand, der breite Ansprech- und Abfallbereich, Verschleiss usw. keine Rolle. Die mehrpoligen Schalter werden in demselben Modul mit und ohne Zeitgeber angeboten. Alle Zeitgeber sind einstellbar und mit verschiedenen Bereichen bis zu maximal 300 s Verzögerung lieferbar.

In der Konstruktion wurden Wiederholbarkeit und Zuverlässigkeit bei allen Geräten betont. Alle Bauelemente sind mit passivem Kunstharz vergossen, und das ganze Aggregat ist in ein anodisiertes Aluminiumgehäuse eingebaut. Die Geräte sind daher sehr unempfindlich gegen feuchte und korrodierende Umgebung, Beschleunigungskräfte und Vibration. Für die meisten Typen ist eine Beschleunigungsgrenze von 150 g vorgeschrieben, für die Verzögerungsschaltuhren mit Relais jedoch 50 g. Alle Geräte können schwingende Äquivalentkräfte von 25 g bei 2 oder 3 kHz und Temperaturen von −65° oder −55°C ... +60°C aushalten.

Ausgangs-Lastströme sind 1,0 ... 5,0 A je nach Typ und die Eingangsleistung —dem Erregerstrom eines Relais entsprechend—niedrig genug für direkte Betätigung durch Transistorschaltungen: 22 mA— oder 5 W∼. Geräte sind für Eingangs- und Ausgangsspannungen von 12 ... 150— und 12 ... 250 V∼ lieferbar.

EE 02 757 *für weitere Einzelheiten*

HF-Abschirmkästen

Hatfield Instruments Ltd, Burrington Way, Plymouth, Devon

(*Abbildung Seite 52*)

Kleine Bauelementegruppen für Anwendung in Abschwächern, Filtern, Netzwerken, Spannungsteilern usw. können in diesen Aluminium-Spritzgussgehäusen wirksam gegen HF geschirmt werden. Die robust konstruierten Kästen werden mit Spritzgussdeckeln geliefert, die durch vier Schrauben befestigt werden. Sie sind auch mit BNC-Steckdosen oder Steckern ausgerüstet für Serienschaltung mit Kabeln oder bestehenden Geräten lieferbar.

Üblicherweise kommen die Kästen mit 50-Ω-BNC-Steckverbindungen, und zwar mit einer Steckdose an einem Ende und einem Stecker am anderen. Sie können ohne merkbare Reflexion in 75-Ω-Systemen bis zu etwa 100 MHz verwendet werden. Grund dafür ist, dass BNC-Steckverbindungen bei niedrigeren Funkfrequenzen nur einen Bruchteil einer Wellenlänge darstellen.

Zur Zeit lieferbar sind drei Grössen: 3,5 × 3,18 × 4,76 cm; 7,3 × 4,76 × 7,3 cm und 4,12 × 4,7 × 14,29 cm.

EE 02 758 *für weitere Einzelheiten*

Kleinstpotentiometer

Pandect Precision Components Ltd, Wellington Road, High Wycombe, Buckinghamshire

(*Abbildung Seite 52*)

Das Pandect-Fertigungsprogramm für Widerstandselemente wurde durch ein Kleinst-Trimmerdrahtpotentiometer ergänzt, das zu den kleinsten derzeitig in England gefertigten gehört. Die Aussenabmessungen entsprechen denen eines Standardtransistors TO-5. Das den strengsten Anforderungen genügende Bauelement ist in erster Linie für Anwendung in der Luftfahrt, militärische Zwecke und hochwertige elektronische Geräte gedacht.

Das neue Potentiometer ist in Widerstandswerten von 5 Ω bis zu 15 kΩ lieferbar und hat die für ein so kleines Element ungewöhnlich hohe Nennbelastbarkeit von 1 W bei +75°C. Grundplatte und Haube sind nach dem Widerstandsverfahren zusammengeschweisst und über den Umgebungstemperaturbereich −70° ... +150° C voll gegen Ausseneinflüsse geschützt.

Das Potentiometer wird mittels Schraubenziehers und geschlitzter Achse eingestellt. Eine eingebaute Rutschkupplung schützt gegen Beschädigung durch Anwendung übermässiger Kraft am Ende der Schleiferbewegung. Ein O-Ring aus Silikonkautschuk dichtet zwischen Gehäuse und Achse.

Die internen Verbindungen werden durch Mikroschweissen erstellt, um auch bei starken Schwingungen höchste Festigkeit zu gewährleisten. Die goldplattierten Anschlussdrähte werden durch Glas-Metallverschmelzungen herausgeführt.

EE 02 759 *für weitere Einzelheiten*

Molekularsieb-Sorptionspumpen

Mullard Ltd, Mullard House, Torrington Place, London, W.C.1

(*Abbildung Seite 52*)

Mullard Ltd hat das Programm für Höchstvakuumgeräte durch zwei neue Molekularsieb-Sorptionspumpen ergänzt. Sie sind beide für schnelles Pumpen vom Atmosphärendruck bis zum Anfangsdruck für Penning-Pumpen (etwa 10^{-2} Torr) herunter konstruiert. Als Sorptionsmaterial dient 13X-Aluminosilikat, das einen höheren Wirkungsgrad als andere Sorten hat. Das Sieb ist so konstruiert, dass die grösstmögliche Sorptionsmaterialfläche dem Kühlmittel ausgesetzt ist.

Die Pumpen VAP-12 und VAP-40 haben eine Volumenpumpfähigkeit von etwa 1 bzw. 10 atmosphärischen Litern. Grössere Volumen werden am besten durch Folgepumpenanordnungen evakuiert, in denen eine Pumpe arbeitet, während die andere sich erholt.

Flansche aus rostfreiem Stahl sind für Anschlüsse vorhanden, die nach dem einfachen Mullard-Golddrahtsystem dicht gemacht werden. Beide Pumpen sind mit einem Sicherheitsventil ausgerüstet, das vollen Schutz gegen Überdruck gewährleistet. Für beide Typen gibt es Spezial-Dewargefässe. In jedem der Gefässe ist genügend Platz für den Fühler des vor kurzem herausgebrachten Mullard-Systems zum Auffüllen mit flüssigem Stickstoff. Mit diesem System wird das Kühlmittelniveau bei unüberwachtem Pumpen automatisch aufrechterhalten. Das grössere Modell VAP-40 hat einen in das Sieb eingebauten Heizer, der das Regenerieren erleichtert.

EE 02 760 *für weitere Einzelheiten*

Mikrowellenmessender

Marconi Instruments Ltd, Sanders Division, Gunnel's Wood Road, Stevenage, Hertfordshire

(*Abbildung Seite 53*)

Der Messender 6459 soll von allen greifbaren Messendern den breitesten Frequenzbereich überstreichen. Er hat folgende Eigenschaften:

- Frequenzbereich 3,5...12 GHz
- Direkt ablesbare Frequenzskala
- Direkt ablesbarer, in Spannung und dBm geeichter Abschwächer
- Hohe Konstanz und Genauigkeit
- Interne FM, CW, Impuls- oder Rechteckwellenmodulation
- Wahlweise für Gestelleinbau lieferbar.

FM, CW, Rechteck- und Impulswellenformen werden intern erzeugt, das Gerät lässt sich jedoch auch extern modulieren. Die Impulsfolgefrequenz ist zwischen 40 und 4000 Imps/s, die Impulsdauer zwischen 0,5 und 10 μs regelbar. Synchronsignale werden entweder gleichzeitig mit dem HF-Impuls oder zwischen 3 und 300 μs vor dem HF-Impuls abgegeben. Der interne Impulsgeber kann auch fremdsynchronisiert werden.

Der Messender enthält einen Einsteck-Klystronoszillator in einem Koaxialleitungsresonator. Die Frequenz wird durch die Position eines beweglichen, nichtberührenden Kolbens bestimmt, der mit einer Frequenzskala und einem automatisch gleichlaufenden Netzwerk gekuppelt ist, dessen Ausgangspegel in dBm und μV von einem direkt geeichten, internen Präzisionsabschwächer ablesbar ist. Durch Temperaturkompensation der Leistungsmesser-Brückenschaltung ist das Gerät praktisch unabhängig von Änderungen der Umgebungstemperatur.

Ausgangsleistung ist wie folgt:

(a) direkt—Leistung bis zu maximal 80 W wird mittels eines Durchgangskopfes ausgekoppelt

(b) 0,223 V...0,1 μV (0...−127 dBm) zwischen 4,5...11,0 GHz und −6 dBm...−127 dBm zwischen 3,5 und 4,5 GHz. Über 11,0 GHz ist die Ausgangsleistung besser als −6 dBm an 50 Ω Abschluss.

EE 02 761 *für weitere Einzelheiten*

Kurvenleser

Normalair Ltd, Yeovil, Somerset

(*Abbildung Seite 53*)

Das "Westland"-Programm der Normalair Ltd für Datenerfassungsgeräte wurde durch den Westland-Kurvenleser ergänzt. Die Arbeitsweise des Gerätes ist sehr einfach, und man kommt ohne Messzeiger, Servos, elektromechanische Teile oder besondere Bedienungskenntnisse aus.

In den Auswerttisch eingebaut ist eine ebene Metallfläche, an der ein lineares elektrisches Potential liegt (das ist ein isoliertes Wechselstromsignal, dessen Amplitude wesentlich unter 1 V liegt). Der abzutastende Registrierstreifen, ein Film oder Foto werden über die empfindliche Fläche gelegt, und die

Auswertung erfolgt durch Positionieren der Stiftspitze einer in der Hand gehaltenen Sonde in dem auszuwertenden Kurvenpunkt.

Die Sonde wird wie ein gewöhnlicher Federhalter oder Bleistift gehalten und hat eine federbelastete Stiftspitze. Der Anwender berührt den digital darzustellenden Kurvenpunkt mit der Stiftspitze und drückt auf den Sondenkörper, wodurch die Spitze den Kurventräger durchdringt und mit der darunter liegenden empfindlichen Fläche Kontakt macht. Die Umsetzung wird dann automatisch durchgeführt und der abgetastete Wert in einen Lochstreifen gestanzt.

Die höchste Arbeitsgeschwindigkeit des Gerätes ist zwei Abtastungen je Sekunde.

Bedienorgane sind nach Funktionen in einer Tastatur gruppiert, die auch Tasten für Eingabe von zusätzlichen Daten wie Kurvenkennzeichnung und Spezialsymbole für das Programmieren des Computers des Anwenders in den erstellten Lochstreifen enthält.

EE 02 762 *für weitere Einzelheiten*

Mehrpoliger Klinkenstecker und -buchse

Render Instruments Ltd, Victoria Road, Burgess Hill, Sussex

(Abbildung Seite 53)

In Ergänzung des bestehenden Programmes 2poliger, 3poliger und Miniatur-Klinkenstecker und Klinkenbuchsen kündigt Render einen mehrpoligen Klinkenstecker mit Klinkenbuchse an.

Die Neueinführung gestattet leichte, schnelle und zuverlässige Erstellung von Verbindungen mittels Miniaturkabel mit bis zu 12 Adern. Zusätzlich zu der Ausführung als Steckverbindung ist das Modell mit Arbeits- und/oder Ruhekontakten in der Buchse in vielen Kombinationen lieferbar.

Der elektrische Kontakt wird durch leichtes Rechtsdrehen des Steckers nach Einführung hergestellt, wonach derselbe automatisch in dieser Stellung verriegelt wird. Durch leichtes Drehen in umgekehrter Richtung wird der Stecker freigegeben und kann aus der Buchse gezogen werden.

Diese Bauelemente geben eine alternative Verbindungsmethode zu den Steckern und Buchsen mit mehreren Stiften und haben den Vorteil zusätzlicher Schalteinrichtungen.

EE 02 763 *für weitere Einzelheiten*

Kurvenfolger-Zusatzgeräte

d-mac Ltd, Queen Elizabeth Avenue, Hillington, Glasgow, S.W.2

(Abbildung Seite 54)

Durch neue Zusatzgeräte wird der Anwendungsbereich des von d-mac Ltd hergestellten "Pencil Follower" erweitert, seine Arbeitsweise beschleunigt und vereinfacht.

Das Gerät, das grafische Information in Digitaldaten für Datenverarbeitung umsetzt, kann jetzt zur Auswertung von Information auf Film mit einem Projektionssystem ausgerüstet werden.

16, 35, 50 oder 70 mm breiter, perforierter oder nichtperforierter Film lässt sich auf den Auswerttisch projizieren. Filmtransport wird in beiden Richtungen durch einen Regelmotor getrieben und kann entkuppelt werden, so dass man spezifische Filmausschnitte von Hand genau positionieren kann.

Sowie der Ausschnitt eingestellt ist, verfolgt der Operator die gewünschten Daten mit einem Schreibstift ("Pencil"), der mit einem unter der Auswertfläche liegenden "Folger" magnetisch verbunden ist. Die Position des Folgers wird in eine Elektronikkonsole übertragen, in der sie in Digitalform umgesetzt in eine Ausgangseinrichtung wie z.B. einen Streifenlocher eingegeben wird.

Der "Pencil Follower" kann auch mit einer Papierrolleneinrichtung ausgerüstet werden, die aus zwei an gegenüberliegenden Seiten des Tisches angebrachten Papierspulen und einer Spannvorrichtung besteht, so dass das Papier sich genau auf der Auswertfläche positionieren lässt. Bis zu 457 mm breite Bahnen können manuell von einer Spule zur anderen gewickelt werden, was Handhabung langer Registrierungen erleichtert.

Mit einem neuen "Pencil" kann man Winkel ablesen. Der "Pencil" wird auf eine Linie gelegt und gibt damit die Koordinaten von zwei Punkten, von denen der Winkel kalkuliert werden kann. Er findet bereits in der Analyse von aus Funkenkammern und von Kinetheodoliten anfallender Information Anwendung.

Eine inkrementale Auswertung gibt es auch. Die Auswertung erfolgt dann in zwischen 1 mm und 1 cm vorgewählten Abständen entlang der X-Achse der Kurve.

Der "Pencil Follower" ist jetzt mit Auswerttischen von 100 × 100 cm anstelle der Standardausführung 100 × 45 cm lieferbar.

EE 02 764 *für weitere Einzelheiten*

Lasergeräte

System Computers Ltd, Fossway, Newcastle upon Tyne, 6

(Abbildung Seite 54)

Im Fertigungsprogramm der System Computers Ltd gibt es unter anderem fünf Helium-Neonlaser und drei Rubinlaser. Ausserdem liefert die Firma Zusatzausrüstungen wie beispielsweise Ausgangsleistungsmesser, passive und Drehprisma-Q-Schalter, Glaswaren und Spezialkristalle für Sonderzwecke.

Der Rubinlaser R1 eignet sich hauptsächlich für allgemeine Vorführungen und Forschungszwecke in Industrie und Schulung. Die vom 51 mm langen Rubinelement abgegebene Leistung reicht für Anwendungen wie z.B. Schneiden oder Schweissen feiner Drähte aus.

Die grösseren Rubinlaser R5 und R10 geben etwa 25 bzw. 50 Joule ab und können in Forschung und Fertigungsverfahren eingesetzt werden. Sondermerkmale sind ein luftgekühlter, hochreiner Aluminium-Hohlraum und ein 165 mm langer Rubin- oder Neodym-in-Glasstab, der je nach Werkstoff bei 6943 Å oder 10600 Å arbeitet. Beide Modelle haben externe Prismen, und gegen Zuschlag werden Drehprismen- oder Trocken-Q-Schalter, optisches Fokussieren, Wasserkühlung des Kristalls und Sonderqualitätkristalle geliefert.

Die Abbildung zeigt den Hochleistungs-Festkörper-Rubinlaser R5.

EE 02 765 *für weitere Einzelheiten*

Drehmomentgeber

Ether Engineering Ltd, Park Avenue, Bushey, Hertfordshire

(Abbildung Seite 54)

In diesem Drehmomentgeber sind Hochleistungs - Festkörper - Dehnungselemente auf einer kurzen Federachse mit runden Kupplungsflanschen angebracht. Der Messwandler ist dünn und flach und eignet sich besonders für Anwendungen wie z.B. Steuerrad-Drehmomentmessungen in der Leistungsprüfung von Kraftfahrzeugen. Der Messwandler wird unter das Steuerrad montiert und ändert die Gesamthöhe nur unwesentlich; die Handhabung des Fahrzeugs wird nicht beeinflusst. Über ein eingebautes Sicherheitsglied bleibt die Steuerung selbst in dem unwahrscheinlichen Fall, dass die Federachse ausfällt, effektiv. Der Geber kann auch für Drehmoment- und Pferdestärkemessungen in eine Wellenkupplung eingebaut werden.

Das hohe Ausgangssignal der Festkörper-Dehnungselemente reicht für direktes Treiben eines robusten Drehspulinstrumentes oder Schreibers. Bei Anwendung in Verbindung mit Schleifringen in einer Wellenkupplung ist der Einfluss der durch die Bürsten verursachten Störung vernachlässigbar klein.

Ausser seinem unbegrenzten Auflösungsvermögen und schnellen Ansprechen ist dieser Wandler erstaunlich unempfindlich gegen Biegebeanspruchung.

Der Standardmessumfang ist 20,8 kg.m.; andere Messbereiche sind gegen Sonderauftrag lieferbar.

Ein batteriebetriebenes, tragbares Anzeigegerät RML 8-225 für Einsatz mit diesem Geber steht zur Verfügung.

EE 02 766 *für weitere Einzelheiten*

Verzögerungsleitung

Sealectro Ltd, Farlington, Portsmouth, Hampshire

(Abbildung Seite 54)

Der Geschäftsbereich "Deltime" der Sealectro kündigt eine neue, preiswerte 500-μs-Verzögerungsleitung an, die in Grosserien für elektronische Tischrechner aufgelegt werden kann.

Die neue Verzögerungsleitung Modell 300 gibt es mit beliebiger Verzögerungszeit bis zu 500 μs. Sie arbeitet nach dem "Rückkehr-zu-Null"-Verfahren bei 1 MHz im schlechtesten Fall mit einem Rauschabstand von 3:1 zwischen +15° und +55° C.

Technische Daten sehen Eingangsspannungen von 20 V bei 50 mA Spitzenstrom vor. Die Ausgangsspannung wird als mindestens 15 mV an einem Abschluss von 2700 Ω gegeben.

EE 02 767 *für weitere Einzelheiten*

Mikrominiaturwiderstände

Vertrieb: Nutec Electronics Ltd, Mercantor House, 5 East Street, Shoreham-by-Sea, Sussex

Die von L. Siegart in der Bundesrepublik hergestellten hochkonstanten Kohleschichtwiderstände RKL2 gehören zu den kleinsten in der Welt. Sie sind bei 0,9 mm Durchmesser 2,6 mm lang.

Konstruktionsmässig ist der neue Widerstand dem RKL ähnlich. Die durch Pyrolyse auf das keramische Substrat aufgebrachte Kohleschicht ist verlängert, so dass sie Hohlräume an den Stabenden überzieht. Anschlussdrähte werden an die die Kohleschicht in diesen Hohlräumen überlagernde Nickelplattierung gelötet. Dadurch wird die übliche aufgedrückte Endkappe vermieden, ein sichererer elektrischer Kontakt gewährleistet und eine sich über die volle Länge des Keramikstabes erstreckende Widerstandsbahn geschaffen.

Die Anschlussdrähte sind zur Erleichterung des Lötens vergoldet. Sie bestehen aus einer Kupfer-Nickellegierung, in der hohe Festigkeit mit niedriger thermischer Leitfähigkeit verbunden ist, was die Gefahr der Wärmebeschädigung während des Lötens verringert. Empfohlen wird jedoch Verwendung eines Lötmetalls mit Schmelzpunkt unter 180° C.

Die in Werten von 47 Ω bis zu 100 kΩ lieferbaren Widerstände sind bei 65° C mit 30 mW belastbar.

EE 02 768 *für weitere Einzelheiten*

Miniatur-Synchronmotor

Magnetic Devices Ltd, Exning Road, Newmarket, Suffolk

(Abbildung Seite 54)

Dieser 90 g wiegende kleine Synchronmotor hat 36 mm Durchmesser und ist 20 mm lang. Der umkehrbare Motor hat bei 50 Hz eine Synchrongeschwindigkeit von 300 UPM. Schnelles Anlaufen und schnelle Umkehr werden durch ein niedriges Trägheitsmoment des Rotors (25 g.cm^2) erreicht. Spannungen bis zu 100 V lassen sich direkt anlegen, aber der Motor kann über Vorwiderstand oder -kondensator ein- oder dreiphasig mit bis zu 380 V betrieben werden. Als Fortschaltmotor kann der RSM36 mit bis zu 300 Schritt/Sek. arbeiten. Getriebe sind für Betrieb mit bis zu 1 Umdrehung in 30 Stunden herunter lieferbar.

EE 02 769 *für weitere Einzelheiten*

HF-Quelle und Demodulator

The Wayne Kerr Co. Ltd, Sycamore Grove, New Malden, Surrey

(Abbildung Seite 55)

Wayne Kerr kündigt Einführung einer Festkörperquelle mit Demodulator an, die Einknopfabstimmung von 100 kHz...100 MHz aufweist. Das hauptsächlich für die HF- und VHF-Messbrücken B201, B601 und B801 entwickelte Modell SR 268 bietet eine breite Auswahl von Quellenausgangspegeln und Empfängerverstärkung und ist daher für die meisten Messzwecke geeignet.

Der Ausgangspegel ist 1 V_{eff} an 75 Ω mit Drucktastenabschwächung in 3-dB-Stufen bis zu −39 dB. Die Kurzzeit-Frequenzkonstanz ist 0,01 Prozent.

Die Demodulatorempfindlichkeit ist 1 μV oder besser; ein Eingangsabschwächer hat vier Stufen von je 20 dB. Bei jeder Einstellung wird die automatische Verstärkungsregelung selbsttätig nachgeregelt, so dass für schnellen Abgleich mit genauer Nullung optimale Bedingungen bestehen. Ein Nullanzeiger ist eingebaut.

Der SR268 ist für Anschluss an 110 oder 230 V mit internem Gleichrichter ausgelegt, kann aber auch aus Batterien gespeist werden.

EE 02 770 *für weitere Einzelheiten*

Motorschutz

Standard Telephones & Cables Ltd, Components Group, Footscray, Sidcup, Kent

(Abbildung Seite 55)

Mit diesem kleinen Festkörper-Einsteckmodul wird die Gefahr des Überhitzens von Elektromotoren beseitigt. Der Baustein unterbricht ohne Kontakte oder bewegliche Teile irgendwelcher Art automatisch die Netzleitung zum Schütz, wenn die Temperatur der Motorwicklungen die zulässige Temperatur überschreitet.

Erfahrungen haben gezeigt, dass selbst geringes Überhitzen der Motorwicklungen die Leistung des Motors beeinträchtigt und bei längerer Dauer die Lebensdauer des Motors wesentlich kürzt.

Der neue Modul regelt die Wechselstromspeisung des Motors mit einem eingebauten Thyristor. Momentaner Schutz gegen Betrieb bei übermässiger Temperatur wird durch einen in die Motorwicklung eingebetteten Thermistor mit positivem Temperaturkoeffizienten erreicht, der das Schalten des Thyristors steuert. Bei ansteigender Motortemperatur wird der Thermistorwiderstand höher, bis er einen kritischen Wert überschreitet, damit den Thyristorzustand ändert und auf diese Weise die Netzleitung zum Schütz unterbricht. Selbstsichernder Betrieb wird durch Zusatz eines externen Widerstandes möglich.

Jeder Thyristor mit positivem Koeffizienten kann Verwendung finden. Drehstrommotoren können mit drei seriengeschalteten Thermistoren—einem je Phase—geschützt werden, so dass alle drei Wicklungen gleichzeitig mit einem Modul überwacht werden.

Da die Wirkungsweise nur auf direkter Überwachung der Istwicklungstemperatur beruht, wird gegen Überhitzung auf Grund von Fehlern oder Missbrauch jeder Art effektiv geschützt.

In der Praxis hat sich herausgestellt, dass diese Moduln schnell Unzulänglichkeiten aufzeigen, die mechanische, elektrische oder Umgebungsursachen in Installation, Konstruktion oder Belastung haben, und sonst für längere Zeit nicht aufgefallen wären, vielleicht nicht vor Ausfall des Motors.

Der Modul besteht aus einer transistorierten Baugruppe, die den Thyristor und seine Steuerschaltung enthält, und ist für Festigkeit und kleine Abmessungen im modularen Bausystem "Ministac" der STC ausgeführt. Einkapselung in ein eloxiertes Aluminiumgehäuse und hermetische Abdichtung erhöhen die Festigkeit. Die kleinen Abmessungen des Moduls erleichtern Einbau in beschränktem Raum, wie z.B. dem Kasten eines Motoranlassers. Anschluss erfolgt mittels eines Internationalen Oktalsockels, so dass im unwahrscheinlichen Fall des Versagens schnelles Auswechseln möglich ist.

Die Zuverlässigkeit ist so hoch, dass die Konstrukteure mit einer Durchschnittszeit von 45 Jahren zwischen Ausfällen rechnen.

EE 02 771 *für weitere Einzelheiten*

Papier-Polyesterkondensatoren

Telegraph Condenser Co. Ltd, Whales Farm Road, Acton, London, W.3

Neue Kondensatoren in rechteckigem Gehäuse mit gemischtem Papier-Polyester-Dielektrikum wurden von der Telegraph Condenser Co Ltd, einem Mitglied der Plessey-Bauelementegruppe, angekündigt. Sie sind für Anwendung in hochwertigen, professionellen elektronischen Geräten bestimmt und nach Anforderungen der DEF-5131, Bauart CP10 und CP11, Klasse 55/100 H6 konstruiert. Sie werden in Kürze zur Musterzulassung eingereicht werden.

Das neue Dielektrikum gestattet höhere Spannungsbeanspruchung, was für die Kondensatoren im Vergleich mit bestehenden Bauarten mit Papierdielektrikum und gleichen Nennwerten zu wesentlich kleineren Abmessungen führt. So werden z.B. die Abmessungen eines 2-μF-Papierkondensators für 5 kV von 229 × 130 mm auf 117 × 130 × 98 mm reduziert. Betriebstemperaturbereich ist −55°C...+70°C; bei entsprechender Leistungsminderung ist Betrieb bis zu 100°C zulässig.

Kapazitäten von 0,5 μF bis zu 12 μF sind für Nenngleichspannungen von 200 V bis zu 10 kV bei 70°C lieferbar. Sowohl die eingeführten Typen wie auch die mit gemischtem Dielektrikum sind besonders für Anwendung in Hochspannungs-Gleichstromschaltungen, als Speicher- und Glättungskondensatoren in Gleichrichtern und für die Entkopplung von Verstärkern geeignet.

EE 02 772 *für weitere Einzelheiten*

Filmwiderstandmonitor

Edwards High Vacuum Ltd, Manor Royal, Crawley, Sussex

(Abbildung Seite 55)

Der Edwards-Filmwiderstandmonitor ist ein Kontrollgerät, das in Verbindung mit einer Vakuumbeschichtungsanlage den sich ändernden Widerstand misst und die Beschichtung bei Erreichen eines vorgewählten Widerstandswertes unterbricht. Der Widerstandsbereich von 10 Ω bis zu 10 kΩ wird in drei Bereichen überstrichen. Der Filmwiderstandmonitor wird eingesetzt, wenn Widerstände aufgestäubt werden, oder in Verbindung mit einem Filmdickenmonitor in der Fertigung von Dünnfilmschaltungen.

Entweder der Widerstand des Dünnfilms selbst oder der eines geeigneten Monitorstreifens wird gemessen. Der Widerstand bildet einen Zweig einer Wheatstone-Brücke, und den Bezugszweig der Brücke kann man von der Frontplatte des Monitors aus einstellen.

Der Frontplatten-Bezugszweig wird mittels eines geeichten Wendelpotentiometers auf den Wert des gewünschten Dünnfilmwiderstands eingestellt.

Nach Erreichen des Sollwertes ist die Brücke ausgeglichen und triggert einen transistorierten Verstärker mit hoher Verstärkung, der seinerseits ein Relais unter Strom setzt und damit durch Betätigung des Quellenverschlusses die Aufstäubung beendet. Der Verschluss bleibt bis zum Drücken einer Rückstelltaste geschlossen.

Das Relais ist ausserdem mit einem Ruhe- und einem Arbeitskontaktsatz für die Steuerung externer Hilfsgeräte bestückt.

Die Brücke ist so ausgelegt, dass die Verlustleistung im überwachten Film für alle Bereiche unter 50 mW liegt. Überhitzen oder teilweises Austrocknen des niedergeschlagenen Films wird dadurch vermieden.

EE 02 773 *für weitere Einzelheiten*

Zusammenfassung der wichtigsten Beiträge

Messung von Geschwindigkeitssprüngen mittels optischer Gitter von D. K. Ewing

Zusammenfassung des Beitrages auf Seite 2-5

Ein beschriebener Frequenz-Spannung-Umsetzer beruht auf dem phasenstarren Oszillatorprinzip, das—mit einem optischen Gitter als Geschwindigkeitsmesswandler—für den Nachweis von Geschwindigkeitssprüngen abgewandelt wurde. Typische Anwendungsmöglichkeiten sind unter anderem das Messen der durch Übertragungsfehler im Antrieb der Gitterwelle hervorgerufenen Geschwindigkeitssprünge und Erstellung einer Geschwindigkeitsrückführung für Werkzeugmaschinensteuerungen in Fällen, in denen tachometrische Rückführung zu laut sein würde.

Entwurf und Abstimmung von MF-Runfunkantennen von P. Knight

Zusammenfassung des Beitrages auf Seite 6-10

Die Leistung einer schwundmindernden Mittelfrequenzantenne wird durch die Form ihres vertikalen Strahlungsdiagramms kritisch beeinflusst. Trotzdem dieses Diagramm hauptsächlich von der Höhe der Antenne und ihrem Querschnitt abhängt, kann es in gewissem Masse modifiziert werden, wenn die Antenne an der Spitze eine Kapazität oder eine serienbelastende Induktivität hat. Die zur Berechnung der vertikalen Strahlungsdiagramme für verschiedene Antennentypen erforderlichen Formeln werden gegeben und Verfahren zur Abstimmung der Antennen zwecks Erzielung spezifischer Diagramme beschrieben.

Ein einfaches, schnelles Analogmultipliziergerät von J. P. Wilson

Zusammenfassung des Beitrages auf Seite 11-14

Ein beschriebenes Analogmultipliziergerät beruht auf den nichtlinearen Röhreneigenschaften. Die Multiplizierunsicherheit ist 2 Prozent mit einer Langzeitdrift von 1 Prozent. Der überstrichene Frequenzbereich hängt von der Wahl der Schaltungseinzelheiten ab und kann zwischen 0 und maximal 2 MHz liegen. Eine Anzahl von Ein- und Ausgangsschaltungen werden besprochen, die Anwendung des Multipliziergerätes für Berechnungen, Modulation, momentane Leistungsmessungen, Korrelation sowie die genaue Regelung der Amplitude oder Hüllkurve hörbarer Frequenzsignale gestatten.

Ein Multivibrator mit breitem, spannungsgesteurten Frequenzbereich von R. J. P. Jones

Zusammenfassung des Beitrages auf Seite 14-15

Ein beschriebener Multivibrator hat einen spannungsgesteuerten Frequenzbereich, der mindestens über 10 Oktaven (1000:1) kontinuierlich regelbar ist. In seiner einfachsten Form werden Frequenz und Tastverhältnis durch kleine Änderungen in Transistoreigenschaften und Bauelementwerten beeinflusst. Eine Stabilisierungsschaltung behebt diese Mängel und linearisiert auch die Beziehung zwischen Frequenz und Steuerspannung.

Ein Zweikanal-Reizgerät von J. W. Hinshelwood und A. G. Seabridge

Zusammenfassung des Beitrages auf Seite 16-19

Ein Rechteckimpulsgeber mit Zweifachausgang wird beschrieben. Der Generator wurde für physiologische Zwecke entwickelt. Die zwei Kanäle haben gemeinsame Frequenzregelung, aber unabhängig voneinander regelbare Amplitude und Impulsdauer. Die höchste Ausgangsamplitude ist 50V. Das Gerät ist für Anregung über zwei verschiedene Wege, d.h. direkt und transneural, geeignet.

Transistorschaltung für logarithmische Strommessungen von K. S. Højberg

Zusammenfassung des Beitrages auf Seite 20-23

Zwei transistorierte Schaltungen für logarithmisches Messen kleiner Ströme werden in bezug auf ihre Anwendung in der Instrumentierung von Kernreaktoren behandelt. Das logarithmische Element liegt im Rückkopplungsweg des Verstärkers, und nur ein Doppeltransistor dient als logarithmische Diode und temperaturkompensierender Transistor. Eine einfache Einzelverstärkerschaltung wird mit einem Zweiverstärkersystem verglichen. Die beschriebenen Schaltungen wurden in Verbindung mit einem Verstärker entwickelt, der eine Doppel-MOST-Eingangsstufe mit diodengeschützten Toren hat.

Belastungseffekte in Zweikreis-RC-Filtern von J. F. Young

Zusammenfassung des Beitrages auf Seite 23-24

Durch einfache Transformation des Schaltungsdiagramms wird gezeigt, dass die Belastungseffekte in Zweikreis-RC-Abzweigfiltern in Form einer Ersatzschaltung für eine umgekehrte Wien-Halbbrücke ausgedrückt werden können. Dadurch wird die Erwägung der Belastungseffekte zwischen den Kreisen erleichtert.

Eine asynchrone binärcodierte Dezimalschaltung mit Torrückkopplung von S. L. Hurst

Zusammenfassung des Beitrages auf Seite 25-28

Binärcodierte Dezimalbausteine arbeiten normalerweise asynchron mit Zählerfassungslogik irgendwelcher Art, die irgendwo während der Zählung den nichtbinären Übergang hervorruft. Hier wird zur Erreichung des notwendigen nichtbinären Übergangs eine Serientorschaltung beschrieben, die den Vorteil hat, die in den meisten binärcodierten Dezimalsystemen auftretenden flüchtigen Falschzählungen zu vermeiden.

Anwendung eines PNPN-Schalters für Temperaturregelung von A. Lupic und B. Kovac

Zusammenfassung des Beitrages auf Seite 28-29

Die Möglichkeit, Temperatur mit Hilfe der Temperaturempfindlichkeit der Kippgeneratorschaltung in Frequenz umzuwandeln, wird besprochen. Die lineare Abhängigkeit der Temperatur und Frequenz wurde im Bereich $-10°$ . . . $+50°C$ gemessen. Während Dauerbetrieb des Oszillators für 1000 Stunden beobachtete Ergebnisse werden gegeben.

Vereinheitlichte Transistorberechnungen von D. W. W. Rogers

Zusammenfassung des Beitrages auf Seite 30-33

Eine beschriebene Methode zur Vereinheitlichung von Flächentransistorberechnungen beruht auf den Impedanzparametern und einer T-Ersatzschaltung. Die Methode ist insofern besonders arbeitssparend, als kanonische Berechnungen in z-, y_1- und h-Parametern ohne Vorbereitungen und ohne Matrixtransformation durchgeführt werden können.

Ein Thermoelement-Wattmeter zum Messen magnetischer Verluste

von J. K. Choudhury, R. K. Mondel und S. N. Bhattacharyya

Zusammenfassung des Beitrages auf Seite 34-37

Der Beitrag beschreibt eine thermische Wattmeterschaltung mit gepaarten Vakuum-Thermoumformern für Kernverlustmessungen. Die von den Autoren angewendete Schaltung unterscheidet sich von konventionellen Schaltungen für thermische Wattmeter. Durch Anwendung eines Drehspulgalvanometers mit Bandaufhängung als Anzeiger wird hohe Empfindlichkeit erreicht.

Ausgewählte Versuchsergebnisse werden als Illustration der Eignung und Einfachheit dieser Methode für Kernverlustmessungen bei normaler und inkrementaler Erregung des Testkerns gegeben. Messungen wurden im Frequenzbereich 50 Hz . . . 50 kHz durchgeführt. Die erzielte Messgenauigkeit war in der Grössenordnung von 1 Prozent des Vollausschlags.

Eine Kombination des beschriebenen thermischen und eines elektrostatischen Wattmeters in einer Prüfeinrichtung, die Messung und Vergleich der Kernverluste unter identischen Testbedingungen gestattet, wurde entwickelt. Ausgezeichnete Übereinstimmung der Ergebnisse beider Methoden wurde erreicht.

Eine Analyse der Wirkungsweise einer Schmitt-Triggerschaltung von D. W. Hampshire und D. Petersen

Zusammenfassung des Beitrages auf Seite 38-40

Dieser Beitrag beschreibt eingehend die verschiedenen möglichen Arbeitsweisen einer Schmitt-Transistortriggerschaltung. Die Bedingungen für entzerrendes Schalten werden analysiert, die Bedingungen für den stabilen Zustand berechnet und mit der Praxis verglichen.

Zündung eines dreiphasigen Wechselrichters mit regelbarer Frequenz von R. L. V. de Lima Mendes

Zusammenfassung des Beitrages auf Seite 41-45

Drei Schaltungen mit steuerbaren Siliziumgleichrichtern für das Zünden eines dreiphasigen Wechselrichters werden beschrieben. Die Vorteile und Nachteile der drei Schaltungen werden besprochen und eingehende Schaltbilder gegeben.